

**Reactions of Cationic (Allyl)Ni(II) Complexes with 1,3-Dienes and Olefins:
Polymerization and Mechanistic Studies**

Abby R. O'Connor

A dissertation submitted to the faculty of the University of North Carolina at Chapel Hill
in partial fulfillment of the requirements for the degree of Doctor of Philosophy in the
Department of Chemistry

Chapel Hill
2008

Approved by:

Advisor: Professor M. Brookhart

Reader: Professor J. L. Templeton

Reader: Professor C. K. Schauer

Professor M. L. Waters

Professor M. R. Gagne

© 2008
Abby R. O'Connor
ALL RIGHTS RESERVED

ABSTRACT

ABBY R. O'CONNOR: Reactions of Cationic (Allyl)Ni(II) Complexes with 1,3-Dienes and Olefins: Polymerization and Mechanistic Studies.
(Under the direction of Professor Maurice Brookhart)

The use of transition metal-based catalysts for diene polymerization has attracted attention because ligand and metal variations offer the possibility that polydispersity, molecular weight, and microstructure of the resulting polymer can be precisely controlled. (Allyl)Ni(II) species have proven to be useful as stereoselective single site catalysts for the polymerization of butadiene as well as for the study of the mechanistic details of polymer chain growth. This dissertation focuses on the synthesis of (allyl)Ni(II) catalysts for the polymerization of 1,3-dienes. Particular attention is diverted towards observation of intermediates and catalyst resting states in the chain growth process and the reactivity of these catalysts towards a variety of 1,3-dienes and α -olefins.

Chapter 2 describes low temperature NMR studies, which allow observation and characterization of key intermediates during polymerization of 1,3-butadiene. Isolation and characterization of wrap-around complexes and the identity of the catalyst resting state, resulting from a 1,2-insertion of butadiene into the growing polymer chain, are also presented.

Chapter 3 presents the synthesis, characterization, and reactivity of highly labile, (2-R-allyl)Ni(mes)⁺ complexes. The reactions with ligands to assess the lability of mesitylene and olefins are described. Intramolecular hydrogen atom transfer is observed upon exposure

of these Ni(II) complexes to olefins. Comparison to the analogous Pd(II) complexes is a feature of this work.

The use of cationic Ni(II) complexes for 1,3-diene and styrene polymerization is outlined in chapter 4. Activity is observed for the polymerization of butadiene, isoprene, 2,3-dimethyl-1,3-butadiene, 1,3-cyclohexadiene, and styrene. Also included is an account of the mechanistic investigations into the chain growth mechanism for other 1,3-dienes. Identification of coupling products and species generated through intramolecular hydrogen atom transfer is presented.

Synthesis of (cyclohexenyl)Ni(II) complexes and their reactivity with 1,3-dienes and olefins is outlined in chapter 5. Characterization of stable ligand-free (cyclohexenyl)Ni(II) and (cyclohexenyl)Ni(II)(η^4 -diene)⁺ species is described. For the first time an η^4 -s-trans coordinated 1,3-diene to a Ni(II) center is reported. Intramolecular hydrogen atom transfer reactions from olefin to the cyclohexenyl moiety are observed and these results suggest this process may be key to understanding the chain termination pathway in the polymerization of dienes catalyzed by (allyl)Ni(II) species.

ACKNOWLEDGEMENTS

I would first like to thank my advisor Brook for his guidance and help throughout the last five years. You are truly a well-balanced individual who values family, education, as well as hard work and I hope to one day achieve a similar balance in life. I have learned so much from working in this lab and know that my future in chemistry will be quite bright due to your tutelage. I will always remember the times I have spent with him working out NMR spectra, preparing talks, and attending our awesome group parties. I would also like to thank you for allowing me to travel to many conferences to present my research over the years. I feel privileged to have been part of your group. I can't believe after 39 years of students I will be your first student hooded in the ceremony! What an honor! I look forward to my post-doctoral position in Seattle and know I will be in close contact with you in the future.

The staff and professors at UNC are a great asset to the Chemistry department at UNC. I owe a lot to Dave Harris and Marc ter Horst in the NMR facility, who have helped me with many NMR studies. I would like to thank Profs. Mike Gagne, Jeff Johnson, Marcey Waters, Wenbin Lin, Joe Templeton, and Cindy Schauer for serving on my committee(s). Joe, I will miss your smile and jokes and leave UNC still not being in your group.

I am grateful to my wonderful parents, Dianne and Andrew who have supported and pushed me to attain my dreams and goals in life. I really appreciate everything that you have provided me with during my schooling. I realize just how much you appreciate all the hard work I have put into my dissertation and studying chemistry. Amy and Kelly are the best sisters that I could possibly ask for in life. We have become so close over the years and have

a blast when we all get to spend time together. Thanks for always caring about me and being there for me over the years. To my grandmother Mimi I am appreciative of ALL the many things you have helped me out with during the years. I am glad you all were able to spend my defense with me! I am sad to leave the east coast for a couple of years because my family is so important to me, but I know I will be back one day.

I have enjoyed working with a great bunch of students (Becky, Jian, Zheng, and Stephanie), post-doc's (Wes, Marc, Azi, and Andy) and undergrads (Indrek and Nick) while in the Brookhart lab. I especially thank Marc (German) who has really been a wonderful asset to this lab, always willing to help out everyone at anytime! I acknowledge the previous members of the group (Amy, Emily, Alison, Mark, Lei) who have helped me prepare for talks, posters, and other requirements during the years and who have been great friends over the years. I would like to acknowledge Tom who mentored me when I first started in the Brookhart lab. Thanks for leaving the nickel chemistry for me to solve! I have really enjoyed this project. I leave behind a fun group and will miss you all dearly. I also want to acknowledge our secretary Ann who does an excellent job keeping this lab in working order.

I would like to acknowledge my high school chemistry teacher Mr. Dave Wilson who introduced me to chemistry and Lafayette College. This leads me to my next shout out to Dr. Chip Nataro, my undergraduate advisor at Lafayette College. You have been there since my freshman year of college pushing me to pursue inorganic chemistry. I was lucky to have accomplished so many projects while doing research at Lafayette. It is crazy to think that I am now on my way to becoming your colleague! Time flies. Thank you for always being there for me and for all the undergrads interested in Chemistry at Lafayette. You have influenced the minds of many students to pursue higher education in chemistry.

I have made some great friends here at Chapel Hill during the last 5 years. To all my fellow 5th years (Jason, Nick, Becca, Matt, Dee, Julie, Heather), thanks for being my classmates and friends over the years and good luck at your future jobs. To the Templeton lab (Chetna, Andy, Ned, and Kristi) thanks for letting me work in your lab during the past 5 years. You guys are all great friends and coworkers. I will always remember our fun times partying it up, at Friday lunches, playing softball, and just talking. I have had two great roommates Julie and Stephanie while living in Chapel Hill. I will miss you guys next year and wish you the best in the future. You two have been great friends over the years and I appreciate all you both have done for me. I will really miss our Thursday night TV nights! To Kristi, you have been one of my closest friends here. Thanks for all the fun times on Franklin St., 80's night, Yo-Po, being my gym buddy, and being there when I needed someone. I will miss your energy, stories, and personality in my life each day! Thanks to my college friends (Katie, Melissa S., Jess, Melissa J., Maureen, and all the AGDs) who are still there when I need to vent or just relax and talk.

Finally, I want to thank my boyfriend Matthew Crowe. If I had not come to UNC, 5 years ago, I would never have met the person that makes so happy each and every day and someone to spend my life with. I really appreciate the drive and passion you have for all things important in your life. You have been the my support system this past year listening to all my problems, taking care of me when I was sick and had a broken leg. I could not have made it through without your love and support. I will not forgot all our wonderful dates in Chapel Hill! I am lucky to have you in my life and look forward to our move to Seattle.

To my Family:
The O'Connor Clan
Dianne, Andrew, Amy, Kelly, and Mimi

TABLE OF CONTENTS

	Page
LIST OF TABLES	xiv
LIST OF SCHEMES	xv
LIST OF FIGURES	xvii
LIST OF ABBREVIATIONS AND SYMBOLS	xviii
 Chapter	
I. Transition Metal-Catalyzed Polymerization of 1-3Dienes:	
Introduction and Background	1
A) Industrial Production of Poly-1,3-Dienes	3
B) Nickel(II) Catalyzed Polymerization of Butadiene	5
C) Chain Transfer in Nickel(II) Catalyzed Polymerization	9
D) Research Goals and Achievements	11
E) References	13
II. The Mechanism of Polymerization of Butadiene	
by “Ligand-Free” Nickel(II) Complexes	16
A) Introduction	16
B) Results and Discussion	17
C) Summary	23
D) Experimental Section	24
1) General Considerations	24
2) Materials	24

3) (Allyl)Ni(II) Complex Synthesis	25
4) In Situ Generation of Cationic Ni(II) Intermediates	28
5) Observation of the Catalyst Resting State	34
6) Polymerization of Butadiene	36
7) Crystal Structure Determination of 6 and 10	36
E) References and Notes	37
III. Synthesis of Labile Cation (Allyl)Nickel(II) and Palladium (II) Arene Complexes and Reactivity with Olefins	39
A) Introduction	39
B) Results and Discussion	42
1) Synthesis of (2-R-Allyl)M(Arene) ⁺ Salts	42
2) Ligand Substitution Reactions of (Allyl)Pd(Arene) ⁺ Complexes	44
(a) Reactions with Diethyl Ether	44
(b) Exchange Reaction with Free Mesitylene	45
(c) Reactions with Olefins and Alkynes	46
3) Reactions of (Allyl)Ni(II)(Arene) ⁺ Complexes	52
(a) Reactions with Diethyl Ether	52
(b) Arene Exchange Reactions	52
(c) Reactions with Olefins	52
4) Mechanism of Hydrogen Transfer	57
C) Conclusions	58
D) Experimental Section	59
1) General Considerations	59
2) Materials	59

3) General Procedure Synthesis for the of [(Allyl)Pd(Arene)][SbF ₆] Complexes	60
4) Synthesis of (Allyl)Pd(II) Bis-Olefin Complexes	62
5) Dynamic Measurements using ¹ H Line Broadening.....	65
6) Synthesis of (2-R-Allyl)Ni(Arene) ⁺ Complexes.....	69
7) Reaction of Olefins with Complexes 5 or 6	72
8) Crystal Structure Determination of 5 and 7	76
E) References	77
IV. Polymerization of 1,3-Dienes Catalyzed by (Allyl)Ni(II) Complexes.....	79
A) Introduction	79
B) Results and Discussion.....	83
1) 1,3-Diene Polymerization Catalyzed by [(2-R-allyl)Ni(NCCH ₃) ₂][B(Ar _F) ₄] in Combination with B(C ₆ F ₅) ₃	83
2) Polymerization of 1,3-Dienes Catalyzed by [(2-R-allyl)Ni(mes)][B(Ar _F) ₄] Complexes	88
(a) Polymerization of Isoprene.....	90
(b) Polymerization of 2,3-Dimethyl-1,3-Butadiene	91
(c) Polymerization of 1,3-Cyclohexadiene	96
3) Polymerization of Styrene	98
C) Summary	102
D) Experimental Section.....	102
1) General Considerations	102
2) Materials.....	113
3) In Situ Generation of Cationic Ni(II) Complexes.....	104

4) General Procedure for BD Polymerization Using In Situ Generated Ligand-Free Species 4	107
5) General Procedure for Polymerization of DMBD with Ligand-Free Species 4	108
6) General Procedure for Polymerization of IP with In Situ Generated Species 4	108
7) General Procedure for BD Polymerization using Complex 5	109
8) General Procedure for Polymerization of 1,3-CHD and IP using Complex 5	109
9) Polymerization of DMBD using 5 or 6	110
10) Polymerization of Styrene with 5 or 6	111
E) References	112
V. Intramolecular Hydrogen Atom Transfer Observed in the Reaction of 1,3-Dienes and Olefins with (Cyclohexenyl)Ni(II) Complexes	115
A) Introduction	115
B) Results and Discussion.....	121
1) Catalyst Synthesis and Structure	121
2) Ligand Exchange Reactions	123
3) Reactions with 1,3-Dienes.....	124
4) Polymerization Screening.....	129
5) Reaction with Olefins.....	129
6) Reaction of 2 with DMBD	131
C) Summary	133
D) Experimental Section.....	143
1) General Considerations	134
2) Materials.....	134

3) Synthesis of (Cyclohexenyl)Ni(II) Complexes	135
4) Generation of [(Cyclohexenyl)Ni(η^4 -Diene)][B(Ar _F) ₄] Complexes.....	137
5) Assessment of the Lability of Coordinated Mesitylene in Complex 2 ..	142
6) Qualitative Competitive Binding Between IP and BD	142
7) In Situ Generation of Ni(II) Species	143
8) General Procedure for Polymerization of 1,3-Dienes	145
9) Crystallographic Information	146
E) References	147
APPENDIX I	150
APPENDIX II	165
APPENDIX III.....	172

LIST OF TABLES

Table 4.1	Polymerization of butadiene using in situ generated complex 4	85
Table 4.2	Polymerization of isoprene using in situ generated complex 4	86
Table 4.3	Polymerization of dimethylbutadiene with in situ generated complex 4 ..	87
Table 4.4	Butadiene polymerization data using complex 5 as initiator.....	90
Table 4.5	Isoprene polymerization data using complex 5 as initiator.....	91
Table 4.6	Dimethylbutadiene polymerization data	92
Table 4.7	1,3-Cyclohexadiene polymerization results	97
Table 4.8	Polymerization of styrene.....	98
Table I.1	X-ray crystal data and structure refinement	150
Table I.2	Selected bond lengths (Å) for complex 6	152
Table I.3	Selected bond angles (°) for complex 6	154
Table I.4	Selected bond lengths (Å) for complex 10	158
Table I.5	Selected bond angles (°) for complex 10	160
Table II.1	X-ray crystallographic data for complexes 5 and 7	165
Table II.2	Selected bond lengths (Å) for complex 5	166
Table II.3	Selected bond angles (°) for complex 5	168
Table II.4	Selected bond angles (Å) for complex 7	172
Table II.5	Selected bond angles (°) for complex 7	174
Table III.1	X-ray crystallographic data for complexes 2	177
Table III.2	Polymerization of 1,3-CHD and DMBD using catalyst 2	178
Table III.3	Selected bond angles (Å) for complex 2	178
Table III.4	Selected bond angles (°) for complex 2	180

LIST OF SCHEMES

Scheme 1.1	Previously investigated (allyl)Ni(II) complexes for butadiene polymerization.....	5
Scheme 1.2	Proposed mechanism for <i>trans</i> -regulating [(allyl)NiL ₂] ⁺ catalysts	8
Scheme 1.3	Proposed mechanism of butadiene insertion in “ligand-free” Ni species, based on DFT calculations.....	9
Scheme 1.4	Taube’s proposed chain transfer mechanism depicting β-hydride elimination from polybutadiene to monomer	10
Scheme 1.5	Methyl migration to form (allyl)M(diimine) ⁺ complexes	11
Scheme 2.1	Taube and Tobisch’s proposed mechanism for for butadiene polymerization.....	17
Scheme 2.2	Reaction of (allyl)Ni(II) ligand-free species with butadiene.....	19
Scheme 2.3	Proposed mechanism for PBD chain growth.....	23
Scheme 3.1	Synthesis of (2-R-allyl)M(arene) ⁺ complexes	43
Scheme 3.2	Formation of Pd(II) bis-ethylene adduct 8	47
Scheme 3.3	Synthesis of (2-Cl-allyl)Pd(cyclopentene) ₂ ⁺ at low temperature.....	49
Scheme 3.4	Synthesis of complexes Pd(II) 14 and 15	51
Scheme 3.5	Reaction of complexes 5 and 6 with 1-hexene at room temperature.....	54
Scheme 3.6	Intramolecular hydrogen atom transfer with complex 5 and 1-octene	55
Scheme 3.7	Mechanism of hydrogen atom transfer in the reaction of 1-hexene with (2-R-allyl)Ni(mes) ⁺ complexes.....	58
Scheme 4.1	Polymerization of 2,3-bis(4-trifluoroethoxy-4-oxobutyl)-1,3-butadiene with in situ generated 4	87
Scheme 4.2	Generation of complex 7 via intramolecular hydrogen atom transfer	95
Scheme 4.3	Proposed mechanism to form coupling product 8	96
Scheme 4.4	Proposed hydrogen atom transfer mechanism to form complex 9	101

Scheme 5.1	Proposed mechanisms for chain transfer in butadiene polymerization based on DFT calculations	120
Scheme 5.2	Synthesis of cationic (cyclohexenyl)Ni(II) complexes	122
Scheme 5.3	Generation of [(cyclohexenyl)Ni][B(Ar _F) ₄], 3 , and [(cyclohexenyl)Ni(η^4 -butadiene)][B(Ar _F) ₄], 4 , at low temperatures	125
Scheme 5.4	Exposure of species 3 to 4 equiv of DMBD	127
Scheme 5.5	Addition of cyclopentadiene to species 3 at -80 °C	129
Scheme 5.6	Reaction of 1-hexene with complex 2 at room temperature.....	130
Scheme 5.7	C-C coupling of complex 2 with DMBD	132

LIST OF FIGURES

Figure 1.1	Polymer microstructures for polybutadiene and 2-substituted poly-1,3-dienes	2
Figure 1.2	<i>Syn</i> and <i>anti</i> allyls control the stereochemistry of the polymer chain.....	3
Figure 2.1	¹ H NMR spectrum of complex 10 (500 MHz) in CD ₂ Cl ₂ at -30°C	20
Figure 2.2	Molecular structure of complex 10	20
Figure 2.3	¹ H NMR overlay displaying insertion of butadiene into complex 10 at -30 °C, generating the catalyst resting state 12	21
Figure 2.4	¹ H NMR overlay displaying insertion of butadiene into complex 11 at -30 °C generating wrap-around complex 12 ; the proposed resting state	22
Figure 3.1	ORTEP diagram of (allyl)Ni(mes) ⁺ , 5	44
Figure 3.2	ORTEP diagram of (2-methallyl)Ni(hmb) ⁺ , 7	44
Figure 3.3	Variable temperature ¹ H NMR overlay of the addition of 1 equiv mesitylene to 1	46
Figure 3.4	¹ H NMR variable temperature overlay showing the formation of (2-Cl-allyl)Pd(ethylene) ₂ ⁺ and exchange with free ethylene	47
Figure 3.5	¹ H NMR overlay showing the formation of (2-Cl-allyl)Pd(cyclopentene) ₂ ⁺ and exchange with free cyclopentene	50
Figure 4.1	Insertion of butadiene into complex 6 to form a wrap-around complex... ..	89
Figure 5.1	Chain termination pathways in the metal-catalyzed polymerization of olefins.....	116
Figure 5.2	Molecular structure of complex 2	123
Figure I.1	ORTEP diagram for complex 6	151
Figure I.2	¹⁹ F NMR overlay showing intramolecular Ar _F exchange for species 2 ..	164
Figure I.3	¹ H NMR spectrum of complex 11 (500 MHz) in CD ₂ Cl ₂ at -40 °C	164

LIST OF ABBREVIATIONS AND SYMBOLS

δ	chemical shift
Å	angstroms
ΔG	change in Gibbs' free energy
°C	degrees Celsius
‡	denotes transition state
ω	spectral linewidth
1,3-CHD	1,3-cyclohexadiene
1,4-CHD	1,4-cyclohexadiene
Ar	aryl
Ar _F	3,5-(CF ₃) ₂ C ₆ H ₃
BD	butadiene
br	broad
CTA	chain transfer agent
COSY	correlated spectroscopy
d	doublet
DFT	density functional theory
DMBD	2,3-dimethyl-1,3-butadiene
DSC	differential scanning calorimetry
equiv	equivalents
g	grams
GPC	gel permeation chromatography
h	hours

HPLC	high performance liquid chromatography
Hz	hertz
hmb	hexamethyl benzene
HMQC	heteronuclear multiple quantum coherence
IP	isoprene
J	scalar coupling constant, in Hz
K	Kelvin (in NMR data)
K	equilibrium constant
k	rate constant
k_p	rate constant for chain propagation
k_u	rate constant for chain termination
kcal	kilocalorie
L	ligand
M	molar
m	multiplet
m	meta
MAO	methylaluminoxane
Me	methyl, -CH ₃
Mes	mesitylene
MHz	megahertz
min	minutes
mL	milliliters
M_n	number average molecular weight

mmol	millimole
mol	moles
M_w	weight average molecular weight
NMR	nuclear magnetic resonance
<i>o</i>	ortho
<i>p</i>	para
P	polymer chain
PBD	polybutadiene
PDI	polydispersity index, M_w/M_n
ppm	parts per million
q	quartet
RT	room temperature
s	seconds
s	singlet (in NMR data)
SBR	polybutadiene polystyrene rubber
solv	solvent
t	triplet
T_g	glass transition temperature
T_m	melt transition temperature
TFA	trifluoroacetato
TOF	turnover frequency
TON	turnover number
VT	variable temperature

CHAPTER ONE

Transition Metal-Catalyzed Polymerization of 1,3-Dienes

Introduction and Background

Homopolymers and copolymers of 1,3-dienes constitute a significant fraction of commodity polyolefins. A prime example is polybutadiene (PBD). In 1999, 2 million tons of polybutadiene were produced worldwide, accounting for 20% of all synthetic rubbers. This polymer is in high demand due to both the low cost of butadiene monomer and the versatility of the microstructure through both 1,2, 1,4 (and for substituted dienes 3,4) enchainment modes (Figure 1.1).¹ Polydienes that have 1,4-units can exist as the *cis* and/or *trans* isomers. For 1,2 or 3,4-enchained polydienes, a chiral polymer is generated with different asymmetric configurations (isotactic, syndiotactic) possible for the polymer chain.² The different polymer enchainment modes are important because they dictate polymer properties. The *cis*-1,4 enchainment isomer of polybutadiene is the most economically important because of its use in the tire industry.³ Butadiene is typically copolymerized with styrene in a 3:1 ratio producing polybutadiene-polystyrene rubber (SBR), which is used for car tire production.⁴ Other polymers that are produced on a large scale each year include polyisoprene, poly-2,3-dimethyl-1,3-butadiene, and polychloroprene.³

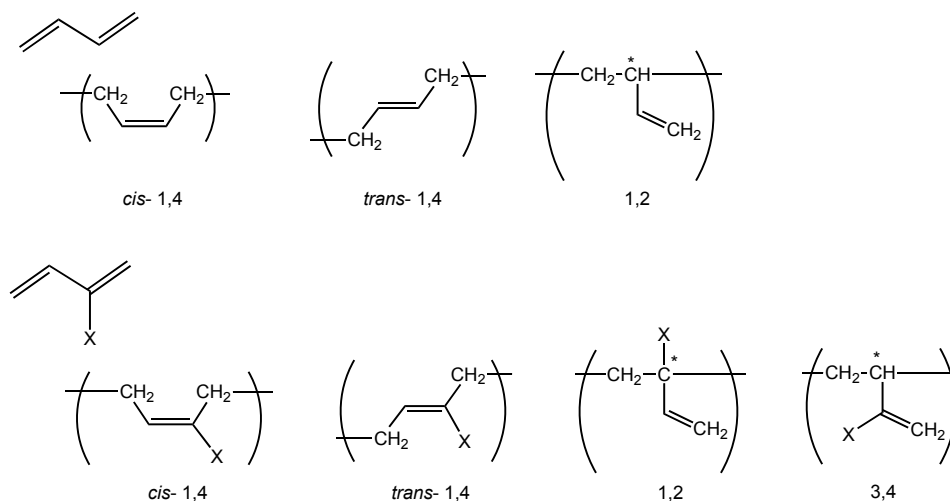


Figure 1.1. Polymer microstructures for polybutadiene and 2-substituted poly-1,3-dienes.

Two general mechanisms have been proposed for the insertion reaction of butadiene into allyl-metal bonds. The first mechanism was proposed by Cossee and Arlman and suggested nucleophilic attack of the σ form of an allyl metal complex (η^1 -allyl) upon bound butadiene.^{5, 6} The second possible mechanism involves direct coupling of complexed butadiene with an η^3 -allyl moiety. This pathway is called the direct allyl-insertion mechanism and is the generally accepted mechanism based on numerous experiments⁷⁻⁹ and calculations.¹⁰⁻¹²

It is well known that *syn-anti* isomerization controls the *cis-trans* stereochemistry in the metal-catalyzed polymerization of dienes. *Syn-anti* isomerization occurs through a σ - π -rearrangement interconverting the two isomers (Figure 1.2). Chain propagation proceeds via an insertion of a diene monomer unit into a preformed π -allyl group on the metal center. The allyl group can exist in two possible orientations *syn* or *anti* in which the polymer chain is *cis* (*syn* isomer) or *trans* (*anti* isomer) to the central hydrogen atom (H_2), respectively.³ Insertion of a monomer unit into the *anti* conformation of an allyl group generates a *cis*-1,4 unit, while insertion into the *syn* conformer yields a *trans*-1,4 unit. It is postulated that controlling the

rate of equilibration between the *syn* and *anti* isomers, relative to their rates of insertion, is key to influencing the resultant microstructure of poly-1,3-dienes.¹⁰

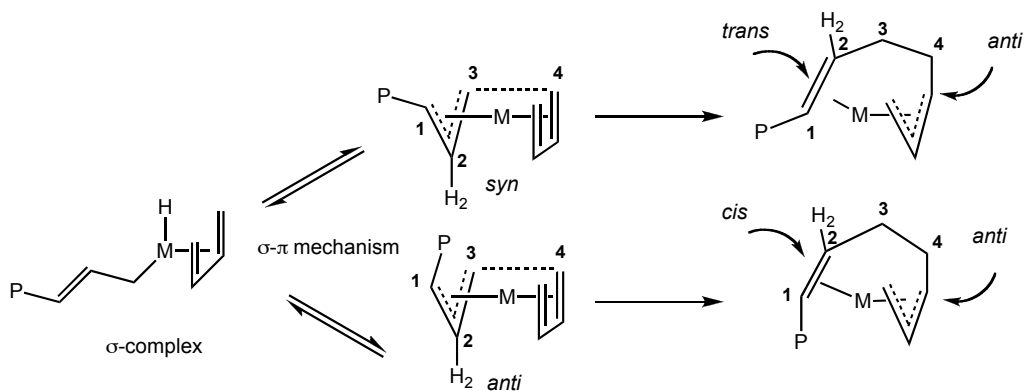


Figure 1.2. *Syn* and *anti* allyls control the stereochemistry of the polymer chain.

Industrial Production of Poly-1,3-Dienes

Polydienes are synthesized in industry via many polymerization mechanisms including free radical, transition metal-mediated insertion, or anionic processes. Polybutadiene is industrially produced using Ziegler-Natta type catalysts of titanium, cobalt, nickel, or neodymium, depending on the microstructure desired. Mixed metal catalysts, containing specific anions, can preferentially yield *cis*-1,4-polybutadiene. For example, combinations of titanium tetrachloride (TiCl_4), aluminum alkyls (R_3Al), and a titanium or aluminum iodide containing species are needed to produce up to 94% *cis*-1,4 enchainment polymer. It is necessary to have an iodide containing metal species to obtain high *cis* stereoselectivity.³ Neodymium¹ or nickel⁸ compounds containing carboxylate, halide, or a combination of carboxylate/halide ligands are also commonly employed as *cis*-1,4 selective polymerization catalysts. *Trans*-1,4 enchainment polybutadiene is achieved through careful variation of the ratio of TiCl_4 to R_3Al .^{1,3} The industrial methods to produce 1,2-units involve

the use of titanium, vanadium, chromium, or cobalt catalysts with alcoholate ligands and a trimethylamine cocatalyst.³

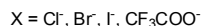
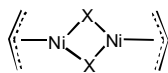
The only synthetically useful method to make polychloroprene is through free radical polymerization in an emulsion process favoring the *trans*-1,4 polymer.³ Polychloroprene is a commodity polymer and most commonly used in the production of wet suits, laptop sleeves, and car fan belts. *Cis*-1,4-polyisoprene, also referred to as natural rubber, has highly elastic properties and is used for production of erasers, rubber bands, and adhesives.¹³ Commercially, the polymer is generally synthesized using anionic initiators including butyllithium. 1,4-Enchained polyisoprene can also be prepared using a vanadium catalyst in combination with aluminum alkyls or halides. The stereochemistry of the polymer can be controlled by adjusting the ratio of vanadium:aluminum. To date there are no methods to synthesize pure 1,2-polyisoprene.³

Unfortunately a major drawback to the metal catalysts used in industry is that the molecular weight distribution of the polymers is broad (PDI 3-4), due to incomplete catalyst activation.¹ The ability to tailor polymer properties, such as molecular weight and stereochemistry is an important area of research in academics and industry. A way to more precisely control these polymer properties is through the development of homogenous catalysts that are single site initiators. Additionally, it is desirable to develop a well-defined catalyst that can be used to probe the mechanistic details, such as the identity of the catalyst resting state and the mode of insertion during the polymerization. The most well-studied examples capable of initiating diene polymerization are those derived from (allyl)Ni(II) complexes (Scheme 1.1).²

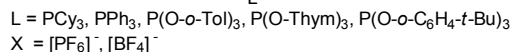
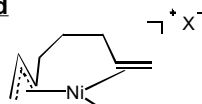
Nickel (II) Catalyzed Polymerization of Butadiene

Scheme 1.1. Previously investigated (allyl)Ni(II) complexes for butadiene polymerization.

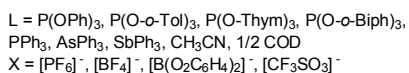
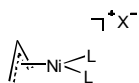
Neutral Dimers - poor activity



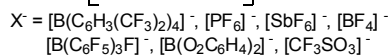
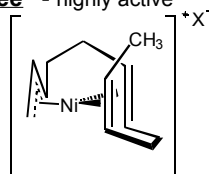
Mono-ligand



Bis-ligand - low activity (except $L = \text{SbPh}_3$)



"Ligand-free" - highly active



The earliest examples of (allyl)Ni(II) complexes shown to polymerize butadiene were developed independently by Porri and Natta¹⁴ as well as Dolgoplosk¹⁵ in the 1960's. These complexes are $[(\text{allyl})\text{NiX}]_2$ dimers ($X = \text{Cl}, \text{Br}, \text{I}$) and exhibit very low activities. It was noted that stereochemical enchainment of the polybutadiene varied as a function of the identity of X . When $X = \text{Cl}$ a predominantly *cis*-1,4 enchainment of the polybutadiene is observed, while when $X = \text{I}$ a *trans*-1,4 polybutadiene is obtained.^{14, 15} These neutral bridging allyl nickel halide dimers when activated with a Lewis acid in benzene are more active and yield polybutadiene with high *cis*-1,4 enchainment in modest to good yields over long periods of time, but unfortunately low molecular weight polymers are obtained. Porri and Natta proposed the active catalyst in solution was a cationic $[(\text{allyl})\text{Ni}(\eta^6\text{-benzene})]^+$ species,¹⁴ but have not proven this experimentally.

In the mid 1970's, Kormer and coworkers studied the mechanism of the [(crotyl)NiI]₂ catalyzed polymerization of 1,3-dienes. They synthesized the [(η³-perdeuterocrotyl)NiI]₂ dimer and studied the stereochemical control in the addition of butadiene to these catalysts. The appearance of allyl resonances in the ¹H NMR spectrum showed that the first monomer unit inserts into the metal-allyl bond followed by subsequent allyl group formation, supporting a direct allyl insertion mechanism. This result was also verified by adding deuterobutadiene to [(crotyl)NiI]₂. ¹H NMR spectroscopic experiments suggested that *syn-anti* isomerization controlled the stereochemistry in the resultant polymer chains.¹⁶⁻¹⁹ Harrod and Wallace also studied this reaction and showed that there is a first-order dependence of chain growth on catalyst and monomer and suggested that the slow step of the reaction is insertion.^{20, 21}

Teyssié reported the first and only living polymerization of butadiene using allyl Ni(II) complexes.²² The most active catalyst they developed was the allyl dimer, [(allyl)Ni(trifluoroacetato)]₂, which yields highly *cis*-1,4 PBD. This system exhibits living polymerization kinetics,²² however the PDIs range from 1.2-2.0, which are quite broad for traditional living polymerization.²³ It was discovered that the choice of ligand and acid in this system affects the stereochemistry. Addition of triphenyl phosphite or chloroanil as ligands to [(allyl)Ni(trifluoroacetato)]₂ dimer drastically influences the stereoselectivity in the polymerization, now favoring the *trans*-1,4 polymer. The *cis:trans* ratio can be adjusted through variation in the ligand and kinetic conditions. Teyssié claims the environment around the metal center dictates the selectivity of the catalyst. He based his proposal on experiments in which the ratio of *cis* to *trans* units varied with the size of the ion coordinated to a (C₁₂H₁₉Ni)⁺ center. Blocking of a coordination site on the metal by a bulky ligand leads

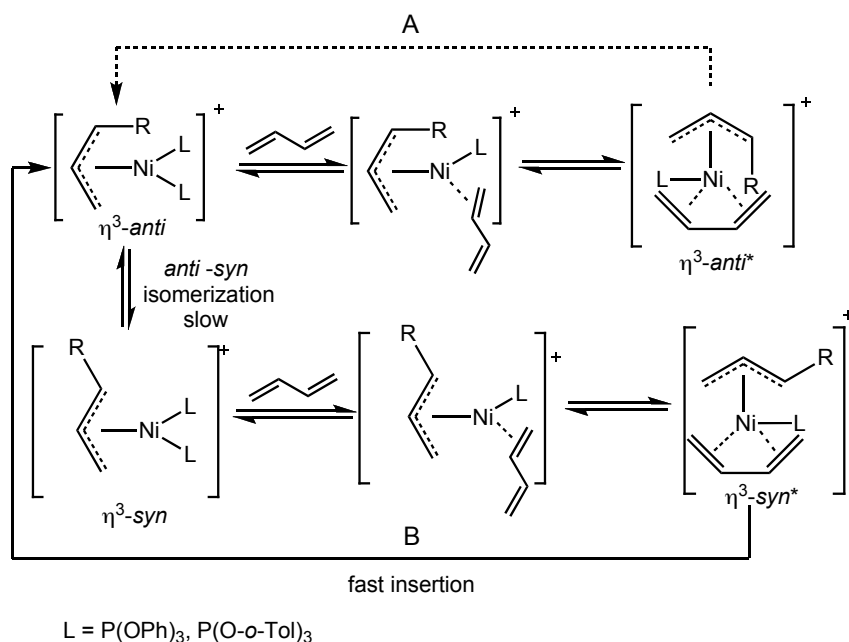
to the formation of complexes with different geometries, therefore affecting the quantity of free coordination sites on the metal. Sterically congested environments generate a more *trans* enriched polybutadiene.²⁴ Thus, the *syn-anti* equilibrium was proposed not to be a factor in controlling the polymer enchainment mode, but later work suggests otherwise.²⁴

The first examples of isolated cationic (allyl)Ni(II) complexes as initiators for 1,3-diene polymerization were [(allyl)NiL₂][X] (X = noncoordinating anion), reported by Taube in the 1980's. These compounds are more active than their neutral analogues previously discussed and contain aryl phosphites, aryl phosphines, aryl arsines, acetonitrile, stibines, or COD as ancillary ligands.²⁵ Complexes that contain triphenyl phosphine, triethyl- and trisopropyl phosphite, and *t*-butylisonitrile ligands are virtually inactive, while those with triphenyl- and tri-*o*-tolyl phosphite ligands exhibit an increase in catalytic activity and are *trans* stereoselective.²⁶ Complexes with weakly coordinated ligands such as triphenyl stibine and triphenyl arsine are very active and more *cis* selective. Overall, the [(allyl)NiL₂][X] complexes generally exhibit low activities except when L = triphenyl stibine.

Taube has attempted to draw conclusions concerning the *trans*-regulating chain growth mechanism through ³¹P{¹H} NMR experiments using the complexes [(allyl)NiP(OPh₃)₂][PF₆] and [(crotyl)NiP(OPh₃)₂][PF₆].⁷ Scheme 1.2 outlines the *trans*-regulating mechanism proposed by Taube. Through these studies, Taube has shown the rate-limiting step to be *syn-anti* isomerization. By ³¹P{¹H} NMR, Taube observed the catalyst resting state to be the less reactive *anti* isomer. The more reactive *syn* isomer rapidly inserts butadiene to generate a *trans*-1,4 unit, followed by rate determining *syn-anti* isomerization.^{7, 8, 27} Path B is proposed to be operative when *syn-anti* isomerization is rate determining, which occurs when there are strong donor ligands present in the coordination sphere of

nickel. Path A is suggested to be essentially non-operative until the donor strength of the ligand decreases substantially.²⁷

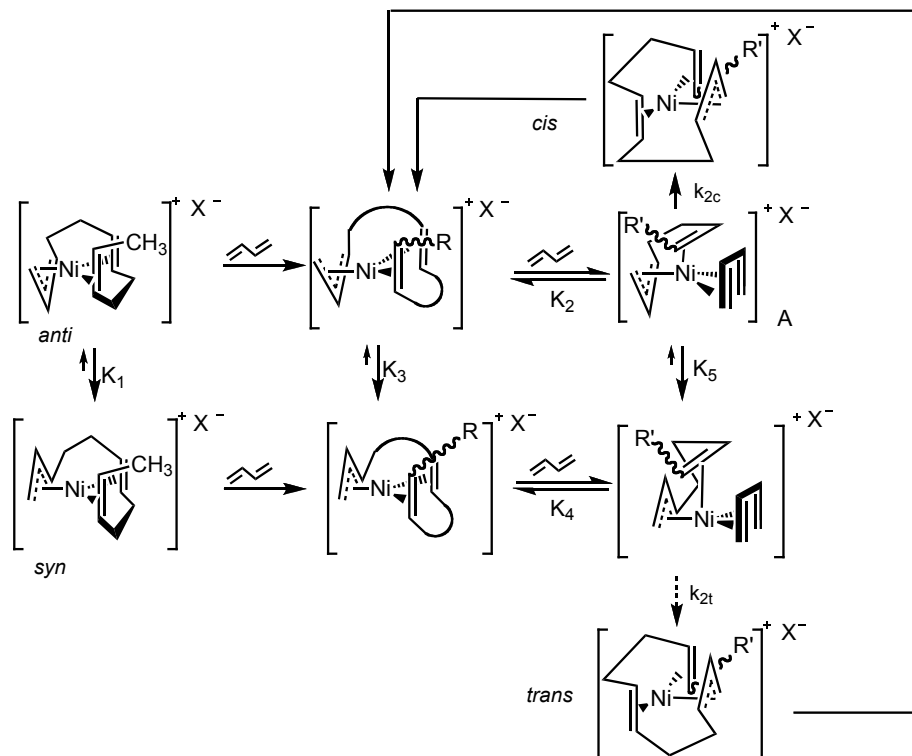
Scheme 1.2. Proposed mechanism for *trans*-regulating [(allyl)NiL₂]⁺ catalysts.



The most active Ni(II) complexes to date were developed by Taube and coworkers and are best described as “ligand-free.”²⁸⁻³⁰ TOFs of 12000/hr are achieved for [Ni(C₁₂H₁₉)]⁺[X]⁻, where X = PF₆⁻, B(Ar_F)₄⁻ or SbF₆⁻, and the polybutadiene prepared is highly *cis*-1,4 enchain.² In collaboration with Tobisch, a DFT supported mechanism for the *cis*-regulating polymerization of butadiene using ligand-free Ni(II) complexes was proposed (Scheme 1.3). It is postulated that both *syn-anti* isomerization and diene insertion play a role in the *cis*-regulating mechanism. The key step in the reaction was proposed to involve a **rapid** *syn-anti* isomerization of the allyl group with rate-determining insertion. A five-coordinate intermediate (see Scheme 1.3, A) is suggested to induce insertion of butadiene

and calculations suggest it to be the catalyst resting state,^{12, 31} but the true identity of the catalyst resting state is still speculative.

Scheme 1.3. Proposed mechanism of butadiene insertion in “ligand-free” Ni species, based on DFT calculations.

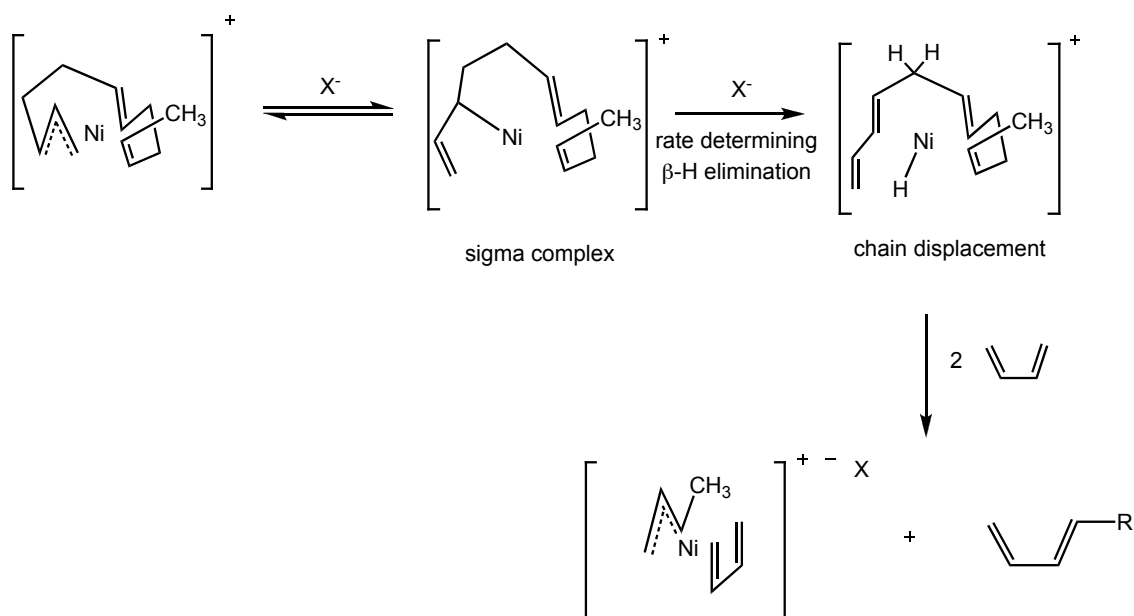


Chain Transfer in Ni(II) Catalyzed Polymerizations

Not much is known about the chain transfer mechanism in the (allyl)Ni(II)-catalyzed polymerization of butadiene. Taube proposes that rate-limiting β -H elimination from the polybutadienyl chain and transfer of the hydrogen atom to butadiene occurs forming a new (allyl)Ni(II) species.^{32, 33} The mechanism for chain termination was supported by the identification of 1,3-diene end groups in Diels-Alder trapping experiments.³³ Through kinetic analysis, the process was shown to be dependent on the concentration of nickel.^{32, 33} DFT calculations have also been performed and point to chain termination occurring through

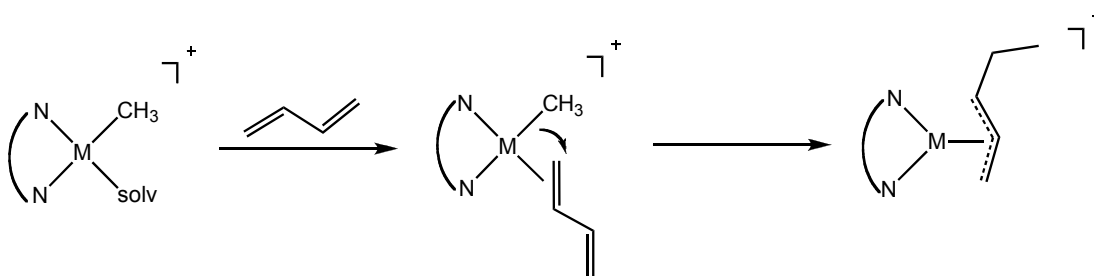
hydrogen atom transfer from the polybutadienyl chain to monomer and not by a direct β -hydrogen elimination mechanism as earlier suggested (Scheme 1.4).³⁴

Scheme 1.4. Taube's proposed chain transfer mechanism depicting β -hydride elimination from polybutadiene to monomer.



The use of late transition metals for the polymerization of olefins has been widely explored over the past few decades. Early metal catalysts of zirconium and titanium exhibit high activity in the polymerization of α -olefins, but due to high oxophilicity of these d^0 metal complexes, incorporation of polar and functionalized monomers are not well tolerated. The Brookhart lab and others have investigated the use of late metal catalysts for the polymerization of ethylene and polar monomers.³⁵⁻³⁷ These Brookhart palladium and nickel complexes yield polyolefins bearing a highly branched microstructure and can incorporate certain polar vinyl monomers into the polyolefin backbone.³⁵ Unfortunately, these catalysts are not well suited for 1,3-diene polymerization due to the formation of a highly stable allyl diimine species (Scheme 1.5).

Scheme 1.5. Methyl migration to form (allyl)M(diimine)⁺ complexes.



Research Goals and Achievements

Significant research in the Brookhart laboratory has been focused at the development of highly active, late transition-metal catalysts for polymerization reactions. Most efforts have focused on α -olefin and polar monomer incorporation into the polyolefin chains using nickel and palladium catalysts. Through carefully designed experiments, details of the mechanism and the kinetics of polyolefin chain growth have been measured. Although there are many examples of well-defined late transition metal complexes that polymerize α -olefins, there are many fewer complexes that are able to initiate polymerization for a wide array of 1,3-dienes. The goals of this research include (1) the synthesis of highly active Ni(II) complexes which can initiate polymerization of butadiene and other 1,3-dienes; (2) elucidation of the mechanism of diene insertion and, for the first time, identification of the catalyst resting state and intermediates prior to and during the chain growth process; and (3) acquisition of a better understanding of the mechanism of chain termination.

Chapter 2 describes the mechanistic investigation into the butadiene polymerization chain growth mechanism using cationic Ni(II) ligand-free species. For the first time, intermediates prior to and during chain growth have been observed through variable temperature NMR studies. Additionally, the identity of catalyst resting state has been determined.

Chapter 3 outlines the synthesis of highly active $[(\text{allyl})\text{Ni}(\text{arene})][\text{B}(\text{Ar}_\text{F})_4]$ complexes and their reactivity with α -olefins. NMR studies investigating the hydrogen atom transfer reaction that occurs when the Ni(II) complexes are exposed to olefins are described. Interestingly, intramolecular hydrogen atom transfer chemistry is observed from an olefin to the allyl moiety. Comparison of the reactivity of these Ni(II) complexes with the analogous $[(\text{allyl})\text{Pd}(\text{arene})][\text{B}(\text{Ar}_\text{F})_4]$ complexes is also presented. Stephanie A. Urbin and Rebecca A. Moorhouse have investigated the Pd(II) systems in these labs.

Chapter 4 describes the use of $[(2\text{-R-allyl})\text{Ni}][\text{B}(\text{Ar}_\text{F})_4]$ and $[(2\text{-R-allyl})\text{Ni}(\text{arene})][\text{B}(\text{Ar}_\text{F})_4]$ ($\text{R} = \text{H}, \text{CH}_3$) for the polymerization of 1,3-dienes and styrene. Additionally, mechanistic information regarding the chain growth mechanism in 2,3-dimethyl-1,3-butadiene and styrene polymerization is outlined.

Chapter 5 describes the reaction of 1,3-dienes and olefins with (cyclohexenyl)Ni(II) complexes performed in hopes to gain insight in the chain transfer mechanism in diene polymerization catalyzed by Ni(II) complexes. This chapter focuses on the synthesis and characterization of “stable” $(\text{cyclohexenyl})\text{Ni}(\eta^4\text{-diene})^+$ complexes. Intramolecular hydrogen atom transfer reactions with olefins and dienes are also discussed.

References

1. Thiele, S. K. H.; Wilson, D. R. *J. Macromol. Sci.* **2003**, *C43*, 581-628.
2. Taube, R.; Sylvester, G. Stereospecific Polymerization of Butadiene or Isoprene. In *Applied Homogeneous Catalysis with Organometallic Complexes*, Cornils, B., Herrmann, W. A. Eds.; VCH: Weinheim, Germany, **1996**; 280-318.
3. Kaminsky, W.; Hinrichs, B. Polymeric Dienes. In *Handbook of polymer synthesis*, 2 ed.; Kricheldorf, H. R., Nuyken, O., Swift, G. Eds.; Marcel Dekker: New York, **2005**; 333-380.
4. Industrial polymers, major. In *Encyclopædia Britannica*.
<http://www.britannica.com/eb/article-76457>.
5. Arlman, E. J. *J. Catal.* **1966**, *5*, 178-189.
6. Cossee, P., In *Stereochemistry of Macromolecules*. Ketley, A. D. Ed.; Marcel Dekker Inc.: New York, **1967**; Vol. 1, p 145.
7. Taube, R.; Gehrke, J. P. *J. Organomet. Chem.* **1985**, *291*, 101-115.
8. Taube, R.; Gehrke, J. P.; Böhme, P. *Wiss. Z. Tech. Leuna-Merseburg* **1987**, *29*, 310-325.
9. Wache, S.; Taube, R. *J. Organomet. Chem.* **1993**, *456*, 137-145.
10. Tobisch, S.; Bögel, H. *Organometallics* **1998**, *17*, 1177-1196.
11. Tobisch, S.; Bögel, H.; Taube, R. *Organometallics* **1996**, *15*, 3563-3571.
12. Tobisch, S.; Taube, R. *Organometallics* **1999**, *18*, 5204-5218.
13. Neoprene. (2008, April 9). In *Wikipedia, The Free Encyclopedia*. Retrieved 13:51, April 10, 2008, from <http://en.wikipedia.org/wiki/Neoprene#Applications>
14. Porri, L.; Natta, G.; Gallazzi, M. C. *J. Polym. Sci., Part C* **1967**, 2525-2537.

15. Babitskii, B. D.; Dolgoplosk, B. A.; Kormer, V. A.; Lobach, M. I.; Tinyakova, E. I.; Yakovlev, V. A. *Isv. Akad. Nauk SSSR Ser. Chem.* **1965**, 1507.
16. Klepikova, V. I.; Kondratenkov, G. P.; Kormer, V. A.; Lobach, M. I.; Churlyayeva, L. A. *J. Polym. Sci., Polym. Lett. Ed.* **1973**, *11*, 193-200.
17. Klepikova, V. I.; Lobach, M. I.; Kormer, V. A. *Dokl. Akad. Nauk SSSR* **1974**, *217*, 352-355.
18. Klepikova, V. I.; Vasil'ev, V. A.; Kondratenkov, G. P.; Lobach, M. I.; Kormer, V. A. *Dokl. Akad. Nauk SSSR* **1973**, *211*, 1111-1114.
19. Kormer, V. A.; Lobach, M. I. *Macromolecules* **1977**, *10*, 572-579.
20. Harrod, J. F.; Wallace, L. R. *Macromolecules* **1969**, *2*, 499-452.
21. Harrod, J. F.; Wallace, L. R. *Macromolecules* **1972**, *5*, 682-684.
22. Hadjiandreou, P.; Julémont, M.; Teyssié, P. H. *Macromolecules* **1984**, *17*, 2455-2456.
23. Coates, G. W.; Hustad, P. D.; Reinhartz, S. *Angew. Chem. Int. Ed.* **2002**, *41*, 2236-2257.
24. Durand, J. P.; Dawans, F.; Teyssié, P. *J. Polym. Sci. Part A* **1970**, *8*, 979-990.
25. Taube, R.; Gehrke, J. P.; Schmidt, U. *J. Organomet. Chem.* **1985**, *292*, 287-296.
26. Taube, R.; Schmidt, U.; Gehrke, J. P.; Anacker, U. *J. Prakt. Chem.* **1984**, *326*, 1-11.
27. Taube, R.; Gehrke, J. P.; Schmidt, U. *Makromol. Chem., Macromol. Symp.* **1986**, *3*, 389-404.
28. Taube, R.; Gehrke, J. P.; Böhme, P.; Scherzer, K. *J. Organomet. Chem.* **1991**, *410*, 403-416.

29. Taube, R.; Langlotz, J.; Sieler, J.; Gelbrich, T.; Tittes, K. *J. Organomet. Chem.* **2000**, *597*, 92-104.
30. Taube, R.; Wache, S. *J. Organomet. Chem.* **1992**, *428*, 431-442.
31. Tobisch, S. *Acc. Chem. Res.* **2002**, *35*, 96-104.
32. Taube, R.; Wache, S.; Langlotz, J. Mol mass regulation in the allyl nickel complex catalyzed 1,4-cis polymerization of butadiene. In *Catalyst design for tailor-made polyolefins. Studies in surface science and catalysis.*, Soga, K., Terano, M. Eds.; Elsevier: Tokyo, **1994**; 315-325.
33. Taube, R.; Wache, S.; Kehlen, H. *J. Mol. Cat. A* **1995**, *97*, 21-27.
34. Tobisch, S. *Macromolecules* **2003**, *36*, 6235-6244.
35. Johnson, L. K.; Killian, C. M.; Brookhart, M. *J. Am. Chem. Soc.* **1995**, *117*, 6414-6415.
36. Ittel, S. D.; Johnson, L. K.; Brookhart, M. *Chem. Rev.* **2000**, *100*, 1169-1203.
37. Leatherman, M. D.; Svejda, S. A.; Johnson, L. K.; Brookhart, M. *J. Am. Chem. Soc.* **2003**, *125*, 3068-3081.

CHAPTER TWO

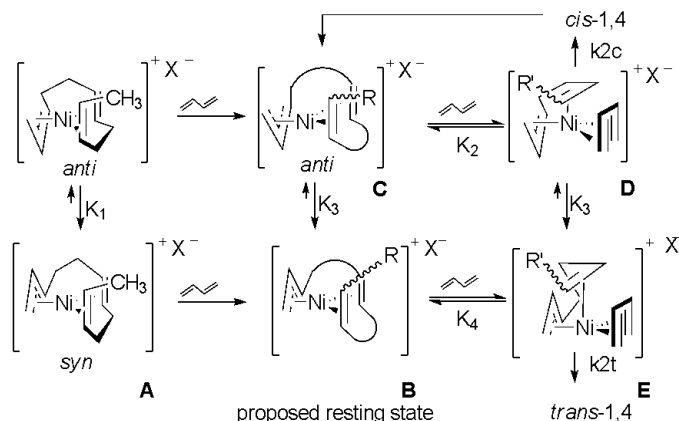
The Mechanism of Polymerization of Butadiene by “Ligand-Free” Nickel(II) Complexes

(Most of this chapter has been published as a *J. Am. Chem. Soc.* communication, with permission, from O'Connor, A. R.; White, P. S.; Brookhart, M. *J. Am. Chem. Soc.* **2007**, *129*, 4142-4243. Copyright 2007, American Chemical Society.)

Introduction

The stereoselective polymerization of butadiene (BD) has been investigated using a variety of transition metal¹⁻⁴ and lanthanide catalysts.⁵ Numerous Ni(II) π -allyl complexes have been used as initiators,⁶⁻⁹ but the most reactive identified to date is “ligand-free” Ni(II) wrap-around complex **A** (Scheme 2.1), which yields polybutadiene (PBD) exhibiting 93% *cis*-1,4 enchainment.^{10, 11}

Scheme 2.1. Taube and Tobisch's proposed mechanism for butadiene polymerization.



The chain growth mechanism proposed by Taube and Tobisch, based largely on DFT calculations,¹²⁻¹⁵ is shown in Scheme 2.1. The most stable form of the propagating species (the catalyst resting state) is assumed to be *syn* complex **B** analogous in structure to initiator **A**. To achieve a *cis*-1,4 enchainment, isomerization to the *anti*-allyl species **C** must occur; C-C coupling is proposed to proceed from η^4 -BD complex **D** formed from **C**. A key finding, based on DFT results, is that insertion is driven by a fifth ligand provided by a π -bond of the growing chain. Species **E** is proposed to account for *trans*-1,4 enchainment.

Results and Discussion

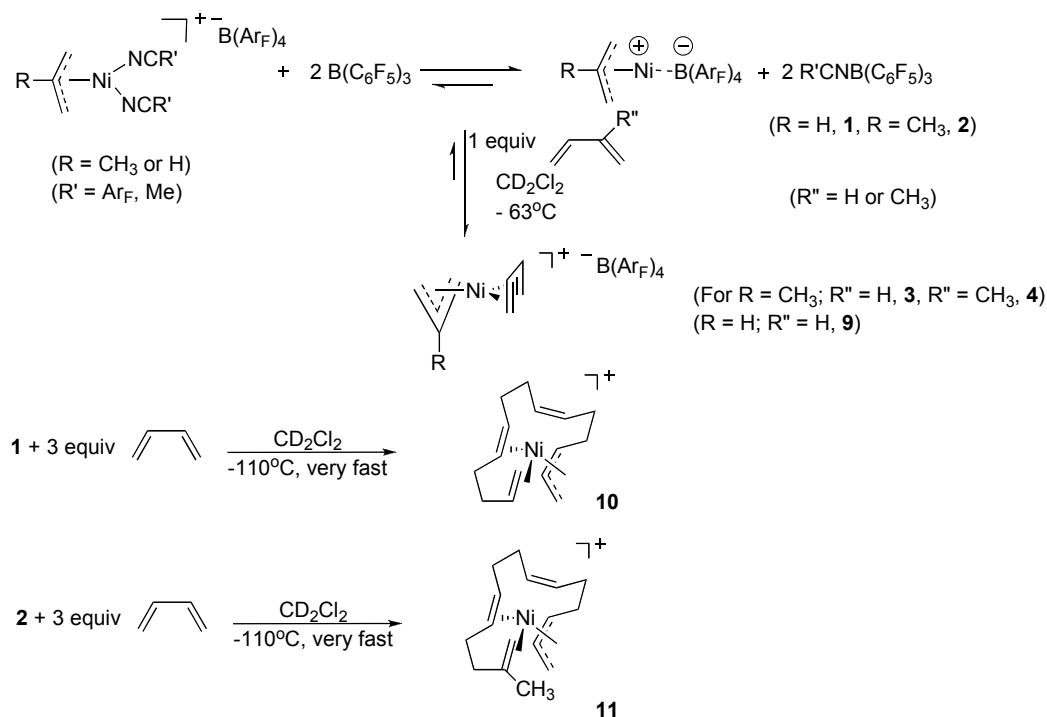
This chapter describes low-temperature observation of highly reactive ligand-free π -allyl complexes $[(\text{allyl})\text{Ni}][\text{B}(\text{Ar}_\text{F})_4]$ (**1**) and $[(2\text{-methallyl})\text{Ni}][\text{B}(\text{Ar}_\text{F})_4]$ (**2**),¹⁶ the first observation of η^4 -BD and η^4 -isoprene (IP) (allyl)Ni(II) complexes, $[(2\text{-methallyl})\text{Ni}(\eta^4\text{-BD})][\text{B}(\text{Ar}_\text{F})_4]$ (**3**) and $[(2\text{-methallyl})\text{Ni}(\eta^4\text{-IP})][\text{B}(\text{Ar}_\text{F})_4]$ (**4**), and their reactions with BD, which provide a modified, more complete mechanism of BD polymerization by ligand-free Ni(II) systems.

As shown in Scheme 2.2, reaction of $\text{B}(\text{C}_6\text{F}_5)_3$ with $[(\text{allyl})\text{Ni}(\text{NCR}')_2][\text{B}(\text{Ar}_\text{F})_4]$ ($\text{R}' = \text{Me}$, **5**, or $3,5\text{-(CF}_3)_2\text{C}_6\text{H}_3$, **6**) or the analogous 2-methallyl derivatives (**7**, **8**) at -60°C

generates the ligand-free complexes **1** or **2** (in equilibrium with the starting complex), which were characterized by ^1H , ^{13}C , and ^{19}F NMR spectroscopy.¹⁷ Ni is coordinated to a single aryl ring; separate ^1H and ^{19}F resonances are observed for the single coordinated and three noncoordinated rings. ^{19}F variable temperature NMR experiments at $-60\text{ }^\circ\text{C}$ to $-18\text{ }^\circ\text{C}$ showed the barrier to intramolecular Ni migration among the rings as $\Delta G^\ddagger = 11.4\text{ kcal/mol}$ for **1** and 11.8 kcal/mol for **2** (see Appendix Figure I.2). Exchange of coordinated $[\text{B}(\text{Ar}_\text{F})_4]^-$ with free $[\text{B}(\text{Ar}_\text{F})_4]^-$ occurs on the NMR timescale at temperatures above $0\text{ }^\circ\text{C}$. Details of the dynamic process are described in the Experimental Section.

Complexes **1** and **2** react at $-80\text{ }^\circ\text{C}$ with 1-2 equiv of BD or IP to yield equilibrium quantities of π -allyl η^4 -diene complexes $[(\text{allyl})\text{Ni}(\eta^4\text{-BD})]^+$ (**9**), $[(2\text{-methallyl})\text{Ni}(\eta^4\text{-BD})]^+$ (**3**), and $[(2\text{-methallyl})\text{Ni}(\eta^4\text{-IP})]^+$ (**4**).¹⁷ Formation of the π -allyl diene complexes is favored for 2-methallyl as the allyl partner and IP as the diene partner, thus **4** is formed nearly quantitatively from **2**.¹⁷ Warming **4** to $-30\text{ }^\circ\text{C}$ results in no observable insertion; however, treatment of **4** ($-50\text{ }^\circ\text{C}$) with BD results in rapid insertion and BD consumption supporting Taube and Tobisch's contention that a fifth ligand drives insertion. Treatment of either **1** or **2** with 3-4 equiv of BD results in rapid insertion of 3 equiv of diene at temperatures as low as $-110\text{ }^\circ\text{C}$ to yield a single species, $\text{Ni}(\text{C}_{15}\text{H}_{23})^+\text{B}(\text{Ar}_\text{F})_4^-$ (**10**) and $\text{Ni}(\text{C}_{16}\text{H}_{25})^+\text{B}(\text{Ar}_\text{F})_4^-$ (**11**),¹⁷ respectively. No intermediates were detected in these reactions.

Scheme 2.2. Reaction of (allyl)Ni(II) ligand-free species with butadiene.



Two-dimensional HMQC and ^1H - ^1H COSY NMR techniques established wrap-around structures as shown in Scheme 2.2 for complexes **10** and **11**.¹⁸ The ^1H NMR spectrum of **10** is shown in Figure 2.1, and the molecular structure was verified by X-ray crystallography (Figure 2.2).¹⁷ The π -allyl moiety is in an *anti* configuration, and all C-C double bonds are *cis* as expected from coupling of an *anti* π -allyl unit with BD. The coordinated π -bonds (C₁-C₂, C₅-C₆) exhibit C-Ni distances between 2.19 and 2.29 Å, while the noncoordinated π -bonds show C-Ni distances of 2.47 and 2.68 Å.

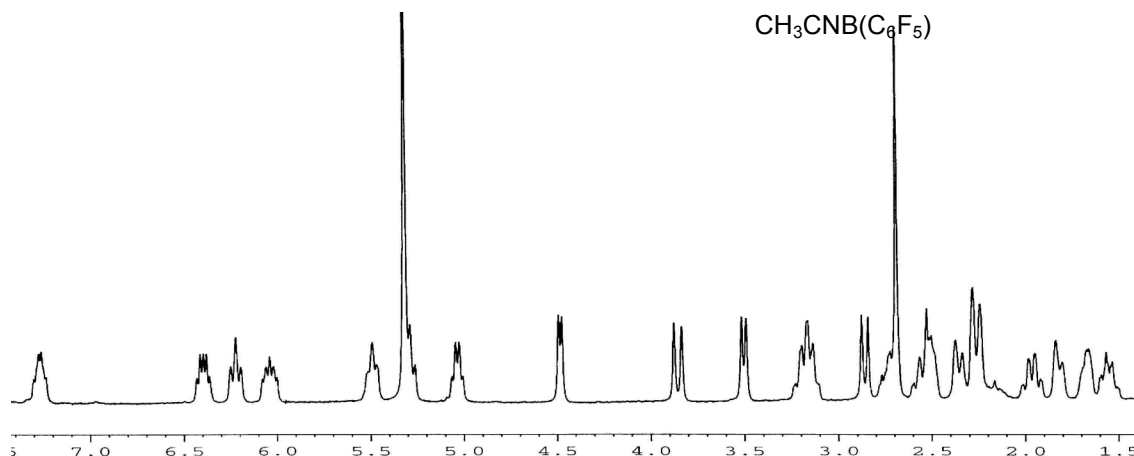


Figure 2.1. ^1H NMR spectrum of complex **10** (500 MHz) in CD_2Cl_2 at $-30\text{ }^\circ\text{C}$.¹⁷

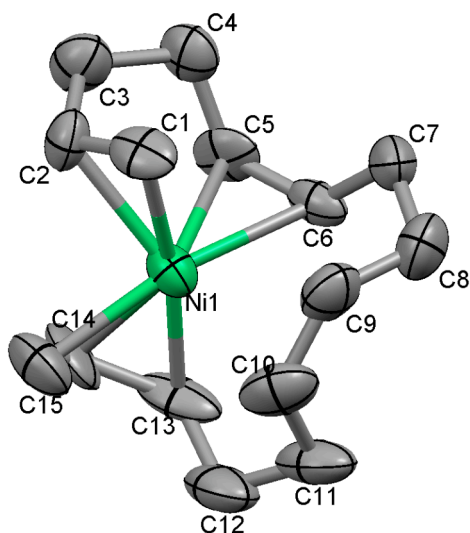


Figure 2.2. Molecular structure of complex **10**. Atomic displacement ellipsoids are drawn at 50% probability. Selected bond lengths (\AA): Ni(1)-C(1) 2.189(8), Ni(1)-C(2) 2.218(8), Ni(1)-C(5) 2.248(7), Ni(1)-C(6) 2.285(7), Ni(1)-C(9) 2.678, Ni(1)-C(10) 2.465(10), Ni(1)-C(13) 2.087(8), Ni(1)-C(14) 2.051(8), Ni(1)-C(15) 2.116(9). Hydrogen atoms and $[\text{B}(\text{Ar}_\text{F})_4]^-$ are omitted for clarity.

We expected that species analogous to **10** and **11** would be the catalyst resting states wherein the growing chain would be attached at C_{15} . This proved *not* to be the case. Exposure of **10** to 45 equiv of BD at $-30\text{ }^\circ\text{C}$ results in uptake of BD and formation of a new

complex, which contains an *anti*- π -allyl Ni unit and a coordinated vinyl group from 1,2 insertion (Figure 2.3).

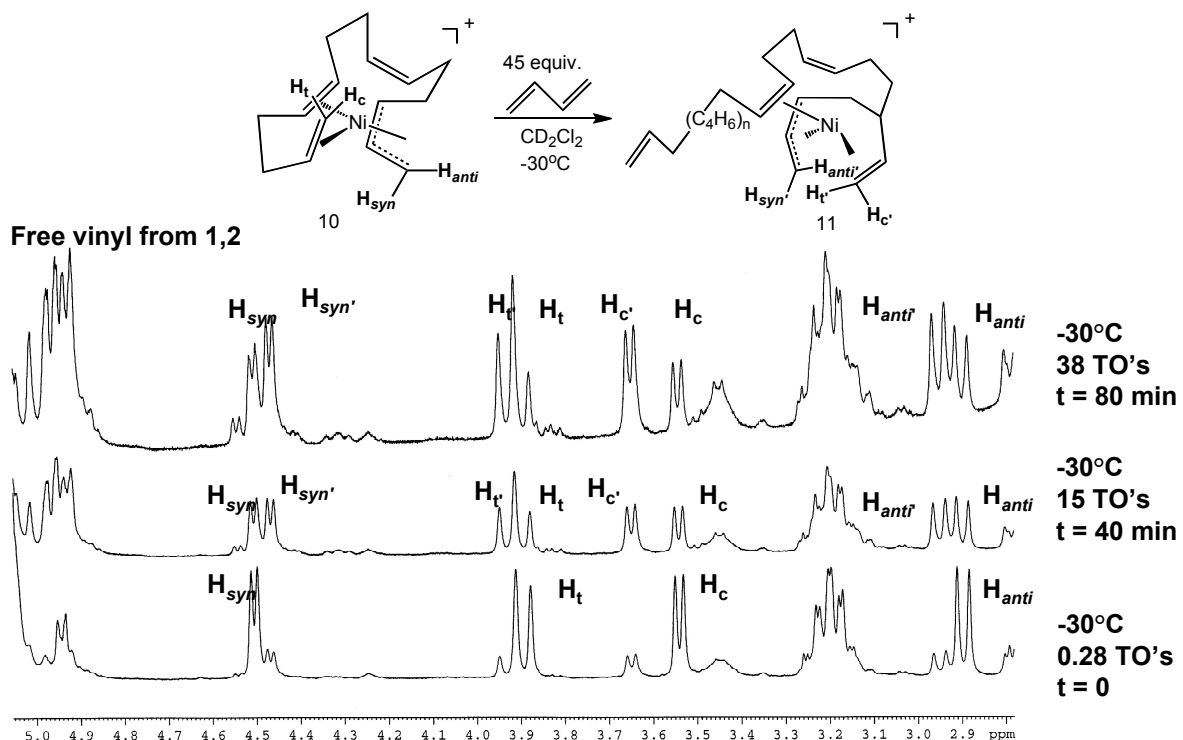


Figure 2.3. ^1H NMR overlay displaying insertion of butadiene into complex **10** at -30°C generating the catalyst resting state, **12**.

After ca. 15 turnovers, only 50% of **10** has been consumed (and after ca. 38 turnovers, 75% consumption), indicating the initial insertion of BD into **10** is slow relative to subsequent insertions. Reaction of **11** with BD is more straightforward and clarifies the situation (Figure 2.4). Treatment with BD (42 equiv) at -30°C results in rapid uptake of 15 equiv of BD and clean quantitative, formation of the vinyl coordinated species with proposed structure **12**. The hydrogens of the free vinylidene end group (δ 4.68 and 4.65) integrate for 1.0 H each relative to the coordinated vinyl end group protons (δ 3.95 (d, $J = 16.5 \text{ Hz}$), 3.65 (d, $J = 9.0 \text{ Hz}$) and the *syn* (δ 4.46 (d, $J = 7.5 \text{ Hz}$) and *anti* (δ 2.94 (d, $J = 13.5 \text{ Hz}$) π -allyl signals.

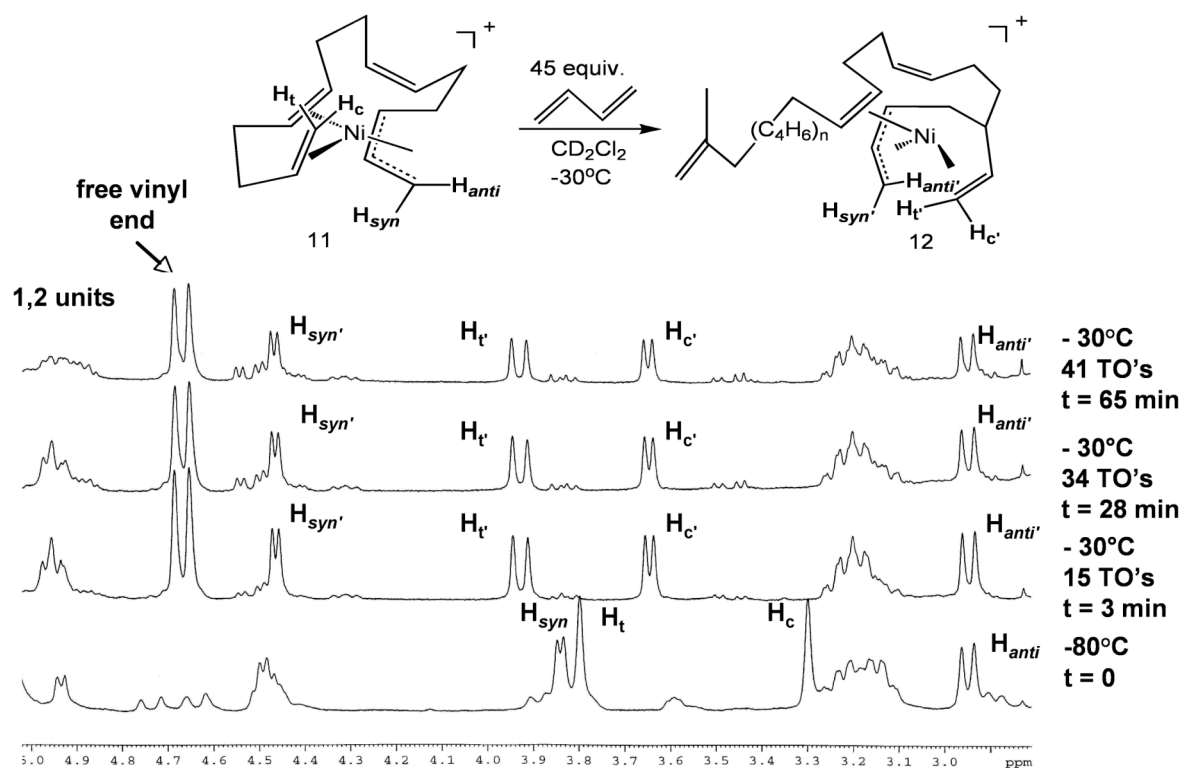


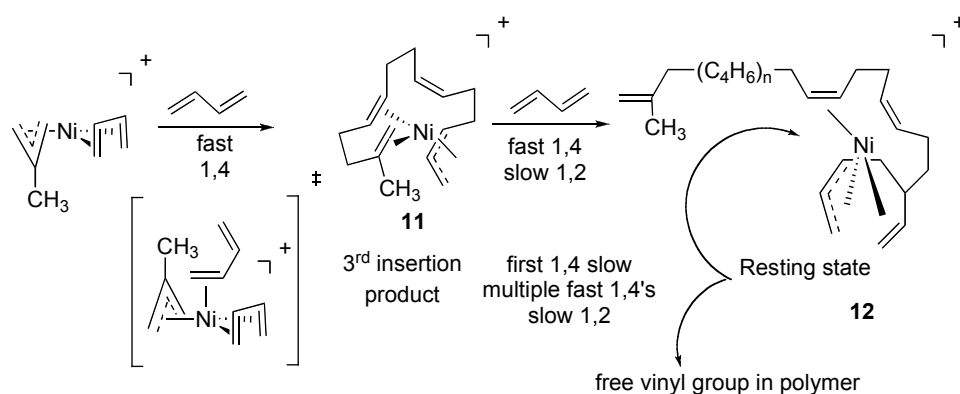
Figure 2.4. ^1H NMR overlay displaying insertion of butadiene into complex **11** at -30°C generating wrap-around complex **12**, the proposed resting state.

Scheme 2.3 summarizes a proposed mechanism for PBD chain growth using catalyst **11**. Complex **11** initiates rapidly, and multiple, fast 1,4 BD insertions occur until a 1,2 insertion takes place to form a stable vinyl-coordinated species, **12**. Subsequent insertions occur via a slow 1,4 insertion of BD into **12** followed by a sequence of rapid 1,4 insertions until another 1,2 insertion takes place and the stable vinyl-coordinated species **12** is regenerated. In the case of **10**, the terminal unsubstituted double bond ($\text{C}_1\text{-C}_2$) is more strongly coordinated than the 2-Me-substituted double bond in **11**; thus, the first 1,4 insertion of BD is slow relative to subsequent 1,4 insertions, and a considerable amount of **10** remains after multiple BD insertions along with formation of a vinyl-coordinated species analogous to **12**. NMR studies establish the vinyl-coordinated species to have the same structures with exception of the end group¹⁷ (Figures 2.3 and 2.4).

These experiments show that the true catalyst resting state is a stable vinyl-coordinated species, **12**, formed following a (rare) 1,2 insertion.¹⁹ The *cis*-1,4 insertions may well proceed through a Taube/Tobisch-type precursor **D** (Scheme 2.1), but if so, it seems likely that a species analogous to complexes **10** or **11**, rather than **C**, would result.

Polymerization of BD, catalyzed by in situ generated complex **2**, was carried out in CH₂Cl₂ at -30 °C under argon yielding PBD, which has the following microstructure: 94% *cis*-1,4, 5% *trans*-1,4 and 1% 1,2 enchainment. The *M_n* values are approximately 8000 with a PDI of 1.5.¹⁷ A more thorough study of the polymerization of **2** with dienes is presented in Chapter 4.

Scheme 2.3. Proposed mechanism for PBD chain growth.



Summary

The identities of key intermediates and catalyst resting states in the polymerization of BD by ligand-free (allyl)Ni(II) species have been observed for the first time. Cationic (2-methallyl)Ni(II) complexes of η^4 -BD and η^4 -IP were prepared and characterized by low-temperature NMR spectroscopy. These highly reactive species insert 3 equiv of BD or IP at very low temperatures to yield stable wrap-around complexes of types **10** and **11**. Although these species insert BD, they do not represent the catalyst resting state(s). The resting states

are formed following a 1,2 BD insertion and exhibit coordination of the resulting vinyl group as shown in structure **12**.

Experimental Section

General Considerations.

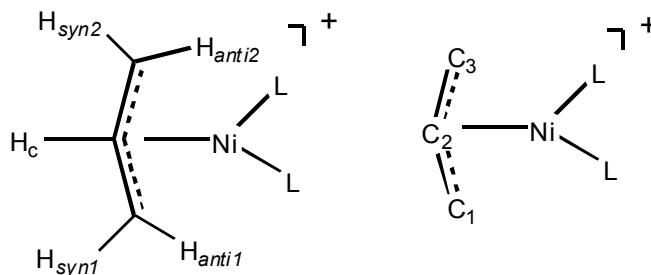
All reactions, unless otherwise stated, were conducted under an atmosphere of dry, oxygen free argon using standard high-vacuum, Schlenk, or drybox techniques. Argon was purified by passage through BASF R3-11 catalyst (Chemalog) and 4Å molecular sieves. All nickel catalysts were stored under argon in an M.Braun glovebox at -35°C. ^1H , ^{13}C , and ^{19}F NMR spectra were recorded on a Bruker DRX 500 MHz, a Bruker DRX 400 MHz, or a Bruker 300 MHz spectrometer. Chemical shifts are referenced relative to residual CHCl_3 (δ 7.24 for ^1H), CH(D)Cl_2 (δ 5.32 for ^1H), CD_2Cl_2 (δ 53.8 for ^{13}C), CDCl_3 (δ 77.0 for ^{13}C). ^{19}F NMR shifts are referenced to external CFCl_3 . Assignments were supported by H-C HMQC, ^1H - ^1H and long range COSY experiments, and through simulation using the Spin Works NMR program. GPC analyses were performed in HPLC grade tetrahydrofuran at 25°C using a Waters Alliance HPLC equipped with Waters Styragel HR2, HR4, and HR5 columns and a Waters 410 refractive index detector. Molecular weights are reported relative to polystyrene standards. Elemental analyses were performed by Atlantic Microlab Inc. of Norcross, GA and Robertson Microlit Laboratories of Madison, NJ.

Materials.

All solvents were deoxygenated and dried by passage over columns of activated alumina.^{20, 21} CD_2Cl_2 , purchased from Cambridge Laboratories, Inc., was dried over CaH_2 , vacuumed transferred to a Teflon sealable Schlenk flask containing 4Å molecular sieves, and degassed via three freeze-pump-thaw cycles. Butadiene and isoprene were purchased from

Aldrich and purified by vacuum transfer through a column of 4Å molecular sieves and stored under argon at -35°C. Ni[COD]₂ and B(C₆F₅)₃ were purchased from Strem and used as received. NaB(Ar_F)₄ (Ar_F = 3,5-(CF₃)₂C₆H₃) was purchased from Boulder Scientific. 3,5-bis(trifluoromethyl)benzonitrile (NCAr_F), acetonitrile, mesitylene (mes), and allyl bromide were purchased from Aldrich and used without further purification. [(Allyl)NiBr]₂ and [(2-methallyl)NiBr]₂ were synthesized according to literature methods.²²

In reporting the chemical shifts, the allyl carbons and protons are labeled as follows:



Spectral Data for [B(Ar_F)₄]⁻. The ¹H and ¹³C spectral data for the B(Ar_F)₄⁻ counteranion were unchanged for all Ni(II) cationic complexes and are not included in the characterization unless otherwise stated. ¹H NMR (400 MHz, CD₂Cl₂, 20 °C): δ 7.72 (s, 8H, Ar_F H_p), 7.57 (s, 4H, Ar_F H_o). ¹³C{¹H} NMR (101 MHz, CD₂Cl₂, 20 °C): δ 162.1 (q, ¹J_{C-B} = 49.8 Hz Ar_F C_{ipso}), 135.2 (s, Ar_F C_o), 129.2 (qq, ³J_{C-B} = 3.0 Hz, ¹J_{C-F} = 34.4 Hz, Ar_F C_m), 122.3 (q, ¹J_{C-F} = 273.2 Hz, Ar_F CF₃), 117.8 (bt, Ar_F C_p).

(Allyl)Ni(II) Complex Synthesis.

[(Allyl)Ni(NCMe)₂][B(Ar_F)₄] (5). A flame-dried Schlenk tube was charged with [(allyl)NiBr]₂ dimer (0.103 g, 0.287 mmol) and NaB(Ar_F)₄ (0.498 g, 0.562 mmol) in the drybox. The reaction flask was cooled to -78 °C and Et₂O (8.0 mL) was added, yielding a red solution. Acetonitrile (50 µL, 0.957 mmol) was added dropwise and the solution became yellow with a grey precipitate. The resulting suspension was allowed to warm to room

temperature and stirred for 2 hours. The yellow solution was collected via cannula transfer and all volatiles were removed in vacuo to yield an orange-yellow oil. Pentane (10.0 mL) was added and the product was vigorously stirred until a yellow powder formed (~1 h). The pentane layer was decanted and the yellow powder was dried in vacuo. Excess $\text{NaB}(\text{Ar}_\text{F})_4$ was removed through an additional filtration step in which the yellow powder was dissolved in CH_2Cl_2 (7.0 mL) and filtered through a Celite pad. The volatiles were removed in vacuo to yield an orange oil. Pentane (5.0 mL) was added and the product was stirred until a yellow powder formed. The pentane layer was decanted and the powder was dried in vacuo overnight to yield 50% of **5** (0.298 g, 0.285 mmol). ^1H NMR (500 MHz, CD_2Cl_2 , 25 °C): δ 5.70 (m, 1H, H_c), 3.66 (d, 2H, $^3J_{\text{H-H}} = 7.2$ Hz, $\text{H}_{\text{syn1\&2}}$), 2.64 (d, 2H, $^3J_{\text{H-H}} = 14$ Hz, $\text{H}_{\text{anti1\&2}}$), 2.21 (bs, 6H, CNCH_3). $^{13}\text{C}\{^1\text{H}\}$ NMR (126 MHz, CD_2Cl_2 , 0 °C): δ 125.3 (bs, CNCH_3), 116.4 (s, C_2), 62.3 (s, $\text{C}_{1\&3}$), 3.70 (bs, CNCH_3). ^{19}F NMR (376 MHz, CD_2Cl_2 , 25 °C): δ -63.4 (s, 24F). Anal. Calcd for $\text{C}_{39}\text{H}_{23}\text{F}_{24}\text{N}_2\text{BNi}$: C, 44.82; N, 2.68; H, 2.21. Found: C, 44.81; N, 2.51; H, 2.28.

[(2-Methallyl)Ni(NCMe)₂][B(Ar_F)₄] (7). This complex was synthesized in an analogous fashion to [(allyl)Ni(NCMe)₂][B(Ar_F)₄], **5**, starting from the [(2-methallyl)NiBr]₂ dimer (0.201g, 0.518 mmol), $\text{NaB}(\text{Ar}_\text{F})_4$ (0.940g, 1.06 mmol), and acetonitrile (300 μL , 5.74 mmol). Yield (1.10 g, 1.04 mmol, 81%). ^1H NMR (400 MHz, CD_2Cl_2 , 25 °C): δ 3.37 (s, 2H, $\text{H}_{\text{syn1\&2}}$), 2.47 (s, 2H, $\text{H}_{\text{anti1\&2}}$), 2.43 (s, 3H, CH_3), 2.20 (bs, 6H, CNCH_3). $^{13}\text{C}\{^1\text{H}\}$ NMR (126 MHz, CD_2Cl_2 , 25 °C): δ 125.0 (bs, CNCH_3), 117.9 (C_2 overlapping Ar_F C_p), 61.7 (s, $\text{C}_{1\&3}$), 22.7 (s, C_2 CH_3), 3.52 (bs, CNCH_3). ^{19}F NMR (376 MHz, CD_2Cl_2 , 25 °C): δ -63.5 (s, 24F). Anal. Calcd for $\text{C}_{40}\text{H}_{25}\text{F}_{24}\text{N}_2\text{BNi}$: C, 45.36; N, 2.64; H, 2.38. Found: C, 45.10; N, 2.47; H, 2.22.

[(Allyl)Ni(NCAr_F)][B(Ar_F)₄] (6).** [(Allyl)NiBr]₂ (0.053 g, 0.148 mmol) and NaB(Ar_F)₄ (0.266 g, 0.300 mmol) were combined in a flame-dried Schlenk flask and cooled to -78 °C under argon. The solids were dissolved in diethyl ether (10.0 mL) to yield a red solution. To this solution 3,5-(bistrifluoromethyl)benzonitrile (100 μL, 0.594 mmol) was added dropwise, producing an orange solution together with a fine light brown precipitate. The suspension was warmed to room temperature and stirred for 1.5 h. The precipitate was filtered off via cannula filtration and the solution was removed in vacuo to yield a thick orange-brown oil. The oil was vigorously stirred overnight in pentane (10.0 mL). The pentane was decanted and the oil was washed with pentane (4 x 10 mL). The oily product was then dried in vacuo and placed in a dry box. Within 7 days in the glovebox, the oily product turned to an orange solid to give **6** (0.336 g, 0.233 mmol) in 79% yield. X-ray quality yellow crystals of the **6** were obtained by dissolving the complex in CH₂Cl₂ (2.0 mL), layering with pentane (6.0 mL) and cooling to -30 °C for 2 days. (X-ray data appears in the Appendix, Figure I.1, and Tables I.1, I.2, and I.3) ¹H NMR (400 MHz, CD₂Cl₂, 25 °C): δ 8.30 (s, 2H, CNAr_F H_p), 8.24 (s, 4H, CNAr_F H_o), 5.93 (m, 1H, H_c), 4.02 (d, ³J_{H-H} = 8.4 Hz, 2H, H_{syn1&2}), 3.00 (d, ³J_{H-H} = 15.6 Hz, 2H, H_{anti1&2}). ¹³C{¹H} NMR (101 MHz, CD₂Cl₂, 25 °C): δ 134.1 (q, ²J_{C-F} = 35.3 Hz, CNAr_F C_m), 133.4 (bs, CNAr_F C_o), 129.2 (bt, CNAr_F C_p), 125.0 (q, ¹J_{C-F} = 272.4 Hz, CNAr_F CF₃), 121.8 (bs, CNAr_F) 118.6 (s, C₂), 112.3 (bs, CNAr_F C_{ipso}), 65.6 (s, C_{1&3}). ¹⁹F (471 MHz, CD₂Cl₂, -80 °C): δ -62.9 (s, 24F, CNAr_F), -63.9 (s, 12F, CNAr_F). Anal. Calcd for C₅₃H₂₃F₃₆N₂BNi: C, 44.17; N, 1.94; H, 1.61. Found: C, 43.66; N, 1.98; H, 1.65.**

[(2-Methallyl)Ni(NCAr_F)₂][B(Ar_F)₄] (8). This complex was synthesized following the previously described procedure for the analogous [(allyl)Ni(NCAr_F)₂][B(Ar_F)₄] complex, **6**,

starting from [(2-methallyl)NiBr]₂ (0.101 g, 0.259 mmol), NaB(Ar_F)₄ (0.460 g, 0.519 mmol), and 3,5-bis(trifluoromethyl)benzonitrile (175 μ L, 1.04 mmol). Yield: 0.650 g, 0.447 mmol (87%). ¹H NMR (400 MHz, CD₂Cl₂, 25 °C): δ 8.30 (s, 2H, CNAr_F H_p), 8.24 (s, 4H, CNAr_F H_o), 3.75 (s, 2H, H_{syn1&2}), 2.85 (s, 2H, H_{anti1&2}), 2.36 (s, 3H, CH₃). ¹³C{¹H} NMR (101 MHz, CD₂Cl₂, 25 °C): δ 134.2 (q, ²J_{C-F} = 35.3 Hz, CNAr_F C_m), 133.6 (s, CNAr_F C_o), 129.5 (bs, CNAr_F C_p), 125.0 (q, ¹J_{C-F} = 272.4 Hz, CNAr_F CF₃), 122.5 (bs, CNAr_F), 117.8 (s, C₂ under CNAr_F C_p), 65.0 (s, C_{1&3}), 22.8 (s, C₂ CH₃). ¹⁹F NMR (376 MHz, CD₂Cl₂, 25 °C): δ -63.4 (s, 24F, CNAr_F), -64.4 (s, 12F, CNAr_F). Anal. Calcd for C₅₄H₂₅F₃₆N₂BNi: C, 44.57; N, 1.93; H, 1.73. Found: C, 44.43; N, 1.97; H, 1.62.

In Situ Generation of Cationic Ni(II) Intermediates.

Note: All complexes described below can be generated starting from either nitrile complex of (2-methallyl)Ni(NCR)₂][B(Ar_F)₄] (R = CH₃ (7) or Ar_F (8)) or (allyl)Ni(NCR)₂][B(Ar_F)₄] (R = CH₃ (5) or Ar_F (6)).

[(Allyl)Ni][B(Ar_F)₄] (**1**). A screw cap NMR tube was charged with **6** (0.015 g, 0.010 mmol) and B(C₆F₅)₃ (0.061 g, 0.120 mmol). The tube was then placed in a -80 °C bath and CD₂Cl₂ (650 μ L) was added via syringe. The tube was inverted quickly to allow mixing and the solution turned yellow-brown. An equilibrium between the starting material **6** and complex **1** exists in solution; the concentration of **1** in solution is dependent upon the temperature. ¹H NMR (500 MHz, CD₂Cl₂, -60 °C): δ 7.89 (s, 1H, coordinated Ar_F H_p), 7.81 (s, 6H, non-coordinated Ar_F H_o), 7.65 (s, 3H, non-coordinated Ar_F H_p), 7.41 (s, 2H, coordinated Ar_F H_o), 5.09 (m, 1H, H_c), 3.56 (d, ³J_{H-H} = 6.5 Hz, 2H, H_{syn1&2}), 1.74 (d, ³J_{H-H} = 12.8 Hz, 2H, H_{anti1&2}). Characteristic peaks: ¹³C{¹H} NMR (126 MHz, CD₂Cl₂, -50 °C): δ 111.2 (s, C₂), 64.0 (s, C_{1&3}). ¹⁹F NMR (471 MHz, CD₂Cl₂, -80 °C): -63.3 (s, 24F, coordinated Ar_F).

Formation of an adduct between the nitrile and B(C₆F₅)₃ was identified by ¹⁹F and ¹H NMR spectroscopy:

(CH₃CN)B(C₆F₅)₃. ¹H NMR (500 MHz, CD₂Cl₂, -80 °C): δ 2.70 (2, 3H). ¹⁹F NMR (471 MHz, CD₂Cl₂, -80 °C): δ -143.5 (s, 6F, F_o), -157.0 (s, 3F, F_p), -164.3 (s, 6F, F_m).

(Ar_FCN)B(C₆F₅)₃. ¹H NMR (500 MHz, CD₂Cl₂, -40 °C): δ 8.42 (bs, 3H, CNAr_F H_{o,m,p}). ¹⁹F NMR (471 MHz, CD₂Cl₂, -40 °C): δ -63.8 (CNAr_F CF₃), -135.0 (dd, ³J_{F-F} = 15.1 Hz, ⁴J_{F-F} = 8.0 Hz, 6F, F_o), -156.5 (t, ³J_{F-F} = 20.7 Hz, 3F, F_p), -163.9 (td, ³J_{F-F} = 23.1 Hz, ⁴J_{F-F} = 8.5 Hz, 6F, F_m).

[(2-Methallyl)Ni][B(Ar_F)₄] (2). This complex was generated following the procedure outlined for complex **1** starting from **8** (0.010 g, 0.007 mmol) and excess B(C₆F₅)₃ (0.033 g, 0.065 mmol). ¹H NMR (500 MHz, CD₂Cl₂, -80 °C): δ 7.83 (s, 6H, non-coordinated Ar_F H_o), 7.62 (s, 4H, 1H coordinated Ar_F H_p, 3H non-coordinated Ar_F H_p), 7.50 (s, 2H, coordinated Ar_F H_o) 3.50 (s, 2H, H_{syn1&2}), 2.22 (s, 3H, CH₃), 1.06 (s, 2H, H_{anti1&2}). Characteristic peaks: ¹³C{¹H} NMR (126 MHz, CD₂Cl₂, -60 °C): δ 111.3 (s, C₂), 64.1 (s, C_{1&3}), 22.0 (s, C₂ CH₃). ¹⁹F NMR (476 MHz, CD₂Cl₂, -50 °C): -63.1 (s, 24 F, coordinated Ar_F).

¹⁹F Line Broadening Experiments to Determine Barriers to Ni Migration Among the B(Ar_F)₄ Rings of **1 and **2**.** A solution of **1** or **2** was prepared in CD₂Cl₂ as described above. Broadening of the ¹⁹F resonance (δ -63.3 ppm) for the three uncoordinated Ar_F rings (which are part of the coordinated [B(Ar_F)₄]⁻ moiety), for complex **1** was monitored between -36 °C and -18 °C. The initial half-height line width at -36 °C was 14 Hz and 59 Hz at -18 °C. The rate constant for **1** was calculated using the slow exchange approximation to yield k_{ex} = 390 s⁻¹: k_{ex} = 3*[π(Δω)] where Δω = 41 Hz (ΔG[‡] = 11.4 kcal/mol). Broadening of the ¹⁹F resonance for the coordinated Ar_F of **2** was examined between -60 °C and -42 °C (See Figure

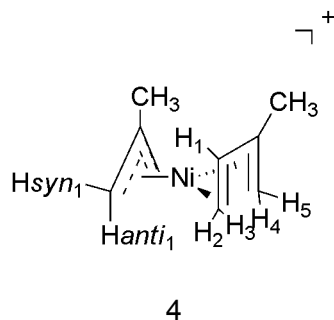
I.2 in the Appendix). The initial half-height line width at -60 °C was 6.2 Hz and 10.0 Hz at -51 °C. The rate constant for complex **2** was calculated from the slow exchange approximation to be $k_{\text{ex}} = 11.9 \text{ s}^{-1}$ ($k_{\text{ex}} = \pi(\Delta\omega)$) where $\Delta\omega = 3.8 \text{ Hz}$ ($\Delta G^\ddagger = 11.8 \text{ kcal/mol}$).

[(2-Methallyl)Ni(η^4 -butadiene)][B(Ar_F)₄] (3**).** To a screw top NMR tube was added complex **8** (0.015 g, 0.010 mmol) and B(C₆F₅)₃ (0.012 g, 0.024 mmol). The tube was cooled in -80 °C and CD₂Cl₂ (700 μ L) was introduced via syringe. The solution was quickly mixed by inversion to allow for generation of the ligand-free complex **2**. Upon formation of **2** the solution turns from yellow-brown to yellow. A solution of butadiene (12.8 μ L, 0.010 mmol) in CD₂Cl₂ (0.781 M) containing exactly one equivalent of butadiene was added to the tube, which was quickly inverted to minimize warming. The solution turned bright yellow, indicative of η^4 -coordination of the diene. The sample was put into a pre-cooled NMR probe at -80 °C without significant warming. ¹H NMR (500 MHz, CD₂Cl₂, -63 °C): δ 6.45 (m, 2H, H_{methineBD}), 5.45 (s, 2H, H_{syn1&2}), 5.43 (d, 2H, H_{cisBD}), 3.20 (d, ³J_{H-H} = 14.0 Hz, 2H_{transBD}), 2.81 (s, 2H, H_{anti1&2}), 2.06 (s, 3H, CH₃). Complexes **8** and **2** were also present in solution.

[(Allyl)Ni(η^4 -butadiene)][B(Ar_F)₄] (9**).** A minor amount of complex **9** can be observed in situ through the reaction of **6** (0.015 g, 0.011 mmol) and B(C₆F₅)₃ (0.014 g, 0.027 mmol) at -60 °C followed by the addition of approximately 1 equiv of butadiene (12.0 μ L, 0.010 mmol). A mixture of starting material **6**, ligand-free **1**, and complex **9** are always observed in solution. ¹H NMR (500 MHz, CD₂Cl₂, -63 °C) of **9**: δ 6.53 (m, 2H, H_{methine BD}), 6.05 (m, 1H, overlapping, H_c) 5.70 (d, ³J_{H-H} = 7.0 Hz, 2H, H_{syn1&2}), 5.53 (d, ³J_{H-H} = 7.5 Hz, 2H, H_{cisBD}), 3.26 (d, ³J_{H-H} = 16.0 Hz, 2H, H_{transBD}), 2.98 (d, ³J_{H-H} = 15.0 Hz, 2H, H_{anti1&2}),

[(2-Methallyl)Ni(η^4 -isoprene)][B(Ar_F)₄] (4**).** A screw top NMR tube was charged with **7** (0.0101 g, 0.010 mmol) and B(C₆F₅)₃ (0.010 g, 0.019 mmol) and cooled to -80 °C. CD₂Cl₂

(600 μL) was added and the solution was mixed to ensure formation of complex **2**. Isoprene (2.0 μL , 0.020 mmol) was then introduced to the tube via syringe and the solution was mixed yielding a bright yellow solution indicative of η^4 -diene coordination. Quantitative conversion to complex **4** is observed at low temperature together with free isoprene. Warming to $-30\text{ }^\circ\text{C}$ consumes the small amount of isoprene, producing a small amount of wrap-around complex. At this point the major species in solution is **4**.

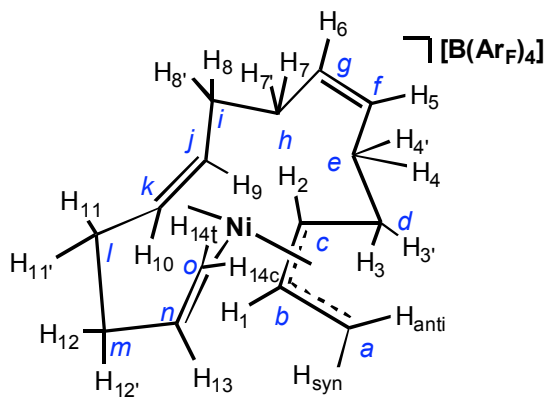


^1H NMR (500 MHz, CD_2Cl_2 , $-60\text{ }^\circ\text{C}$): δ 6.24 (dd, $^3J_{\text{H-H}_{cis}} = 9.5\text{ Hz}$, $^3J_{\text{H-H}_{trans}} = 16.0\text{ Hz}$, 1H, H_1), 5.36 (dd, $^3J_{\text{H-H}} = 9.5\text{ Hz}$, $^2J_{\text{H-H}} = 2.0\text{ Hz}$, 1H, H_2), 5.35 (s, 1H, H_{syn2}), 5.28 (s, 1H, H_{syn1}), 5.16 (s, 1H, H_5), 3.18 (dd, $^3J_{\text{H-H}} = 16.5\text{ Hz}$, $^2J_{\text{H-H}} = 2.5\text{ Hz}$, 1H, H_3), 2.92 (d, $^2J_{\text{H-H}} = 2.0\text{ Hz}$, 1H, H_4), 2.76 (s, 1H, H_{anti1}), 2.73 (s, 1H, H_{anti2}), 2.33 (s, 3H, CH_{3IP}), 2.05 (s, 3H, CH_3).

The analogous $[(\text{allyl})\text{Ni}(\eta^4\text{-isoprene})][\text{B}(\text{Ar}_F)_4]$ complex could not be observed at low temperatures. Only species with wrap-around structures were observed in the ^1H NMR spectrum.

$[\text{C}_{15}\text{H}_{23}\text{Ni}][\text{B}(\text{Ar}_F)_4]$ (10). Complex **6** (0.021 g, 0.015 mmol) and $\text{B}(\text{C}_6\text{F}_5)_3$ (0.020 g, 0.039 mmol) were added to a dry screw-cap NMR tube and cooled to $-80\text{ }^\circ\text{C}$. CD_2Cl_2 (600 μL) was added via syringe and the tube was inverted to allow for formation of compound **5**. At this point, butadiene (100 μL , 0.054 mmol), a 0.54 M solution in CD_2Cl_2 , was added to the yellow-brown solution. Upon mixing, the solution color turned bright orange-red, signifying

formation of the Ni(II) wrap-around complex **10**. Quantitative conversion to **10** is observed at low temperature. Extra care was taken to ensure that the tube was kept cold. The sample was placed into a pre-cooled NMR probe set at -80 °C.



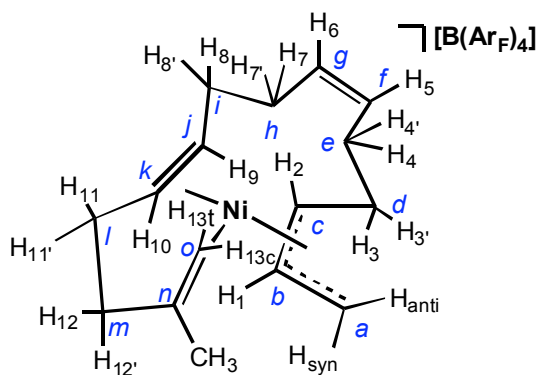
10

^1H NMR (500 MHz, CD_2Cl_2 , -40 °C): δ 7.28 (dt, $^3J_{\text{H-H}_{\text{cis}}} = 5.8$ Hz, $^3J_{\text{H-H}} = 10.7$ Hz, 1H, H_5), 6.41 (dt, $^3J_{\text{H-H}_{\text{anti}}} = 13.7$ Hz, $^3J_{\text{H-H}_{\text{syn}}} = 7.3$ Hz, 1H, H_1), 6.26 (ddd, $^3J_{\text{H-H}} = 12.3$ Hz, $^3J_{\text{H-H}} = 9.5$ Hz, $^3J_{\text{H-H}} = 5.0$ Hz, 1H, H_6), 6.06 (ddt, $^3J_{\text{H-H}_{\text{trans}}} = 16.5$ Hz, $^3J_{\text{HH}_{\text{cis}}} = 7.8$ Hz, $^3J_{\text{H-H}} = 7.6$ Hz, 1H, H_{13}), 5.52 (ddd, $^3J_{\text{H-H}} = 12.3$ Hz, $^3J_{\text{H-H}} = 8.7$ Hz, $^3J_{\text{H-H}} = 1$ Hz, H_{10}), 5.31 (overlapping CD_2Cl_2 , 1H, H_9), 5.06 (dt, $^3J_{\text{H-H}} = 8.4$ Hz, $^3J_{\text{H-H}_{\text{syn}}} = 8.0$ Hz, 1H, H_2), 4.50 (d, $^3J_{\text{H}_{\text{syn}}-\text{H}} = 7.2$ Hz, 1H, H_{syn}), 3.88 (d, $^3J_{\text{H}_{\text{trans}}-\text{H}} = 16.5$ Hz, 1H, $\text{H}_{14\text{t}}$), 3.53 (d, $^3J_{\text{H-H}} = 9.3$ Hz, 1H, $\text{H}_{14\text{c}}$), 3.22 (two overlapping dt, 2H, $\text{H}_{7,4'}$), 2.88 (d, $^3J_{\text{H}_{\text{anti}}-\text{H}} = 13.6$ Hz, 1H, H_{anti}), 2.74 (m, 1H, H_{12}), 2.55 (m, 2H, $\text{H}_{7,8'}$), 2.37 (m, 1H, H_8), 2.28 (m, 2H, $\text{H}_{4,12'}$), 1.99 (m, 1H, H_{11}), 1.82 (m, 1H, $\text{H}_{11'}$), 1.68 (m, 1H, H_3), 1.57 (m, 1H, $\text{H}_{3'}$). $^{13}\text{C}\{^1\text{H}\}$ NMR (126 MHz, CD_2Cl_2 , -20 °C): δ 137.5 (s, C_g), 130.8 (s, C_f), 121.8 (s, C_k), 120.6 (s, C_n), 112.1 (s, C_b), 111.2 (s, C_j), 95.9 (s, C_c), 78.5 (s, C_o), 62.9 (s, C_a), 34.9 (s, C_d), 34.0 (s, C_m), 31.3 (s, C_i), 27.1 (s, C_h), 26.4 (s, C_e), 22.6 (s, C_l).

Isolation of $[\text{C}_{15}\text{H}_{23}\text{Ni}][\text{B}(\text{ArF})_4]$ (10**).** A flame-dried Schlenk flask was charged with compound **5** (0.101 g, 0.097 mmol) and $\text{B}(\text{C}_6\text{F}_5)_3$ (0.098 g, 0.192 mmol) and cooled to -80

°C. CH₂Cl₂ (5.0 mL) was added via syringe and the solution was warmed slightly to allow for formation of “ligand-free” complex **1**. At this point a 0.41 M solution of butadiene in CD₂Cl₂ (700 µL, 0.287 mmol) was added. Immediate color change to deep orange-red was observed and the solution was allowed to stir at -80 °C for 10 min. The solvent was removed in vacuo at -80 °C to yield a red oily product. The product was washed with pentane (3 x 5.0 mL) and dried in vacuo. X-ray suitable crystals were obtained by dissolving complex **10** in CH₂Cl₂ (2.0 mL), layering with pentane (6.0 mL) and storing at -30 °C for 3 days. Two distinct sets of crystals were obtained. One fraction was orange ((CH₃CNB(C₆F₅)₃ adduct) and the other was deep red complex **10** (See Figure 2.2 and Appendix Tables I.1, II.4, and II.5 for X-ray structural details).

[C₁₆H₂₅Ni][B(Ar_F)₄] (11). This species was generated in situ following the procedure described previously for **10** starting from **7** (0.015 g, 0.011 mmol) and B(C₆F₅)₃ (0.013 g, 0.026 mmol) and 0.781 M butadiene solution (40.0 µl, 0.031 mmol) (see Appendix Figure I.3 for ¹H NMR spectrum).



11

¹H NMR (500 MHz, CD₂Cl₂, -40 °C): δ 7.15 (dt, ³J_{H-H_{cis}} = 6.1 Hz, ³J_{H-H} = 10.7 Hz, 1H, H₆), 6.40 (ddd, ³J_{H-H} = 12.8 Hz, ³J_{H-H} = 9.8 Hz, ³J_{H-H_{cis}} = 6.1 Hz, 1H, H₅), 6.26 (dt, ³J_{H-H_{anti}} = 13.7, ³J_{H-H_{syn}} = 7.3 Hz, 1H, H₁), 5.50 (ddd, ³J_{H-H} = 12.4 Hz, ³J_{H-H} = 8.4 Hz, ³J_{H-H} = 7.0 Hz, 1H,

H₁₀), 5.25 (ddd, $^3J_{\text{H-H}} = 11.7$ Hz, $^3J_{\text{H-H}} = 9.5$ Hz, $^3J_{\text{H-H}} = 7$ Hz, 1H, H₉), 4.57 (dt, $^3J_{\text{H-H}} = 8.0$ Hz, $^3J_{\text{H-H}_{\text{syn}}} = 7.3$ Hz, 1H, H₂), 3.92 (d, $^3J_{\text{H}_{\text{syn}}-\text{H}} = 7.3$ Hz, 1H, H_{syn}), 3.88 (s, 1H, H_{13t}), 3.39 (s, 1H, H_{13c}), 3.28 (ddq, $^2J_{\text{H-H}} = 4.6$ Hz, $^3J_{\text{H-H}} = 11.3$ Hz, 1H, H₄), 3.22 (ddq, $^2J_{\text{H-H}} = 4.4$ Hz, $^3J_{\text{H-H}} = 12.7$ Hz, 1H, H₇), 3.04 (d, $^3J_{\text{H}_{\text{anti}}-\text{H}} = 13.7$ Hz, 1H, H_{anti}), 2.74 (m, 2H, H_{12,8'}), 2.60 (m, 1H, H_{7'}), 2.44 (m, 1H, H_{4'}), 2.38 (m, 1H, H₈), 2.31 (m, 1H, H₁₁), 2.06 (overlapping CH₃, m, 1H, H_{11'}), 2.05 (s, 3H, CH₃), 1.95 (m, 1H, H_{12'}), 1.54 (m, 1H, H₃), 1.42 (m, 1H, H_{3'}). $^{13}\text{C}\{^1\text{H}\}$ NMR (126 MHz, CD₂Cl₂, -60 °C): δ 138.0 (s, C_g), 131.0 (s, C_f), 122.6 (s, C_k), 121.4 (s, C_n), 111.3 (s, C_b), 110.9 (s, C_j), 89.4 (s, C_c), 76.6 (s, C_o), 67.9 (s, C_a), 39.0 (s, C_d), 34.8 (s, C_m), 31.3 (s, C_i), 28.9 (s, CCH₃), 26.2 (s, C_e), 26.3 (s, C_h), 22.7 (s, C_l).

Opening “wrap-around” complexes **10 and **11** with NCAr_F.** A solution of complex **10** or **11** was generated in situ following the procedure described previously. To complex **10** or **11** held at -30 °C was added 2 equiv of CNAr_F via syringe and the solution instantaneously turned from orange-red to yellow. The ^1H NMR displayed shifts indicative of uncoordinated olefins. Characteristic peaks for open chain form of **10**: ^1H NMR (500 MHz, CD₂Cl₂, -30 °C): δ 5.78 (m, 1H, H_c), 4.99 (d, $^3J_{\text{H-H}} = 17.1$ Hz, 1H, H_{trans-end-olefin}), 4.92 (d, $^3J_{\text{H-H}} = 10.1$ Hz, H_{cis-end-olefin}), 4.03 (d, $^3J_{\text{H-H}} = 8.3$ Hz, 1H, H_{syn}), 3.20 (d, $^3J_{\text{H-H}} = 14.9$ Hz, H_{anti}).

Observation of the Catalyst Resting State.

Observation of the resting state following a 1,2-insertion using **7 as the precursor (12-vinylidene).** Complex **11** was generated in situ through reaction of **7** (0.010 g, 0.009 mmol), B(C₆F₅)₃ (0.010 g, 0.019 mmol), and a 1.31 M solution of butadiene in CD₂Cl₂ (300 μL , 0.393 mmol), 42 equiv, at -80 °C following the above procedure. The NMR tube was placed in a precooled spectrometer held at -80 °C and formation of complex **11** was determined by ^1H NMR spectroscopy. At this point, the tube was warmed to -30 °C in the probe of the

spectrometer and then the reaction of the wrap-around complex **11** with excess butadiene was monitored by NMR spectroscopy. Upon warming, further insertion of butadiene into the wrap-around complex is observed and conversion to a new complex containing a coordinated vinylidene group is observed in solution (**12**). The ^1H NMR overlay in Figure 2.3 shows the growth of 12-vinylidene over time at $-30\text{ }^\circ\text{C}$. Characteristic peaks: ^1H NMR (500 MHz, CD_2Cl_2 , $-30\text{ }^\circ\text{C}$): δ 4.46 (d, $^3J_{\text{H-H}} = 7.5\text{ Hz}$, 1H, H_{syn}), 3.95 (d, $^3J_{\text{H-H}} = 16.5\text{ Hz}$, 1H, $\text{H}_{\text{trans-vinyl}}$), 3.65 (d, $^3J_{\text{H-H}} = 9.0\text{ Hz}$, 1H, $\text{H}_{\text{cis-vinyl}}$), 2.94 (d, $^3J_{\text{H-H}} = 13.5\text{ Hz}$, 1H, H_{anti}), with 2-Me substituted end group 4.68 (s, 1H) and 4.65 (s, 1H). In the ^1H NMR spectrum free vinyl groups appear at δ 4.95.

Observation of the Resting State following 1,2 insertion using 6 as the precursor (12-vinyl). Complex **10** was generated in situ through reaction of **6** (0.011 g, 0.008 mmol), $\text{B}(\text{C}_6\text{F}_5)_3$ (0.011 g, 0.021 mmol), and a 1.0 M solution of butadiene in CD_2Cl_2 (350 μL , 0.350 mmol), 45 equiv, at $-80\text{ }^\circ\text{C}$ following the above procedure. The NMR tube was placed in a precooled spectrometer held at $-80\text{ }^\circ\text{C}$ and formation of complex **10** was determined by ^1H NMR spectroscopy. Upon warming, further insertion of butadiene into the wrap-around complex is observed and conversion to a new complex containing a coordinated vinyl group is observed in solution (**12**). Figure 2.4, a ^1H NMR overlay, shows the growth of **12** overtime at $-30\text{ }^\circ\text{C}$. Characteristic peaks: ^1H NMR (500 MHz, CD_2Cl_2 , $-30\text{ }^\circ\text{C}$): δ 4.46 (d, $^3J_{\text{H-H}} = 7.5\text{ Hz}$, 1H, H_{syn}), 3.95 (d, $^3J_{\text{H-H}} = 16.5\text{ Hz}$, 1H, $\text{H}_{\text{trans-vinyl}}$), 3.65 (d, $^3J_{\text{H-H}} = 9.0\text{ Hz}$, 1H, $\text{H}_{\text{cis-vinyl}}$), 2.94 (d, $^3J_{\text{H-H}} = 13.5\text{ Hz}$, 1H, H_{anti}), vinyl end group $\sim 5\text{ ppm}$. In the ^1H NMR spectrum free vinyl groups appear at δ 4.95.

Polymerization of Butadiene.

A flame-dried Schlenk flask was charged with complex **7** (0.005 g, 0.005 mmol) and $\text{B}(\text{C}_6\text{F}_5)_3$ (0.005 g, 0.010 mmol) and cooled to $-30\text{ }^\circ\text{C}$. A solution of butadiene (1.5 M in CH_2Cl_2) (3.0 mL, 4.5 mmol) was added via syringe. The reaction was stirred at $-30\text{ }^\circ\text{C}$ for 7.5 h. After the polymerization was complete, 2,6-Di-*tert*-butyl-4-methylphenol (BHT) (0.001 g, 0.005 mmol) was added to prevent cross-linking and the solution was pipetted into a flask of cold MeOH (15.0 mL). The MeOH solution turned cloudy white and was allowed to settle over night in the freezer. The MeOH was then decanted and the polymer was dried in vacuo over night to yield 17% polybutadiene (0.040 g, 0.741 mmol). Refer to Chapter 4 for a more complete description of the polymerization study.

Crystal Structure Determination of **6** and **10**.

The crystallographic information for structures **6** and **10** is given in Table I.1 of the Appendix. The data was collected on a Bruker SMART APEX-2 X-ray diffractometer at $-173\text{ }^\circ\text{C}$ using Mo- $\text{K}\alpha$ radiation for complex **6** and Cu- $\text{K}\alpha$ radiation for **10**. Tables I.2-I.5 located in the Appendix list the selected bond lengths and angles for complexes **6** and **10**. An ORTEP diagram for complex **6** is found in Figure I.1.

References and Notes

1. Durand, J. P.; Dawans, F.; Teyssié, P. *J. Polym. Sci., Part A* **1970**, *8*, 979-990.
2. Porri, L.; Giarrusso, A.; Ricci, G. *Prog. Polym. Sci.* **1991**, *16*, 405-441.
3. Taube, R.; Sylvester, G. Stereospecific Polymerization of Butadiene or Isoprene. In *Applied Homogeneous Catalysis with Organometallic Complexes*, Cornlis, B., Herrmann, W. A. Eds.; VCH: Weinheim, Germany, **1996**; 280-318.
4. Thiele, S. K.-H.; Wilson, D. R. *J. Macromol. Sci. Part C: Polym. Rev.* **2003**, *C43*, (4), 581-628.
5. Taube, R.; Windisch, H.; Weissenborn, H.; Hemling, H.; Schumann, H. *J. Organomet. Chem.* **1997**, *548*, 229-236.
6. Kormer, V. A.; Baitskii, B. D.; Lobach, M. I.; Chesnokova, N. N. *J. Polym. Sci. Polym. Symp.* **1969**, *16*, 4351-4359.
7. Porri, I.; Natta, G.; Gallazzi, M. C. *J. Polym. Sci., Part C* **1967**, *16*, 2525-2537.
8. Taube, R.; Gehrke, J. P.; Schmidt, U. *J. Organomet. Chem.* **1985**, *292*, 287-296.
9. Taube, R.; Schmidt, U.; Gehrke, J. P.; Anacker, U. *J. Prakt. Chem.* **1984**, *326*, 1-11.
10. Taube, R.; Gehrke, J. P.; Böhme, P.; Scherzer, K. *J. Organomet. Chem.* **1991**, *410*, 403-416.
11. Taube, R.; Langlotz, J.; Sieler, J.; Gelbrich, T.; Tittes, K. *J. Organomet. Chem.* **2000**, *597*, (92-104).
12. Tobisch, S. *Acc. Chem. Res.* **2002**, *35*, 96-104.
13. Tobisch, S. *Chem.-Eur. J.* **2002**, *8*, (20), 4756-4766.
14. Tobisch, S.; Taube, R. *Organometallics* **1999**, *18*, 5204-5218.
15. Tobisch, S.; Taube, R. *Chem.-Eur. J.* **2001**, *7*, (17), 3681-3695.
16. There is precedence for η^6 -coordination of bulky arenes to Ni(II) complexes. Cámpora, J.; Conejo, M. d. M.; Reyes, M. L.; Mereiter, K.; Passaglia, E. *Chem. Commun.* **2003**, 78-79.
17. See Experimental Section.

18. Reaction of complex **10** with 2 equiv of $\text{NC}(\text{C}_6\text{H}_3(\text{CF}_3)_2)$ results in decoordination of the olefins as evidenced by the downfield shifts in the ^1H NMR spectrum. See Experimental Section.
19. From the presence of ca. 1% vinyl groups in the PBD formed, on average, 100 1,4 insertions must occur prior to a 1,3-insertion. These ratios are consistent with our NMR observations.
20. Alaimo, P. J.; Peters, D. W.; Arnold, J.; Bergman, R. G. *J. Chem. Educ.* **2001**, 78, (1), 64.
21. Pangborn, A. B.; Giardello, M. A.; Grubbs, R. H.; Rosen, R. K.; Timmers, F. J. *Organometallics* **1996**, 15, 1518-1520.
22. Wilke, G.; Bogdanovic, B.; Hardt, P.; Heimbach, P.; Keim, W.; Kröner, M.; Oberkirch, W.; Tanaka, K.; Steinrücke, E.; Walter, D.; Zimmermann, H. *Angew. Chem. Int. Ed. Eng.* **1966**, 5, 151-164.

CHAPTER THREE

Synthesis of Labile Cationic (Allyl)Nickel(II) and Palladium(II) Arene Complexes and Reactivity with Olefins

All of the experiments conducted with the [(2-R-allyl)Pd(mes)][SbF₆] derivatives were performed by Stephanie A. Urbin and Rebecca A. Moorhouse.

Introduction

An important goal in the field of transition metal-catalyzed polymerizations is the synthesis of highly active and easily prepared metal complexes that can serve as initiators for the polymerization of olefins and dienes. Many research groups have addressed this issue and found that the use of transition metal complexes containing a labile ligand are key targets for use as polymerization catalysts.¹⁻³ The presence of a labile ligand at the metal center allows for facile displacement of the ligand by an incoming monomer unit. This is an important feature for metal catalysts used in living polymerization because ideally initiation should be fast or occur at a rate similar to propagation.⁴

The Brookhart lab has shown that nickel and palladium diimine complexes possessing the weakly bound diethyl ether ligand serve as highly active, well-defined catalysts for the polymerization of ethylene and α -olefins.^{3, 5} Recently, Goodall and coworkers have reported the polymerization of norbornene using (crotyl)Ni(COD)⁺ as the active catalyst.^{6, 7} Quantitative conversion to polynorbornene is achieved within minutes. They proposed the labile COD (cyclooctadiene) ligand could be displaced by norbornene to

generate a highly active metal center.⁷ Unfortunately, mechanistic studies showed COD was strongly coordinated to the nickel center leading to slow initiation relative to propagation. The monomer does not readily displace the COD ligand, making only a fraction of the nickel catalyst active for polymerization, yielding high molecular weight polymer quickly.⁷

Arenes have been used as weakly coordinating ligands yielding interesting metal complexes that exhibit high activity.⁸ Neutral group 10 arene metal complexes have been shown to exhibit high lability, for example the $(\text{C}_6\text{F}_5)_2\text{-Ni-}\pi\text{-arene}$ species prepared using harsh metal deposition conditions. The arene ligands in this system are highly fluxional, and undergo rapid exchange with free arenes at room temperature.⁸ The $(\text{C}_6\text{F}_5)_2\text{-Ni-(tolyl)}$ complex is highly active for polymerization of norbornadiene and cyclic telomerization of butadiene.⁹ This contrasts with the lability of the arene of $\text{RuCl}_2(\text{arene})\text{PR}_3$, which must be irradiated or thermally activated to cause aryl ring exchange.¹⁰ Both studies show that the more electron-donating arenes displace the original arene fragment more readily than electro-neutral or electron-withdrawing arenes.^{9,10}

(Allyl)Ni(II) complexes have been investigated for diene polymerization.¹¹⁻¹⁴ Taube and coworkers reported the active $[(\text{C}_{12}\text{H}_{19})\text{Ni}]^+$, which can polymerize butadiene to yield highly *cis*-1,4 enchaind polybutadiene.¹⁵⁻¹⁷ We recently reported a detailed account of the mechanism of butadiene polymerization using “naked” (allyl)Ni(II) cations. These complexes are highly active for butadiene polymerization at low temperatures, yielding highly *cis*-1,4 enchaind polybutadiene.¹⁸

Rare-examples of cationic allyl Pd(II) complexes containing weakly bound arene or diene ligands were reported by Maitilis and Goodall. Cationic $(\text{allyl})\text{Pd}(\eta^4\text{-diene})/(\eta^6\text{-arene})^+$ (diene = COD, COT, 1,5-hexadiene; arene = hexamethylbenzene [hmb]) complexes

were readily synthesized and examined by Maitilis. He has shown that the diene or arene ligand is weakly coordinated to Pd, as evidenced by exchange with excess diene/arene in solution at room temperature.¹⁹ Goodall has reported the use of (crotyl)Pd(COD)⁺ for the polymerization of norbornene. Polymerization of norbornene with Pd was sluggish,⁶ in contrast to previous observations using the analogous Ni(II) complex.²⁰ The COD ligand was shown to be strongly coordinated to Pd, but these complexes proved to be useful models to observe insertion products that form during norbornene chain growth.⁶

Recently, Cámpora and coworkers have reported the synthesis of (allyl)Ni(arene)⁺ complexes, where the arene is 2,6-di-*tert*-butyl-4-methylphenol or 1,3,5-tris(*tert*-butyl)benzene. These compounds serve as active catalysts for the polymerization of butadiene and styrene. After 1 h at 60 °C in toluene, *cis*-1,4-butadiene is synthesized in good yield²¹ and the activity of these catalysts is comparable to Taube's ligand-free Ni(II) catalyst. Cámpora proposes the active species, (allyl)Ni(η^4 -butadiene)⁺, forms prior to polymerization²¹ and this is supported by experiments and calculations performed by Taube and Tobisch.^{11, 17, 22} We have also shown that an η^4 -diene species exists prior to insertion of butadiene.¹⁸

This chapter details the synthesis and characterization of cationic (allyl)Ni(II) and Pd(II) arene complexes that possess highly labile arene ligands. The reactions of these complexes with olefins and alkynes are described. The Pd complexes rapidly coordinate two equivalents of olefin at low temperature (-80 °C) and upon warming, exchange with excess free olefin in solution. The dynamics of the exchange process will be outlined in this chapter. Continued warming to room temperature leads to olefin oligomerization. Additionally, alkynes displace mesitylene and coordinate to the Pd(II) center at low

temperatures. The reactivity observed with the analogous (allyl)Ni(II) complexes and olefins is quite different. When (allyl)Ni(arene)⁺ complexes are reacted with olefins, a hydrogen atom transfer reaction from the olefin to the allyl group is observed, liberating an equivalent of propene/isobutylene and generating a new (allyl)Ni(II) complex, as seen in ¹H NMR spectroscopic experiments. Mechanistic details regarding intramolecular hydrogen atom transfer observed during the reaction of olefins with the nickel complexes will be discussed.

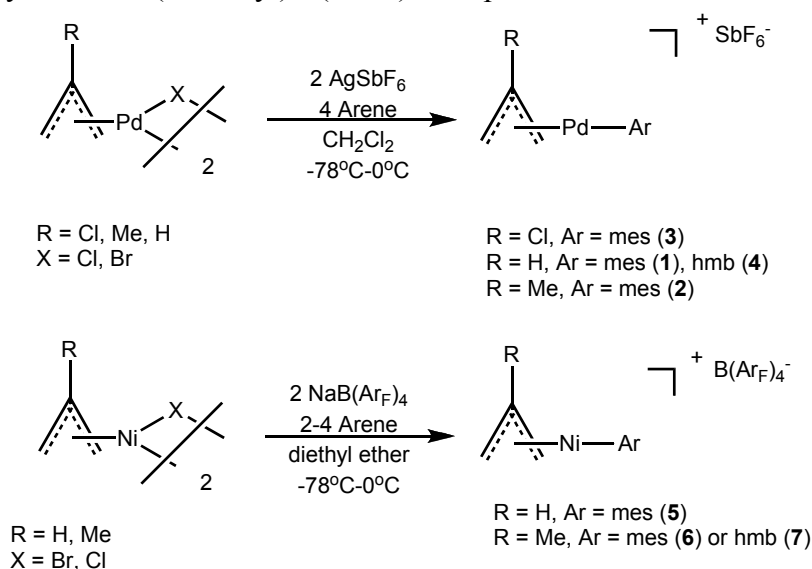
Results and Discussion

Synthesis of (2-R-allyl)M(Arene)⁺ Salts (M = Pd, Arene = mes, R = H (1), R = Me (2), R = Cl (3); M = Pd, Arene = hmb, R = H (4); M = Ni, Arene = mes, R = H (5), R = Me (6); M = Ni, Arene = hmb, R = Me (7)). Synthesis of the (2-R-allyl)M(arene)⁺ complexes was achieved by salt metathesis of the well-known allyl halide [2-R-allyl(M)X]₂ dimers²³⁻²⁶ in the presence of a slight excess of arene. Scheme 3.1 summarizes the complexes prepared and the general methods used. NaB(Ar_F)₄ (Ar_F = 3,5-(CF₃)₂C₆H₃) was used for preparation of the Ni complexes, while AgSbF₆ was required for synthesis of the Pd complexes. The Ni complexes are quite robust and can be handled at room temperature, while the Pd derivatives need to be isolated and stored at low temperatures. ¹H and ¹³C{¹H} NMR spectroscopy was used to characterize the complexes. As characteristic of these complexes, allyl ¹H resonances of Ni complex **5** appear at δ 5.85 (m), 3.69 (d, ³J_{H-H} = 6.6 Hz), and 2.45 (d, ³J_{H-H} = 12.6 Hz) for the central, *syn*, and *anti* protons respectively, while those of the Pd analog, **1**, appear at δ 5.65 (m), 4.54 (d, ³J_{H-H} = 4.8 Hz), 3.30 (d, ³J_{H-H} = 11.4 Hz) for the central, *syn*, and *anti* protons respectively. The mesitylene signals for the aromatic hydrogens (δ 6.66) of **5** are shifted upfield relative to free mesitylene (δ 6.79) in the

Ni complex, while in Pd complex **1** the signals are shifted downfield to δ 7.03 relative to free mesitylene (see Experimental Section for complete characterization of complexes **1-7**).

Single crystal X-ray analysis provided structural details for complexes **5** and **7** and confirmed the η^6 -coordination mode of the arene. The crystallographic information is collected in Tables II.1 – II.5 of the Appendix. ORTEP drawings for **5** and **7** appear in Figures 3.1 and 3.2, respectively. The Ni-C arene bond lengths in complex **5** range from 2.12-2.19 Å indicating the ring is coordinated nearly symmetrically to the Ni center (Figure 3.1). This is in good agreement with the arene coordination in the crystal structure reported by Cámpora for the analogous [(allyl)Ni(2,6-di-*tert*-butyl-4-methyl-phenol)][B(Ar_F)₄].²¹ The angle between the mesitylene plane and the allyl plane is 17.2°. The arene bond lengths for complex **7** vary from 2.12-2.26 Å (Figure 3.2), similar to those obtained for compound **5**, indicating once again a symmetrically bound arene ring. The angle between the hexamethylbenzene and allyl planes is 15.43°. The arene ring is slightly tilted away from the 2-methallyl moiety.

Scheme 3.1. Synthesis of (2-R-allyl)M(arene)⁺ complexes.



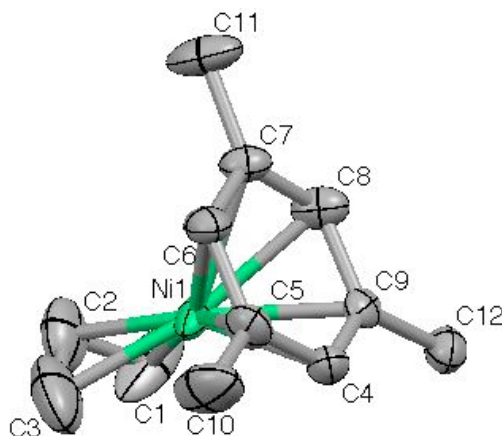


Figure 3.1. ORTEP diagram of (allyl)Ni(mes)⁺, **5**. Thermal ellipsoids drawn at 50% probability, [B(Ar_F)₄]⁻ omitted for clarity. Selected bond lengths (Å): Ni(1)-C(2) = 1.962(4), Ni(1)-C(1) = 1.994(4), Ni(1)-C(3) = 2.061 (6), Ni(1)-C(6) = 2.121(4), Ni(1)-C(8) = 2.130(4), Ni(1)-C(5) = 2.142(4), Ni(1)-C(9) = 2.157(3), Ni(1)-C(4) = 2.176(4), Ni(1)-C(7) = 2.192(4).

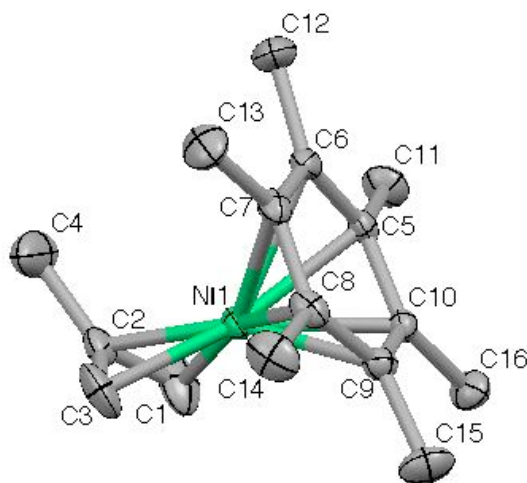
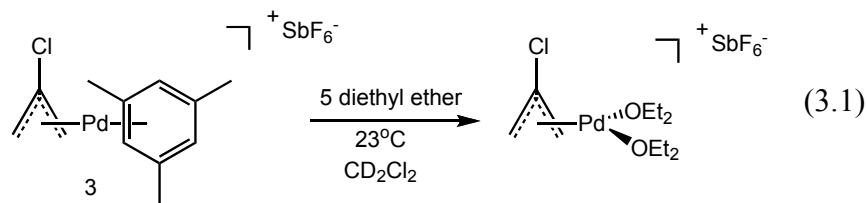


Figure 3.2. ORTEP diagram of (2-methallyl)Ni(hmb)⁺, **7**. Thermal ellipsoids drawn at 50% probability, [B(Ar_F)₄]⁻ is omitted for clarity. Selected bond lengths (Å): Ni(1)-C(2) = 1.978(2), Ni(1)-C(1) = 2.001(2), Ni(1)-C(3) = 2.007(2), Ni(1)-C(8) = 2.1205(19), Ni(1)-C(5) = 2.1392(18), Ni(1)-C(10) = 2.1426(18), Ni(1)-C(7) = 2.1857(19), Ni(1)-C(9) = 2.1901(19), Ni(1)-C(6) = 2.2563(18).

Ligand Substitution Reactions of (Allyl)Pd(II)(Mes)⁺ Complexes.

Reactions with Diethyl Ether. The rapid reaction of **3** with diethyl ether illustrates the high lability of the bound arene. At room temperature in CD₂Cl₂, 5 equiv of diethyl ether displaced the mesitylene ligand of **3** to yield a diethyl ether complex shown in eq 3.1.



Free mesitylene is generated (δ 6.80) and new allyl signals appear at δ 4.43 (s, H_{syn}) and H_{anti} overlaps with the coordinated ether signal for **3**. The bound ether ligands exchange with free ether at room temperature and show resonances at 3.51 (CH_3) and 1.21 (CH_2) ppm. We assume this is a four-coordinate square planar complex, but the averaging of free and bound ether ligand resonances precludes establishing this through peak integration.

Exchange reaction with Free Mesitylene. Reaction of $[(allyl)Pd(mes)][SbF_6]$, **1**, with excess mesitylene results in exchange of the free and bound mesitylene. This exchange is rapid at room temperature on the NMR timescale, but at low temperatures the resonances for free and bound mesitylene decoalesce (Figure 3.3). Due to poor solubility of **1** in CD_2Cl_2 at low temperatures, the slow exchange limit could not be quite reached. However, when **1** is exposed to 2, 4, or 6 equiv of free mesitylene at $-67^\circ C$, the peak width at half-height for the aromatic signal of the bound mesitylene (26 Hz) did not change, indicating that the exchange is independent of the concentration of free mesitylene. The linewidth at slow exchange is estimated to be 20 Hz, from which the rate constant for exchange, k_{ex} , can be estimated as $18\ s^{-1}$, corresponding to $\Delta G^\ddagger_{avg} = 10.5\ kcal/mol$. This data eliminates an associative exchange mechanism involving external mesitylene in the transition state for exchange. Possible mechanisms would include a fully dissociative process, a solvent-assisted process, or a process in which the rate-limiting step is formation of an η^4 or η^2 -mesitylene complex (potentially solvent stabilized) followed by associative displacement.

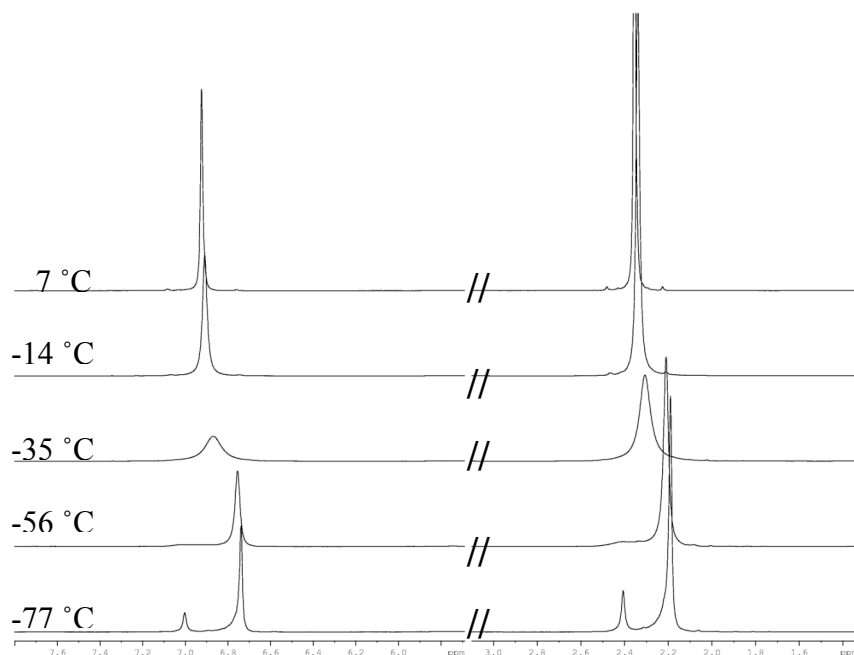


Figure 3.3. Variable temperature ^1H NMR overlay of the addition of 1 equiv mesitylene to **1**. Mesitylene aryl (δ 6.0 – 7.5) and methyl regions (δ 1.8 – 3.0) are shown.

Reactions with Olefins and Alkynes. Treatment of $[(2\text{-Cl-allyl})\text{Pd}(\text{mes})][\text{SbF}_6]$, **3**, with excess olefin at temperatures as low as $-120\text{ }^\circ\text{C}$ results in displacement of mesitylene and formation of bis-olefin adducts. Scheme 3.2 shows the reaction of **3** with ethylene to form **8**, the η^2 -coordinated bis-ethylene palladium allyl species. Exposure of **3** to three equiv of ethylene in CDCl_2F at $-110\text{ }^\circ\text{C}$ generates free mesitylene and the bis-ethylene complex whose ^1H NMR spectrum is shown in Figure 3.4. At $-110\text{ }^\circ\text{C}$, resonances for the *syn* and *anti* protons appear as singlets at 5.14 and 3.91 ppm, respectively, which are shifted downfield from the analogous resonances in the mesitylene complex (δ 4.72 and 3.57). Two sets of bound ethylene resonances are seen at 5.24 (4.0H) and 5.00 (4.0H) ppm suggesting that rotation of ethylene is rapid on the NMR timescale and that both $\text{H}_1/\text{H}_{1'}$ and $\text{H}_2/\text{H}_{2'}$ protons average. The sharp free ethylene signal is seen at 5.33 ppm. Upon warming to $-60\text{ }^\circ\text{C}$, the bound ethylene signals begin to broaden. At $-20\text{ }^\circ\text{C}$, the signal for bound ethylene has nearly

coalesced with the signal for free ethylene, implying rapid exchange between bound and free ethylene at this temperature. ^1H NMR variable temperature line broadening experiments at $-77\text{ }^\circ\text{C}$ to $-56\text{ }^\circ\text{C}$ showed the barrier for intermolecular exchange of free and bound ethylene to be $\Delta G^\ddagger_{\text{avg}} = 11.4\text{ kcal/mol}$. When the sample is warmed to $25\text{ }^\circ\text{C}$, the ethylene and allyl resonances vanish. High field signals in the aliphatic region as well as mass spectral results suggest formation of ethylene oligomers.

Scheme 3.2. Formation of Pd(II) bis-ethylene adduct **8**.

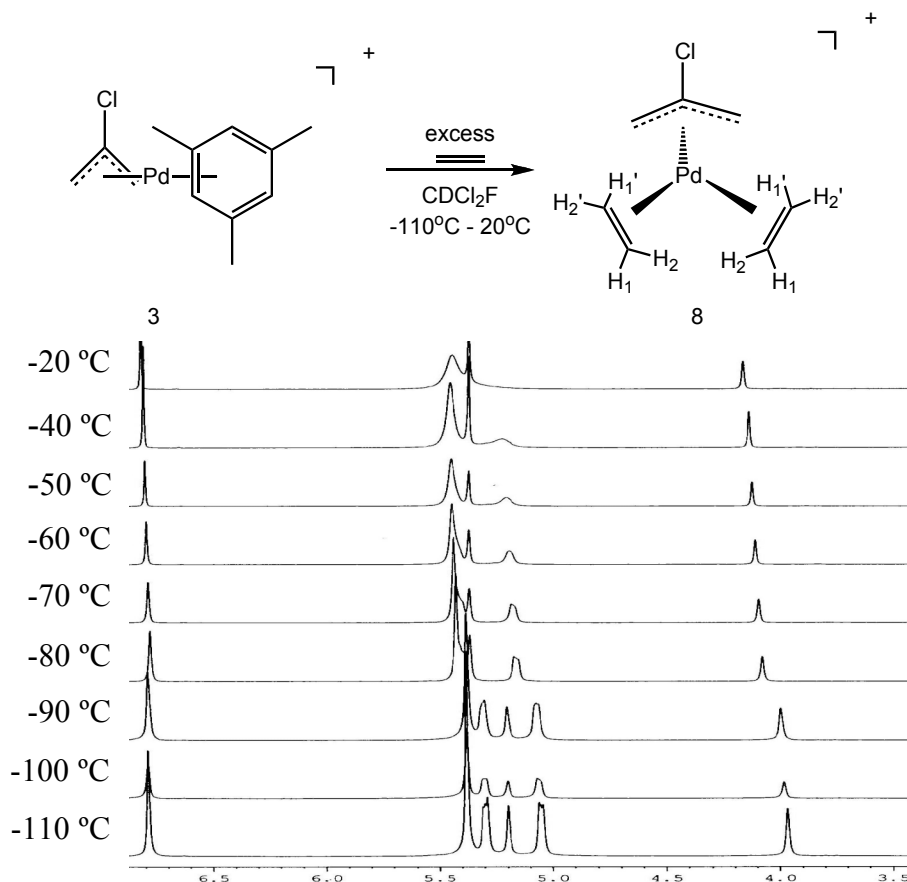
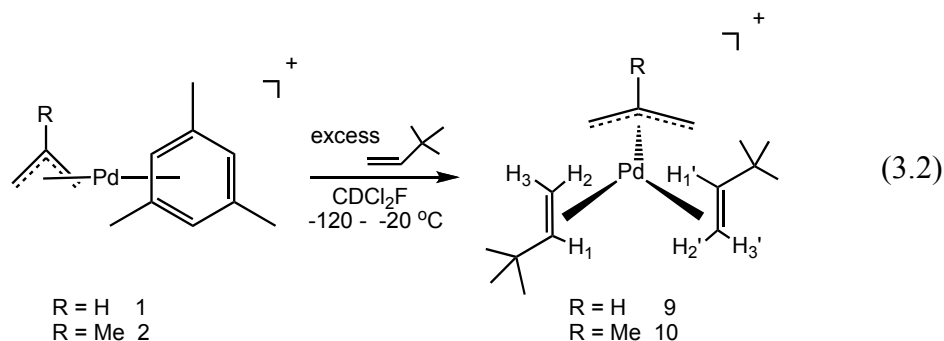


Figure 3.4. ^1H NMR variable temperature overlay showing the formation of $(2\text{-Cl-allyl})\text{Pd}(\text{ethylene})_2^+$ and exchange with free ethylene at higher temperatures. At $-110\text{ }^\circ\text{C}$, the resonances for H_1 and H_1' appear at 5.24 ppm and at 5.00 ppm for H_2 and H_2' . The *syn* and *anti* protons are at 5.14 and 3.91 ppm, respectively.

Similar to the formation of the bis-ethylene adduct, reaction of $[(\text{allyl})\text{Pd}(\text{mes})][\text{SbF}_6]$, **1**, and $[(2\text{-methallyl})\text{Pd}(\text{mes})][\text{SbF}_6]$, **2**, with excess *tert*-butylethylene (TBE) in CDCl_2F at temperatures as low as $-120\text{ }^\circ\text{C}$ results in displacement of mesitylene and subsequent formation of bis-(TBE) species **9** and **10**, respectively (eq 3.2). Only one isomer is formed due to the steric bulk of the *t*-butyl group in the TBE ligand. Free mesitylene appears at 6.79 (Ar) and 2.20 (CH_3) ppm upon formation of either complex **9** or **10**. The two *syn* and *anti* allyl ^1H resonances are inequivalent and appear for species **9** at δ 5.10 (br. d, H_{syn}), 5.02 (br. d, H_{syn}), 3.89 (d, $^3J_{\text{H-H}} = 13.0\text{ Hz}$, H_{anti}), and 3.25 (d, $^3J_{\text{H-H}} = 12.5\text{ Hz}$, H_{anti}). The central allyl resonance appears at δ 5.78 (m) (see Experimental Section for structural assignments). The coordinated TBE ligands of **9** are also inequivalent as shown by six separate vinyl signals at δ 6.24 (1.0H, m, H_1), 6.13 (1.0H, m, H_1'), 5.40 (2.0H d, $^3J_{\text{H-H}} = 16.5\text{ Hz}$, H_3 and H_3' are coincident), 4.77 (1.0H, d, $^3J_{\text{H-H}} = 8.5\text{ Hz}$, H_2) and 4.41 (1.0H, d, $^3J_{\text{H-H}} = 9.0\text{ Hz}$, H_2'). The structure shown below for **9** is consistent with the NMR data. ^1H NMR resonances for **10** are similar to those of **9** and indicate the coordination of 2 equiv of TBE to the cationic (2-methallyl)Pd(II) center (see Experimental Section for complete characterization).

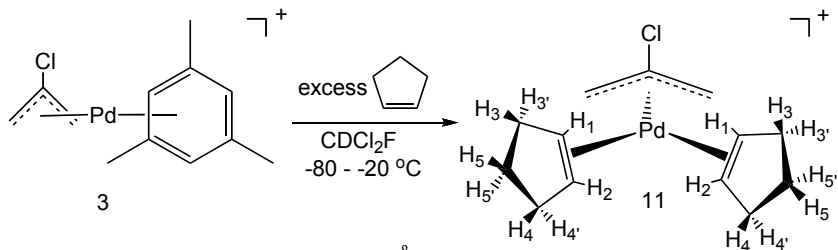


Treatment of **3** with excess cyclopentene in CD_2Cl_2 at $-70\text{ }^\circ\text{C}$ results in formation of bis-cyclopentene complex **11** and free mesitylene (Scheme 3.3). Two new resonances at 6.16

(2.0H) and 5.86 (2.0H) ppm correspond to the vinylic protons (H_1 and H_2) on bound cyclopentene and are shifted downfield from free cyclopentene (δ 5.76), as seen in the 1H NMR spectrum shown in Figure 3.5. The *syn* and *anti* protons appear as two singlets at δ 5.28 (2.0H) and 3.96 (2.0H), respectively. The allylic protons of bound cyclopentene appear as a broad 8.0H band at 2.51 ppm, while the two 2.0H resonances at 1.92 and 1.05 ppm are assigned to H_5 and $H_{5'}$ for the *endo* and *exo* hydrogens. At temperatures above -56 $^{\circ}C$, the resonances for the bound and free cyclopentene broaden as the exchange rate increases.

As with the mesitylene case, this exchange process was analyzed quantitatively. Screw-cap NMR tubes were charged with **3** and 6, 9 and 12 equiv respectively of cyclopentene, and methylene chloride was added to reach the same total volume in each tube. Broadening of the bound vinyl 1H resonance (6.16 ppm) of cyclopentene was monitored between -56 $^{\circ}C$ and -45 $^{\circ}C$. The peak width at half-height at -56 $^{\circ}C$ was 12 Hz for both 6 and 9 equiv and 13 Hz for 12 equiv of cyclopentene. At -45 $^{\circ}C$ the peak widths at half-height were 22 Hz (6 equiv), 23 Hz (9 equiv), and 24 Hz (12 equiv). These line widths are within experimental error and clearly show there is no dependence of the exchange rate on added cyclopentene, suggesting either a dissociative or solvent-assisted exchange mechanism. The rate constant for cyclopentene dissociation can be estimated using the slow exchange approximation as $k_{ex} = 30$ s^{-1} at -45 $^{\circ}C$, corresponding to $\Delta G^{\ddagger} = 11.7$ kcal/mol.

Scheme 3.3. Synthesis of $(2\text{-Cl-allyl})Pd(\text{cyclopentene})_2^+$ at low temperature.



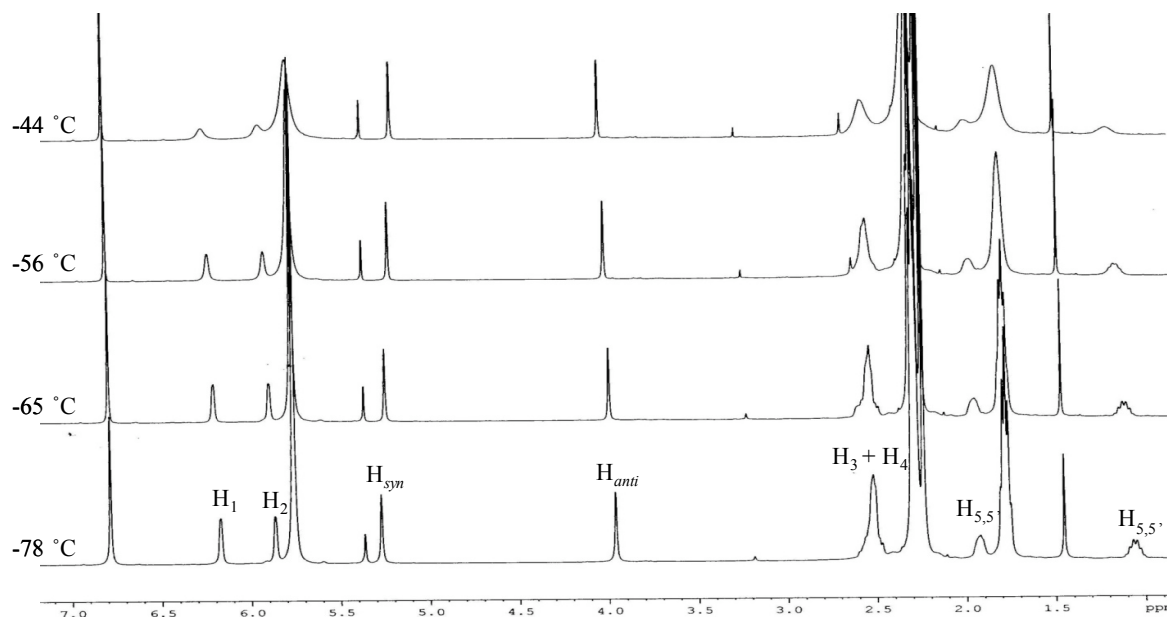
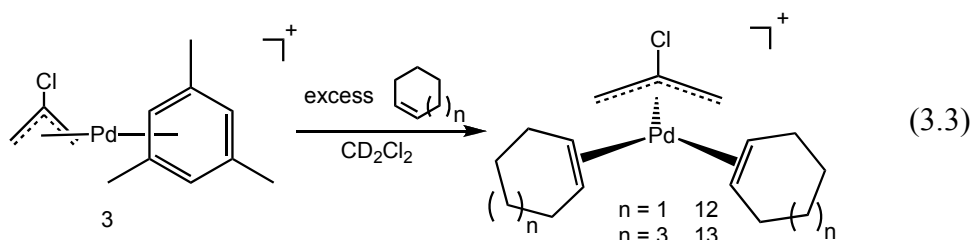


Figure 3.5. ^1H NMR overlay showing the formation of $(2\text{-Cl-allyl})\text{Pd}(\text{cyclopentene})_2^+$ and exchange with free cyclopentene at higher temperatures.

Similar to cyclopentene, cyclohexene, and cyclooctene react with **3** to form bis-olefin adducts **12** and **13**, respectively (see eq 3.3). ^1H NMR spectra for these species are similar to that of the bis-cyclopentene adduct and are reported in the Experimental Section.

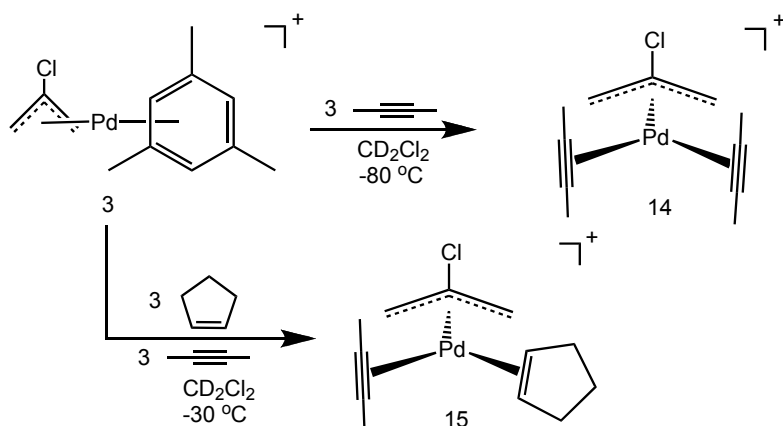


Exposure of **3** to α -olefins propene or 1-hexene results in the formation of a mixture of bis-olefin isomer adducts, and no attempt was made to structurally assign these species.

Exposure of **3** to 3 equiv of 2-butyne in CD_2Cl_2 at $-80\text{ }^\circ\text{C}$ results in displacement of mesitylene and formation of the bis-alkyne adduct **14** (Scheme 3.4). NMR studies were performed in the presence of 3 equiv of 2-butyne in CD_2Cl_2 from $-80\text{ }^\circ\text{C}$ to $23\text{ }^\circ\text{C}$. At $-80\text{ }^\circ\text{C}$ mesitylene has been displaced to form free mesitylene. The *syn* and *anti* protons appear as

singlets at 4.83 and 3.94 ppm, while the methyl groups give rise to a singlet at 2.18 (12.0H) ppm. The equivalence of the methyl resonances suggests rapid rotation of the alkyne ligands on the NMR timescale at -80 °C. Line broadening of the methyl resonances for free and bound 2-butyne begins at -40 °C due to intermolecular ligand exchange; at 23 °C free and bound methyl signals are present as one broad resonance. ^1H variable temperature NMR studies conducted at -66 °C to -24 °C showed the barrier to intermolecular exchange between free and bound 2-butyne to be $\Delta G^\ddagger_{\text{avg}} = 12.6$ kcal/mol. After a period of two days at room temperature, the color of the solution has changed from colorless to dark purple. A small amount of free 2-butyne remains and a new intense sharp singlet has grown in at 2.20 ppm, likely due to 2-butyne oligomers.

Scheme 3.4. Synthesis of Pd(II) complexes **14** and **15**.



The addition of equivalent amounts of cyclopentene and 2-butyne, both in excess, to **3** in CD_2Cl_2 at -70°C , cleanly gives rise to the mixed ligand species $(2\text{-Cl-allyl})\text{Pd}(\text{2-butyne})(\text{cyclopentene})^+$ (**15**), with no observable formation of either the bis-cyclopentene (**11**) or bis-2-butyne (**14**) adducts (Scheme 3.4). At -70°C all four *syn* and *anti* allyl protons are inequivalent and appear as singlets at 5.05, 5.01, 4.19, and 4.11 ppm in a 1:1:1:1 ratio. Resonances for the vinylic protons on bound cyclopentene occur at 6.22 (1.0H) and 5.63

(1.0H) ppm and the two methyl resonances for 2-butyne appear as a 6.0H singlet at 2.10 ppm. At 0 °C, all allylic, vinylic, and methyl resonances of **15** begin to exhibit dynamic behavior; broadening and exchanging with free substrates.

Reactions of (Allyl)Ni(II)(Arene)⁺ Complexes.

Reactions with Diethyl Ether. In contrast to the Pd systems, exposure of allyl nickel complex **5** at 23 °C to 4.2 equiv of diethyl ether results in no displacement of mesitylene. Monitoring the reaction at 23 °C results in slow decomposition of the allyl complex (22% after 3 days) and formation of free mesitylene, but no evidence for production of a bis-ether complex.

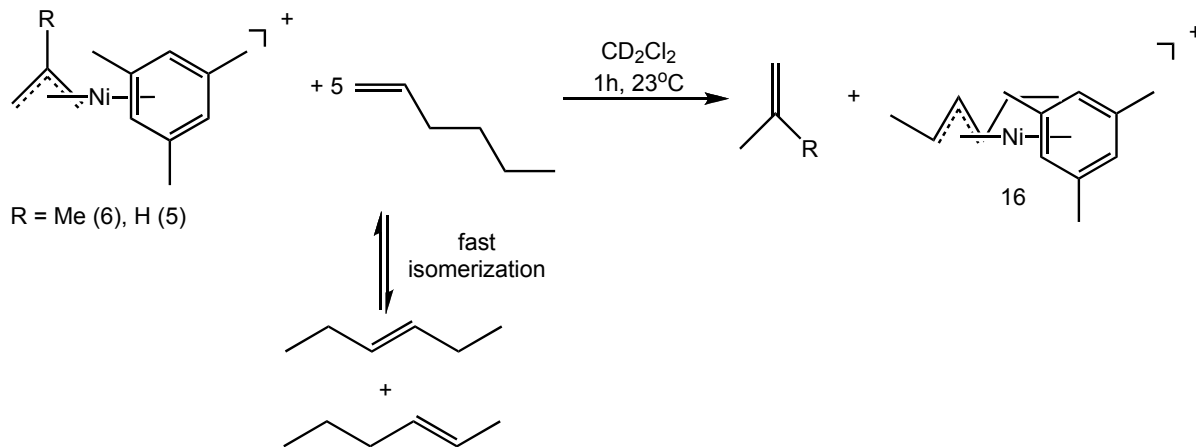
Arene Exchange Reactions. No line broadening of free or bound arene signals is observed upon treatment of **5** with excess mesitylene in CD₂Cl₂ up to temperatures of 23 °C, indicating degenerate exchange is far slower than in the case of the Pd analogs described above. However, exchange on a preparative time scale could be observed. Treatment of **5** with 2.6 equiv of hexamethylbenzene at 23 °C in CD₂Cl₂ results in rapid, quantitative displacement of mesitylene (δ 6.80) to form (allyl)Ni(C₆Me₆)⁺ as supported by an 18.0H singlet at 2.31 ppm in the ¹H NMR spectrum for coordinated hexamethylbenzene and allyl resonances at 3.24 ppm (2.0H, d, ³J_{H-H} = 6.6 Hz, H_{syn}). The H_{anti} 2.0H doublet is masked by excess hexamethylbenzene. The central allyl hydrogen resonance appears at 5.73 ppm. Within 10 min, 100% conversion to (allyl)Ni(C₆Me₆)⁺ is achieved.

Reactions with Olefins. Relative to the previously described Pd analogs, a quite different reactivity pattern is observed when the Ni complexes **5** or **6** are treated with α -olefins. The reaction of **6** with 4 equiv of 1-hexene was monitored at low temperature by ¹H NMR spectroscopy. At -80 °C there is no evidence for ligand substitution and formation of a

bis-olefin adduct. Only free 1-hexene and starting complex **6** are observed. Upon warming to -30 °C, no change in the structure of the (2-methallyl)Ni(II) complex is observed, but 1-hexene is partially isomerized to internal 2- and 3-hexenes. After 1.5 h at -30 °C, complete isomerization of 1-hexene is achieved. At -10 °C, a new (allyl)Ni(mes)⁺ complex begins to appear together with free isobutylene (4.65 and 1.72 ppm).

In a second experiment, monitoring the reaction of **5** and 5 equiv of 1-hexene at room temperature showed that complete isomerization to the internal isomers of hexene (both *cis* and *trans*) was achieved in 30 min together with consumption of 80% of **5**, formation of the new (allyl)Ni(mes)⁺ complex, and propene. After ca. 1 h, quantitative conversion to the new allyl complex identified as (2-hexenyl)Ni(mes)⁺, **16**, had occurred (Scheme 3.5). There are two allyl resonances, one a triplet at 5.46 ppm (1.0H), ³J_{H-H} = 11.2 Hz, assigned to the central allyl H and the other two overlapping 1.0H multiplets centered at 3.14 ppm corresponding to the *anti* H's. A 2.0H pentet at 1.32 ppm, ³J_{H-H} = 6.4 Hz, is assigned to the CH₂ of the ethyl group. There are two methyl resonances at 1.05 (t, ³J_{H-H} = 7.2 Hz) and 1.02 (d, ³J_{H-H} = 6.8 Hz) ppm. Additionally, a new mesitylene aryl proton resonance at 6.44 ppm, shifted upfield from 6.66 ppm for complex **5**, is observed in the ¹H spectrum, indicating the formation of **16**. ¹³C{¹H} NMR also validates the identity of complex **16** by the presence of three new allylic carbons (105.4, 83.0, and 76.3 ppm) and three aliphatic carbons (26.4, 19.5, and 18.8 ppm).

Scheme 3.5. Reaction of complexes **5** and **6** with 1-hexene at room temperature.



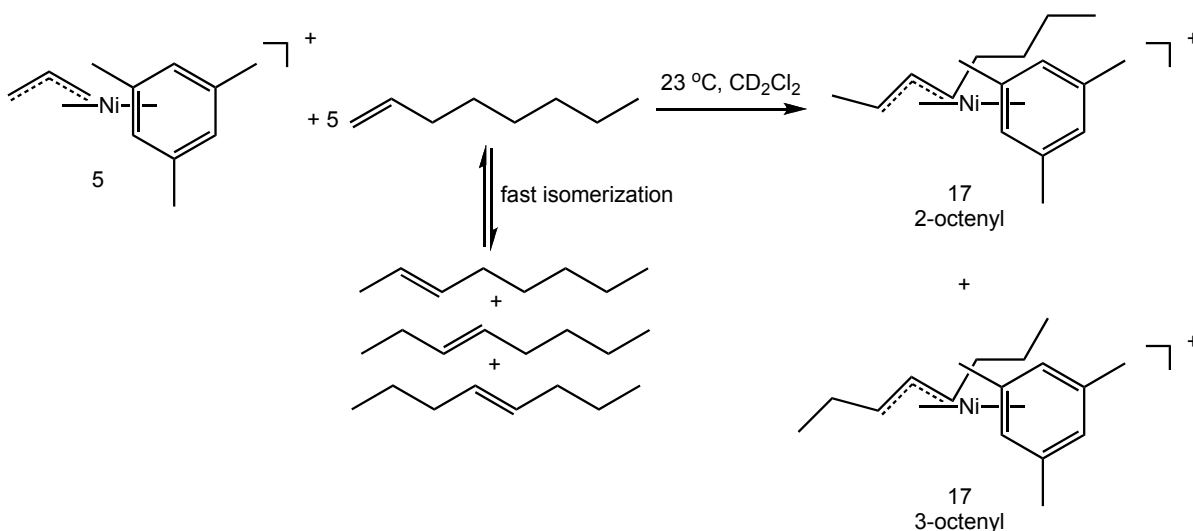
The evolution of propylene, as detected in the ^1H NMR spectrum, is evidence that an intramolecular hydrogen atom transfer reaction has occurred (see Experimental Section for NMR data). This reaction has never been observed with the analogous Pd complexes as the catalyst.

Goodall investigated the use of α -olefins as chain transfer agents (CTAs) to control the molecular weight in the polymerization of norbornene.^{7, 27} Using the cationic complex $(\text{allyl})\text{Pd}(\text{PCy}_3)(\text{OEt}_2)^+$ as a catalyst and 1-hexene as a CTA, he observed complete isomerization to internal hexene isomers within 30 minutes. This contrasts his previous results using the cationic $(\text{allyl})\text{Ni}(\text{COD})^+$ complex, in which olefins do not undergo isomerization, but simply serve as CTAs.²⁰ He reported that the use of α -olefins as chain transfer agents in the Pd catalyzed polymerization of norbornene is much less effective than in the Ni systems. Goodall suggests that in the case of Pd, isomerization to the internal olefin isomers makes them less effective as CTAs.²⁷ We see the opposite trend for (2-R-allyl)Ni(mes)⁺ and (2-Cl-allyl)Pd(mes)⁺. Olefins coordinate to form bis-olefin adducts and

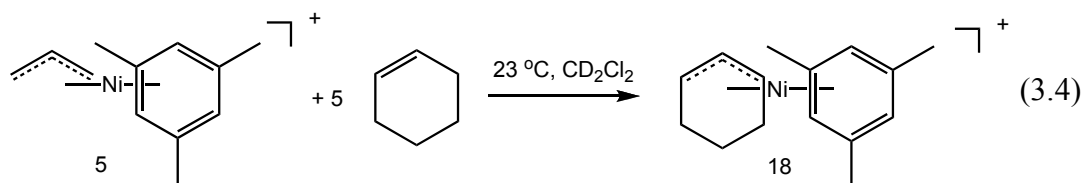
then oligomerize in the case of the Pd complexes, while in the case of the Ni complexes, α -olefins isomerize and undergo hydrogen atom transfer.

To ascertain if this reactivity held true for other 1-olefins, 1-octene was added to complex **5**. The intramolecular hydrogen atom transfer reaction does take place in the presence of 1-octene. In the presence of **5**, isomerization of 5 equiv of 1-octene to the internal 2-, 3-, and 4-octenes is observed within 30 minutes at room temperature, together with the formation of (*n*-octenyl)Ni(mes)⁺, **17**, over the course of an hour (Scheme 3.6). ¹H NMR data suggests that there are two isomers in solution in approximately a 50/50 ratio. The two isomers are assigned to the 2- and 3-octenyl positional isomers of the allyl moiety. The mesitylene arene resonance shifts upfield to 6.44 ppm. The allyl resonances centered at 5.45 (1.0H, appears as two overlapping triplets) and 3.13 (2.0H, appears as overlapping multiplets) ppm are assigned to the central hydrogen and *anti* H's of both isomers, respectively. The aliphatic methylene and methyl protons for both isomers appear as multiplets centered at 1.32 and 0.95 ppm.

Scheme 3.6. Intramolecular hydrogen atom transfer with complex **5** and 1-octene.



Internal isomers of hexene also exhibit similar activity with complexes **5** and **6**. When 5 equivalents of *cis* or *trans* 2-hexene were reacted with (allyl)Ni(mes)⁺, a new allyl species, **16**, is generated, which possesses the same ¹H and ¹³C NMR spectra as observed when **5** is reacted with 1-hexene to generate **16**. Hexene isomers (*cis* and *trans* 2- and 3- isomers) are also seen in the ¹H NMR spectrum. Cyclohexene also reacts with **5** liberating an equivalent of propene and forming (cyclohexenyl)Ni(mes)⁺, **18**, (eq 3.4) as evidenced by ¹H NMR spectroscopy. Complex **18** can be synthesized independently on a preparative scale and the details of this synthesis can be found in Chapter 5 of this thesis. All of these reactions are fast and are complete within 1 h.



When complex **5** is exposed to an atmosphere of 1-butene, rapid isomerization of 1-butene to *cis* and *trans*-2-butene is observed. Within 10 min at room temperature, all of the 1-butene has isomerized, while complex **5** is still present in solution. After 24 h, all of complex **5** is consumed and dimerization of butene occurs forming internal isomers of octene. ¹H NMR resonances corresponding to (crotyl)Ni(mes)⁺ are present in the baseline (see Experimental Section for characterization). This product is generated from hydrogen atom transfer from 2-butene.

The reaction becomes more complicated when ethylene is used. Within 10 min, reaction of **6** with an atmosphere of ethylene at 23 °C, generates *cis*- and *trans*-2-butene as the major species in solution, together with remaining complex **6** and isobutylene. The observed products indicate rapid dimerization of ethylene at room temperature. After 24 h,

complex **6** is no longer present and new signals for polyethylene oligomers and other mesitylene resonances are now seen in the ^1H spectrum. There is no clear indication of a new (allyl)Ni(II) complex in solution.

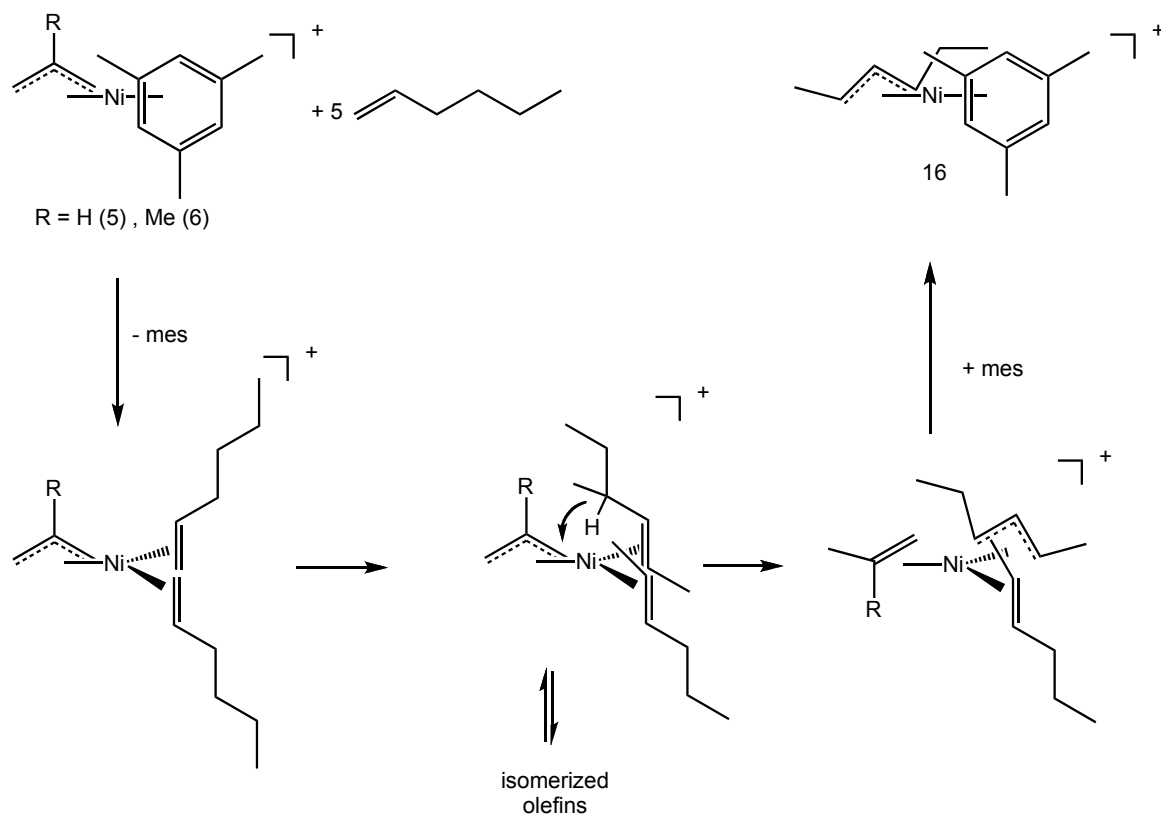
There are relatively few examples of (allyl)Ni(II) complexes that can isomerize olefins and undergo hydrogen atom transfer reactions. Wilke has reported the isomerization and dimerization of internal olefins by (allyl)Ni(II) halide dimers activated with Lewis acids in the presence of phosphines. This system dimerizes propene favoring the most substituted isomers (2-methylpentene and 2,3-dimethylbutene),²⁸ in contrast with our results yielding only isomerized linear α -olefins. Additionally, Wilke observed that isomerization of hexene generated predominantly 2,3-dimethyl-2-butene and minor amounts of the linear isomers.²⁸ Wilke's results clearly are indicative of a cationic pathway. No branched isomers have been observed under our reactions conditions.

Mechanism of Hydrogen Transfer

The proposed mechanism for intramolecular hydrogen atom transfer with 1-hexene is shown in Scheme 3.7. We have no spectral evidence, even at low temperatures that bis-olefin complexes form in the case of Ni. We propose these species as viable intermediates since they have been observed spectroscopically for the analogous Pd complexes. The first step involves the displacement of mesitylene by 2 equiv of 1-hexene to generate a very reactive bis-olefin species. We believe isomerization to the internal olefin then occurs. However, the mechanism for isomerization is not yet clear. Following isomerization, intramolecular hydrogen atom transfer from the internal hexene isomers to the allyl group would generate propene or isobutylene coordinated to a (2-hexenyl)Ni⁺ fragment. The

propene/isobutylene is displaced by mesitylene, generating the (2-hexenyl)Ni(mes)⁺ complex, **16**.

Scheme 3.7. Mechanism of hydrogen atom transfer in the reaction of 1-hexene with (2-R-allyl)Ni(mes)⁺ complexes.



Conclusions

Highly labile (allyl)Ni(II) and Pd(II) arene complexes have been synthesized and characterized. The arene in the Pd complexes is quite labile, and is rapidly displaced by diethyl ether. The (allyl)Pd(II) compounds coordinate two equiv of acyclic and cyclic olefins, as well as alkynes, to yield bis-olefin or bis-alkyne complexes, which exchange with free olefin/alkyne on the NMR timescale at low temperatures. At room temperature

oligomerization is observed. The dynamics of olefin/alkyne exchange were measured for the (allyl)Pd(II) bis-olefin/alkyne complexes. The (allyl)Ni(II) complexes reacted differently to form new allyl species, after intramolecular hydrogen atom transfer. This reaction is observed with cyclic and acyclic olefins. We are currently studying this reaction to better understand the mechanism of hydrogen atom transfer and how these results may help elucidate the mechanism of chain transfer in the polymerization of 1,3-dienes.

Experimental

General Considerations.

All reactions, unless otherwise stated, were conducted under an atmosphere of dry, oxygen free argon atmosphere using standard high-vacuum, Schlenk, or drybox techniques. Argon was purified by passage through BASF R3-11 catalyst (Chemalog) and 4Å molecular sieves. All nickel and palladium catalysts were stored under argon in an M.Braun glovebox at -35 °C. ^1H , ^{13}C , and ^{19}F NMR spectra were recorded on a Bruker DRX 500 MHz, a Bruker DRX 400 MHz, or a Bruker 300 MHz spectrometer. Chemical shifts are referenced relative to residual $\text{CH}(\text{D})\text{Cl}_2$ (δ 5.32 for ^1H) and $^{13}\text{CD}_2\text{Cl}_2$ (δ 53.8 for ^{13}C) in CD_2Cl_2 and CHCl_2F (δ 7.16 for ^1H) in CDCl_2F . Chemical shift assignments were supported through 2D HMQC and ^1H - ^1H -COSY experiments. Elemental analyses were performed by Robertson Microlit Laboratories of Madison, NJ.

Materials.

All solvents were deoxygenated and dried by passage over columns of activated alumina.^{29, 30} CD_2Cl_2 , purchased from Cambridge Laboratories, Inc., was dried over CaH_2 , vacuum transferred to a Teflon sealable Schlenk flask containing 4Å molecular sieves, and degassed via three freeze-pump-thaw cycles. CDCl_2F was synthesized according to literature

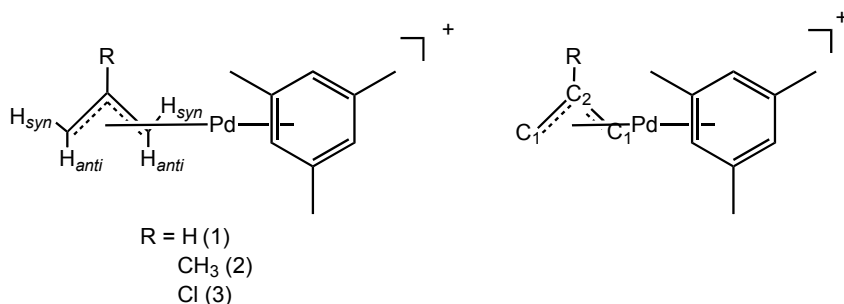
methods.³¹ 1-Hexene, *cis*-2-hexene, *trans*-2-hexene, 1-octene, cyclooctene, and cyclohexene were purchased from Aldrich and dried over CaH₂ and vacuum transferred to a Teflon sealable Schlenk flask. 1-Butene was purchased from Aldrich and 99.99% ethylene was purchased from National Welders and used as received. Ni[COD]₂, [(2-methallyl)NiCl]₂, and B(C₆F₅)₃ were purchased from Strem. PdCl₂ was purchased from J&J Materials and used as received. Carbon monoxide was purchased from National Welders and used as received. NaB(Ar_F)₄ (Ar_F = 3,5-(CF₃)₂C₆H₃) was synthesized using literature methods.³² Mesitylene (Mes), 2-butyne, 2,3-dichloropropene, 3-bromo-2-methyl-propene, allyl chloride, and allyl bromide were purchased from Aldrich and used without further purification. *tert*-Butyl ethylene purchased from Aldrich was distilled prior to use and hexamethyl benzene was purchased from Aldrich and sublimed prior to use. [(allyl)NiBr]₂, [(2-methallyl)NiBr]₂, [(allyl)NiCl]₂,²⁶ [(allyl)PdBr]₂, [(allyl)PdCl]₂, [(2-Cl-allyl)PdCl]₂, [(2-methallyl)PdBr]₂, and [(2-methallyl)PdCl]₂²³⁻²⁵ were synthesized according to literature methods.

Spectral data for [B(Ar_F)₄]⁻. The ¹H and ¹³C spectral data for the [B(Ar_F)₄]⁻ counteranion were unchanged for all Ni(II) cationic complexes and are not be included in the characterization unless otherwise stated. ¹H NMR (400 MHz, CD₂Cl₂, 20 °C): δ 7.72 (s, 4H, Ar_F H_p), 7.57 (s, 8H, Ar_F H_o). ¹³C{¹H} NMR (101 MHz, CD₂Cl₂, 20 °C): δ 162.1 (q, ¹J_{C-B} = 49.8 Hz, Ar_F C_{ipso}), 135.2 (s, Ar_F C_o), 129.2 (qq, ³J_{C-B} = 3.0 Hz, ³J_{C-F} = 34.4 Hz, Ar_F CF₃), 122.3 (q, ¹J_{C-F} = 273.2 Hz, Ar_F CF₃), 117.8 (bt, Ar_F C_p).

General Procedure for the Synthesis of [(Allyl)Pd(Arene)][SbF₆] Complexes.

Under an argon atmosphere, the corresponding palladium halide dimer was dissolved in dry methylene chloride (20 mL) and the resulting yellow solution was stirred at room temperature for five minutes to dissolve the solid. Four equivalents of the corresponding

arene were then added via syringe, and the resulting solution cooled to -78 °C. A solution of two equivalents silver hexafluoroantimonate in 5 mL methylene chloride was then added dropwise at -78 °C and the mixture was stirred for ca. 30 min at low temperature before the solution was allowed to warm slowly to room temperature. The resulting solution was cannula filtered and the solvent evaporated in vacuo. The product was washed with 3 x 10 mL of pentane and dried under vacuum to yield product as a yellow powder, which was immediately stored in the glove box at -35 °C to prevent thermal degradation.



[(Allyl)Pd(mes)][SbF₆] (1). [(Allyl)PdBr]₂ (0.160 g, 0.440 mmol), mesitylene (240 μ L, 1.76 mmol), and AgSbF₆ (0.300 g, 0.880 mmol). Yield: 0.419 g (94%). ¹H NMR (400 MHz, CD₂Cl₂, 25 °C): δ 7.03 (s, 3H, Mes_{Ar}), 5.65 (m, 1H, R = H_c), 4.54 (d, 2H, ³J_{H-H} = 4.8 Hz, H_{syn}), 3.30 (d, 2H, ³J_{H-H} = 11.4 Hz, H_{anti}), 2.44 (s, 9H, MesCH₃). ¹³C{¹H} NMR (400 MHz, CD₂Cl₂, 0 °C): δ 133.4 (s, MesC_{ipso}), 116.8 (s, MesC_{Ar}), 109.1 (s, C₂), 65.7 (s, C₁), 20.9 (s, MesCH₃). Anal. Calcd for C₁₂H₁₇F₆SbPd: C, 28.63; H, 3.41. Found: C, 28.60; H, 3.34.

[(2-Methallyl)Pd(mes)][SbF₆] (2). [(2-Methallyl)PdBr]₂ (0.350 g, 0.720 mmol), mesitylene (500 μ L, 2.88 mmol), and AgSF₆ (0.600 g, 1.44 mmol). Yield: 0.677 g (82%). ¹H NMR (400 MHz, CD₂Cl₂, 25 °C): δ 7.03 (s, 3H, Mes_{Ar}), 4.32 (s, 2H, H_{syn}), 3.10 (s, 2H, H_{anti}), 2.44 (s, 9H, MesCH₃), 2.08 (s, 3H, R = CH₃). ¹³C{¹H} NMR (400 MHz, CD₂Cl₂, 0 °C): δ 133.7 (s,

MesC_{ipso}), 126.9 (s, C₂), 117.4 (s, MesC_{Ar}), 64.6 (s, C₁), 21.7 (s, R = CH₃), 20.9 (s, MesCH₃).

Anal. Calcd for C₁₃H₁₉F₆SbPd: C, 30.17; H, 3.71. Found: C, 29.99; H, 3.59.

[(2-Cl-allyl)Pd(mes)][SbF₆] (3). [(2-Cl-allyl)PdCl]₂ (0.192 g, 0.440 mmol), mesitylene (240 μ L, 1.76 mmol), and AgSbF₆ (0.302 g, 0.880 mmol). Yield: 0.393 g (83%). ¹H NMR (400 MHz, CD₂Cl₂, 25 °C): δ 7.12 (s, 3H, Mes_{Ar}), 4.72 (s, 2H, H_{syn}), 3.57 (s, 2H, H_{anti}), 2.44 (s, 9H, ArCH₃). ¹³C{¹H} NMR (400 MHz, CD₂Cl₂, 25 °C): δ 134.0 (s, MesC_{ipso}), 124.9 (s, C₂), 117.1 (s, MesC_{Ar}), 65.6 (s, C₁), 20.9 (s, MesCH₃). Anal. Calcd for C₁₂H₁₆F₆SbPd: C, 26.79; H, 3.00. Found: C, 27.70; H, 3.23.

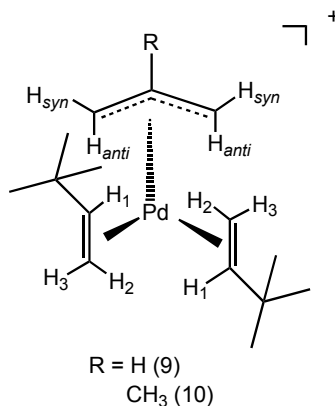
[(Allyl)Pd(C₆Me₆)][SbF₆] (4). [(2-Methallyl)PdCl]₂ (0.160 g, 0.440 mmol), hexamethylbenzene (0.286 g, 1.76 mmol), and AgSbF₆ (0.302 g, 0.880 mmol). Yield: 0.370 g (76%). ¹H NMR (400 MHz, CD₂Cl₂, 25 °C): δ 5.55 (m, 1H, R = H_c), 4.10 (d, ³J_{H-H} = 6.5, 2H, H_{syn}), 3.01 (d, ³J_{H-H} = 11.5 Hz, 2H, H_{anti}), 2.50 (s, 18H, hmbCH₃). ¹³C{¹H} NMR (400 MHz, CD₂Cl₂, 25 °C): δ 126.5 (s, hmbC_{ipso}), 109.1 (s, C₂), 64.0 (s, C₁), 17.2 (s, hmbCH₃). Anal. Calcd for C₁₅H₂₃F₆SbPd: C, 33.02; H, 4.26. Found: C, 33.33; H, 4.31.

¹H Line Broadening Experiments for the Exchange of Bound with Free Mesitylene.

Three screw-cap NMR tubes were each charged with [(allyl)Pd(mes)][SbF₆], **1**, (0.011 g, 0.020 mmol) and dissolved in CD₂Cl₂. **2** (4.0 μ L, 0.040 mmol), **4** (8.0 μ L, 0.080 mmol), and **6** (12 μ L, 0.120 mmol) equivalents of mesitylene were added respectively for a total volume of 500 μ L. The tubes were quickly shaken to allow for mixing and ¹H NMR spectra were recorded for each sample at low temperature after 5 minutes of equilibration. Due to poor solubility, NMR spectra could not be recorded below ca. -80 °C; however the changes in line-width at half-height of the coordinated mesitylene resonance (δ 7.90 ppm) were monitored for each of the three samples at -77 °C and -67 °C. The rate constant was calculated using the

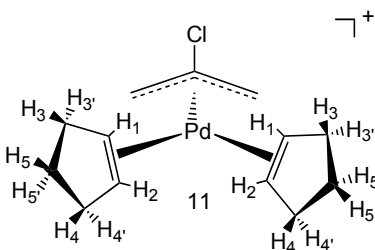
slow exchange approximation to yield $k_{\text{ex}} = 22$, 16, and 16 s^{-1} for 6, 4, and 2 equivalents of added mesitylene, respectively, at $-67\text{ }^{\circ}\text{C}$: $k_{\text{ex}} = \pi(\Delta\omega)$ where $\Delta\omega$ (6 equiv) = 6.9 Hz ($\Delta G^{\ddagger} = 10.7\text{ kcal/mol}$); $\Delta\omega$ (4 equiv) = 5.0 Hz ($\Delta G^{\ddagger} = 10.8\text{ kcal/mol}$); $\Delta\omega$ (2 equiv) = 5.1 Hz ($\Delta G^{\ddagger} = 10.8\text{ kcal/mol}$).

Synthesis of (Allyl)Pd(II) Bis-Olefin Complexes.



In situ generation of [(allyl)Pd(TBE)₂][SbF₆] (9). A screw-cap NMR tube was charged with [(allyl)Pd(mes)][SbF₆], **1**, (0.011 g, 0.020 mmol) and dissolved in ca. 400 μL CD_2Cl_2 . The tube was placed in a $-78\text{ }^{\circ}\text{C}$ bath and 2 equivalents *tert*-butyl ethylene (TBE) were added via syringe. The tube was shaken to allow for mixing and a color change from yellow to colorless was observed. Exchange of bound and free TBE occurs at $-95\text{ }^{\circ}\text{C}$ on the NMR time scale. ^1H NMR (400 MHz, CDCl_2F , $-120\text{ }^{\circ}\text{C}$): δ 6.24 (br. m, 1H, H₁), 6.13 (br. m, 1H, H₁), 5.78 (m, 1H, R = H_c), 5.40 (d, $^3J_{\text{H-H}} = 16.5\text{ Hz}$, 2H, H₃, other H₃ overlapping), 5.10 (br. d, 1H, H_{syn}), 5.02 (br. d, 1H, H_{syn}), 4.77 (d, $^3J_{\text{H-H}} = 8.5\text{ Hz}$, 1H, H₂), 4.41 (d, $^3J_{\text{H-H}} = 9.0\text{ Hz}$, 1H, H₂), 3.89 (d, $^3J_{\text{H-H}} = 13.0\text{ Hz}$, 1H, H_{anti}), 3.25 (d, $^3J_{\text{H-H}} = 12.5\text{ Hz}$, 1H, H_{anti}), 1.06-0.98 (br. s, 18H, TBE-CH₃). Characteristic shifts for free mesitylene: ^1H (400 MHz, CDCl_2F , $-120\text{ }^{\circ}\text{C}$): δ 6.79 (s, 3H, mes_{Ar}), 2.20 (s, 9H, mes_{CH₃}).

In situ generation of [(2-methallyl)Pd(TBE)₂][SbF₆] (10). A screw-cap NMR tube was charged with [(2-methallyl)Pd(mes)][SbF₆], **2**, (0.012 g, 0.020 mmol) dissolved in ca. 500 μ L CD₂Cl₂. The tube was placed in a -78 °C bath and 2 equivalents TBE were added via syringe. The tube was quickly shaken to allow for mixing and a color change from yellow to colorless was observed. Exchange of bound and free TBE occurs at -60 °C on the NMR time scale. ¹H NMR (500 MHz, CD₂Cl₂, -40 °C): δ 6.32 (m, 1H, H₁), 6.25 (m, 1H, H₁), 5.36 (m, 1H, H₃), 5.30 (m, 1H, H₃), 4.84 (s, 2H, H_{syn}), 4.81 (d, 1H, H₂, masked by H_{syn}), 4.45 (d, ³J_{H-H} = 8.5 Hz, 1H, H₂), 3.81 (s, 1H, H_{anti}), 3.16 (s, 1H, H_{anti}), 1.99 (s, 3H, CH₃), 1.06-0.98 (br. s, 18H, TBE-CH₃). Characteristic shifts for free mesitylene: ¹H NMR (500 MHz, CD₂Cl₂, -50 °C): δ 6.79 (s, 3H, Mes_{Ar}), 2.20 (s, 9H, Mes_{CH₃}).

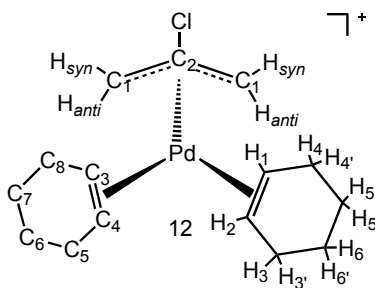


In situ generation of [(2-Cl-allyl)Pd(cyclopentene)₂][SbF₆] (11). A screw-cap NMR tube was charged with [(2-Cl-allyl)Pd(mes)][SbF₆], **3**, (0.010 g, 0.019 mmol) dissolved in 500 μ L CD₂Cl₂. The tube was then placed in a -78 °C bath and 5 equivalents of cyclopentene (10 μ L, 0.093 mmol) were added via syringe. The tube was inverted quickly to allow mixing and the solution turned from yellow to colorless. Exchange of free and bound olefin occurs on the NMR time scale at -40 °C. ¹H NMR (500 MHz, CD₂Cl₂, -76 °C): δ 6.16 (s, 2H, H₁ or H₂), 5.86 (s, 2H, H₂ or H₁), 5.28 (s, 2H, H_{syn}), 3.96 (s, 2H, H_{anti}), 2.51 (br. m, 8H, H_{4,4'} and H_{3,3'}), 1.92 (br. m, 2H, H₅ or H_{5'}), 1.05 (m, 2H, H_{5'} or H₅). ¹³C{¹H}NMR (100 MHz, CD₂Cl₂, -87 °C): δ 126.8 (C₂), 113.7 (C₃ or C₄), 113.3 (C₃ or C₄), 83.6 (C₁), 35.0 (C₅ or C₇), 34.8 (C₇ or

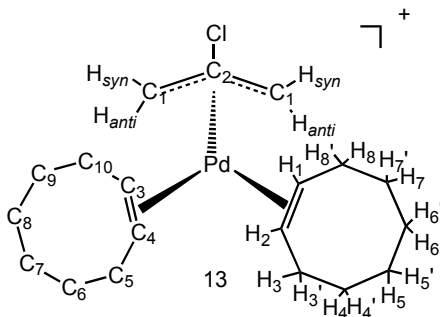
C₅), 22.6 (C₆). Characteristic peaks for free mesitylene: ¹H NMR (500 MHz CD₂Cl₂, -76 °C): δ 6.79 (s, 3H, mes_{Ar}), 2.24 (s, 9H, mes_{Ar}CH₃). ¹³C{¹H} NMR (100 MHz, CD₂Cl₂, -87 °C): δ 137.7 (s, mesC_{Ar}CH₃), 126.8 (s, mesC_{Ar}H), 21.4 (s, CH₃). Characteristic peaks for free cyclopentene: ¹H NMR (500 MHz CD₂Cl₂, -76 °C): δ 5.76 (s, 2H, H_{1,2}), 2.27 (t, ³J_{H-H} = 7.5 Hz, 4H, H_{3,4}), 1.78 (m, 2H, H₅). ¹³C{¹H} NMR (100 MHz, CD₂Cl₂, -87 °C): δ 130.8 (s, C_{3,4}), 32.6 (s, C_{5,7}), 23.0 (s, C₆).

Dynamic Measurements using ¹H Line Broadening.

¹H Line broadening experiments to determine the mechanism of displacement of bound cyclopentene by free cyclopentene. Three separate screw-cap NMR tubes were charged with [(2-Cl-allyl)Pd(mes)][SbF₆] (**3**) (0.010 g, 0.019 mmol). In a -78 °C dry ice-acetone bath, 6 equiv (0.01 μL, 0.11 mmol), 9 equiv (0.01 μL, 0.17 mmol), and 12 equiv (0.01 μL, 0.22 mmol) respectively, of cyclopentene were added to the three NMR tubes, followed by the addition of CD₂Cl₂ to reach a total volume of 500 μL. Broadening of the bound vinyl ¹H resonance (6.16 ppm) was monitored between -56 °C and -45 °C. The initial half height line width at -56 °C was 12 Hz for 6 and 9 equiv, and 13 Hz for 12 equiv; and at -45 °C 22 Hz for 6 equiv, 23 Hz for 9 equiv and 24 Hz for 12 equiv. The rate constant was calculated using the slow exchange approximation to give k_{ex} = 31 s⁻¹ at 6 equiv, 35 s⁻¹ at 9 equiv 33 s⁻¹ at 12 equiv: k_{ex} = π(Δω) where Δω = 10 Hz (ΔG[‡] = 11.7 kcal/mol) for 6 equiv, 11 Hz (ΔG[‡] = 11.7 kcal/mol) for 9 equiv, and 11 Hz (ΔG[‡] = 11.7 kcal/mol) for 12 equiv.

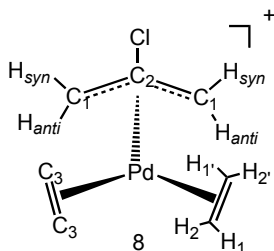


In situ generation of [(2-Cl-allyl)Pd(cyclohexene)₂][SbF₆] (12). This compound was generated according to the above procedure, using **3** (0.010 g, 0.019 mmol) dissolved in 500 μ L of CD₂Cl₂ and 5 equivalents of cyclohexene (10 μ L, 0.0980 mmol) as the olefin. ¹H NMR (500 MHz, CD₂Cl₂, -77 °C): δ 6.47 (s, 2H, H₁ or H₂), 5.95 (s, 2H, H₂ or H₁), 4.82 (s, 2H, H_{syn}), 4.03 (s, 2H, H_{anti}), 2.40 (bm, 8H, H_{4,4'} and H_{3,3'}), 1.05 (m, 8H, H_{5,5'} and H_{6,6'}). ¹³C{¹H}NMR (100 MHz, CD₂Cl₂, -87 °C): δ 130.0 (s, C₂), 116.4 (s, C₃ or C₄), 114.3 (s, C₃ or C₄), 80.6 (s, C₁), 26.7 (s, C₅ or C₈), 26.4 (s, C₅ or C₈), 21.2 (s, C₆ or C₇), 20.9 (s, C₆ or C₇). Characteristic peaks for free cyclohexene: ¹H NMR (500 MHz, CD₂Cl₂, -77 °C): δ 5.73 (s, 2H, H_{1,2}), 2.24 (bs, 4H, H_{3,4}), 1.15 (bs, 4H, H_{5,6}). ¹³C{¹H} NMR (100 MHz, CD₂Cl₂, -87 °C): δ 127.3 (s, C_{3,4}), 25.3 (s, C_{5,8}), 22.8 (s, C_{6,7}).



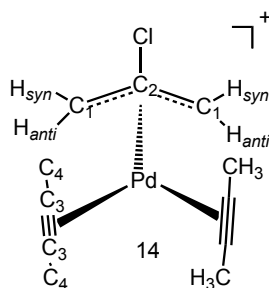
In situ generation of [(2-Cl-allyl)Pd(cyclooctene)₂][SbF₆] (13). This compound was generated according to the above procedure; in this instance **3** (0.010 g, 0.019 mmol) dissolved in 500 μ L CD₂Cl₂ and 2.2 equivalents of cyclooctene (5.2 μ L, 0.040 mmol) were employed. ¹H NMR (500 MHz, CD₂Cl₂, -50 °C): δ 6.08 (s, 2H, H₁ or H₂), 5.78 (s, 2H, H₂ or

H₁), 4.72 (s, 2H, H_{syn}), 3.94 (s, 2H, H_{anti}), 2.48 (bm, 8H, H_{8,8'} and H_{3,3'} or H_{4,4'} and H_{7,7'}), 2.35 (bm, 8H, H_{8,8'} and H_{3,3'} or H_{4,4'} and H_{7,7'}), 1.88 (bm, 8H, H_{5,5'} and H_{6,6'}). ¹³C{¹H} NMR (100 MHz, CD₂Cl₂, -51 °C): δ 132.4 (s, C₂), 117.7 (s, C₃ or C₄), 116.0 (s, C₄ or C₃), 80.7 (s, C₁), 30.3 (s, C₅ or C₁₀), 30.2 (s, C₁₀ or C₅), 28.7 (s, C₆ or C₉), 28.5 (s, C₉ or C₆), 25.8 (s, C₇ or C₈), 25.6 (s, C₈ or C₇). Characteristic NMR shifts for free cyclooctene: ¹H NMR (500 MHz, CD₂Cl₂, -50 °C): δ 5.70 (s, 2H, H_{1,2}), 2.24 (bs, 4H, H_{3,8}), 2.17 (bs, 4H, H_{4,7}), 1.51 (bs, 4H, H_{5,6}). ¹³C{¹H} NMR (100 MHz, CD₂Cl₂, -51 °C): δ 130.2 (s, C_{3,4}), 29.3 (s, C_{5,10}), 26.3 (s, C_{6,9}), 25.6 (s, C_{7,8}).



In situ generation of [(2-Cl-allyl)Pd(ethylene)₂][SbF₆] (8). A J-Young NMR tube was charged with [(2-Cl-allyl)Pd(mes)][SbF₆] (**3**) (0.010 g, 0.019 mmol) dissolved in 500 μL CD₂Cl₂. The yellow solution was frozen at -196 °C, and approximately 3 equivalents (93 torr, 0.056 mmol) of ethylene was admitted via a 10.94 mL calibrated gas bulb on a high vacuum line. The tube was then moved to a -78 °C dry ice-acetone bath. The tube was inverted to allow mixing and the solution turned from yellow to colorless. ¹H NMR (500 MHz CD₂Cl₂, -90 °C): δ 5.24 (m, 4H, H_{1,1'} or H_{2,2'}), 5.00 (m, 4H, H_{2,2'} or H_{1,1'}), 5.14 (s, 2H, H_{syn}), 3.91 (s, 2H, H_{anti}). ¹³C{¹H} NMR (100 MHz, CD₂Cl₂, -90 °C) δ 128.3 (s, C₂), 96.4 (s C₃), 80.7 (s, C₁). Characteristic Peaks for free ethylene: ¹H NMR (500 MHz CD₂Cl₂, -90 °C): δ 5.33 (s, 2H, vinyl). ¹³C{¹H} NMR (100 MHz, CD₂Cl₂, -90 °C): 122.7 (s, C₃).

Using line-broadening techniques, the rate of exchange of bound and free ethylene was determined upon the addition of ca. 3 equivalents of ethylene. Broadening of the coordinated ethylene groups (^1H NMR resonance 5.19 ppm) was monitored between $-77\text{ }^\circ\text{C}$ to $-56\text{ }^\circ\text{C}$. The initial half height width at $-77\text{ }^\circ\text{C}$ was 16 Hz. The line width was 18 Hz at $-66\text{ }^\circ\text{C}$ and 24 Hz at $-56\text{ }^\circ\text{C}$. The rate constants calculated using the slow exchange approximation are $k_{\text{ex}} = 7.4\text{ s}^{-1}$ at $-66\text{ }^\circ\text{C}$ and $k_{\text{ex}} = 21\text{ s}^{-1}$: where $\Delta\omega = 2.4\text{ Hz}$ at $-66\text{ }^\circ\text{C}$ and $\Delta\omega = 7.7\text{ Hz}$ at $-56\text{ }^\circ\text{C}$. The average $\Delta G^\ddagger_{\text{avg}} = 11.4\text{ kcal/mol}$, assuming a dissociative mechanism as previously observed for cyclopentene exchange.

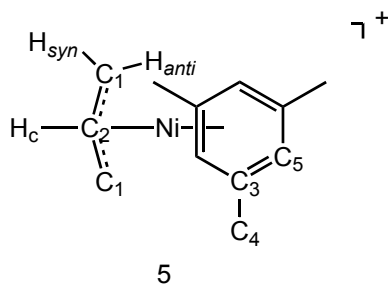


In situ generation of [(2-Cl-allyl)Pd(2-butyne)₂][SbF₆] (14). This compound was generated according to the above procedure, with [(2-Cl-allyl)Pd(mes)][SbF₆] (**3**) (0.020 g, 0.037 mmol) dissolved in 500 μL CD_2Cl_2 using 2-butyne (14 μL , 0.098 mmol) as the alkyne. ^1H NMR (500 MHz, CD_2Cl_2 , $-90\text{ }^\circ\text{C}$): δ 4.83 (s, 2H, H_{syn}), 3.94 (s, 2H, H_{anti}), 2.18 (s, 12H, butyne- CH_3). $^{13}\text{C}\{^1\text{H}\}$ NMR (100 MHz, CD_2Cl_2 , $25\text{ }^\circ\text{C}$): δ 132.1 (s, C_2), 75.8 (s, C_1), 68.6 (s, C_3), 7.32 (s, C_4). Characteristic Peaks for free 2-butyne: ^1H NMR (500 MHz, CD_2Cl_2 , $-90\text{ }^\circ\text{C}$): δ 1.70 (s, 6H, CH_3). $^{13}\text{C}\{^1\text{H}\}$ NMR (100 MHz, CD_2Cl_2 , $-90\text{ }^\circ\text{C}$): δ 74.6 (s, C_3), 3.3 (s, C_4).

Using line-broadening techniques, the rate of exchange of bound and free 2-butyne was determined for the addition of ca. 3 equivalents of 2-butyne. Broadening of the methyl resonance (2.13 ppm) of 2-butyne was monitored between $-66\text{ }^\circ\text{C}$ and $-24\text{ }^\circ\text{C}$. The initial half

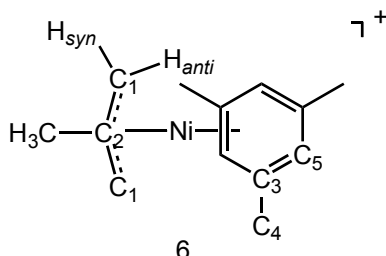
height line width at -66 °C was 3.7 Hz. The line widths were measured as 5.2 and 15 Hz at -45 °C and -24 °C, respectively. The rate constants, calculated using the slow exchange approximation, are $k_{\text{ex}} = 4.6 \text{ s}^{-1}$ at -45 °C and $k_{\text{ex}} = 36 \text{ s}^{-1}$ at -24 °C: where $\Delta\omega = 1.5 \text{ Hz}$ at -45 °C and $\Delta\omega = 11.6 \text{ Hz}$ at -24 °C. $\Delta G_{\text{avg}}^{\ddagger} = 12.6 \text{ kcal/mol}$ assuming a dissociative exchange mechanism as previously observed for cyclopentene exchange.

Synthesis of (2-R-Allyl)Ni(Arene)⁺ Complexes.

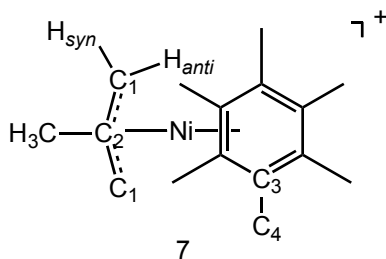


[(Allyl)Ni(mes)][B(Ar_F)₄] (5). A flame dried Schlenk flask was charged with [(allyl)NiBr]₂ (0.270 g, 0.751 mmol) and NaB(Ar_F)₄ (1.33 g, 1.50 mmol). The flask was cooled to -80 °C and Et₂O (12.0 mL) was added. To the stirring deep orange-red solution was added mesitylene (550 μL, 3.95 mmol) and the reaction was warmed to 0 °C and allowed to stir for 1h. The volatiles were then removed in vacuo and the red residue was dissolved CH₂Cl₂ and filtered through Celite. The solvent was removed in vacuo and the solid product was washed with pentane (3 x 10 mL). The pentane was decanted and the product was dried in vacuo to give **5** (0.920 g, 0.849 mmol) in 57 % yield. Red X-ray quality crystals were obtained by dissolving **5** in CH₂Cl₂ (2.0 mL) and layering with pentane (6.0 mL) and placing in a -30 °C freezer for 2 days. ¹H NMR (300 MHz, CD₂Cl₂, 25 °C): δ 6.66 (s, 3H, Mes_{Ar}), 5.85 (m, 1H, H_c), 3.69 (d, ³J_{H-H} = 6.6 Hz, 2H, H_{syn}), 2.45 (d, ³J_{H-H} = 12.6 Hz, 2H, H_{anti}), 2.35 (s, 9H, MesCH₃). ¹³C{¹H} NMR (126 MHz, CD₂Cl₂, 25 °C): δ 124.8 (s, C₃), 109.5 (s, C₅), 107.5 (s,

C₂), 59.7 (s, C₁), 20.6 (s, C₄). ¹⁹F NMR (376 MHz, CD₂Cl₂, 25 °C): δ -63.4 (s, 24F). Anal. Calcd for C₄₄H₂₉F₂₄BNi: C, 48.79; H, 2.70. Found: C, 48.40; H, 2.68.



[(2-Methallyl)Ni(mes)][B(Ar_F)₄] (6). This complex was synthesized following the above procedure for **6** starting from [(2-Me- π -allyl)NiBr]₂ (0.101 g, 0.260 mmol), NaB(Ar_F)₄ (0.460 g, 0.519 mmol), and mesitylene (215 μ L, 1.55 mmol). Yield of **6**: 83 % (0.474 g, 0.432 mmol). ¹H NMR (400.1 MHz, CD₂Cl₂, 25 °C): δ 6.62 (s, 3H, Mes_{Ar}), 3.54 (s, 2H, H_{syn}), 2.34 (s, 2H, H_{anti}), 2.35 (s, 9H, MesCH₃) 2.13 (s, 3H, CH₃). ¹³C{¹H} NMR (126 MHz, CD₂Cl₂, 25 °C): δ 124.5 (s, C₃), 109.2 (s, C₅ overlapping C₂), 60.1 (s, C₁), 22.2 (s, CH₃ overlapping C₄). ¹⁹F NMR (376 MHz, CD₂Cl₂, 25 °C): δ -63.4 (s, 24F). Anal. Calcd for: C₄₅H₃₁F₂₄BNi: C, 49.26; H, 2.85. Found: C, 48.89; H, 2.63.



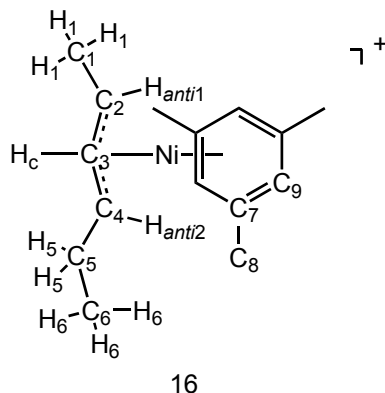
[(2-Methallyl)Ni(hexamethylbenzene)][B(Ar_F)₄] (7). A Schlenk flask was charged with (0.100 g, 0.340 mmol) of [(2-methallyl)NiCl]₂ and NaB(Ar_F)₄ (0.604 g, 0.683 mmol) and dissolved in 8.0 mL of diethyl ether in a -78 °C dry ice-acetone bath. To this, hexamethylbenzene (0.224 g, 12.2 mmol) dissolved in 2.0 mL of CH₂Cl₂ was added via

cannula. The mixture was removed from the cooling bath until a color change was observed, then the reaction mixture was held at 0 °C for an additional 2 hours. The reaction mixture was then cannula filtered into a second Schlenk, and taken to dryness in dynamic vacuum. The resulting red solid was washed with pentane (3 x 10.0 mL) and dried in vacuo. Red X-ray quality crystals were obtained by dissolving **7** in CH₂Cl₂ (2.0 mL) layering with pentane (6.0 mL) and placing in a -30 °C freezer until solvent evaporation occurred. ¹H NMR (500 MHz, CD₂Cl₂, 25 °C): δ 3.04 (s, 2H, H_{syn}), 2.31 (s, 18H, hmb_{CH3}), 2.09 (s, 2H, H_{anti}), 2.03 (s, 3H, CH₃). ¹³C{¹H} NMR (CD₂Cl₂, 100 MHz, 25 °C): δ 123.8 (s, C₂), 119.5 (s, C₃), 59.1 (s, C₁), 21.8 (s, CH₃), 17.2 (s, C₄). Anal. Calcd for: C₄₈H₃₇F₂₄BNi: C, 50.60; H, 3.27. Found: C, 50.32; H, 3.08.

In situ generation of (allyl)Ni(hmb)⁺. A screw top NMR tube was charged with **5** (0.010 g, 0.009 mmol), and dissolved in 600 μL of CD₂Cl₂. Hexamethylbenzene (0.004 g, 0.025 mmol) was added and the NMR tube was inverted to allow for mixing. (Allyl)Ni(hmb)⁺ was generated quantitatively as determined by ¹H NMR. This reaction was complete within 10 minutes. ¹H NMR (300 MHz, CD₂Cl₂, 25 °C): δ 6.80 (s, 3H, free mes, Mes_{Ar}), 5.73 (m, 1H, H_c), 3.24 (d, ³J_{H-H} = 6.6 Hz, 2H, H_{syn}), 2.31 (s, 18H, hmb_{CH3}), 2H *anti* doublet under mesitylene and hexamethylbenzene.

Addition of diethyl ether to (allyl)Ni(mes)⁺. A screw top NMR tube was charged with **5** (0.010 g, 0.009 mmol) and dissolved in 600 μL of CD₂Cl₂. Diethyl ether (4.1 μL, 0.039 mmol) was added and the solution was mixed via inversion. The formation of free mesitylene and broadened ether signals were monitored by ¹H NMR. After 3 days, slow decomposition of complex **5** (ca. 22%) had occurred as evidenced by black precipitate and free mesitylene (δ 6.79) in the ¹H NMR spectrum.

Reaction of Olefins with Complexes **5** or **6**.



In situ generation of [(2-hexenyl)Ni(mes)][B(Ar_F)₄] (16**).** A J-Young tube was charged with **5** (0.010 g, 0.009 mmol) and dissolved in CD₂Cl₂ (500 μL). 1-Hexene (4.50 μL, 0.037 mmol) was added via microliter syringe and the solution was mixed. The reaction was monitored by ¹H NMR spectroscopy at room temperature. Complete formation of (2-hexenyl)Ni(Mes)[B(Ar_F)₄], **16**, was observed within an hour.

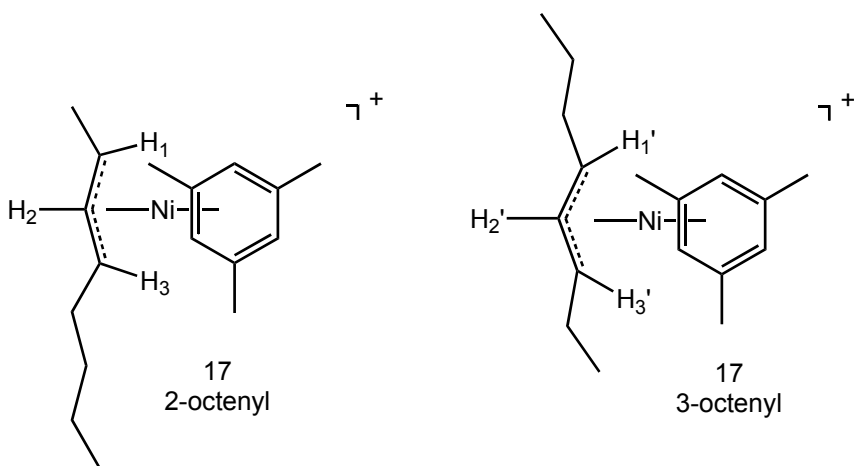
The same procedure, as described above was followed to generate **16** using *cis*-2-hexene. Complex **5** (0.099 g, 0.009 mmol) was treated with *cis*-2-hexene (5.70 μl, 0.045 mmol) in CD₂Cl₂ (600 μL). The reaction was complete within 1 h.

The same procedure, as described above, was followed to generate **16** using *trans*-2-hexene. Complex **5** (0.010 g, 0.009 mmol) was treated with *trans*-2-hexene (5.70 μl, 0.045 mmol) in CD₂Cl₂ (600 μL). The reaction was complete within 1 h.

To obtain complete NMR characterization of **16**, the volatiles were removed in vacuo and the solid residue was redissolved in CD₂Cl₂ in the drybox. ¹H NMR (400 MHz, CD₂Cl₂, 25 °C): δ 6.44 (s, 3H, Mes_{Ar}), 5.46 (t, ³J_{H-H} = 11.2 Hz, 1H, H_c), 3.14 (m, 2H, H_{anti1} overlapping H_{anti2}), 2.32 (s, 9H, Mes_{CH₃}), 1.32 (pent., ³J_{H-H} = 6.4 Hz, 2H, H₅), 1.05 (t, ³J_{H-H} = 7.2, 3H, H₆), 1.01 (d, 3H, ³J_{H-H} = 6.8 Hz, H₁). ¹³C{¹H} NMR (101 MHz, CD₂Cl₂, 25 °C): δ 123.2 (s,

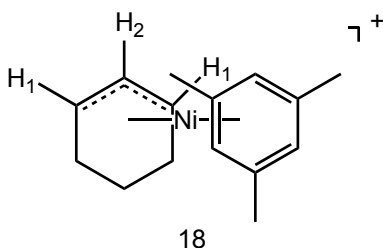
C₇), 109.0 (s, C₉), 105.4 (s, C₃), 83.0 (s, C₄), 76.3 (s, C₂), 26.4 (s, C₄), 19.5 (s, C₈), 18.8 (s, C₁), 12.6 (s, C₆). Characteristic ¹H NMR shifts for propene: ¹H NMR (400 MHz, CD₂Cl₂, 25 °C): δ 5.84 (m, 2H, H_{vinyl}), 5.03 (d, ³J_{H-H} = 16.0 Hz, 1H, H_{trans}), 4.93 (d, ³J_{H-H} = 8.0 Hz, 1H, H_{cis}), 1.71 (d, 3H, ³J_{H-H} = 8.0 Hz, CH₃). Characteristic ¹H NMR shifts for isobutylene: ¹H NMR (400 MHz, CD₂Cl₂, 25 °C): δ 4.65 (s, 2H, vinyl CH₂), 1.72 (s, 6H, CH₃).

Low temperature ¹H NMR study of the reaction of **6 and 1-hexene.** A screw top NMR tube was charged with complex **6** (0.010 g, 0.009 mmol) and dissolved in CD₂Cl₂ (600 μL). The tube was placed in a dry ice/acetone bath at -80 °C. At this point, 1-hexene (4.4 μL, 0.035 mmol) was added via microliter syringe. The reaction was monitored by low temperature ¹H NMR spectroscopy. No change in the spectrum occurred until -30 °C. At this temperature isomerization occurred. Monitoring the reaction at this temperature, showed isomerization was complete within 1.5 h. At -10 °C, complex **16** began to grow in while starting complex **6** was slowly being consumed.

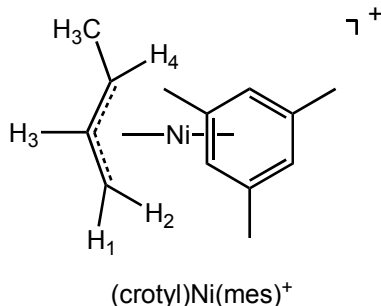


In situ generation of (2/3-octenyl)Ni(mes)][B(Ar_F)₄] (17**).** A J-Young tube was charged with **5** (0.011 g, 0.010 mmol) and dissolved in CD₂Cl₂ (600 mL). The solution was mixed to ensure the catalyst was completely dissolved. 1-Octene (8.0 μL, 0.051 mmol) was then added and the NMR tube was inverted to mix the sample. The reaction was monitored by ¹H

NMR spectroscopy and complete conversion to complex **17** was obtained within an hour. There appears to be two isomers in approximately 50/50 mixture in solution. These are tentatively assigned as the 2- and 3-octenyl positional isomers of complex **17**. ^1H NMR (400 MHz, CD_2Cl_2 , 25 °C): δ 6.43 (s, 3H, Mes_{Ar}), 5.45 (t, 1H, overlapping H_2 and $\text{H}_{2'}$), 3.12 (m, 2H, overlapping $\text{H}_{1\&3}$ and $\text{H}_{1'\&3'}$), 2.31 (s, 9H, Mes_{CH_3}), the methylene groups appear in a range from 1.60-1.29 ppm and the methyl groups appear in a range from 1.10-0.88 ppm for both isomers.



In situ generation of [(Cyclohexenyl)Ni(mes)][B(Ar_F)₄] (18**).** Complex **5** (0.0102 g, 0.0094 mmol) was added to a J-Young tube and dissolved in CD_2Cl_2 (600 μL). The solution was mixed and cyclohexene (4.7 μL , 0.046 mmol) was added via syringe. The reaction was monitored by ^1H NMR spectroscopy. Formation of [(cyclohexenyl)Ni(mes)][B(Ar_F)₄], **18**, and propene were observed immediately in the ^1H NMR spectrum. Complete conversion was observed within 1 hour. ^1H NMR (400 MHz, CD_2Cl_2 , 25 °C): δ 6.55 (s, 3H, Mes_{Ar}), 5.86 (t, $^3J_{\text{H-H}} = 6.4$ Hz, 1H, H_2), 4.81 (br. t, 2H, H_1), 2.34 (s, 9H, Mes_{CH_3}), 1.50-1.00 (m, 6H, CH_2).



Reaction of 5 with 1-butene. A J-Young tube was charged with **5** (0.010 g, 0.009 mmol) and dissolved in CD₂Cl₂ (500 μ l). The NMR tube was removed from the drybox and cooled to -78 °C and evacuated. A lecture cylinder of 1-butene was attached to a glass T, which was attached to the J-Young tube. The whole system was evacuated and then back filled with an atmosphere of 1-butene. The J-Young tube was opened and 1-butene was condensed in the tube. Extra caution was used to avoid over-pressure in the tube. The reaction was monitored by ¹H NMR spectroscopy. Isomerization to the internal 2-butene is observed immediately. Dimerization to internal octenes is observed, as well as minor amounts of [(crotyl)Ni(Mes)][B(Ar_F)₄]. ¹H NMR (300 MHz, CD₂Cl₂, 25 °C): δ 6.55 (s, 3H, Mes_{Ar}), 5.65 (m, 1H, H₃), 3.45 (d, ³J_{H-H} = 6.6 Hz, 1H, H₁), 3.35 (m, 1H, H₄), 2.34 (s, 9H, MesCH₃), ~ 2.2 (d, 1H, under mes, H₂), 1.08 (d, ³J_{H-H} = 6.6 Hz, 3H, CH₃).

Reaction of 6 with ethylene. A dry J-Young tube was charged with **6** (0.010 g, 0.009 mmol) and dissolved in CD₂Cl₂. The reaction was mixture by inversion and cooled to -78 °C. The tube was evacuated and backfilled with a pressure of ethylene. The reaction was warmed to room temperature and monitored by ¹H NMR spectroscopy. Within about 5 minutes, the major products observed in the ¹H NMR spectrum were *cis* and *trans* 2-butenes, resulting from the dimerization of ethylene. After long reaction times (1-2 days) degradation of the mesitylene and the [B(Ar_F)₄] counteranion is observed.

Crystal Structure Determination of **5 and **7**.**

The crystallographic information for **5** and **7** is reported in Table II.1. The data was obtained on a Bruker SMART APEX-2 X-ray diffractometer at -173 °C using Mo-K α radiation for **5** and Cu-K α radiation for **7**. A list of selected bond angles and lengths for complex **5** are located in the Appendix on Tables II.2 and II.3 and for complex **7** on Tables II.4 and II.5.

References

1. Connor, E. F.; Younkin, J. I.; Waltman, A. W.; Grubbs, R. H. *Chem. Commun.* **2003**, 2272-2273.
2. Ittel, S. D.; Johnson, L. K.; Brookhart, M. *Chem. Rev.* **2000**, *100*, 1169-1203.
3. Johnson, L. K.; Killian, C. M.; Brookhart, M. *J. Am. Chem. Soc.* **1995**, *117*, 6414-6415.
4. Coates, G. W.; Hustad, P. D.; Reinhartz, S. *Angew. Chem. Int. Ed.* **2002**, *41*, 2236-2257.
5. Leatherman, M. D.; Svejda, S. A.; Johnson, L. K.; Brookhart, M. *J. Am. Chem. Soc.* **2003**, *125*, 3068-3081.
6. Goodall, B. L. Cycloaliphatic polymers via late transition metal catalysis. In *Late Transition Metal Polymerization Catalysis*, Rieger, B., Saunders Baugh, L., Kacker, S., Striegler, S. Eds.; Wiley-VCH: Weinheim, **2003**; 101-133.
7. Goodall, B. L.; Benedikt, G. M.; McIntosh, L. H. I.; Barnes, D. A. U. S. 5468819, **1995**.
8. Klabunde, K. J.; Anderson, B. B.; Bader, M.; Radonovich, L. J. *J. Am. Chem. Soc.* **1978**, *100*, 1313-1314.
9. Gastinger, R. G.; Anderson, B. B.; Klabunde, K. J. *J. Am. Chem. Soc.* **1980**, *102*, 4959-4966.
10. Bennett, M. A.; Smith, A. K. *J. Chem. Soc. Dalton Trans.* **1974**, 233-241.
11. Taube, R.; Sylvester, G. Stereospecific Polymerization of Butadiene or Isoprene. In *Applied Homogeneous Catalysis with Organometallic Complexes*, Cornils, B., Herrmann, W. A. Eds.; VCH: Weinheim, Germany, **1996**; 280-318.
12. Porri, L.; Natta, G.; Gallazzi, M. C. *J. Polym. Sci., Part C* **1967**, 2525-2537.
13. Durand, J. P.; Dawans, F.; Teyssié, P. *J. Polym. Sci. Part A* **1970**, *8*, 979-990.
14. Babitskii, B. D.; Dolgoplosk, B. A.; Kormer, V. A.; Lobach, M. I.; Tinyakova, E. I.; Yakovlev, V. A. *Isv. Akad. Nauk SSSR Ser. Chem.* **1965**, 1507.
15. Taube, R.; Gehrke, J. P.; Böhme, P.; Scherzer, K. *J. Organomet. Chem.* **1991**, *410*, 403-416.

16. Taube, R.; Langlotz, J.; Sieler, J.; Gelbrich, T.; Tittes, K. *J. Organomet. Chem.* **2000**, 597, 92-104.
17. Taube, R.; Wache, S. *J. Organomet. Chem.* **1992**, 428, 431-442.
18. O'Connor, A. R.; White, P. S.; Brookhart, M. *J. Am. Chem. Soc.* **2007**, 129, 4142-4143.
19. Mabbott, D. J.; E., M. B.; Maitlis, P. M. *J. Chem. Soc. Dalton Trans.* **1977**, 294-299.
20. Goodall, B. L.; Barnes, D. A.; Benedikt, G. M.; Jayaraman, S.; McIntosh, L. H. I.; Rhodes, L. F.; Shick, R. A. *Polym. Prepr.* **1998**, 39, 216-217.
21. Cámpora, J.; Conejo, M. D. M.; Reyes, M. L.; Mereiter, K.; Passaglia, E. *Chem. Commun.* **2003**, 78-79.
22. Tobisch, S.; Taube, R. *Organometallics* **1999**, 18, 5204-5218.
23. Aranyos, A.; Szabó, K. J.; Castaño, A. M.; Bäckvall, J.-E. *Organometallics* **1997**, 16, 1058-1064.
24. Auburn, P. R.; Mackenzie, P. B.; Bosnich, B. *J. Am. Chem. Soc.* **1985**, 107, 2033-2046.
25. Dent, W. T.; Long, R.; Wilkinson, A. J. *J. Chem. Soc.* **1964**, 1585-1588.
26. Wilke, G.; Bogdanovic, B.; Heimbach, P.; Keim, W.; Kröner, M.; Oberkirch, W.; Tanaka, K.; Steinrücke, E.; Walter, D.; Zimmerman, H. *Angew. Chem. Int. Ed.* **1966**, 5, 151-164.
27. Lipian, J.; Mimna, R. A.; Fondran, J. C.; Yandulov, D.; Shick, R. A.; Goodall, B. L.; Rhodes, L. F.; Huffman, J. C. *Macromolecules* **2002**, 35, 8969-8977.
28. Wilke, G.; Bogdanovic, B. DE 1924628, **1969**.
29. Alaimo, P. J.; Peters, D. W.; Arnold, J.; Bergman, R. G. *J. Chem. Educ.* **2001**, 78, (1), 64.
30. Pangborn, A. B.; Giardello, M. A.; Grubbs, R. H.; Rosen, R. K.; Timmers, F. J. *Organometallics* **1996**, 15, 1518-1520.
31. Siegel, J. S.; Anet, F. A. *J. Org. Chem.* **1988**, 53, 2629-2630.
32. Yakelis, N. A.; Bergman, R. G. *Organometallics* **2005**, 24, 3579-3581.

CHAPTER FOUR

Polymerization of 1,3-Dienes and Styrene Catalyzed by (Allyl)Nickel(II) Complexes

Introduction

The stereoselective polymerization of 1,3-dienes has been a significant challenge and efforts have been made in both academia and industry to design metal catalysts that polymerize 1,3-dienes in a selective fashion.¹ The unique microstructures (*cis*-1,4, *trans*-1,4, 1,2, 3,4) that exist for diene polymers influence polymer properties and therefore applications and potential uses of these materials (see chapter 1). For example, *cis*-1,4-polybutadiene is important because of its industrial use for synthetic rubber production.² The integrity of synthetic rubber is highly dependent on the percent 1,4-*cis* content. There is a significant difference in the elastic properties between 98% and 99% *cis*-1,4-polybutadiene.³ Complexes containing early metals, lanthanides (Ln), and late metals have been synthesized and used as stereoselective 1,3-diene polymerization catalysts.

Early transition metal complexes in conjunction with an activator have been employed as initiators in the polymerization of 1,3-dienes. The polymer stereochemistry is highly dependent on the catalyst, temperature, and ratio of metal to MAO (methylaluminoxane).¹ CpTiCl₃ activated with MAO is highly active for *cis*-stereoselective polymerization of butadiene (BD), 2,3-dimethyl-1,3-butadiene (DMBD), and 4-methyl-

1,3-pentadiene at room temperature. Using the same catalyst system at -20 °C, yields 1,2-syndiotactic polymers with good productivity.^{4, 5} Zirconocene complexes are much less active for 1,3-diene polymerization. *Ansa*-zirconocenes with bulky substituents on the indenyl moiety are required for polymerization.⁶ Ricci has shown that a V(acac)₃/MAO catalyst can be employed as a *trans*-selective butadiene polymerization catalyst.⁷ Chromium catalysts of the type Cr(allyl)₃⁸ and CrCl₂(dmpe)^{9, 10} have also been shown to be active and produce 1,2-enchained polybutadiene.

The most active and selective catalysts are those containing lanthanides. Three types of lanthanide catalysts have been reported for 1,3-diene polymerization. Catalysts of the type LnCl₃·nL (L = THF, alcohol) and Ln(OCOR)₃ are highly effective for butadiene polymerization, where Ln commonly is neodymium, gadolinium, cerium, or praseodymium. These catalysts are highly *cis*-1,4 selective yielding up to 98% *cis*-1,4 enchained polybutadiene.¹¹⁻¹³ Lanthanide complexes derived from (allyl)₃Ln (Ln = La, Nd) are *trans*-selective catalysts, but in the presence of MAO become *cis*-selective.^{14, 15} Additionally, lanthocenes in conjunction with MAO or [Ph₃C][B(C₆F₅)₄] are efficient catalysts,^{16, 17} with [(C₅Me₅)₂Gd][B(C₆F₅)₄] in combination with Al(*i*-Bu)₃ yielding >99.9% *cis*-1,4-enchained polybutadiene, the highest selectivity reported to date.³

In many of the above examples cocatalysts have been added to activate the metal. With cocatalysts such as MAO in the system, it is difficult to study the coordination-insertion mechanism predicted for the polymerization of 1,3-dienes. The active metal center may not be well defined and the large excess of MAO makes it difficult to observe any metal-containing species during polymerization. Additionally, metal complexes activated with MAO often yield polymers with broad PDI. Quirk and coworkers recently

reported a neodymium complex activated with $\text{Al}_2\text{Et}_3\text{Cl}_3$ and $\text{Al}(i\text{-Bu})_2\text{H}$ which yields 98-99% *cis*-1,4-enchaind polybutadiene, but the PDIs range from 3.0-5.3.¹³ In contrast to late metal catalysts, these early metal catalysts are not functional group tolerant due to high oxophilicity of the metal center, making these catalysts ineffective to polymerize functionalized 1,3-dienes.

Late transition metal complexes of nickel have been employed as single component catalysts in 1,3-diene polymerization. Both neutral and cationic (allyl)Ni(II) catalysts with a variety of ligands have been examined. Neutral complexes based on [(allyl)NiX]₂ dimers have been shown to be active 1,3-diene polymerization catalysts. The identity of X influences the reactivity and selectivity in butadiene polymerization, where X = I⁻ *trans* selectivity is observed and where X = Cl⁻^{18, 19} or TFA²⁰ *cis* selectivity is seen. Dolgoplosk has also shown that these complexes initiate 1,3-cyclohexadiene and 2,3-dimethylbutadiene polymerization in the presence of added chloroanil.²¹ Polymers of 1,3-cyclohexadiene are interesting because the 1,4-enchaind polymer allows for the production of unbranched poly(*p*-phenylenes) after dehydrogenation. Such polymers have applications in the electronics field.²² Overall, the halogen bridged [(allyl)NiX]₂ dimers exhibit poor activity and yield low molecular weight polymers.^{18, 19}

Cationic [(allyl)NiL₂][X] complexes with a variety of ligands (L = P(OAr)₃, COD, SbPh₃) have been investigated in butadiene polymerization. Varying the ligand bound to nickel has a significant effect on the activity and selectivity. [(Allyl)Ni(P(OPh)₃)₂][X] (X = noncoordinating anion) exhibits slow reaction rates and yields *trans*-1,4-polybutadiene selectively, while [(allyl)Ni(SbPh₃)₂][X] is highly active and is *cis*-selective. Removing ligands from the coordination sphere of nickel creates a

highly active butadiene polymerization catalyst.²³⁻²⁶ The most active well-defined Ni(II) initiator, a so-called “ligand-free” system, $[\text{Ni}(\text{C}_{12}\text{H}_{19})][\text{PF}_6]$, was reported by Taube (see chapter 1). This catalyst is reported to achieve turnover frequencies (TOFs) of 12000/h for butadiene polymerization at room temperature and yields 93% *cis*-1,4-polybutadiene.^{27, 28} Unfortunately, the utility of this catalyst was never expanded to polymerize an array of conjugated dienes.

Cámpora reported the polymerization of styrene and butadiene in toluene using $[(\text{allyl})\text{Ni}(2,6\text{-di-}i\text{-tert-butyl-4-methylphenol})][\text{B}(\text{Ar}_\text{F})_4]$ as the active catalyst. The activity of this complex is comparable to Taube’s ligand-free catalyst. Butadiene could be polymerized to high conversions (up to 99%) at 60 °C after 1 h. The polybutadiene obtained was up to 94% *cis*-1,4-enchained and of high molecular weight. Using CH_2Cl_2 as solvent, he observed a marked decrease in the polymerization activity. He proposed that polymerizations performed in aromatic solvents help stabilize the active $(\text{allyl})\text{Ni}(\text{II})$ centers. When the polymerizations run in CH_2Cl_2 , the $(\text{allyl})\text{Ni}(\text{II})$ complex does not gain extra stabilization from the solvent resulting in short catalyst lifetimes. Styrene was polymerized to 56-77% conversion after 1 h at 60 °C. Low molecular weight, atactic polystyrene was obtained using this catalyst.^{29, 30}

We have previously reported that $[(2\text{-R-allyl})\text{Ni}(\text{NCR}')_2][\text{B}(\text{Ar}_\text{F})_4]$ ($\text{R} = \text{H}, \text{CH}_3$, $\text{R}' = \text{CH}_3$ or Ar_F , $\text{Ar}_\text{F} = 3,5\text{-bis(trifluoromethyl)benzene}$) when activated with $\text{B}(\text{C}_6\text{F}_5)_3$ (which abstracts the nitrile ligands) generates a “naked-Ni” center that is active for butadiene polymerization. Key intermediates prior to and during the chain growth process were observed for the first time.³¹ Additionally, we reported the synthesis of $[(2\text{-R-allyl})\text{Ni}(\text{mesitylene})][\text{B}(\text{Ar}_\text{F})_4]$ ($\text{R} = \text{H}, \text{CH}_3$) complexes which were shown to be

effective as olefin isomerization catalysts as well as induce hydrogen atom transfer from an added olefin to the allyl moiety, generating a new (allyl)Ni(II) complex, as detailed in chapter 3.³²

This chapter focuses on the development and improvement of cationic (allyl)Ni(II) complexes for 1,3-diene polymerization. Catalysts [(2-R-allyl)Ni(NCMe)₂][B(Ar_F)₄] activated with B(C₆F₅)₃ and [(2-R-allyl)Ni(mes)][B(Ar_F)₄] (R = H, CH₃) have been investigated as catalysts for polymerization of butadiene (BD), isoprene (IP), 2,3-dimethyl-1,3-butadiene (DMBD), and 1,3-cyclohexadiene (1,3-CHD), as well as styrene and a functionalized diene. The polymerization results are summarized in this chapter. Additionally, some preliminary observations regarding the mechanism of DMBD and styrene polymerization are unveiled.

Results and Discussion

1,3-Diene Polymerization Catalyzed by [(2-R-Allyl)Ni(NCCH₃)₂][B(Ar_F)₄] in Combination with B(C₆F₅)₃

The polymerization of butadiene (BD), 2,3-dimethyl-1,3-butadiene (DMBD) and isoprene (IP) was examined using [(allyl)Ni(NCCH₃)₂][B(Ar_F)₄], **1**, and [(2-methallyl)Ni(NCCH₃)₂][B(Ar_F)₄], **2**, as catalysts in the presence of 2 equiv of tris(pentafluorophenyl)boron (B(C₆F₅)₃) in methylene chloride. This reaction generates ligand-free [(allyl)Ni][B(Ar_F)₄], **3**, or [(2-methallyl)Ni][B(Ar_F)₄], **4**, in solution, which serves as the active initiator. We previously reported η^4 -diene coordination of IP and BD to ligand-free species **2** and **3**. We can extend this series to include 1,3-CHD. Exposure of 1 equiv of 1,3-CHD to ligand-free species **4** at -80 °C generates [(2-methallyl)Ni(η^4 -1,3-cyclohexadiene)][B(Ar_F)₄]. The ¹H NMR spectrum at -70 °C exhibits two roofed broad singlets at 6.31(2.0H) and 6.11(2.0H) ppm corresponding to the vinylic hydrogens

of the coordinated cyclohexadiene. There are three singlets at 5.14 (2.0H), 2.59 (2.0H), 2.15 (3.0H) ppm that are assigned to the *syn*, *anti*, and CH₃ group protons of the allyl ligand, respectively. The final resonance is a roofed multiplet at 1.77 ppm assigned to the diastereotopic methylene hydrogens.

To effect the polymerization reactions, the ligand-free species is generated at -30 °C and the reactions are warmed (if necessary) after monomer addition. The results for the polymerization of BD, IP, and DMBD using catalysts **1** or **2** in the presence of B(C₆F₅)₃ are found in Tables 4.1, 4.2, and 4.3. Each polymerization trial was run in duplicate. Most of the trials were run with the 2-methallyl derivative, **2**, because the methyl-substituted wrap-around complex, formed from 3 insertions of BD, opens readily in the presence of added 1,3-diene, as shown previously³¹ and in chapter 2 of this thesis.

Results for the polymerization of butadiene are found in Table 4.1. Polymerization of butadiene at -30 °C using in situ generated **4** (monomer:catalyst = 1100:1) yields 48% polybutadiene (PBD) after 6 h. (see entry 1) ¹³C{¹H} NMR analysis of this polymer indicates the polymer microstructure is 93% *cis*-1,4, 6% *trans*-1,4 and 1% 1,2 enchain, similar to PBD obtained by Taube using his ligand-free catalyst.^{28, 33} At 0 °C, ligand-free **4** is a highly active initiator for butadiene polymerization (monomer:catalyst = 1800:1). Within 30 min, ~70% conversion is achieved and within 1 h the polymerization reaction is complete (see entry 4). Again the polymer microstructure assigned by ¹³C{¹H} NMR spectroscopy is 93% *cis*-1,4, 6% *trans*-1,4 and 1% 1,2. Frequently at temperatures above 0 °C, the polymerization yields a highly cross-linked polymer which is insoluble in common organic solvents (entry 4). Cross-linking of PBD has been observed while terminating the polymerizations with MeOH and also

during the runs at elevated temperatures (0 °C – 23 °C). We are not sure how or why cross-linking occurs, but optimal conditions have been developed to minimize the chance of cross-linking upon quenching the polymerizations. Adding cold MeOH and 2,6-di-*tert*-butyl-4-methyl-phenol (BHT) prevents cross-linking during workup. Another problem encountered during these reactions is that ligand-free species **4** is air and moisture sensitive. Often with these polymerizations the solution will turn colorless upon the addition of butadiene, indicating catalyst deactivation. This issue makes obtaining reproducible results with these catalysts very difficult.

Table 4.1. Polymerization of butadiene using in situ generated complex **4**.^a

Entry	Ratio ^b	Time (h)	Conversion (Isolated) (%)	M _n ^c	PDI
1	1100:1:2	6	48	12200	1.75
2	620:1:2	5	86	6700	1.65
3 ^d	1800:1:2	0.5	68	12200	3.38
4 ^d	1500:1:2	1	100	- ^e	-

^aReaction conditions: Vol. 2.0 mL, CH₂Cl₂, -30 °C. ^b[BD]:[Ni]:[B(C₆F₅)₃]. ^cMolecular weights determined by GPC in THF versus polystyrene standards. ^dTemperature 0 °C. ^eCross-linked.

The isoprene polymerization data is located on Table 4.2. With a monomer:catalyst ratio of 940:1, isoprene is polymerized to ca. ~50% conversion using in situ generated species **4** as catalyst at 23 °C. Low conversion is observed when the polymerization temperature is lowered to -30 °C with a monomer:catalyst ratio of 2100:1 (entry 1). Varying the solvent from toluene to CH₂Cl₂ had no apparent effect on the polymerization activity (entry 2 vs. entry 3). Molecular weight data for polyisoprene was determined using GPC analysis in THF. The M_n's range from 2,300-6,700 for the polymerizations conducted at 23 °C. At -30 °C with an IP:Ni ratio of 2100:1 a polymer

with an M_n of 29,000 is obtained. The high M_n value, coupled with low conversion, suggests a slow initiation step relative to propagation at -30 °C. In all cases the PDI is broad. Evaluation of the microstructure with $^{13}\text{C}\{^1\text{H}\}$ analysis shows the polyisoprene exhibits 64% *trans*-1,4, 23% *cis*-1,4, and 13% 3,4 enchainment, indicating poor selectivity with this system. Cross-linking is often a complication during these polymerization reactions, similar to the results found for BD polymerizations.

Table 4.2. Polymerization of isoprene using in situ generated complex **4**.^a

Entry	Ratio ^b	Time (h)	Conversion (Isolated) (%)	M_n^c	PDI
1	2100:1:2	4	8	29000	2.61
2 ^d	940:1:2	5	54	6700	3.90
2 ^e	940:1:2	15	60	3400	6.30
3 ^e	940:1:2	7	47	2300	2.70
4 ^e	940:1:2	7	42	2300	2.26

^aReaction conditions: Volume 3.0 mL, CH_2Cl_2 , -30 °C. ^b[IP]:[Ni]:[B(C₆F₅)₃]. ^cMolecular weights determined by GPC in THF versus polystyrene standards. ^dTemperature 23 °C. ^eTemperature 23 °C, 1.5 mL toluene, 0.5 mL CH_2Cl_2 .

Polymerization of 2,3-dimethyl-1,3-butadiene was also conducted using in situ generated species **4** (Table 4.3). Formation of ligand-free complex **4** was performed at -30 °C and the reaction was warmed to room temperature upon addition of DMBD. No polymerization activity was observed at -30 °C. Inconsistent results have been obtained for these polymerizations as one trial yields only ~50% conversion after 3.5 h, while another experiment yields 81% conversion (entry 1 vs. entry 2). The polymer is insoluble in CH_2Cl_2 and precipitates out of solution as a white powder. No information regarding the molecular weights could be obtained due to poor solubility in organic solvents at room temperature.

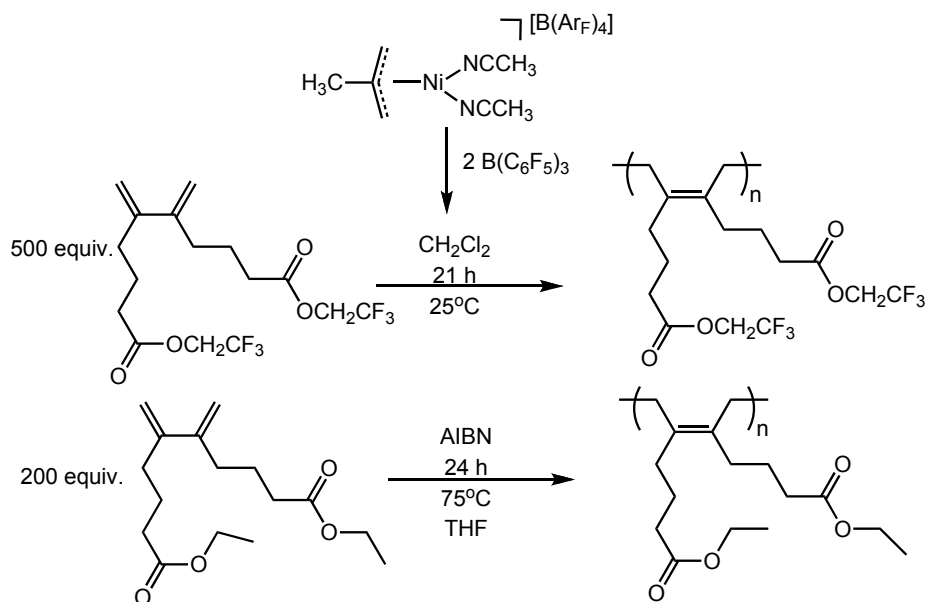
Table 4.3. Polymerization of dimethylbutadiene with in situ generated complex **4**.^a

Entry	Ratio ^b	Time (h)	Conversion (Isolated) (%)
1	875:1:2	3	49
2	940:1:2	3	81

^aReaction conditions: 1.0 mL CH₂Cl₂, 23 °C. ^b[DMBD]:[Ni]:[B(C₆F₅)₃].

In situ generated ligand-free species **4** is also tolerant of functional groups. Room temperature polymerization of 2,3-bis(4-trifluoroethoxy-4-oxobutyl)-1,3-butadiene is observed within 24h. GPC analysis yields an M_n value of 113,000 for this polymer. A higher molecular weight polymer is achieved using Ni complex **4**, compared to the M_n of 20,000 observed for the free radical polymerization of analogous 2,3-bis(4-ethoxy-4-oxobutyl)-1,3-butadiene.³⁴

Scheme 4.1. Polymerization of 2,3-bis(4-trifluoroethoxy-4-oxobutyl)-1,3-butadiene with in situ generated **4**.



Polymerization of 1,3-Dienes Catalyzed by [(2-R-allyl)Ni(mes)][B(Ar_F)₄] Complexes

As previously mentioned, the active species, ligand-free [(2-R-allyl)Ni][B(Ar_F)₄] (R = H, CH₃), is quite air and moisture sensitive, which has led to inconsistent results in the polymerization studies. To combat this, we developed stable arene complexes, (R-allyl)Ni(mes)[B(Ar_F)₄] (R = CH₃, **5**, R = H, **6**), as described in chapter 3, and examined their activity for 1,3-diene polymerization. These complexes mimic the ligand-free species with a coordinated arene moiety, but now are more robust and do not need to be activated with B(C₆F₅)₃. Additionally, the mesitylene catalysts are highly *cis*-1,4 selective for polymerization of DMBD, IP, and BD. Most polymerizations have been performed using **5** because our previous findings show that the 2-methallyl derivatives generate wrap-around complexes, which rapidly dissociate an olefin arm in the presence of butadiene,³¹ and therefore could possibly be used as living polymerization initiators.

To verify that complex **6** undergoes the same reaction with butadiene as ligand-free species **6**, a low temperature ¹H NMR study was performed (Figure 4.1). The addition of 4 equiv of BD to **6** at -80 °C results in no reaction and only free BD and starting catalyst **6** are present as indicated in the ¹H NMR spectrum shown in Figure 4.1. Reaction between BD and complex **6** occurs slowly upon warming to -50 °C as evidenced by decrease in the [BD] and starting catalyst **6**. New ¹H resonances begin to grow in and precisely match those for the wrap-around complex generated from ligand-free **3** and 3 equiv of BD.³¹ Warming to -10 °C leads to fast conversion to the wrap-around complex.

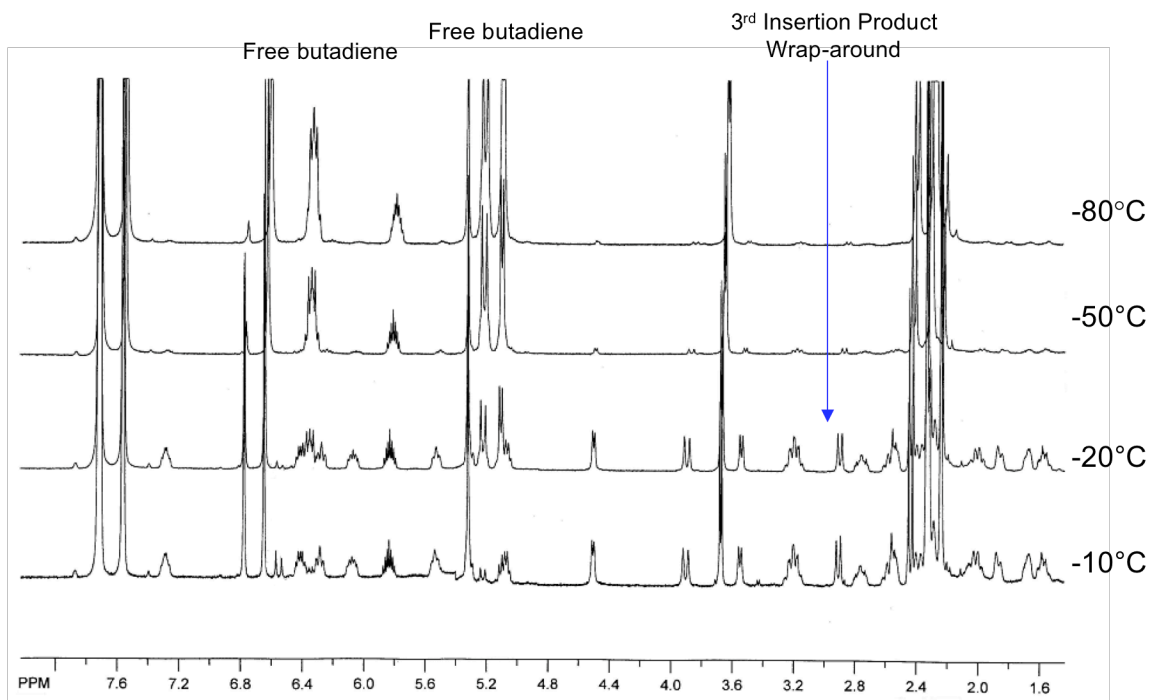


Figure 4.1. Insertion of butadiene into complex **6** to form a wrap-around complex.

The polymerization of butadiene was examined using catalyst **5** at $-30\text{ }^{\circ}\text{C}$ and $0\text{ }^{\circ}\text{C}$ in CH_2Cl_2 and the results are summarized in Table 4.4. When the ratio of $[\text{BD}]:[\text{Ni}]$ is 1100:1, up to ca. ~40% conversion to PBD is obtained at $-30\text{ }^{\circ}\text{C}$ (entry 1). This polymer M_n is 32,000. Doubling the solvent volume results in 44% conversion in approximately double the time (entry 2). Lower concentrations of butadiene (150:1) result in only 21% conversion after 2 h (entry 3). An increase in the rate of the reaction is observed upon raising the temperature to $0\text{ }^{\circ}\text{C}$. With a butadiene:nickel ratio of 2100:1, complete conversion is achieved within 15 min at $0\text{ }^{\circ}\text{C}$. $^{13}\text{C}\{^1\text{H}\}$ NMR of the PBD shows the microstructure is 94% *cis*-1,4, 5% *trans*-1,4, and 1% 1,2, slightly better than Taube's reported selectivity.^{28, 33} The M_n 's were determined using GPC analysis in THF. Polymerizations run at $0\text{ }^{\circ}\text{C}$ exhibit an extremely broad PDI, and this is commonly

observed at high concentrations of BD (entry 4). At such high concentrations, the reactions are exothermic and this may explain the broad PDI. At -30 °C the PDI is less broad at lower conversion, but broadens with conversion as previously observed by Winter in his study of the polymerization of BD using [(allyl)Ni(TFA)₂].³⁵

Table 4.4. Butadiene polymerization data using complex **5** as initiator.^a

Entry	Ratio ^b	Time (h)	Conversion (Isolated) (%)	M _n ^c	PDI
1	1200:1	3	42	32000	2.19
2 ^d	1100:1	6	44	18000	2.39
3	150:1	2	21	19000	1.85
4 ^e	2100:1	0.25	100	20700	7.75

^aReaction conditions: 1.0 mL CH₂Cl₂, -30 °C. ^b[BD]:[Ni]. ^cMolecular weights determined by GPC in THF versus polystyrene standards. ^d2.0 mL of CH₂Cl₂. ^eTemperature 0 °C.

Polymerization of Isoprene

The polymerization of isoprene was investigated using complex **5** and the results are summarized in Table 4.5. Polymerizations were initiated at room temperature in CH₂Cl₂. In these polymerizations, 11 equiv of BD are added prior to IP monomer because the addition of butadiene to complex **5** generates a wrap-around complex and this species should initiate polymerization rapidly. With a IP:Ni ratio of 1100:1, polyisoprene can be obtained in up to 60% yield after 15 h at 23 °C (entry 4). Comparing entries 1-5, only a slight increase in conversion is observed as time progresses. GPC results in THF show these polymers to have M_n's of ~7000. The PDI's for all polyisoprenes are quite broad. The polymer microstructure is 84% *cis*-1,4, 15% *trans*-1,4, and 1% 3,4 as determined by ¹³C{¹H} NMR spectroscopy. Interestingly, the polymers formed from **5** are predominantly *cis*-1,4 enchain, while the polymers

synthesized by ligand-free **4** are more *trans*-1,4 enchainned. We are in the process of investigating this finding to try to understand the selectivity, which may be linked to the choice of solvent. Again at higher conversions, cross-linking is observed making characterization of the polymer difficult.

Table 4.5. Isoprene polymerization data using complex **5** as initiator.^a

Entry	Ratio ^b	Time (h)	Conversion (Isolated) (%)	Mn ^c	PDI
1	1100:1	4.5	36	7600	3.10
2	1100:1	6.5	41	6700	3.98
3	1100:1	10	40	10100	10.8
4	1100:1	15	60	- ^e	-
5 ^d	550:1	8.5	32	6800	2.39

^aReaction conditions: 1.0 mL CH₂Cl₂, 11 equiv BD, 23 °C. ^b[IP]:[Ni]. ^cMolecular weights determined by GPC in THF versus polystyrene standards. ^d1.5 mL of CH₂Cl₂. ^eCross-linked.

Polymerization of 2,3-Dimethyl-1,3-Butadiene

The activity of (allyl)Ni(mes)⁺ catalysts **5** and **6** for the polymerization of DMBD was investigated at two ratios of [DMBD]:[Ni]. All polymerizations were carried out at 23 °C by the addition of 11 equiv of BD to **5** or **6** dissolved in dry CH₂Cl₂ followed by DMBD addition. The polydimethylbutadiene (PDMBD) formed precipitates out of solution during the course of the reaction. The polymerizations were terminated by the addition of MeOH. Catalysts **5** and **6** are highly active for DMBD polymerization as seen on Table 4.6, with complex **6** showing slightly better activities (entries 5-9). Comparing entries 5-7, (DMBD:Ni = 900:1), the conversion to PDMBD increases as time progresses. At lower DMBD:Ni ratios (460:1), higher conversions are noted at earlier times (entries 8 and 9).

Table 4.6. Dimethylbutadiene polymerization data.^a

Entry	Ratio ^b	Time (h)	Conversion (Isolated) (%)
1 ^c	460:1	3.2	92
2 ^c	450:1	5	78
3	940:1	2.5	77
4	940:1	8	88
5 ^d	900:1	2.5	52
6 ^d	900:1	6.5	66
7 ^d	900:1	15	98
8 ^{d,e}	460:1	4	93
9 ^{d,e}	460:1	8	100

^aReaction conditions: complex **5**, 1.0 mL CH₂Cl₂, 11 equiv BD, 23 °C. ^b[DMBD]:[Ni]. ^c1.5 mL CH₂Cl₂. ^dReaction conditions: complex **6**, 1.0 mL of CH₂Cl₂, 11 equiv BD, 23 °C. ^e1.5 mL CH₂Cl₂.

The polymer obtained is insoluble in all common organic solvents at room temperature, but at high temperatures (80 °C) is partially soluble in C₆D₅Br to allow for characterization by ¹H and ¹³C{¹H} NMR spectroscopy. Using ¹H and ¹³C{¹H} NMR spectroscopy, the enchainment mode of PDMBD was determined to be predominantly 1,4 with minor amounts of vinyl (1,2) also present. PDMBD exhibits two aliphatic carbon resonances at 34.06 and 18.84 ppm, assigned to the methylene and methyl group carbons, respectively. The olefinic carbon appears at 128.9 ppm. The chemical shifts of PDMBD indicate that enchainment is likely to be *cis*-1,4.

Assignment of the PDMBD stereochemistry is difficult based upon ¹³C NMR data alone. Literature reports claim samples of *cis*-1,4-PDMBD and *trans*-1,4-PDMBD exhibit nearly identical resonances in the ¹³C NMR.³⁶ The ¹³C NMR for the *trans* isomer in *o*-dichlorobenzene at 90 °C exhibits a methyl carbon resonance at 18.43 ppm and a resonance at 33.88 ppm assigned to the allylic methylene carbon. For the *cis* isomer the methyl carbon resonates at 18.84 ppm and the allylic methylene carbon appears at 34.04

ppm, in *o*-dichlorobenzene at 90 °C. The olefinic signals, for the *cis* and *trans* isomers, are nearly identical.³⁶

Additional support for a *cis*-1,4 enchainment polymer comes from IR spectroscopy. The IR spectrum of PDMBD exhibits a strong band at 1384 cm⁻¹ and a minor band at 1375 cm⁻¹, characterized as the symmetric stretch for the methyl group, and are assigned to the *cis*-1,4 and 1,2 enchainment polymer based on literature report.³⁷ There is no IR evidence for the *trans*-1,4 isomer. A *cis*-1,4 enchainment polymer is expected based upon our previous results concerning the mechanism of butadiene insertion into nickel allyl complexes.³¹

Studies using thermal analysis and GPC proved to be less fruitful. The DSC showed a melting transition at 181 °C with no observable glass transitions found for these polymer samples. The reported T_m values for *cis*- and *trans*-1,4-PDMBD are 190 °C and 260 °C, respectively.^{36, 38} In our case, a T_m of 181 °C supports the assignment of a *cis*-1,4 enchainment polymer. Due to poor solubility in THF at room temperature, molecular weights of these polymers could not be obtained. High temperature GPC in 1,2,4-trichlorobenzene was not successful.

Very few (allyl)Ni(II) complexes have been shown to be active for DMBD polymerization. Dolgoplosk reported the polymerization of DMBD using [(crotyl)NiCl]₂ and chloroanil at 30 °C, but after 8 h only 12% conversion was achieved.²¹ The polymers are *trans*-1,4 enchainment as determined by IR and thermomechanical (TMA) measurements. Dolgoplosk reports a T_m of 120 °C for *trans*-1,4-PDMBD,²¹ which is quite low compared to literature value of 260 °C reported by Yamada and Vogel.^{36, 38} Compared to Dolgoplosk's system, complexes **5** and **6** are much more active, allowing

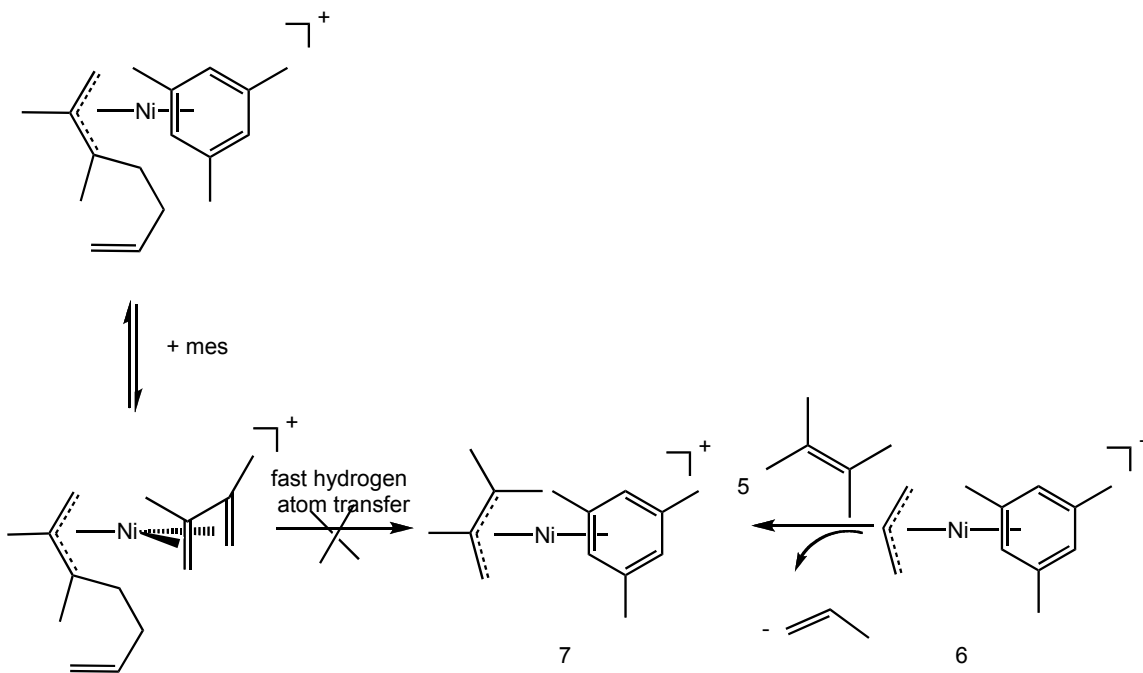
for quantitative conversion of DMBD to polymer within 15 h. Additionally, these polymers appear to be highly *cis*-1,4 enchainned.

Interestingly, when orange-red complex **6** is exposed to DMBD under polymerization conditions (25 °C) a bright yellow solution is immediately generated. In contrast, when BD is added to **6**, the reactions remain bright orange-red. To investigate the color change, we studied this reaction by ¹H NMR spectroscopy. At low temperature there is no change in the ¹H NMR spectrum upon exposure of 38 equiv of DMBD to complex **6**. Upon warming to 0 °C, complete conversion to a new (allyl)Ni(II) species occurs with complete consumption of catalyst **6**. The coordinated mesitylene ring appears as two singlets at 6.42 (3.0H) and 2.28 (9.0H) ppm, corresponding to the arene and methyl hydrogens, respectively. The new species shows a complex multiplet centered at 5.77 ppm, which resembles the internal olefin signal of 1-hexene. Based upon the splitting pattern of this resonance, it has been determined that this H shows coupling to *cis* and *trans* olefinic H's as well as a methylene group consistent with an α-olefin unit. The *syn* and *anti* protons resonate at 3.43 (1.0H) and 2.53 (1.0H) ppm and there are two methyl singlets at 2.07 (3.0H) and 1.22 (3.0H) ppm. There is no evidence of propene, which would be generated if hydrogen atom transfer had occurred. Therefore, a C-C coupling product between DMBD and an allyl unit must be present in solution.

In an attempt to identify this new allyl species, complex **6** was exposed to 4 equiv of 2,3-dimethyl-2-butene at room temperature. This reaction generates an equivalent of propene and [(1,1,2-trimethallyl)Ni(mes)][B(Ar_F)₄], **7**, via intramolecular hydrogen atom transfer from 2,3-dimethyl-2-butene to the allyl moiety (Scheme 4.2). Complex **7**

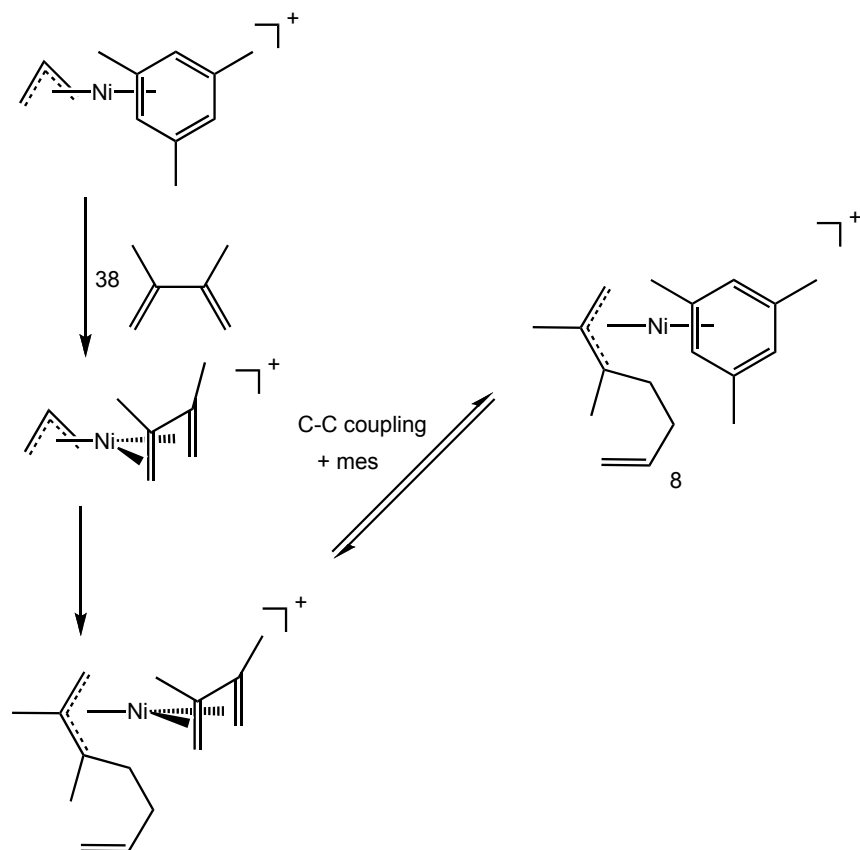
exhibits three singlet resonances corresponding to methyl groups at δ 2.10, 1.19, 0.89 and two singlets for *syn* and *anti* protons at 3.39 and 2.66 ppm, respectively. The mesitylene resonances shift to 6.44 and 2.31 ppm, for the aryl and methyl group protons, respectively. The ^1H NMR spectrum of complex **7** does not match exactly with the (allyl)Ni(II) species generated when DMBD is exposed to complex **6**, but lends some information about the identity of the new allyl species.

Scheme 4.2. Generation of complex **7** via intramolecular hydrogen atom transfer.



A plausible mechanism for the reaction of complex **6** with DMBD is outlined in Scheme 4.3. C-C coupling occurs first to generate a new allyl species, $[(\text{C}_9\text{H}_{15})\text{Ni}(\eta^4\text{-DMBD})][\text{B}(\text{Ar}_\text{F})_4]$, which is unobservable. The DMBD is then displaced by mesitylene to form $[(\text{C}_9\text{H}_{15})\text{Ni}(\text{mes})][\text{B}(\text{Ar}_\text{F})_4]$, **8**. We believe the species observed during the NMR studies of **6** with DMBD to be the coupling product **8** (Scheme 4.2). Currently, we are studying this reaction to completely characterize the coupled allyl species.

Scheme 4.3. Proposed mechanism to form coupling product **8**.



Polymerization of 1,3-Cyclohexadiene

Complex **5** has been examined for polymerization of 1,3-CHD in CH_2Cl_2 at room temperature and $-30\text{ }^\circ\text{C}$ and the results are found on Table 4.7. 11 equiv of BD were added to complex **5** in CH_2Cl_2 to form a wrap-around species prior to monomer addition. Polycyclohexadiene (PCHD) is insoluble in CH_2Cl_2 and precipitates out of solution as a powder. These reactions are very exothermic and within 2 min of initiation the reaction temperature rises. Within 5 min at room temperature quantitative conversion to polymer is observed. As seen in entry 3, the reaction rate decreases when the polymerization is run at $-30\text{ }^\circ\text{C}$, and only 21% of PCHD is isolated after 1 h. These polymerizations can

also be run under more dilute conditions (entry 4) although much longer reaction times are necessary to achieve high yields.

Table 4.7. 1,3-Cyclohexadiene polymerization results.^a

Entry	Ratio ^b	Time (min)	Conversion (Isolated) (%)
1	1100:1	5	96
2	1100:1	5	88
3 ^c	1100:1	60	21
4 ^d	1000:1	330	35

^aReaction conditions: complex **5**, 1.0 mL CH₂Cl₂, 11 equiv BD, 23 °C. ^b[CHD]:[Ni]. ^c-30 °C. ^d5.0 mL CH₂Cl₂.

The polymer microstructure was studied using DSC and NMR spectroscopy. The observed ¹³C NMR shifts are very broad and are centered at of 131.1, 40.64, and 26.0 ppm. The presence of broad ¹³C NMR resonances makes determining the enchainment difficult. The polymer is likely atactic. According to the literature, characteristic resonances for 1,2 enchainment PCHD appear at 25 and 125 ppm and at 131, 40, and 26 ppm for 1,4-enchainment PCHD.³⁹ DSC data for our samples of PCHD displays a *T_m* at 231 °C, suggesting 1,4-enchainment.²¹ Literature reports show purely 1,4-enchainment crystalline PCHD exhibits high melting temperatures between 370 and 380 °C.³⁸ The lower *T_m* for the PCHD samples prepared here are consistent with an atactic structure and possibly some contamination from 1,2 enchainment.

Dolgoplosk reported the polymerization of 1,3-CHD using (allyl) and (crotyl)Ni(II) halide dimers in combination with added chloroanil or a Ni(II) species. Only 37% conversion could be achieved after 2 days at room temperature. The polymer was characterized to be predominantly 1,4-*trans* enchainment based upon TMA and IR

analyses.²¹ Complex **5** is much more active than that investigated by Dolgoplosk, as we can achieve quantitative conversion within minutes at room temperature.

Studying this polymerization reaction by ¹H NMR spectroscopy shows that most of the catalyst remains after all the 1,3-CHD is consumed. This indicates slow initiation relative to propagation; only a small amount of Ni is actually active for the polymerization of 1,3-CHD.

Polymerization of Styrene

Complexes **5** and **6** are highly active for the polymerization of styrene (Table 4.8). Within 1 h at 0 °C (styrene:Ni = 900:1), quantitative conversion to polystyrene is observed (entry 3). The polymers obtained are soluble in common organic solvents and can be easily characterized. Additionally, the polymerizations can be initiated at temperatures as low as -30 °C, without much loss in activity (entries 4 and 5). The ¹³C NMR spectra of these polymers reveal there is little stereoregularity in the polymer. GPC analysis in THF shows the polymers are of low molecular weights with *M_n*'s ranging from 2,500-6,500. The PDI of approximately 2.0 indicates molecular weights of these polymers are chain-transfer limited.

Table 4.8. Polymerization of styrene.^a

Entry	Ratio ^b	Time (h)	Conversion (Isolated) (%)	<i>M_n</i> ^c	PDI
1	890:1	1	88	5300	2.04
2	910:1	0.5	92	3500	2.45
3	910:1	1	100	6100	1.94
4 ^d	910:1	2	72	3300	1.95
5 ^d	900:1	0.5	59	4500	1.72

^aReaction conditions: 3.0 mL CH₂Cl₂, 0 °C. ^b[Styrene]:[Ni]. ^cMolecular weights determined by GPC in THF versus polystyrene standards. ^dTemperature -30 °C.

Complex **6** exhibits higher activity and conversions for styrene polymerization when compared to Cámpora's [(allyl)Ni(2,6-di-*tert*-butyl-4-methylphenol)][B(Ar_F)₄] catalyst.³⁰ Additionally, catalyst **6** yields polymers of slightly higher molecular weight; Cámpora reports an M_n of 1,090 for the polystyrene synthesized with his catalyst.^{29, 30} The reactions with our catalyst can also be run at much lower temperatures. Cámpora initiates polymerization at 60 °C to observe acceptable activities. With Cámpora's catalyst at 60 °C in CH₂Cl₂, (styrene:nickel = 35,000:1) only 77% conversion to polystyrene is achieved compared to 100% at 1 h at 0 °C (styrene:nickel = 900:1) using complex **6**. In toluene, Cámpora observes lower activity for styrene polymerization (56% after 1 h). Both catalysts generate atactic polystyrene.

Others groups have oligomerized styrene with (allyl)Ni(II) complexes. Dias reported the oligomerization of styrene using [(2-methallyl)Ni(COD)][PF₆].⁴⁰ Valerga recently described the polymerization of styrene using an [(allyl)Ni(allyldiphenylphosphine)₂][PF₆] catalyst.⁴¹ Dias observes low conversion (~20%) of styrene and Valerga reports 94% conversion within 1 h at 40 °C. Complex **6** shows superior activity to both catalysts because within 1 h at 0 °C 100% conversion is observed. In both cases the polymerizations are stereoselective generating isotactic polystyrene. Also, the molecular weights of the polymers are quite low, with M_n 's ranging from 200-1,900. Complex **6** yields polystyrene of the highest molecular weights, when comparing the available molecular weight data for polymerization initiated by a cationic nickel complexes.

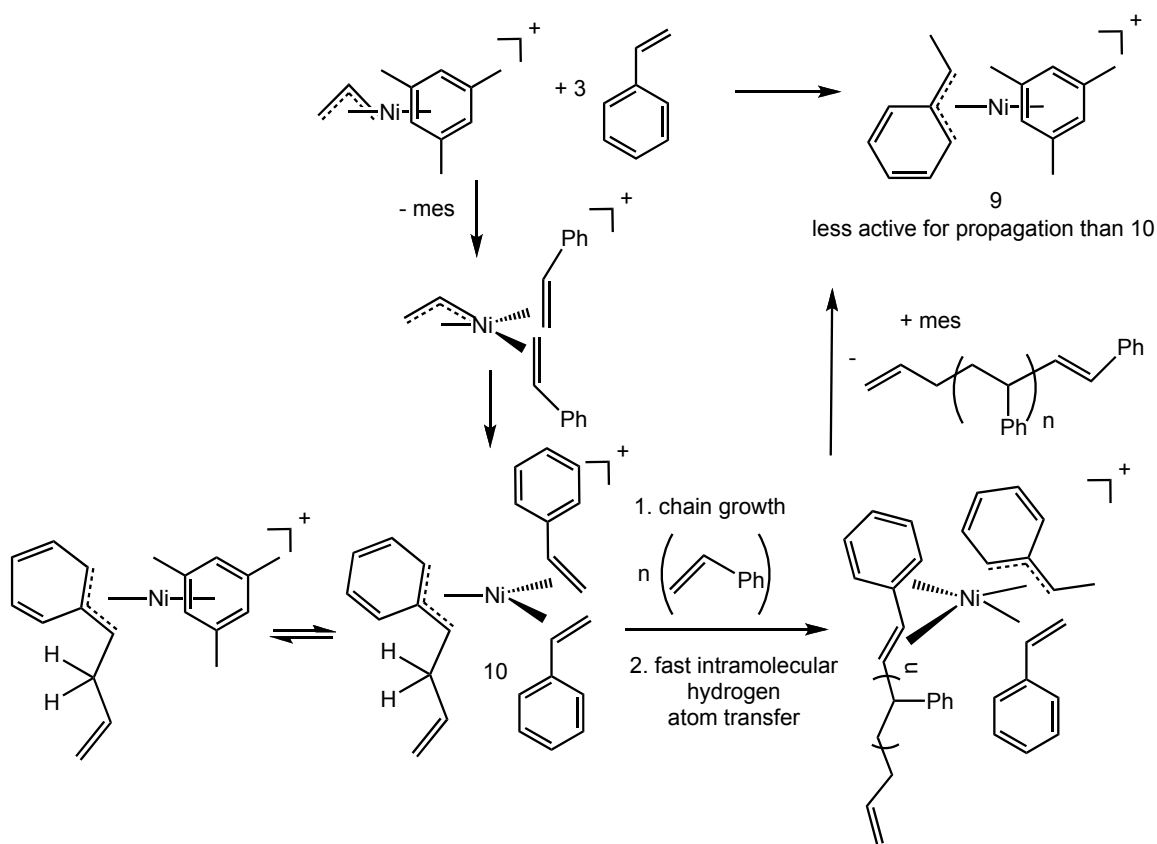
Using ¹H NMR spectroscopy we are able to gain some information regarding the chain growth pathway in the polymerization of styrene. Addition of 3 equiv of styrene to

complex **6** at 23 °C immediately generates a new species in solution. Starting complex **6** is still present in solution, while all of the styrene has been consumed to form polystyrene. Monitoring the reaction by variable-temperature ^1H NMR shows that styrene consumption begins to occur at -33 °C and is completely consumed upon warming to 23 °C. A new allyl nickel complex appears in the ^1H NMR spectrum, which is characterized as $[(\eta^3\text{-1-methylbenzyl})\text{Ni}(\text{mes})][\text{B}(\text{Ar}_\text{F})_4]$, **9**. Some key ^1H NMR features aid in the characterization of **9**. A doublet at 1.47 ppm is characteristic for a methyl group *syn* on an allyl moiety, coupling to one hydrogen atom. A broad singlet at 6.32 ppm is assigned to the allyl hydrogen contained on the ring. Additionally, a multiplet integrating for 1.0H centered at 3.65 ppm showing coupling to a methyl group represents the *anti* allyl hydrogen. There is also a new aryl signal for coordinated mesitylene at 6.65 ppm. The rest of the signals are masked by resonances for polystyrene.

A plausible mechanism to form a nickel species of this nature is shown in Scheme 4.4. Since there are no allylic hydrogens on styrene, C-C coupling of the allyl moiety and styrene must occur first. This is further evidenced by a lack of signals for propene formation in the ^1H NMR spectrum. Formation of propene would be expected if hydrogen atom transfer occurred. After C-C coupling, a new allyl complex, **10**, is generated. Chain propagation from **10** must be more rapid than from **9**, as **9** is observable in solution. After a number of styrene insertions, intramolecular hydrogen transfer from the growing polystyrene tail to a monomer of styrene could occur. Displacement of the resulting diene by mesitylene would then generate species **9**. Intramolecular hydrogen atom transfer is a viable pathway, since previous studies have shown this reaction to

occur readily with olefins as seen in chapter 3 of this thesis.³² Dias reports a similar η^3 -benzylic species observed during styrene polymerization using [(2-methallyl)Ni(COD)][PF₆] as initiator for styrene polymerization although they propose a Ni-H as intermediate,⁴⁰ which seems unlikely.

Scheme 4.4. Proposed hydrogen atom transfer mechanism to form complex **9**.



These results once again indicate that only a small fraction of the catalyst is active for polymerization, as most of the starting complex **6** is present in solution. Once coupling of the allyl group and styrene has occurred a stable nickel complex is generated, which appears to be slow to insert styrene monomer. At this point, there is now competition between insertion of more styrene or intramolecular hydrogen atom transfer

to release a chain. Only a small fraction of Ni is active in these polymerization and Initiation is slow relative to propagation.

Summary

The polymerization of 1,3-dienes and styrene was evaluated using ligand-free complexes **3** and **4** as well as mesitylene complexes **5** and **6**. All polymers are 1,4-enchainment. Polybutadiene exhibits high stereoregularity at 94% *cis*-1,4-enchainment. High activities for DMBD, styrene, and 1,3-CHD are obtained using catalysts **5** and **6**. These are some of the highest activities reported for the polymerizations of these monomers using (allyl)Ni(II) based catalysts. In reactions with styrene, C-C coupling occurred initially followed by hydrogen atom transfer from the coupled product to styrene, generating $(\eta^3\text{-1-methylstyrenyl})\text{Ni}(\text{mes})^+$ as an observable intermediate. In the case of DMBD, C-C coupling occurred to generate a $(\text{C}_9\text{H}_{15})\text{Ni}(\text{mes})^+$ complex. No hydrogen atom transfer was observed at 0 °C. We expect that hydrogen atom transfer plays a role in chain transfer processes in diene polymerization and this is the focus of the next chapter.

Experimental

General Considerations.

All reactions, unless otherwise stated, were conducted under an atmosphere of dry, oxygen free argon atmosphere using standard high-vacuum, Schlenk, or drybox techniques. Argon was purified by passage through BASF R3-11 catalyst (Chemalog) and 4Å molecular sieves. All nickel catalysts were stored under argon in an M. Braun glovebox at -35 °C. ^1H , ^{13}C , and ^{19}F NMR spectra were recorded on a Bruker DRX 500 MHz, a Bruker DRX 400 MHz, or a Bruker 300 MHz spectrometer. Chemical shifts are

referenced relative to residual CHCl_3 (δ 7.24 for ^1H), CH(D)Cl_2 (δ 5.32 for ^1H), $^{13}\text{CD}_2\text{Cl}_2$ (δ 53.8 for ^{13}C), $^{13}\text{CD}_3\text{Br}$ (δ 125.5 for ^{13}C), and $^{13}\text{CDCl}_3$ (δ 77.0 for ^{13}C). GPC analyses were performed in HPLC grade tetrahydrofuran at 25 °C using a Waters Alliance HPLC equipped with Waters Styragel HR2, HR4, and HR5 columns and a Waters 410 refractive index detector. Molecular weights are reported relative to polystyrene standards. High temperature GPC was run at Cornell University. DSC measurements were run on a Seiko Instruments DSC220C. To standardize the measurements, the sample was heated above the melting temperature of the polymer followed by rapid cooling and data was collected at a rate of 10 °C/min (second heat). FT-IR measurements were recorded on a ReactIR 1000 from ASI Applied Systems. Elemental analyses were performed by Robertson Microlit Laboratories of Madison, NJ.

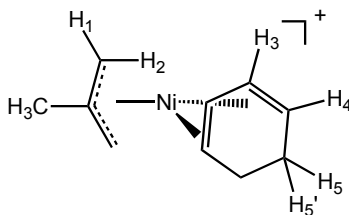
Materials.

All solvents were deoxygenated and dried by passage over columns of activated alumina.⁴² CD_2Cl_2 , purchased from Cambridge Laboratories, Inc., was dried over CaH_2 , vacuumed transferred to a Teflon sealable Schlenk flask containing 4Å molecular sieves, and degassed via three freeze-pump-thaw cycles. Butadiene and isoprene were purchased from Aldrich and purified by vacuum transfer through a column of 4Å molecular sieves and stored under argon at -35 °C. 1,3-Cyclohexadiene was purified by drying over NaBH_4 overnight, vacuum transferred into a Teflon sealable flask and degassed via three freeze-pump-thaw cycles. 2,3-Dimethyl-1,3-butadiene and 2,3-dimethyl-2-butene were purified by degassing via three freeze pump thaw cycles. $\text{Ni}[\text{COD}]_2$ and $\text{B}(\text{C}_6\text{F}_5)_3$ were purchased from Strem. $\text{NaB}(\text{Ar}_\text{F})_4$ ($\text{Ar}_\text{F} = 3,5\text{-(CF}_3)_2\text{C}_6\text{H}_3$), was synthesized according to literature methods.⁴³ 2,3-(Bis-4-trifluoroethoxy-4-oxobutyl)-1,3-butadiene was

synthesized and donated by the Ashby group. Styrene was purchased from Aldrich, purified by passing through a plug of alumina and then dried over CaH₂, and vacuum transferred into a sealable flask. Acetonitrile and mesitylene (mes) were purchased from Aldrich and Acros respectively and used without further purification. [(Allyl)Ni(NCMe)₂][B(Ar_F)₄], **1**, [(2-methallyl)Ni(NCMe)₂][B(Ar_F)₄],³¹ **2**, [(allyl)Ni(mes)][B(Ar_F)₄], **6**, and [(2-methallyl)Ni(mes)][B(Ar_F)₄],³² **5**, were synthesized according to literature procedure (see chapters 2 and 3).

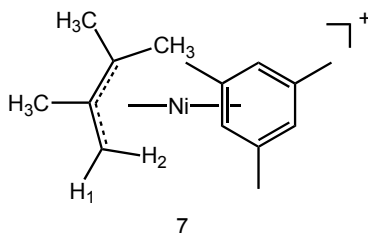
Spectral Data for [B(Ar_F)₄]. The ¹H and ¹³C spectral data for the B(Ar_F)₄⁻ counteranion were unchanged for all Ni(II) cationic complexes and are not be included in the characterization unless otherwise stated. ¹H NMR (400 MHz, CD₂Cl₂, 25 °C): δ 7.72 (s, 2H, Ar_F H_p), 7.57 (s, 4H, Ar_F H_o). ¹³C{¹H} NMR (101 MHz, CD₂Cl₂, 25 °C): δ 162.1 (q, ¹J_{C-B} = 49.8 Hz, Ar_F C_{ipso}), 135.2 (s, Ar_F C_o), 129.2 (qq, ³J_{C-B} = 3.0 Hz, ³J_{C-F} = 34.4 Hz, Ar_F CF₃), 122.3 (q, ¹J_{C-F} = 273.2 Hz, Ar_F CF₃), 117.8 (bt, Ar_F C_p).

In Situ Generation of Cationic Ni(II) Complexes.

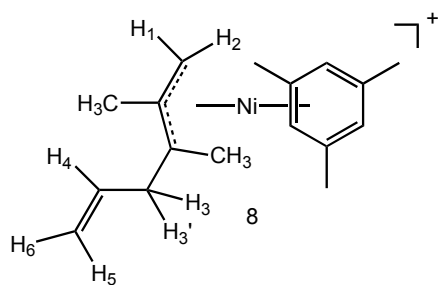


[(2-Methallyl)Ni(η⁴-1,3-cyclohexadiene)][B(Ar_F)₄]. A screw top NMR tube was charged with [(2-methallyl)Ni(NCMe)₂][B(Ar_F)₄] (0.015 g, 0.014 mmol) and B(C₆F₅)₃ (0.015 g, 0.028 mmol) and cooled to -80 °C. CD₂Cl₂ (600 μL) was introduced to the tube and the solids were quickly mixed by inversion. The solution turned yellow-brown. 1,3-Cyclohexadiene (1.35 μL, 0.014 mmol) was then added via syringe and the tube was quickly inverted again to mix. The solution color changed to bright yellow, indicative of

η^4 -diene coordination. The sample was then placed in a precooled NMR probe to monitor the reaction by ^1H NMR spectroscopy. ^1H NMR (500 MHz, CD_2Cl_2 , $-70\text{ }^\circ\text{C}$): δ 6.31 (br. s, 2H, H_3), 6.11 (d, 2H, $^3J_{\text{H-H}} = 5.5\text{ Hz}$, H_4), 5.14 (s, 2H, H_1), 2.59 (s, 2H, H_2), 2.15 (s, 3H, CH_3), 1.77 (complex AA'BB', 4H, $\text{H}_{5,5'}$). Insertion was observed upon warming to $-30\text{ }^\circ\text{C}$.

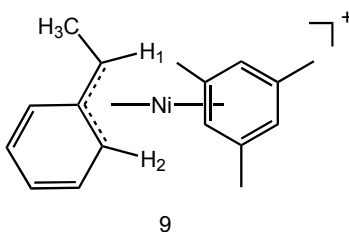


[(1,1,3-trimethallyl)Ni(mes)][B(Ar_F)₄] (7). A J-Young tube was charged with complex **6** (0.010 g, 0.009 mmol) and dissolved in CD_2Cl_2 (600 μL) in the dry box. 2,3-Dimethyl-2-butene (4.4 μL , 0.037 mmol) was added via syringe and the reaction was monitored by ^1H NMR spectroscopy. ^1H NMR (400 MHz, CD_2Cl_2 , $25\text{ }^\circ\text{C}$): δ 6.44 (s, 3H, mes-Ar), 5.84 (m, 1H, propene), 5.02 (d, 1H, $^3J_{\text{H-H}} = 16.8\text{ Hz}$, propene), 4.92 (d, 1H, $^3J_{\text{H-H}} = 9.6\text{ Hz}$, propene), 3.39 (s, 1H, H_1), 2.66 (s, 1H, H_2), 2.31 (s, 9H, mes- CH_3), 2.10 (s, 3H, CH_3 -center), 1.70 (d, $^3J_{\text{H-H}} = 6.3\text{ Hz}$, 3H, propene), 1.19 (s, 3H, CH_3 -syn), 0.89 (s, CH_3 -anti).



Coupling product from 6 and DMBD to form species 8. A screw top NMR tube was charged with complex **6** (0.010 g, 0.009 mmol) and dissolved in CD_2Cl_2 (600 μL). The NMR tube was cooled to $-80\text{ }^\circ\text{C}$ and DMBD (40.0 μL , 0.035 mmol) was introduced via

syringe. The tube was inverted to allow for mixing. The reaction was monitored by low temperature ^1H NMR spectroscopy. Complete consumption of **6** is observed within 20 min at $-23\text{ }^\circ\text{C}$ and formation of a new species resulting from coupling is observed. There is no evidence of propene formed in this reaction. ^1H NMR (500 MHz, CD_2Cl_2 , $0\text{ }^\circ\text{C}$): δ 6.42 (s, 3H, mes-Ar), 5.77 (m, 1H, H_4), 3.43 (s, 1H, H_1), 2.53 (s, 1H, H_2), 2.28 (s, 9H, mes- CH_3), 2.07 (s, 3H, CH_3 -center), allylic CH_2 , vinyl H's, and one methyl group are masked by excess DMBD, 1.22 (s, 3H, CH_3). As the reaction is warmed from -80 to $0\text{ }^\circ\text{C}$ the solution changes color from red to bright yellow.



$[(\eta^3\text{-1-Methylstyrenyl})\text{Ni}(\text{mes})][\text{B}(\text{Ar}_\text{F})_4]$ (9). Complex **6** (0.011 g, 0.010 mmol) was added to a screw top NMR tube and dissolved in CD_2Cl_2 (600 μL) and cooled to $-80\text{ }^\circ\text{C}$. Styrene (3.2 μL , 0.028 mmol) was added via syringe and the NMR tube was inverted to allow for mixing. The sample was placed in a precooled NMR probe and the reaction was monitored by ^1H NMR spectroscopy. As the reaction temperature is raised, a small amount of polystyrene becomes evident in the ^1H spectrum at $-70\text{ }^\circ\text{C}$. Formation of species **9** is not observed until $-20\text{ }^\circ\text{C}$. After all styrene is consumed $\sim 50\%$ of starting complex **6** is present in solution together with complex **9**. ^1H NMR (500 MHz, CD_2Cl_2 , $25\text{ }^\circ\text{C}$): δ 6.42 (s, 3H, mes-Ar), 6.32 (s, 1H, H_2), 3.65 (q, 1H, $^3J_{\text{H-H}} = 6.5\text{ Hz}$, H_1), 2.25 (s, 9H, mes- CH_3), 1.46 (d, 3H, $^3J_{\text{H-H}} = 7\text{ Hz}$, CH_3). The other aromatic hydrogens of protons

of the η^3 -benzyl fragment are masked by polystyrene. As the reaction is warmed, the solution changes color from red to yellow-brown.

General Procedure for BD Polymerization using In Situ Generated Ligand-Free Species 4.

A flame dried Schlenk tube was charged with [(2-methallyl)Ni(mes)][B(Ar_F)₄], **2**, (0.010 g, 0.010 mmol) and B(C₆F₅)₃ (0.010 g, 0.019 mmol). The flask was cooled to -30 °C and the solids were dissolved in CH₂Cl₂ (total volume of 2.5 mL) to generate the ligand-free species [(2-methallyl)Ni][B(Ar_F)₄], **4**. Butadiene was added via cannula to another flame dried, preweighed Schlenk flask held at -80 °C. The flask was then warmed to -30 °C and the butadiene was added via cannula to the flask containing the nickel ligand-free species. The solution turned deep orange. The reaction was held at -30 °C and stirred until the polymerization was quenched. The polymerizations were terminated by adding 1.0 mg of 2,6-di-tert-butyl-4-methylphenol (BHT) followed by 5.0 mL of cold MeOH. The polymer was allowed to settle overnight by placing the flask in a -30 °C freezer. The MeOH layer was decanted and the polymer was dried in vacuo overnight. Each polymerization was run in duplicate. Polymerization results are summarized in Table 4.1. ¹³C{¹H} NMR spectroscopy was used to distinguish between different enchainment modes. The PBD enchainment was 93% *cis*-1,4 6% *trans*-1,4, and 1% 1,2. ¹³C{¹H} NMR (100 MHz, CDCl₃, 25 °C): δ 129.6 (vinyl CH, *cis* and *trans* overlap), 114.1 (vinyl CH, 1,2), 27.38 (CH₂-*cis*-1,4), 32.67 (CH₂-*trans*-1,4), 43.72 (CH-1,2).

General Procedure for Polymerization of DMBD with Ligand-Free Species 4.

A flame dried Schlenk flask was charged with complex **2** (0.011 g, 0.010 mmol) and $\text{B}(\text{C}_6\text{F}_5)_3$ (0.0103 g, 0.020 mmol). The flask was cooled $-30\text{ }^\circ\text{C}$ and CH_2Cl_2 (total volume 2.0 mL) was added and the mixture was allowed to stir. Then, DMBD was added via syringe and the polymerization was warmed to room temperature. The solution changed color from yellow-brown to bright yellow. The PDMBD formed is insoluble and precipitates from solution as a white powder. MeOH (5.0 mL) was added to terminate the polymerizations. The polymer was collected on a preweighed frit and dried in a vacuum oven at $120\text{ }^\circ\text{C}$. The polymerization data is found in Table 4.3. The observed IR and $^{13}\text{C}\{^1\text{H}\}$ NMR resonances are characteristic of *cis*-1,4 enchainment. $^{13}\text{C}\{^1\text{H}\}$ NMR (125 MHz, $\text{C}_6\text{D}_5\text{Br}$, $80\text{ }^\circ\text{C}$): δ 128.93 (CH olefin), 34.06 (CH_2), 18.83 (CH_3). IR (KBr): for symmetric CH_3 vibrations: 1384 cm^{-1} , 1372 cm^{-1} . For the DSC measurements, the samples was cooled to $-40\text{ }^\circ\text{C}$ and held for 10 min and warmed at $10\text{ }^\circ\text{C}/\text{min}$ to $300\text{ }^\circ\text{C}$. T_m : $181\text{ }^\circ\text{C}$.

General Procedure for Polymerization of IP with In Situ Generated Species 4.

A flame dried Schlenk tube was charged with complex **2** (0.010 g, 0.009 mmol) and $\text{B}(\text{C}_6\text{F}_5)_3$ (0.010 g, 0.019 mmol). The tube was cooled to $-30\text{ }^\circ\text{C}$ and the solids were dissolved in 0.50 mL of CH_2Cl_2 . Toluene or more CH_2Cl_2 (total volume is always 3.0 mL) was added. Isoprene was then added via syringe. The reaction was warmed to the desired temperature if necessary. The polymerizations were terminated by adding cold MeOH (5.0 mL). The polymer was allowed to settle in a $-30\text{ }^\circ\text{C}$ freezer. The MeOH layer was decanted and the polymer was dried in vacuo overnight. Each polymerization was run in duplicate. The polymerization data are summarized in Table 4.2. $^{13}\text{C}\{^1\text{H}\}$

NMR spectroscopy was used to determine the enchainment modes. The PIP enchainment was 64% *trans*-1,4, 23% *cis*-1,4, and 13% 3,4. $^{13}\text{C}\{^1\text{H}\}$ NMR (MHz, CDCl_3 , 25 °C): δ 23.41 (CH_3), 32.19 (CH_2) (characteristic signals for *cis*-1,4), 15.91 (CH_3), 38.2 (CH_2) (characteristic signals for *trans*-1,4), 40.02 (allylic CH_2), 111.5 (vinylic) (characteristic for 1,2).

General Procedure for BD Polymerization Using Complex 5.

A flame dried Schlenk flask was charged with complex **5** (0.006 g, 0.005 mmol) and CH_2Cl_2 (1.0 mL, unless specified in Table 4.4). The flask was cooled to -30 °C. Butadiene was added to another flame dried Schlenk flask, held at -30 °C, via cannula. The butadiene was then added to the nickel solution via cannula and the solution remained dark orange. The reaction was stirred at the desired temperature until the polymerization was terminated. The polymerizations were terminated by the addition of 1.0 mg of BHT and 5.0 mL of cold MeOH. The polymer was allowed to settle in the freezer at -30 °C. The MeOH layer was decanted and the polymer was dried in vacuo. Polymerization results are summarized in Table 4.4. The PBD enchainment was 94% *cis*-1,4, 5% *trans*-1,4, and 1% 1,2. $^{13}\text{C}\{^1\text{H}\}$ NMR (100 MHz, CDCl_3 , 25 °C): δ 129.6 (vinyl CH, *cis* and *trans* overlap), 114.1 (vinyl CH, 1,2), 27.38 (CH_2 -*cis*-1,4), 32.67 (CH_2 -*trans*-1,4), 43.72 (CH-1,2).

General Procedure for Polymerization of 1,3-CHD and IP using Complex 5.

NOTE: It is imperative that 1,3-CHD is dried over NaBH_4 before use to ensure consistent polymerization results.

Complex **5** (0.0100 g, 0.0091 mmol) was added to a flame dried Schlenk flask and dissolved in CH_2Cl_2 (total volume 2.0 mL). A butadiene solution 1.95 M in CD_2Cl_2 ,

(50 μL , 0.098 mmol)) was added and the solution was dark orange. Monomer was then added and the solution turned color to bright yellow. For 1,3-CHD, the polymer precipitates out of solution. Cold MeOH (5.0 mL) was added to terminate the polymerizations. For isoprene, the polymer was allowed to settle in a $-30\text{ }^{\circ}\text{C}$ freezer overnight. The MeOH layer was decanted and the polymer was dried in vacuo. The polymerization data are found in Table 4.5. The PIP enchainment was determined to be 84% *cis*-1,4, 15% *trans*-1,4, and 1% 1,2. $^{13}\text{C}\{^1\text{H}\}$ NMR (MHz, CDCl_3 , $25\text{ }^{\circ}\text{C}$): δ 23.41 (CH_3), 32.19 (CH_2) (characteristic signals for *cis*-1,4), 15.91 (CH_3), 38.2 (CH_2) (characteristic signals for *trans*-1,4), 40.02 (allylic CH_2), 111.5 (vinylic) (characteristic for 1,2).

For 1,3-CHD, the polymer was collected on a frit and dried in a vacuum oven overnight at $120\text{ }^{\circ}\text{C}$. All polymerizations were run in duplicate. The 1,3-CHD polymerization results are summarized in Table 4.7. The reported $^{13}\text{C}\{^1\text{H}\}$ NMR shifts indicated an atactic 1,4-enchainment with some 1,2-units present. $^{13}\text{C}\{^1\text{H}\}$ NMR (125 MHz, CDCl_3 , $60\text{ }^{\circ}\text{C}$, 1,4): δ 131.1 (CH olefin), 40.64 (CH allylic), 26.02 (CH_2). All the resonances are very broad making characterization of the polymer enchainment modes difficult. The DSC samples were cooled to $25\text{ }^{\circ}\text{C}$ and held for 15 min and then the temperature was raised $10\text{ }^{\circ}\text{C}/\text{min}$ to $350\text{ }^{\circ}\text{C}$ to obtain the data. T_m : $231\text{ }^{\circ}\text{C}$.

Polymerization of DMBD using **5 or **6**.**

A flame dried Schlenk flask was charged with complex **5** or **6** (0.0100 g) and dissolved in CH_2Cl_2 (total volume 2.0 mL). A 1.95 M butadiene solution in CD_2Cl_2 (20 μL , 0.039 mmol) was added and the reaction was allowed to stir. 2,3-Dimethyl-1,3-butadiene was added via a dry gas tight syringe and the reaction was stirred at room

temperature for the desired time. The polymer is insoluble in CH₂Cl₂ and precipitates from solution. The polymerizations were terminated by the addition on 5.0 mL of MeOH. The polymer was collected on a frit and was dried in a vacuum oven at 120 °C overnight. The polymerizations were run in triplicate. The polymerization results are found in Table 4.6. ¹³C{¹H} NMR (125 MHz, C₆D₅Br, 80 °C): δ 128.93 (CH olefin), 34.06 (CH₂), 18.83 (CH₃). IR (KBr): for symmetric CH₃ vibration: 1384 cm⁻¹, 1372 cm⁻¹.

Polymerization of Styrene with 5 or 6.

A flame dried Schlenk flask was charged with complex **5** or **6** (0.0100 g) and dissolved in CH₂Cl₂ (total volume 3.0 mL). The reaction flask was cooled to the desired temperature and styrene was added via a dry glass gas tight syringe. The reaction was allowed to stir for the desired time. The polymerization was terminated by the addition of 5.0 mL of MeOH, which precipitated the polymer as a white, fluffy powder. The polymer was collected on a frit and dried in a 120 °C vacuum oven overnight. The polymerizations were run in triplicate. The polymerization results are summarized in Table 4.8. The ¹H and ¹³C{¹H} NMR spectroscopic assignments are difficult due to broad resonances. ¹³C{¹H}NMR (101 MHz, CDCl₃, 25 °C) δ 128.0 (Ar C_o), 127.3 (Ar C_m), 125.6 (Ar C_p), and 40.6 (allylic CH₂).

References

1. Osakada, K.; Takeuchi, D. Coordination polymerization of dienes, allenes, and methylenecycloalkanes. In *Advances in Polymer Science*, Eds.; Springer-Verlag: Berlin, **2004**; Vol. 171, 137-194.
2. Industrial polymers, major. In *Encyclopædia Britannica*.
<http://www.britannica.com/eb/article-76457>.
3. Kaita, S.; Hou, Z.; Nishiura, M.; Kurazumi, J.; Horiuchi, A. C.; Wakatsuki, Y. *Macromol. Rapid Commun.* **2003**, *24*, 179-184.
4. Ricci, G.; Italia, S. *J. Organomet. Chem.* **1993**, *451*, 67-72.
5. Ricci, G.; Italia, S. *Macromolecules* **1994**, *27*, 868-869.
6. Pragliola, S.; Forlenza, E.; Longo, P. *Macromol. Rapid Commun.* **2001**, *22*, 783-786.
7. Ricci, G.; Italia, S.; Comitani, C.; Porri, L. *Polym. Commun.* **1991**, *32*, 514-517.
8. Dolgoplosk, B. A.; Tinyakova, E. I.; Stefanovskaya, N. N.; Oreshkin, I. A.; Shmonina, V. L. *Eur. Polym. J.* **1974**, *10*, 605-615.
9. Ricci, G.; Battistella, M. *Macromolecules* **2001**, *34*, 5766-5769.
10. Ricci, G.; Battistella, M.; Bertini, F.; Porri, L. *Polym. Bull.* **2002**, *48*, 25-31.
11. Kobayashi, E.; Hayashi, N.; Aoshima, S.; Furukawa, J. *J. Polym. Sci. Part A* **1998**, *36*, 1707-1716.
12. Nickaf, J. B.; Burford, R. P.; Chaplin, R. P. *J. Polym. Sci. Part A* **1995**, *33*, 1125-1132.
13. Quirk, R. P.; Kells, A. M.; Yunlu, K.; Cuif, J.-P. *Polymer* **2000**, *41*, 5903-5908.
14. Taube, R.; Windisch, H.; Maiwald, S.; Hemling, H.; Schumann, H. *J. Organomet. Chem.* **1996**, *513*, 49-61.
15. Taube, R.; Windisch, H.; Weissenborn J. *Organomet. Chem.* **1997**, *548*, 229-236.
16. Cui, L.; Ba, X.; Teng, H.; Ying, L.; Li, L.; Jin, Y. *Polym. Bull.* **1998**, *40*, 729-734.
17. Kaita, S.; Hou, Z.; Wakatsuki, Y. *Macromolecules* **2001**, *34*, 1539-1541.

18. Babitskii, B. D.; Dolgoplosk, B. A.; Kormer, V. A.; Lobach, M. I.; Tinyakova, E. I.; Yakovlev, V. A. *Isv. Akad. Nauk SSSR Ser. Chem.* **1965**, 1507.
19. Porri, L.; Natta, G.; Gallazzi, M. C. *J. Polym. Sci., Part C* **1967**, 2525-2537.
20. Durand, J. P.; Dawans, F.; Teyssié, P. *J. Polym. Sci. Part A* **1970**, 8, 979-990.
21. Dolgoplosk, B. A.; Beilin, S. I.; Korshak, Y. V.; Chernenko, G. M.; Vardanyan, L. M.; Teterina, M. P. *Eur. Polym. J.* **1973**, 9, 895-908.
22. Quirk, R. P.; You, F.; Zhu, L.; Cheng, S. Z. D. *Macromol. Chem. Phys.* **2003**, 204, 755-761.
23. Taube, R.; Gehrke, J. P. *J. Organomet. Chem.* **1985**, 291, 101-115.
24. Taube, R.; Gehrke, J. P.; Schmidt, U. *J. Organomet. Chem.* **1985**, 292, 287-296.
25. Taube, R.; Gehrke, J. P.; Schmidt, U. *Makromol. Chem., Macromol. Symp.* **1986**, 3, 389-404.
26. Taube, R.; Schmidt, U.; Gehrke, J. P.; Anacker, U. *J. Prakt. Chem.* **1984**, 326, 1-11.
27. Taube, R.; Gehrke, J. P.; Böhme, P.; Scherzer, K. *J. Organomet. Chem.* **1991**, 410, 403-416.
28. Taube, R.; Sylvester, G. Stereospecific Polymerization of Butadiene or Isoprene. In *Applied Homogeneous Catalysis with Organometallic Complexes*, Cornils, B., Herrmann, W. A. Eds.; VCH: Weinheim, Germany, **1996**; 280-318.
29. Cámpora, P. J.; Carmona, G. E.; Consejo Argandon, M. d. M. ES2200698, **2004**.
30. Cámpora, J.; Conejo, M. D. M.; Reyes, M. L.; Mereiter, K.; Passaglia, E. *Chem. Commun.* **2003**, 78-79.
31. O'Connor, A. R.; White, P. S.; Brookhart, M. *J. Am. Chem. Soc.* **2007**, 129, 4142-4143.
32. O'Connor, A. R.; Moorhouse, R. M.; Urbin, S. A.; White, P. S.; Brookhart, M. *Manuscript in Preparation* **2008**.
33. Taube, R.; Wache, S. *J. Organomet. Chem.* **1992**, 428, 431-442.
34. Beery, M. D.; Rath, M. K.; Sheares, V. V. *Macromolecules* **2001**, 34, 2469-2475.
35. Winter, H.; Aagaard, O. *Macromol. Rapid Commun.* **1998**, 19, 345-348.

36. Grossman, S.; Yamada, A.; Vogl, O. *J. Macromol. Sci. Chem.* **1981**, *A16*, 897-927.
37. Assioma, F.; Marchal, J.; Schue, F.; Friedmann, G.; Maillard, A. *J. Polym. Sci. Part C* **1968**, *16*, 3089-3095.
38. Kaminsky, W.; Hinrichs, B. Polymeric Dienes. In *Handbook of polymer synthesis*, 2 ed.; Kricheldorf, H. R., Nuyken, O., Swift, G. Eds.; Marcel Dekker: New York, **2005**; 333-380.
39. Sharaby, Z.; Martan, M.; Jagur-Grodzinski, J. *Macromolecules* **1982**, *15*, 1167-1173.
40. Ascenso, J. R.; Dias, A. R.; Gomes, P. T.; Ramão, C. C.; Pham, Q.-T.; Neibecker, D.; Tkatchenko, I. *Macromolecules* **1989**, *22*, 998-1000.
41. Hyder, I.; Jiménez-Tenorio, M.; Puerta, M. C.; Valerga, P. *Dalton Trans.* **2007**, 3000-3009.
42. Pangborn, A. B.; Giardello, M. A.; Grubbs, R. H.; Rosen, R. K.; Timmers, F. J. *Organometallics* **1996**, *15*, 1518-1520.
43. Yakelis, N. A.; Bergman, R. G. *Organometallics* **2005**, *24*, 3579-3581.

CHAPTER FIVE

Intramolecular Hydrogen Atom Transfer Observed in the Reaction of 1,3-Dienes and Olefins with (Cyclohexenyl)Ni(II) Complexes

Introduction

The molecular weight and the molecular weight distribution, (MWD), or polydispersity (PDI), of a polymer influences polymer properties including T_g , tensile strength, viscosity, and processability.¹ In transition metal-catalyzed polymerizations molecular weights and molecular weight distributions are largely controlled by chain transfer (often called chain termination) processes in which the growing polymer chain is cleaved from the metal center and a new chain is initiated. Furthermore, chain transfer processes allow formation of many polymer chains per metal center reducing the required loading of a metal catalyst. Therefore it is valuable to understand how chain transfer occurs in metal-catalyzed polymerization reactions and how catalyst features control these termination reactions.

There are four common modes of chain transfer in metal-catalyzed olefin polymerizations (Figure 5.1).² The first is chain transfer via β -hydride elimination, which generates an alkene end group and a M-H that can reinitiate chain propagation. The second mechanism is chain transfer to monomer, which involves the transfer of a hydrogen atom from the polyolefin to a monomer unit, generating a M-alkyl complex and a polymer chain

with an alkenyl end group. The third pathway is chain transfer by added hydrogen, which cleaves the M-polymer bond, regenerating a M-H and a free polymer chain containing a saturated alkyl end group. The fourth mode is transmetalation with an aluminum alkyl, AlR_3 , which generates an active M-R and a free polymer chain bound to aluminum.

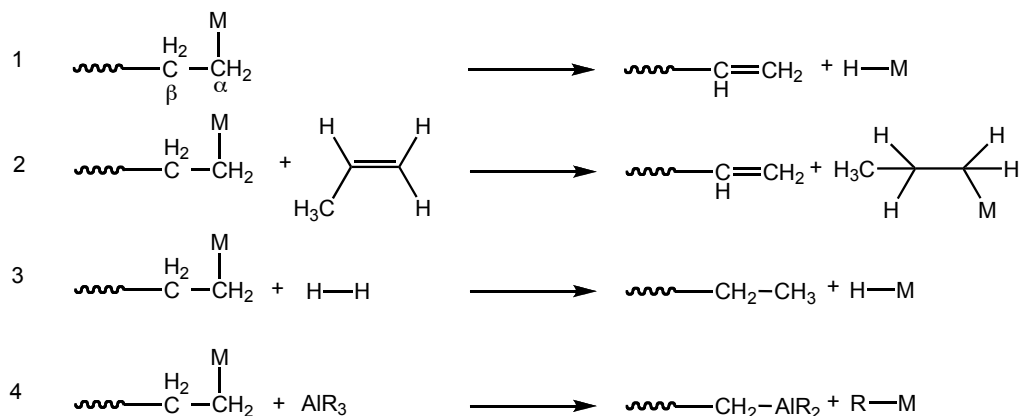


Figure 5.1. Chain termination pathways in the metal-catalyzed polymerization of olefins.

A common method that has been employed to control the molecular weight in the polymerization of α -olefins and dienes is through the use of chain transfer agents. Addition of α -olefins, hydrogen, and aluminum reagents has been shown to induce chain termination. Kaita recently reported the use of Al^iBu_3 as a chain transfer agent to control the molecular weight of polybutadiene formed using bimetallic lanthanide catalysts.³

Living polymerization using transition metal catalysts has been used as a technique to synthesize polymers of controlled molecular weights and unique architectures. The term “living” polymerization was defined by Szwarc and refers to a polymer chain that does not involve a termination step and thus the polymer will ‘live’ for a period of an extended time.⁴ In living polymerization, the rate of chain termination is negligible compared to the rate of

propagation allowing for the formation of higher molecular polymer chains and controlled molecular weight on a single metal center.⁵ Living polymerization allows for the consecutive addition of monomers to create block copolymers with segments of precisely controlled molecular weights. This can be envisioned to occur through a polymerization in which there are no chain transfer events.

The Brookhart lab reported the use of α -diimine palladium and nickel complexes for the living polymerization of α -olefins.^{6, 7} Polyethylene can be synthesized using these catalysts, yielding polymers that possess interesting morphologies and properties. Schrock and Grubbs are well-known for their work in the development of metal catalysts that produce living polymers through ring-opening metathesis polymerization (ROMP) of cyclic olefins.⁸⁻¹⁰ A variety of functionalized polymers with controlled molecular weights and structures can be prepared. The industrial application of living polymerization employing transition metal catalysts is still a major challenge because each polymer chain grows from a single metal center, making such processes economically unattractive.

Many groups have focused research on the development of catalysts¹¹ for the polymerization of butadiene (BD) using metal catalysts ranging from cobalt^{12, 13} and nickel¹⁴⁻¹⁶ to lanthanides.^{3, 17-20} The likely mechanisms of chain growth have been reviewed^{21, 22} and subjected to detailed mechanistic studies in the case of Ni(II) complexes (See chapter 2).²³ Tessy  has reported the only living polymerization of butadiene using the $[(\text{allyl})\text{Ni}(\text{TFA})]_2$ (TFA = trifluoroacetato) dimer and chloroanil as an added ligand, but the molecular weight distribution is broad for traditional living polymerization.²⁴ Copolymers of *cis* and *trans* 1,4-polybutadiene could also be synthesized using this catalyst. Additionally, Novak and

Deming have demonstrated the living polymerization in the copolymerization of butadiene with isocyanide using a bimetallic nickel TFA catalyst.²⁵

Although there are many studies on the polymerization of 1,3-dienes, there is very little experimental information regarding the mechanism of chain transfer in the polymerization of butadiene using (allyl)Ni(II) catalysts. Recently, Winter and coworkers reexamined Teyssié's [(allyl)Ni(TFA)]₂ catalyst in conjunction with chloroanil for butadiene polymerization, specifically interested in studying the chain transfer during polymerization of butadiene. By careful investigation of polymer molecular weight at various concentrations and times, they showed that the PDI begins to broaden and M_n remains constant at higher conversions²⁶ and this suggests that chain-transfer plays a more important role than previously proposed.²⁴ These results support that this catalyst system is far from living.

Taube has studied the chain transfer in the polymerization of butadiene using [(C₁₂H₁₉)Ni][B(Ar_F)₄] as a catalyst. The identity of a 1,3-diene end group was determined by trapping the diene using a Diels-Alder reaction with (Z)-diethyl diazene 1,2-dicarboxylate. Taube puts forward the idea that a diene end group points to β -hydride elimination as the main pathway to chain termination. He proposes that β -hydride elimination is rate-determining for chain transfer and that substitution of butadiene monomer for the polymer chain and the subsequent β -hydride elimination are both fast.^{27, 28} Therefore he suggests that the degree of polymerization can be controlled by the ratio of [BD]/[Ni], since the rate of propagation is dependent on [BD] where the chain transfer is independent of [BD].

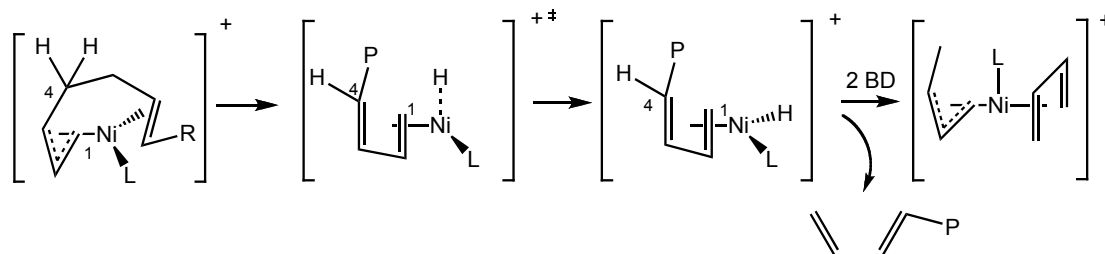
Additionally, Taube speculates that there may be an anion dependence because the chain transfer rate constant (k_u) decreases upon an increase in the catalyst concentration. The decrease in k_u may imply that the anion influences the rate of β -hydride elimination through

ion pair formation. In separate experiments, he has shown that addition of varying amounts NEt_4PF_6 influences the ratio of the rate of chain propagation to the rate of chain termination (k_p/k_u). A three-fold increase in the ratio of k_p/k_u was observed upon the addition of 100 equiv of NEt_4PF_6 to the reaction.²⁷

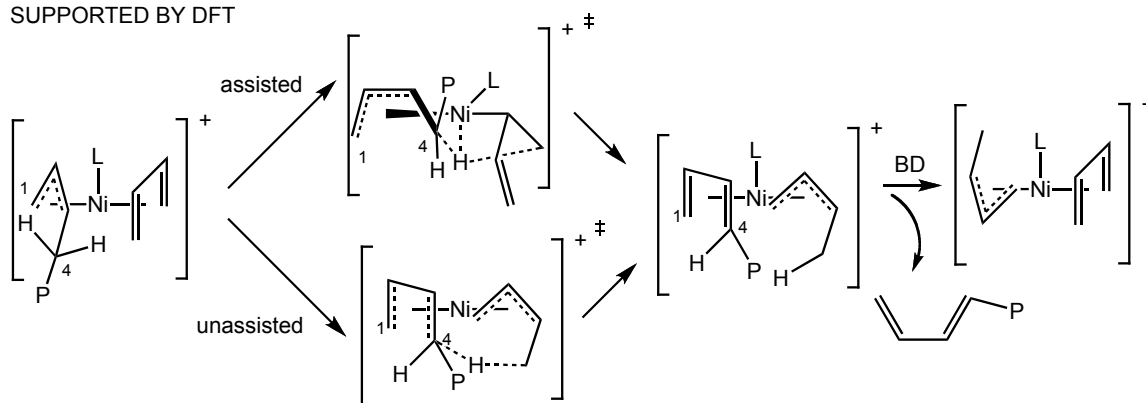
DFT calculations have been used to evaluate two possible mechanistic pathways in the chain termination using (allyl)Ni(II) catalysts for the polymerization of butadiene (Scheme 5.1).²⁹ The first mechanism is a hydrogen elimination pathway, in which a transient metal hydride exists as proposed by Taube.^{27, 28} The latter pathway is a hydrogen transfer mechanism, which involves concerted hydrogen atom transfer from the polybutadienenyl group to a monomer unit of butadiene. The hydrogen atom transfer could be envisioned to occur by either a metal-assisted or non-metal-assisted pathway. The calculations support a hydrogen transfer mechanism, which occurs without metal assistance. The ΔG^\ddagger for the hydrogen elimination path is at least 25.2 kcal/mol, while the ΔG^\ddagger 's for assisted and non-assisted hydrogen transfer mechanisms are 20.9 and 18.6 kcal/mol, respectively.²⁹ These values contradict Taube's previous experiments in which he proposes a discrete Ni-H is generated as a possible intermediate.^{27, 28}

Scheme 5.1. Proposed mechanisms for chain transfer in butadiene polymerization based on DFT calculations.

HYDROGEN ELIMINATION MECHANISM



HYDROGEN TRANSFER MECHANISM
SUPPORTED BY DFT



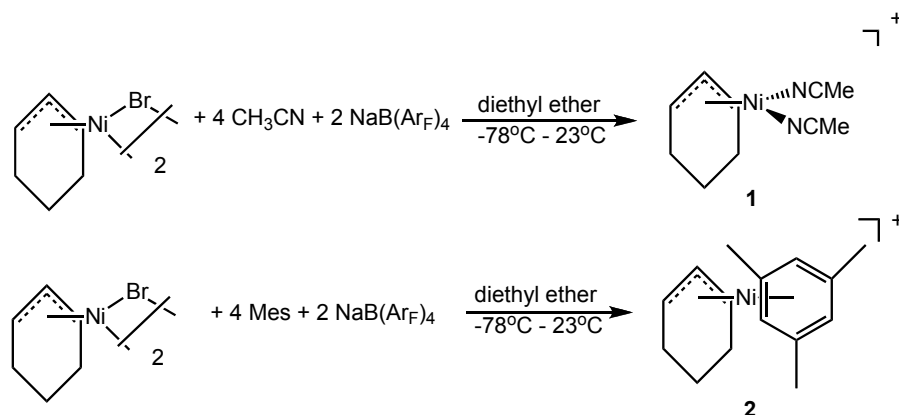
Previously, we reported the synthesis of complexes $[(2\text{-R-allyl})\text{Ni}(\text{NCMe})_2][\text{B}(\text{Ar}_\text{F})_4]$ ($\text{R} = \text{H}, \text{CH}_3$, $\text{Ar}_\text{F} = (\text{C}_6\text{H}_3)(\text{CF}_3)_2$), which serve as precursors to a naked nickel center. In the presence of 1 equiv of butadiene (BD) and 2 equiv $\text{B}(\text{C}_6\text{F}_5)_3$, η^4 -coordination of BD occurs, and the $(2\text{-R-allyl})\text{Ni}(\eta^4\text{-diene})^+$ complexes can be observed. However, upon exposure to greater than 1 equiv of BD rapid insertion occurs to yield wrap-around complexes as described in Chapter 2.²³ Additionally, we have shown that $[(2\text{-R-allyl})\text{Ni}(\text{mes})][\text{B}(\text{Ar}_\text{F})_4]$ ($\text{R} = \text{H}, \text{CH}_3$, $\text{mes} = \text{mesitylene}$) complexes exhibit interesting reactivity with olefins³⁰ and are highly active polymerization catalysts for 1,3-diene and styrene polymerization, as described in chapter 4 of this thesis.

The work described in this chapter focuses on the synthesis of $[(\text{cyclohexenyl})\text{Ni}(\text{NCMe})_2][\text{B}(\text{Ar}_\text{F})_4]$, **1**, and $[(\text{cyclohexenyl})\text{Ni}(\text{mes})][\text{B}(\text{Ar}_\text{F})_4]$, **2**, and investigation of the reactivity of these complexes with 1,3-dienes and α -olefins, which sheds light on the possible chain termination pathway in 1,3-diene polymerization. Similar to previous experiments using acyclic allyl complexes, a cationic ligand-free (cyclohexenyl)Ni(II) complex, in which a single Ar_F ring is coordinated to nickel, can be observed at low temperature. Interestingly, in contrast to the acyclic allyl complexes, the $(\text{cyclohexenyl})\text{Ni}(\eta^4\text{-diene})^+$ complexes are stable up to $-20\text{ }^\circ\text{C}$ to $-10\text{ }^\circ\text{C}$, at which insertion of diene occurs. The reactions of **2** with olefins and 1,3-dienes and the observed intramolecular hydrogen atom transfer will also be discussed. Additionally, we describe the first observation of an *s-trans*-coordinated 1,3-diene.

Results and Discussion

Catalyst Synthesis and Structure. The synthesis of complexes $[(\text{cyclohexenyl})\text{Ni}(\text{NCMe})_2][\text{B}(\text{Ar}_\text{F})_4]$, **1**, and $[(\text{cyclohexenyl})\text{Ni}(\text{mes})][\text{B}(\text{Ar}_\text{F})_4]$, **2**, was achieved using methods previously described for the preparation of the analogous allyl compounds.²³ Salt metathesis of $[(\text{cyclohexenyl})\text{NiBr}]_2$, readily synthesized via literature methods,¹³ with 2 equiv $\text{NaB}(\text{Ar}_\text{F})_4$ in diethyl ether in the presence of 4 equiv of ligand (mesitylene (mes) or acetonitrile (NCMe)) generates compounds **1** and **2** in good yields (Scheme 5.2). Characterization of the compounds was achieved using ^1H and ^{13}C NMR spectroscopy and elemental analysis.

Scheme 5.2. Synthesis of cationic (cyclohexenyl)Ni(II) complexes.



The structure of **2** was established using X-ray crystallography (Figure 5.2, Tables III.1, III.3, and III.4 of the Appendix).³¹ In the molecular structure of complex **2** the mesitylene ligand exhibits no puckering or bending upon coordination. The C₅ methylene group of the cyclohexenyl ligand is bent out of the plane pointing away from the mesitylene ring. The Ni-C₁, Ni-C₂, and Ni-C₃ bond lengths of the allyl moiety are nearly identical, consistent with similar bond distances observed for the analogous [(allyl)Ni(mes)][B(Ar_F)₄] complex.²³ Interestingly, this structure shows variation in the Ni-C bond lengths to the arene. The Ni-C₁₁, Ni-C₁₂, Ni-C₇, and Ni-C₈ exhibit bond lengths in the range of 2.15-2.16 Å, while the Ni-C₁₀ and Ni-C₉ bond lengths are elongated to 2.19 and 2.22 Å, respectively. The significant differences in the bond lengths, suggest a ring slippage away from an ideal η^6 binding scheme and a stronger interaction of Ni with the C₈-C₇-C₁₁-C₁₂ “ η^4 ” diene unit relative to the C₁₀-C₉ “ η^2 ” olefinic unit.

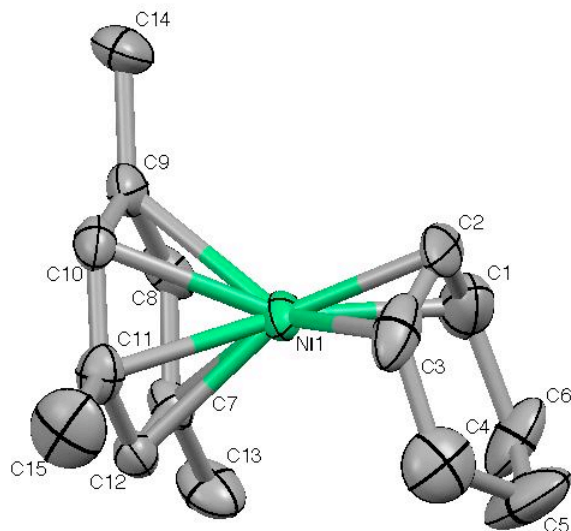


Figure 5.2. Molecular structure of complex **2**. Thermal ellipsoids drawn at 50% probability. Hydrogen atoms and [B(Ar_F)₄], omitted for clarity. Selected bond lengths (Å): Ni(1)-C(2) 1.934(5), Ni(1)-C(3) 2.015(5), Ni(1)-C(1) 2.063(6), Ni(1)-C(8) 2.149(5), Ni(1)-C(12) 2.154(4), Ni(1)-C(11) 2.157(5), Ni(1)-C(7) 2.159(4), Ni(1)-C(10) 2.193(5), Ni(1)-C(9) 2.224(5).

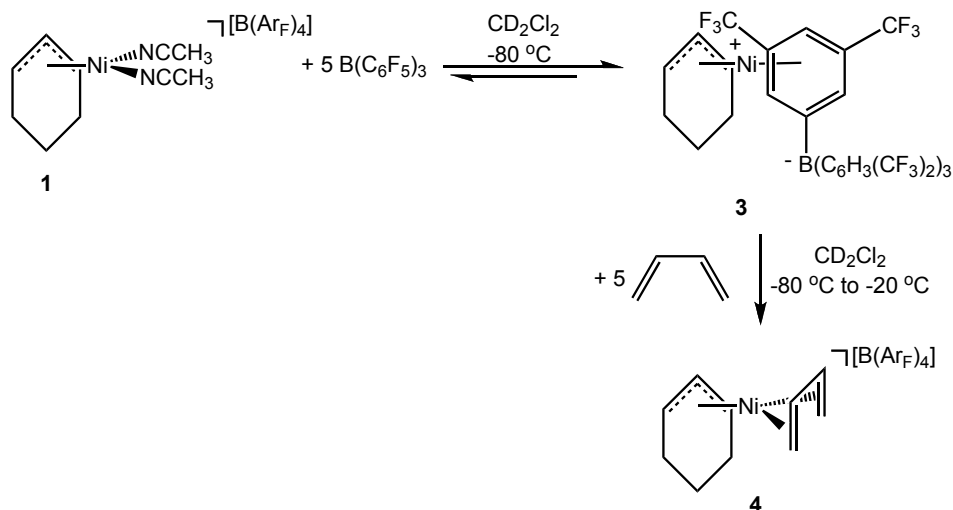
Ligand Exchange Reactions. The lability of the mesitylene group coordinated to the (cyclohexenyl)Ni(II) fragment was probed through the addition of various ligands. Addition of 5 equiv of mesitylene-*d*₁₂ to complex **2** generates a resonance in the mesityl aryl region at δ 6.79, indicative of free mesitylene, along with a resonance for the coordinated mesityl group at 6.55 ppm. This indicates that mesitylene exchange occurs on the chemical time scale. Equilibrium is reached within 4 h. The ratio of coordinated:free mesitylene is 3:7 approximately 10 min after mixing complex **2** with mesitylene-*d*₁₂. After 4 h, the ratio of coordinated to free mesitylene changes to 1:6 and this ratio remained constant after 1 day. No line broadening is observed in the ¹H NMR spectrum when protio mesitylene is added to complex **2**, which means arene exchange is slow on the NMR time scale. Complete displacement of the mesitylene by hexamethylbenzene (hmb) occurs to form [(cyclohexenyl)Ni(hmb)]⁺ within 4 h. The ratio of **2**:[(cyclohexenyl)Ni(hmb)]⁺ was 1:9

within 10 min of adding hmb to compound **2**. Complete conversion to the hexamethyl benzene species is achieved within 1 h and is much slower than that previously reported for the $[(\text{allyl})\text{Ni}(\text{mes})]^+$ analog.³⁰ Exposure of **2** to 9 equiv of diethyl ether results in very minor displacement of mesitylene after 1 day indicating that diethyl ether does not effectively compete with mesitylene for binding to Ni.

Reactions with 1,3-Dienes. The reaction of **1** in the presence of 5 equiv of $\text{B}(\text{C}_6\text{F}_5)_3$ generates $[(\text{cyclohexenyl})\text{Ni}][\text{B}(\text{Ar}_\text{F})_4]$, **3**, at low temperatures (Scheme 5.3). This species was identified spectroscopically by ^1H and ^{19}F NMR and shows the presence of four new resonances in the ^1H spectrum for the coordinated $[\text{B}(\text{Ar}_\text{F})_4]^-$ anion. The ratio of the new proton signals in the ^1H NMR spectrum is 1:6:3:2. In the ^{19}F NMR spectrum there are two signals for coordinated $[\text{B}(\text{Ar}_\text{F})_4]^-$ in a 1:3 ratio, corresponding to the coordinated:uncoordinated Ar_F rings. This pattern indicates one Ar_F ring is coordinated to nickel, while the remaining 3 aryl rings are uncoordinated as previously observed for $[(\text{allyl})\text{Ni}][\text{B}(\text{Ar}_\text{F})_4]$ and $[(2\text{-methallyl})\text{Ni}][\text{B}(\text{Ar}_\text{F})_4]$.²³

Intramolecular exchange is observed for the Ar_F rings at $-40\text{ }^\circ\text{C}$ through broadening of the coordinated Ar_F resonances as previously observed for similar species.²³ ^1H VT NMR experiments at $-70\text{ }^\circ\text{C}$ to $-35\text{ }^\circ\text{C}$ showed the barrier to intramolecular Ni migration among the rings to be $\Delta G^\ddagger = 11.9\text{ kcal/mol}$. Intermolecular exchange of coordinated $[\text{B}(\text{Ar}_\text{F})_4]^-$ with free $[\text{B}(\text{Ar}_\text{F})_4]^-$ occurs on the NMR timescale at temperatures above $0\text{ }^\circ\text{C}$. Details of this dynamic process are described in the Experimental Section. Species **3** is in equilibrium with starting complex **1** and the equilibrium is temperature dependent shifting towards species **3** at higher temperatures. At $-20\text{ }^\circ\text{C}$, the ratio of **3**:**1** is 4:1.

Scheme 5.3. Generation of [(cyclohexenyl)Ni][B(Ar_F)₄], **3**, and [(cyclohexenyl)Ni(η^4 -butadiene)][B(Ar_F)₄], **4**, at low temperatures.



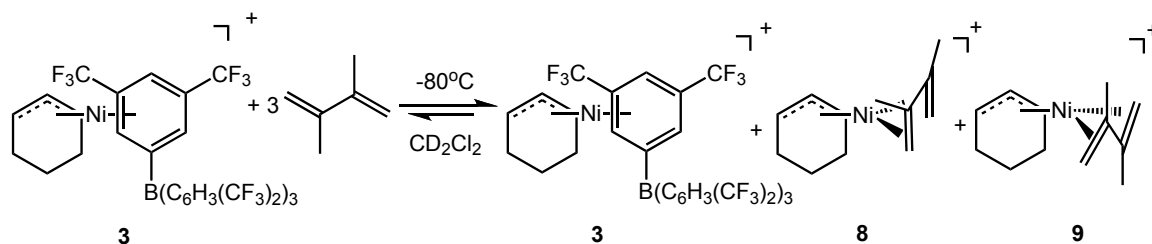
Species **3** rapidly coordinates butadiene at -80 °C to form η^4 -diene adduct [(cyclohexenyl)Ni(η^4 -butadiene)][B(Ar_F)₄], **4**, (Scheme 5.3). Only one isomer, the *s-cis* η^4 -diene complex **4**, is observed in the ¹H NMR spectrum and this species is the most stable structure predicted by DFT calculations.³² At temperatures below -20 °C, insertion reactions do not take place in the presence of excess butadiene. This contrasts with our previous result, in which [(allyl)Ni][B(Ar_F)₄] rapidly inserts 3 equiv of butadiene to form stable wrap-around complexes below -110 °C.²³ The cyclohexenyl insertion product, formed at -20 °C, has a characteristic ¹H NMR spectrum for a wrap-around complex, but the spectrum is too complex to assign.

Addition of 2 equiv of isoprene (IP), 1,3-cyclohexadiene (1,3-CHD), and 1,4-cyclohexadiene (1,4-CHD) to ligand-free species **3** at -80 °C yields [(cyclohexenyl)Ni(η^4 -IP)][B(Ar_F)₄], **5**, [(cyclohexenyl)Ni(η^4 -1,3-CHD)][B(Ar_F)₄], **6**, and [(cyclohexenyl)Ni(η^4 -1,4-CHD)][B(Ar_F)₄], **7**, respectively. Complexes **5** and **6** undergo insertion of diene at -20

°C, while **7** is stable at room temperature. Each of the CH₂ groups of the cyclohexenyl ring is diastereotopic when diene or arene is coordinated, facilitating their assignment in the ¹H NMR spectrum (see Experimental Section for complete characterization).

When the diene partner used is 2,3-dimethyl-1,3-butadiene (DMBD), an interesting result is obtained. Two isomers of an η⁴-diene species, one major and one minor, in addition to ligand-free complex are observed at -80 °C. Upon warming to -20 °C, there is no spectral evidence for **3** in solution. This indicates that there is an equilibrium between the diene complexes and the ligand-free species **3**. Through spectroscopic data provided from ¹H-¹H-COSY and ¹H NMR experiments, the identities of the 2 isomers were established as: [(cyclohexenyl)Ni(η⁴-*s-cis*-DMB)]⁺, **8**, the major isomer, and [(cyclohexenyl)Ni(η⁴-*s-trans*-DMB)]⁺, **9**, the minor isomer (Scheme 5.4). This is the first observation of an η⁴-*trans* coordinated diene on a nickel complex. In the ¹H NMR spectrum at -20 °C, **9** exhibits four signals (each integrating for 1.0H) that appear in the region for a coordinated olefin (δ 5.19, 5.04, 4.46 and 4.30) as well as two methyl resonances (δ 1.94, 1.50), each correlating to a different set of olefinic signals. Additionally, for the minor isomer, separate H₁ and H₂ allyl peaks (each integrating for 1.0H) appear at 6.32 (H₁) and 6.30 (H₁') and 5.32(H₂) ppm, respectively. These ¹H NMR characteristics point to an η⁴-diene complex in which the DMBD moiety is in the *s-trans* geometry. The ¹H NMR spectrum for the *s-cis* coordinated diene fragment of species **8** exhibits two olefinic signals at δ 4.97 (2.0H) and 2.93 (2.0H) and a single 6.0H methyl resonance (δ 2.21). The ratio of the two isomers (*cis:trans*) is 4:1 at -20 °C, and this ratio does not change over time, suggesting this is the thermodynamic ratio.

Scheme 5.4. Exposure of species **3** to 4 equiv of DMBD.

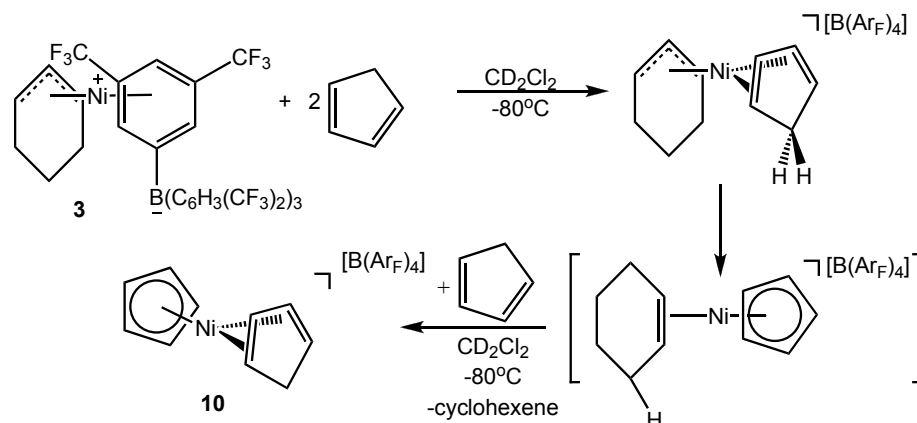


The identification of an η^4 -*trans* diene coordinated to Ni may have implications concerning the mechanism for *trans*-1,4-enchainment of polybutadiene. It is proposed that the chain growth mechanism to form *trans*-enchained polybutadiene occurs from an η^4 -*trans* coordinated butadiene species because a *syn* allyl forms after insertion. This correlation was first established through separate experiments performed by Porri³³ and Tolman.³⁴ We will continue to study this reaction to try to gain more information regarding the coupling of *trans*-DMBD to the (cyclohexenyl)Ni(II) moiety.

Qualitative experiments were performed to assess the binding strengths of 1,3-dienes to the (cyclohexenyl)Ni(II) fragment. Exposing a solution of η^4 -butadiene species **4** at -60°C to 2 equiv of IP leads to a 3:1 ratio of complexes **5**:**4**, indicating a slight preference for binding the more electron rich IP to the nickel center. Similarly, we have observed this trend for preferential coordination of more electron rich arenes to cationic (allyl)Ni(II) and Pd(II) fragments as described in chapter 3.³⁰ No insertion of BD or IP is observed at this temperature. Upon warming, the resonances for the η^4 -BD coordinated species **4** broaden, while those for the η^4 -IP species remain fairly sharp. At -10°C , the resonances for **4** are broadened into the baseline and at 0°C both species exhibit broad resonances, indicating exchange of diene on the NMR timescale.

An interesting reaction is observed upon the addition of ligand-free **3** or mesitylene complex **2** to cyclopentadiene. Exposure of species **3** to 2 equiv of cyclopentadiene at -80 °C results in a rapid color change from yellow-brown to green-yellow. The ^1H NMR spectrum is indicative of the formation of $[(\text{cyclopentadienyl})\text{Ni}(\eta^4\text{-cyclopentadiene})][\text{B}(\text{Ar}_\text{F})_4]$ (**10**), which was independently synthesized through protonation of Cp_2Ni with $[\text{H}(\text{OEt}_2)][\text{B}(\text{Ar}_\text{F})_4]$. $[(\text{Cyclopentadienyl})\text{Ni}(\eta^4\text{-cyclopentadiene})]^+$ with BF_4^- ³⁵ or OTf^- ³⁶ as counterions has previously been reported. This species is quite robust and is not active for butadiene polymerization. Similarly, exposure of complex **2** to 3 equiv of cyclopentadiene at 0 °C leads to the direct formation of species **10** and one equiv of cyclohexene. This product forms via hydrogen atom transfer from cyclopentadiene to the cyclohexenyl group. In the ^1H NMR spectrum, all mesitylene is now uncoordinated, as indicated by a downfield shift of the aryl singlet resonance to 6.79 ppm. We propose this reaction occurs through a similar mechanism as observed for the hydrogen atom transfer reactions when 1-hexene is exposed to $[(2\text{-R-allyl})\text{Ni}(\text{mes})]^+$ ³⁰ (Scheme 5.5). It is proposed that $\eta^4\text{-cyclopentadiene}$ coordination occurs prior to hydrogen atom transfer. This assignment is supported by observation of a transient, minor amount of a complex, tentatively assigned as $[(\text{cyclohexenyl})\text{Ni}(\eta^4\text{-cyclopentadiene})]^+$ in the ^1H NMR spectrum at -80 °C.

Scheme 5.5. Addition of cyclopentadiene to species **3** at -80 °C.

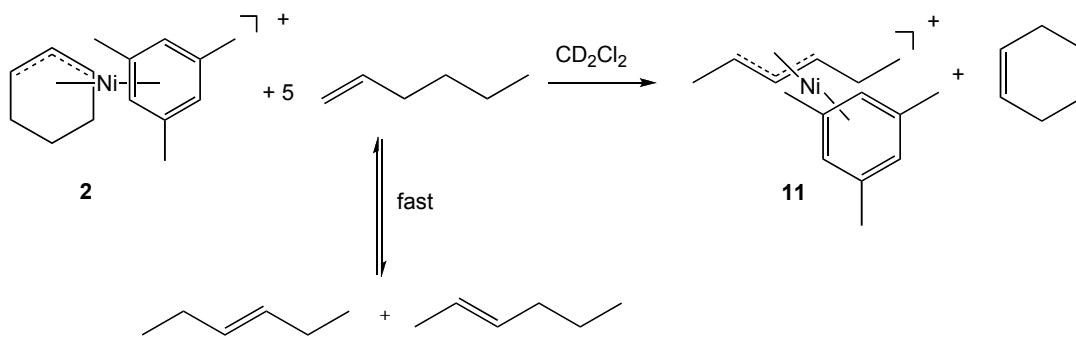


Polymerization Screening. $[(\text{Cyclohexenyl})\text{Ni}(\text{mes})][\text{B}(\text{Ar}_\text{F})_4]$, **2**, is active for the polymerization of 1,3-dienes. The polymerization of 850 equiv of 1,3-CHD is achieved within 1 h at room temperature in methylene chloride. Upon monomer addition, the solution changes color from red-orange to yellow. The reaction is highly exothermic and within two min the solution temperature has risen substantially. The polymer produced is insoluble in CH_2Cl_2 and therefore precipitates out of solution as a white powder (85% isolated). Additionally, catalyst **2** is active for DMBD polymerization at room temperature in CH_2Cl_2 . Within 6 h, 32% conversion is achieved in the polymerization of DMBD using initiator **2**. The polymer produced is also insoluble in CH_2Cl_2 and precipitates from solution. Within 6 h catalyst decomposition has occurred as evidenced by a colorless solution. The mesitylene catalyst is not active for polymerization of 1,3-CHD or DMBD at temperatures much below 0°C . All polymerization results are tabulated in Table III.2 of the Appendix. A more detailed screening of polymerization activity will be the focus of future work.

Reaction with Olefins. Reaction of mesitylene complex **2** with olefins leads to hydrogen atom transfer products, analogous to the findings reported for the [(2-R-

allyl)Ni(mes)][B(Ar_F)₄] complexes (R = H, CH₃) (see chapter 3).³⁰ Exposure of 4-5 equiv of 1-hexene to species **2** at room temperature generates one equiv of cyclohexene and a new allyl complex, [(2-hexenyl)Ni(mes)][B(Ar_F)₄] (**11**), after 24 h (Scheme 5.6). Rapid isomerization of 1-hexene to the internal 2- and 3-isomers is observed within 10 min of olefin addition and only minor formation of the new allyl species is achieved. After 2.5 h, the ¹H spectrum shows a signal for the olefinic hydrogens of cyclohexene at 5.66 ppm and a new allyl resonance integrating for 2.0H at 3.11 ppm, with complex **2** still present in solution. Species **11** is completely characterized in the Experimental Section of chapter 3. This intramolecular hydrogen atom transfer reaction in the cyclohexenyl system is much slower when compared to the [(allyl)Ni(mes)]⁺ system. Similar to previous experiments, the addition of ethylene produced ethylene oligomers.³⁰

Scheme 5.6. Reaction of 1-hexene with complex **2** at room temperature.



Experiments to rule out the involvement of Ni(0) in the isomerization and hydrogen atom transfer reaction have been performed. To ensure that the reaction was not catalyzed by Ni(0), the solution was filtered through a 0.2 μ filter before addition of 1-hexene. The isomerization and hydrogen atom transfer reactions occurred after filtration, supporting a

Ni(II)-catalyzed reaction. Isomerization of 1-hexene was not observed in the absence of Ni(II).

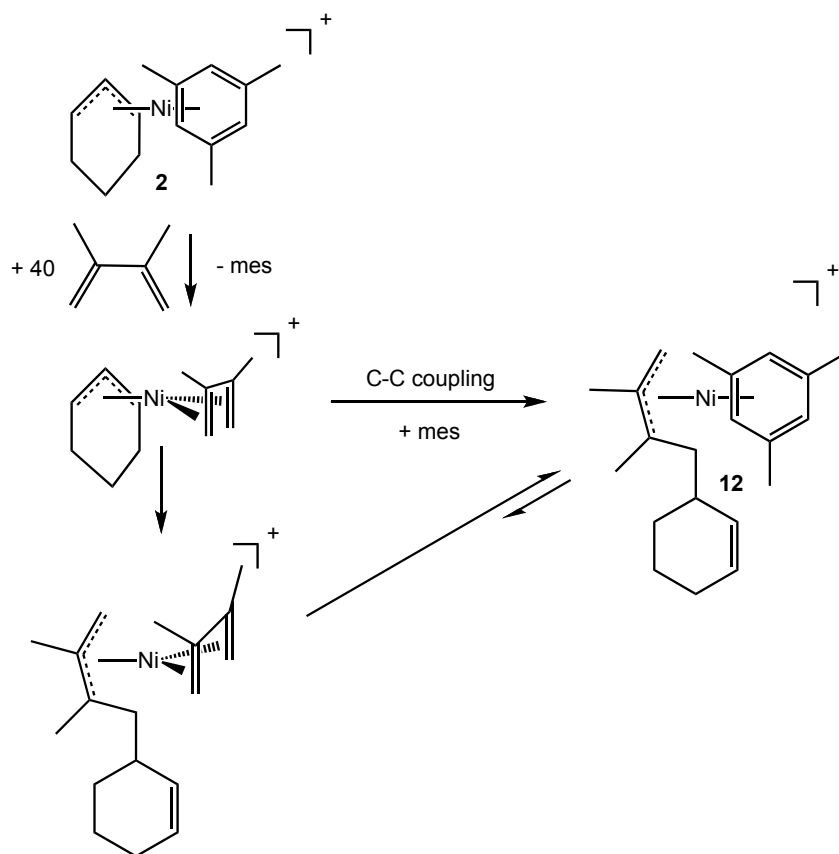
The mechanism to form complex **11** involves intramolecular hydrogen atom transfer from hexene to the cyclohexenyl moiety. ^1H NMR studies show that rapid isomerization of 1-hexene to the 2- and 3-hexene isomers occurs prior to hydrogen atom transfer, however the details of the isomerization mechanism are still unclear. We know from previous experiments, as described in chapter 3, that the internal *cis*-2-hexene and *trans*-2-hexene isomers also undergo hydrogen atom transfer reactions with $(\text{allyl})\text{Ni}(\text{mes})^+$. It is uncertain as to which isomer or isomers of hexene are needed to generate complex **11**. Following isomerization, hydrogen atom transfer from hexene would generate one equiv of cyclohexene and complex **11** after trapping with mesitylene. Further experiments are planned to evaluate this interesting reactivity.

Reaction of 2 with DMBD. When complex **2** is treated with DMBD, a new $(\text{allyl})\text{Ni}(\text{II})$ product from carbon-carbon coupling is formed. The reaction of 40 equiv of DMBD and **2** was monitored at $-20\text{ }^\circ\text{C}$ using ^1H NMR spectroscopy. A new allyl species containing two allyl resonances, a *syn* resonance 3.38 ppm (s, 1.0H) and an *anti* resonance at 2.65 ppm (s, 1.0H) are present in solution. This species also exhibits two broad olefinic triplets characteristic of an unsymmetrically substituted cyclohexene at 5.43 and 5.66 ppm. There is no evidence of cyclohexene (δ 5.66, 1.61, 1.26) in the ^1H NMR spectrum, as would be expected if hydrogen atom transfer to the cyclohexenyl ligand occurred.

Scheme 5.7 describes a plausible mechanism to form the coupling product, followed by the intramolecular hydrogen atom transfer. We propose that η^4 -coordination of DMBD occurs first, and this species then undergoes C-C coupling. Although the formation of η^4 -

diene complexes has never been observed at low temperature by ^1H NMR when **2** is exposed to 1,3-dienes, we believe DMBD must coordinate in an η^4 -fashion to facilitate C-C coupling. After the coupling reaction, a new (allyl)Ni(II) species is formed and coordinates mesitylene. Coupling of DMBD and the cyclohexenyl moiety would generate a product as drawn in Scheme 5.7 (**12**). This new allyl species, **12**, is similar to the previously reported assignment for the coupling product of an allyl moiety and DMBD as described in chapter 4 for the product formed after the reaction of $[(\text{allyl})\text{Ni}(\text{mes})][\text{B}(\text{Ar}_\text{F})_4]$ with 40 equiv of DMBD. The resonances for the methyl groups for species **12** are masked by excess DMBD and oligomers present in solution. There is still uncertainty as to the identity of the coupled molecule, as many of the aliphatic proton resonances are masked by excess DMBD.

Scheme 5.7. C-C coupling of complex **2** with DMBD.



The above experiments support the hypothesis that chain transfer in 1,3-diene polymerization probably occurs through intramolecular hydrogen atom transfer; a discrete Ni-H intermediate as previously proposed by Taube is unlikely.^{27, 28} Observation of intramolecular hydrogen atom transfer from added olefin to the cyclohexenyl fragment supports a mechanism in which chain transfer occurs via a hydrogen atom transfer, adding experimental credence to Tobisch's DFT calculations.²⁹ We are further examining these systems to gain information about the rate of hydrogen transfer in these reactions.

Summary

The reactivity of (cyclohexenyl)Ni(II) complexes was investigated using olefins and 1,3-dienes. Exposure of [(cyclohexenyl)Ni(NCMe)₂][B(Ar_F)₄] to 2 equiv B(C₆F₅)₃ generated a ligand-free species [(cyclohexenyl)Ni][B(Ar_F)₄], **3**, at low temperatures. Stable (η^4 -diene)Ni(cyclohexenyl)⁺ complexes (diene = BD, IP, DMBD, 1,3-CHD, and 1,4-CHD) have been observed for the first time by reaction of **3** with dienes. Significantly, we have identified the first η^4 -*s-trans* coordinated diene to an (allyl)Ni(II) species. The ability to form these stable η^4 -diene complexes, which will be useful for the study of chain transfer reactions that occur in diene polymerization and will be the focus of future work. Additionally, we have observed for the first time intramolecular hydrogen atom transfer reactions from monomer (olefin) to the cyclohexenyl moiety when [(cyclohexenyl)Ni(mes)][B(Ar_F)₄] was treated with α -olefins. We will further probe this reaction to determine whether the hydrogen atom transfer is reversible. Hydrogen atom transfer from cyclopentadiene to the cyclohexenyl moiety was observed, preliminarily suggesting that chain transfer occurs through hydrogen transfer from the diene to the allyl

group. Study of this reaction will be continued through addition of deuterium labeled dienes to monitor the transfer of a hydrogen atom.

Experimental

General Considerations.

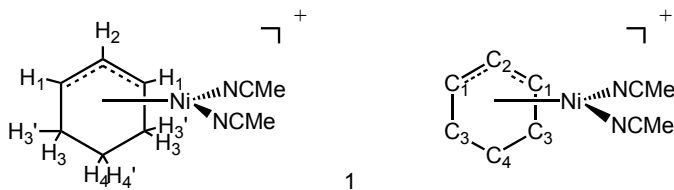
All reactions, unless otherwise stated, were conducted under an atmosphere of dry, oxygen free argon atmosphere using standard high-vacuum, Schlenk, or drybox techniques. Argon was purified by passage through BASF R3-11 catalyst (Chemalog) and 4Å molecular sieves. All nickel catalysts were stored under argon in an M.Braun glovebox at -35 °C. ^1H , ^{13}C , and ^{19}F NMR spectra were recorded on a Bruker DRX 500 MHz, a Bruker DRX 400 MHz, or a Bruker 300 MHz spectrometer. Chemical shifts are referenced relative to residual CHCl_3 (δ 7.24 for ^1H), CH(D)Cl_2 (δ 5.32 for ^1H), $^{13}\text{CD}_2\text{Cl}_2$ (δ 53.8 for ^{13}C), $^{13}\text{CDCl}_3$ (δ 77.0 for ^{13}C). Elemental analyses were performed by Robertson Microlit Laboratories of Madison, NJ.

Materials.

All solvents were deoxygenated and dried by passage over columns of activated alumina.³⁷ CD_2Cl_2 , purchased from Cambridge Laboratories, Inc., was dried over CaH_2 , vacuumed transferred to a Teflon sealable Schlenk flask containing 4Å molecular sieves, and degassed via three freeze-pump-thaw cycles. Butadiene and isoprene were purchased from Aldrich and purified by vacuum transfer through a column of 4Å molecular sieves and stored under argon at -35 °C. 1,3-Cyclohexadiene was purified by drying over NaBH_4 overnight, vacuum transferred into a Teflon sealable flask and degassed via three freeze-pump-thaw cycles. 2,3-Dimethyl-1,3-butadiene and 1,4-cyclohexadiene were purified by degassing via three freeze pump thaw cycles. $\text{Ni}[\text{COD}]_2$ and $\text{B}(\text{C}_6\text{F}_5)_3$ were purchased from Strem.

NaB(Ar_F)₄ (Ar_F = 3,5-(CF₃)₂C₆H₃),³⁸ nickolecene (Cp₂Ni),³⁹ and [H(OEt₂)] [B(Ar_F)₄]⁴⁰ were synthesized according to literature methods. Cyclopentadiene was distilled fresh prior to use through cracking of dicyclopentadiene purchased from Aldrich and stored cold. 1-Hexene was purchased from Aldrich, dried over CaH₂, and vacuum transferred into a sealable flask. Acetonitrile, mesitylene (mes), hexamethyl benzene (hmb) mesitylene-*d*₁₂, and 3-bromocyclohexene were purchased from Aldrich and Acros respectively and used without further purification. [(cyclohexenyl)NiBr]₂ was synthesized according to literature methods.¹³

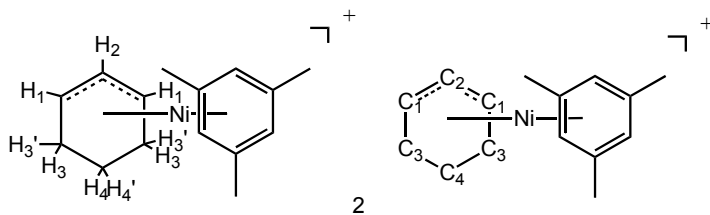
Spectral data for [B(Ar_F)₄][−]. The ¹H and ¹³C spectral data for the B(Ar_F)₄[−] counteranion were unchanged for all Ni(II) cationic complexes and are not be included in the characterization unless otherwise stated. ¹H NMR (400 MHz, CD₂Cl₂, 20 °C): δ 7.72 (s, 4H, Ar_F H_p), 7.57 (s, 8H, Ar_F H_o). ¹³C{¹H} NMR (101 MHz, CD₂Cl₂, 20 °C): δ 162.1 (q, ¹J_{C-B} = 49.8 Hz, Ar_F C_{ipso}), 135.2 (s, Ar_F C_o), 129.2 (qq, ³J_{C-B} = 3.0 Hz, ³J_{C-F} = 34.4 Hz, Ar_F CF₃), 122.3 (q, ¹J_{C-F} = 273.2 Hz, Ar_F CF₃), 117.8 (bt, Ar_F C_p).



Synthesis of (Cyclohexenyl)Ni(II) Complexes.

[(Cyclohexenyl)Ni(NCMe)₂][B(Ar_F)₄] (1). A flame-dried Schlenk tube was charged with [(cyclohexenyl)NiBr]₂ (0.070 g, 0.159 mmol) dimer and NaB(Ar_F)₄ (0.282 g, 0.318 mmol) and cooled to -78 °C. The solids were dissolved in diethyl ether (10.0 mL) to yield an orange solution with a fine precipitate. Acetonitrile (33.2 μL, 0.636 mmol) was added and the solution turned yellow. The reaction was then warmed to room temperature and stirred for

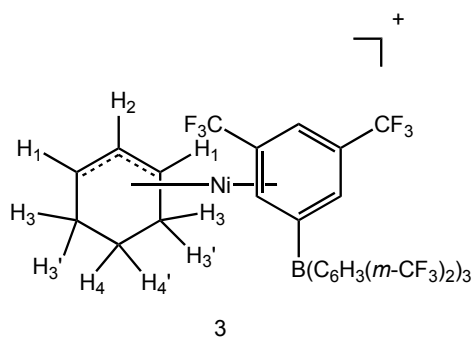
1h. The solution was filtered via cannula and the volatiles were removed in vacuo to yield a yellow oily product. The oil was washed with pentane (6.0 mL) and stirred vigorously for 30 min. At this point a yellow powder was allowed to settle and the liquid layer was decanted. The powder was dried in vacuo. Excess $\text{NaB}(\text{Ar}_\text{F})_4$ was removed through an additional filtration step in which the yellow powder was dissolved in CH_2Cl_2 (5.0 mL) and filtered through a Celite pad. The volatiles were removed in vacuo to yield a yellow-oil. Pentane (5.0 mL) was added and the product was again stirred until a yellow powder formed. The pentane layer was decanted and the yellow powder was dried in vacuo overnight to yield 56% of **1** (0.190 g, 0.175 mmol). ^1H NMR (500 MHz, CD_2Cl_2 , 20 °C): δ 5.70 (t, $^3J_{\text{H-H}} = 6.5$ Hz, 1H, H₂), 5.86 (t, $^3J_{\text{H-H}} = 6.5$ Hz, 2H, H₁), 2.23 (s, 6H, CH₃), 1.71 (br. m, 2H, H₃), 1.61 (m, 1H, H₄), 1.41 (m, 2H, H_{3'}), 0.78 (m, 1H, H_{4'}). $^{13}\text{C}\{^1\text{H}\}$ NMR (100 MHz, CD_2Cl_2 , 25 °C): δ 107.6 (s, C₂), 77.6 (s, C₁), 29.1 (s, C₃), 17.6 (s, C₄), 3.5 (br. s, NCCCH_3). Nitrile carbon could not be located. Anal. Calcd for $\text{C}_{42}\text{H}_{27}\text{N}_2\text{BNi}$: C, 46.49; N, 2.58; H, 2.47. Found: C, 46.40; N, 2.41; H, 2.34.



[(Cyclohexenyl)Ni(mes)][B(Ar_F)₄] (2). A flame-dried Schlenk flask was charged with [(cyclohexenyl)NiBr]₂ (0.150 g, 0.314 mmol) dimer and $\text{NaB}(\text{Ar}_\text{F})_4$ (0.604 g, 0.682 mmol) and cooled to -78 °C in a dry ice-isopropanol bath. Dry diethyl ether (10.0 mL) was added, yielding an orange solution with a fine brown precipitate. After approximately 5 min of stirring, mesitylene (190 μL , 1.36 mmol) was added dropwise via syringe. The solution was warmed to 0 °C and stirred for 1 h. The solution was filtered via cannula and the solvent was

removed in vacuo to yield a red powder. The solid was purified by dissolving in a minimal amount of methylene chloride and filtering through Celite. The volatiles were then removed in vacuo to give **2** in 65% yield (0.491 g, 0.437 mmol). Brick red X-ray quality crystals of the complex were obtained by dissolving complex **2** in CH₂Cl₂ (2.0 mL), layered with pentane (6.0 mL) and placed in the freezer at -35 °C for 4 days. ¹H NMR (300 MHz, CD₂Cl₂, 25 °C): δ 6.52 (s, 3H), 5.86 (t, ³J_{H-H} = 6.3 Hz, 1H, H_c), 4.81 (td, ³J_{H-H} = 6.3 Hz, ³J_{H-H} = 1.8 Hz, 2H, H_{syn}), 2.34 (s, 9H, MesCH₃), 1.57-1.17 (m, 6H, CH₂). ¹³C NMR (100 MHz, CD₂Cl₂, 25 °C): 123.9 (s, mesC_{Ar}), 109.7 (s, mesC_{Ar}CH₃), 100.4 (s, C₂), 78.4 (s, C₁), 28.5 (s, C₃), 20.2 (s, C₄), 20.2 (s, mesCH₃, overlapping with C₄). Anal. Calcd for C₄₇H₃₃F₂₄BNi: C, 50.26; H, 2.97. Found: C, 49.04; H, 2.97.

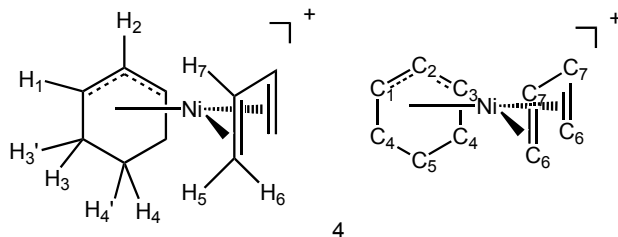
Generation of [(Cyclohexenyl)Ni(η⁴-Diene)][B(Ar_F)₄] Complexes.



[(Cyclohexenyl)Ni(B(Ar_F)₄)] (3**).** A screw top NMR tube was charged with **1** (0.010 g, 0.009 mmol) and B(C₆F₅)₃ (0.024 g, 0.047 mmol). The NMR tube was cooled to -80 °C in a dry ice-acetone bath. The tube was placed under an argon stream and the two solids were dissolved in CD₂Cl₂. The NMR tube was quickly inverted to allow for mixing and placed again in the cold bath. The solution turned from bright yellow to yellowish-brown, which is indicative of the ligand free complex formation. The tube was placed into a precooled NMR probe and the reaction was monitored by ¹H NMR spectroscopy. An equilibrium exists

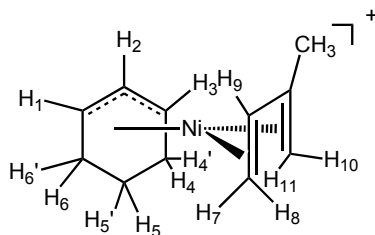
between starting complex **1** and species **3**. The ratio of **1**:**3** is 1:4 at -20 °C. ^1H NMR (500 MHz, CD_2Cl_2 , -60 °C): δ 8.04 (s, 1H, Ar_{Fp} coordinated), 7.74 (s, 6H, Ar_{Fm}), 7.66 (s, 3H, Ar_{Fp}), 7.22 (s, 2H, Ar_{Fm} coordinated), 4.60 (br. s, 2H, H_1), 4.00 (br. t, 1H, H_2), 2.70 (s, borane adduct), 2.32 (s, 2H, H_3), 1.10 (br. s, 4H, H_3' , H_4 , H_4'). ^{19}F NMR (471 MHz, CD_2Cl_2 , -40 °C): δ -62.7 (s, 6F), -62.9 (s, 18F).

^1H NMR line broadening experiments to determine barrier to Ni migration among the Ar_{F} rings of $[\text{B}(\text{Ar}_{\text{F}})_4]^-$ in species **3.** A solution of **3** was prepared in CD_2Cl_2 as described above. Broadening of the coordinated Ar_{F} ^1H resonance corresponding Ar_{F} H_p (8.04 ppm) was monitored between -70 °C and -35 °C. The initial half-height line width at -70 °C was 10 Hz, 12 Hz at -56 °C, 15 Hz at -46 °C, and 23 Hz at -35 °C. The rate constants, calculated from the slow exchange approximation ($k_{\text{ex}} = \pi\Delta\omega$) at the above listed temperatures, are $k_{\text{ex}} = 6.3, 15.7, 40.8 \text{ s}^{-1}$, where $\Delta\omega = 2, 5, 13 \text{ Hz}$, respectively ($\Delta G_{\text{avg}}^\ddagger = 11.9 \text{ kcal/mol}$, average of three values).



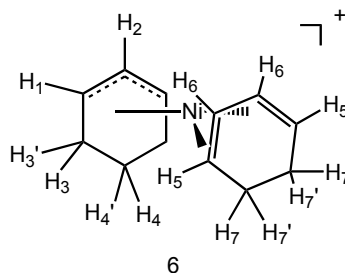
$[(\text{Cyclohexenyl})\text{Ni}(\eta^4\text{-butadiene})][\text{B}(\text{Ar}_{\text{F}})_4]$ (4**).** A dry screw top NMR tube was charged with **1** (0.010 g, 0.009 mmol) and $\text{B}(\text{C}_6\text{F}_5)_3$ (0.009 g, 0.018 mmol) and cooled to -78 °C. The tube was placed under argon and the solids were dissolved in CD_2Cl_2 and quickly mixed by inversion of the tube. Two equivalents of butadiene (0.37 M in CD_2Cl_2) (50 μL , 0.019 mmol) were added via syringe and the NMR tube was quickly inverted to allow for mixing. The NMR tube was placed in a precooled probe and monitored by ^1H NMR spectroscopy.

^1H NMR (500 MHz, CD_2Cl_2 , $-53\text{ }^\circ\text{C}$): δ 6.77 (t, $^3J_{\text{H-H}} = 6.5\text{ Hz}$, 2H, H_1), 6.25 (m, 2H, H_7), 5.91 (t, $^3J_{\text{H-H}} = 6.5\text{ Hz}$, 1H, H_2), 5.20 (d, $^3J_{\text{H-H}} = 7.0\text{ Hz}$, 2H, H_5), 3.26 (dd, $^3J_{\text{H-H}} = 14.0\text{ Hz}$, $^2J_{\text{H-H}} = 1.5\text{ Hz}$, 2H, H_6), 2.09 (br. m, 2H, H_3), 1.21 (m, 1H, H_4), 0.73 (m, 1H, H_4'), 0.59 (m, 2H, H_3'). $^{13}\text{C}\{^1\text{H}\}$ NMR (126 MHz, CD_2Cl_2 , $-53\text{ }^\circ\text{C}$): δ 111.4 (s, C_2), 109.2 (s, C_7), 90.4 (s, $\text{C}_{1,3}$), 83.0 (s, C_6), 28.8 (s, C_4), 14.3 (s, C_5). The solution remained yellow in color until insertion occurred and then the solution turned orange ($0\text{ }^\circ\text{C}$).

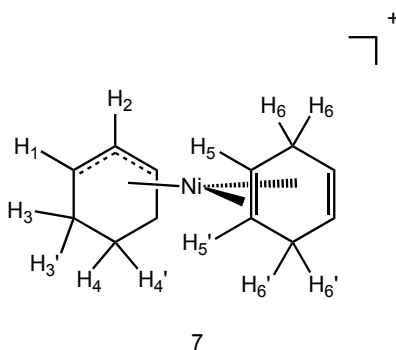


5

[(Cyclohexenyl)Ni(η^4 -isoprene)][B(Ar_F) $_4$] (5). A screw top NMR tube was charged with **1** (0.010 g, 0.009 mmol) and $\text{B}(\text{C}_6\text{F}_5)_3$ (0.009 g, 0.018 mmol) and cooled to $-78\text{ }^\circ\text{C}$. The solid was dissolved in CD_2Cl_2 and then isoprene ($1.8\text{ }\mu\text{L}$, 0.018 mmol) was added. The tube was inverted quickly to allow mixing. The NMR tube was placed in a precooled probe and the reaction was monitored by low temperature ^1H NMR spectroscopy. ^1H NMR (500 MHz, CD_2Cl_2 , $-60\text{ }^\circ\text{C}$): δ 6.68 (t, $^3J_{\text{H-H}} = 6.8\text{ Hz}$, 1H, H_1), 6.62 (t, $^3J_{\text{H-H}} = 6.8\text{ Hz}$, 1H, H_3), 6.01 (dd, $^3J_{\text{H-H}} = 16.0\text{ Hz}$, $^2J_{\text{H-H}} = 1.5\text{ Hz}$, 1H, H_9), 5.83 (t, $^3J_{\text{H-H}} = 6.8\text{ Hz}$, 1H, H_2), 5.13 (dd, $^3J_{\text{H-H}} = 9.5\text{ Hz}$, $^2J_{\text{H-H}} = 1.5\text{ Hz}$, 1H, H_7), 4.98 (s, 1H, H_{10}), 3.20 (dd, $^3J_{\text{H-H}} = 16.6\text{ Hz}$, $^2J_{\text{H-H}} = 1.5\text{ Hz}$, 1H, H_8), 2.95 (s, 1H, H_{11}), 2.27 (s, 3H, CH_3), 2.17 (br. m, 2H, H_6 , H_4), 1.24 (m, 1H, H_5), 0.83-0.61 (m, 2H, H_5' , H_6'), 0.55 (m, 1H, H_4'). Isoprene insertion products are observed as the sample is warmed to $-20\text{ }^\circ\text{C}$.

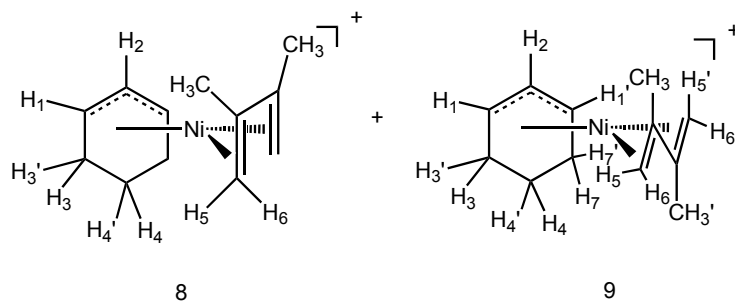


[(Cyclohexenyl)Ni(η^4 -1,3-cyclohexadiene)][B(Ar_F)₄] (6). This complex was generated following the procedure previously described for complex **5**. Compound **1** (0.010 g, 0.009 mmol) and B(C₆F₅)₃ (0.009 g, 0.018 mmol) were dissolved in CD₂Cl₂ (600 μ L) and 1,3-cyclohexadiene (1.8 μ L, 0.019 mmol) was added via syringe. ¹H NMR (500 MHz, CD₂Cl₂, -20 °C): δ 6.46 (t, ³J_{H-H} = 6.0 Hz, 2H, H₁), 6.01 (br. m, 2H, H₆), 5.97 (br. m, 2H, H₅), 5.87 (t, ³J_{H-H} = 6.0 Hz, 1H, H₂), 2.18 (m, 2H, H₃), 1.84 (complex AA'BB' 4H, H₇, H_{7'}), 1.26 (br. s, 1H, H₄), 0.76 (br. m, 3H, H_{3'}, H_{3''}, H_{4'}). Insertion of 1,3-cyclohexadiene is observed upon warming to -20 °C.



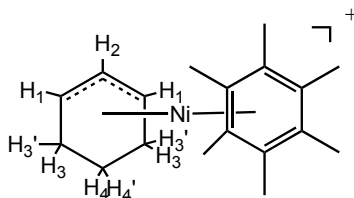
[(Cyclohexenyl)Ni(η^4 -1,4-cyclohexadiene)][B(Ar_F)₄] (7). Complex **7** was generated following the procedure previously outlined for **5**. A screw cap NMR tube was charged with **1** (0.010 g, 0.009 mmol) and B(C₆F₅)₃ (0.009 g, 0.018 mmol) and dissolved in CD₂Cl₂ (600 μ L) and 1,4-cyclohexadiene (1.87 μ L, 0.020 mmol) was added via syringe. ¹H NMR (500 MHz, CD₂Cl₂, -33 °C): δ 5.85 (t, ³J_{H-H} = 6.5 Hz, 1H, H₂), 5.70 (m, 4H, H₅, H_{5'}, overlapping with free 1,4-CHD), 5.10 (t, ³J_{H-H} = 6.5 Hz, 2H, H₁), 4.29 (br. m, 1H, H₆), 3.84 (br. m, 1H,

H₆), 3.38 (br. m, 1H, H_{6'}), 2.99 (br. m, 1H, H_{6'}), 1.95 (br. m, 2H, H₃), 1.56 (m, 1H, H₄), 1.21 (m, 2H, H_{3'}), 0.75 (m, 1H, H_{4'}). Insertion of 1,4-cyclohexadiene is never observed. This species is stable at room temperature.



[(Cyclohexenyl)Ni(η^4 -*cis*-2,3-dimethyl-1,3-butadiene)][B(Ar_F)₄] (8) and [(cyclohexenyl)Ni(η^4 -*trans*-2,3-dimethyl-1,3-butadiene)][B(Ar_F)₄] (9). This experiment was conducted using the above procedure described for the formation of complex **5**. Complex **1** (0.010 g, 0.009 mmol) and B(C₆F₅)₃ (0.009 g, 0.018 mmol) were dissolved in CD₂Cl₂ (600 μ L) and 2,3-dimethyl-1,3-butadiene (1.1 μ L, 0.010 mmol) was added. Species **9** is observed in solution along with **3** and **8** at -80 °C. At -20 °C only **8** and **9** are observed in solution. The ratio of **8**:**9** in solution at -20 °C is 4:1. Complex **8**: ¹H NMR (500 MHz, CD₂Cl₂, -80 °C): δ 6.54 (t, ³J_{H-H} = 6.8 Hz, 2H, H₁), 5.77 (t, ³J_{H-H} = 6.5 Hz, 1H, H₂), 4.97 (s, 2H, H₅), 2.93 (s, 2H, H₆), 2.21 (s, 6H, CH₃), 2.18 (br. m, 2H, H₃), 1.27 (br. s, 1H, H₄), 0.85-0.48 (br. m, 3H, H_{4'}, H_{3'}). Complex **9**: ¹H NMR (500 MHz, CD₂Cl₂, -20 °C): δ 6.32 (br. m, 1H, H₁), 6.30 (br. m, 1H, H_{1'}), 5.33 (t, 1H, H₂, under CDHCl₂), 5.19 (s, 1H, H₅), 5.04 (s, 1H, H_{5'}, under free DMBD), 4.46 (s, 1H, H₆), 4.30 (s, 1H, H_{6'}), 1.94 (s, 3H, CH_{3'}), 1.50 (s, 3H, CH₃), CH₂ groups masked by *cis* isomer and oligomers of DMBD. Insertion of DMBD occurs upon warming to -10 °C.

Assessment of the Lability of Coordinated Mesitylene in Complex 2.



Reaction of complex 2 with hexamethylbenzene (hmb). A screw top NMR tube was charged with **2** (0.005 g, 0.004 mmol) and hmb (0.004 g, 0.022 mmol) and dissolved at room temperature in CD_2Cl_2 (500 μL). The NMR tube was shaken to allow for mixing. Within 10 mins of addition of CD_2Cl_2 to the tube, the ^1H NMR spectrum was recorded for this reaction. The reaction was then monitored by ^1H NMR spectroscopy every hour until complete conversion. After 10 min, the ratio of **2**:[(cyclohexenyl)Ni(hmb)] $^+$ was 1:9 and after 1h complete conversion to the hmb complex was achieved. ^1H NMR (300 MHz, CD_2Cl_2 , 25 $^\circ\text{C}$): δ 5.68 (t, $^3J_{\text{H-H}} = 6.6$ Hz, 1H, H₂), 4.26 (br. t, 2H, H₁), 2.28 (s, 18H, CH₃), 1.47-1.37 (m, 3H, H₃, H₃, H₄), 1.11-0.99 (m, 3H, H₃, H₃, H₄).

Reaction of 2 with mesitylene- d_{12} . A screw cap NMR tube was charged with **2** (0.005 g, 0.004 mmol) and dissolved in CD_2Cl_2 (500 μL) in the glove box. Mesitylene- d_{12} (3.1 μL , 0.022 mmol) was then introduced via syringe. The reaction was monitored at room temperature by ^1H NMR spectroscopy. The first spectrum was recorded 10 min after the addition of mesitylene- d_{12} and at this point the ratio of **2**:**2**- d_{12} was 3:7 as determined from integrating free (δ 6.79) vs. bound mesitylene (δ 6.55). After 4h, the ratio changed to 1:6 and this value did not change overnight.

Qualitative Relative Binding Affinities of IP and BD.

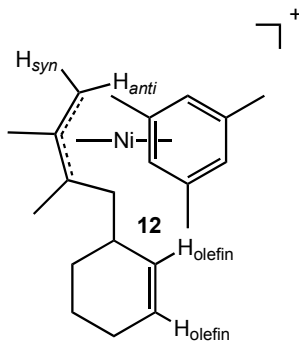
A screw cap NMR tube was charged with complex **1** (0.010 g, 0.009 mmol) and $\text{B}(\text{C}_6\text{F}_5)_3$ (0.009 g, 0.018 mmol). The NMR tube was cooled to -80 $^\circ\text{C}$ and the solids were

dissolved in 600 μL CD_2Cl_2 . After quick mixing, the solution turned yellow-brown. Butadiene, a 0.92 M solution in CD_2Cl_2 , (50 μL , 0.046 mmol) was added and the solution turned bright yellow, indicative of η^4 -diene coordination. Isoprene (1.84 μL , 0.018 mmol) was then added and the solution was mixed, making sure to keep the tube cold. The reaction was monitored by low temperature NMR spectroscopy. Isoprene displaces butadiene and the ratio of η^4 -diene complexes **5:4** is 3:1. Diene exchange is observed at 0 $^\circ\text{C}$ on the NMR timescale.

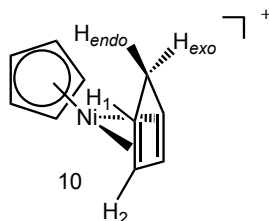
In Situ Generation of Ni(II) Species.

In situ observation of [(2-hexenyl)Ni(mes)][B(Ar_F)₄] (11**).** A J-Young tube was charged with complex **2** (0.010 g, 0.009 mmol) and dissolved in 500 μL of CD_2Cl_2 . After mixing, 1-hexene (5.0 mL, 0.040 mmol) was added and the tube was inverted to allow for mixing. The reaction was monitored by ^1H NMR spectroscopy. Only the observable resonances for complex **11**, which are not masked by excess hexene, are reported here. See chapter 3 for complete characterization of **11**. Formation of cyclohexene is also observed in the ^1H NMR spectrum. Characteristic resonances: ^1H NMR (300 MHz, CD_2Cl_2 , 25 $^\circ\text{C}$): δ 6.44 (s, 3H, mesAr_H), 5.66 (br. s, free cyclohexene), 3.11 (m, 2H, H_{anti}), 2.32 (s, 9H, MesCH₃).

In situ reactions with ethylene. Complex **2** (0.010 g, 0.009 mmol) was added to a J-Young tube and dissolved in 600 μL of CD_2Cl_2 . The tube was cooled in a dry ice-acetone bath and back filled with an atmosphere of ethylene. The reaction was warmed to room temperature and monitored by ^1H NMR spectroscopy. Oligomers of ethylene were observed in ^1H NMR spectrum.



In situ identification of coupling product (12). Complex **2** (0.010 g, 0.009 mmol) was added to a screw cap NMR and dissolved in CD₂Cl₂ (600 μ L). The NMR tube was cooled to -80 °C and then charged with 2,3-dimethyl-1,3-butadiene (60.4 μ L, 0.534 mmol) and quickly mixed by tube inversion. The solution remained deep red. The reaction was monitored at low temperatures using ¹H NMR spectroscopy. Polymerization of DMBD occurred upon warming to 10 °C, with polyDMBD precipitating out of solution. Formation of **12**, the C-C coupling product of DMBD and complex **2**, is observed at 10 °C. Complete identification of all resonances for **12** could not be established due to the presence of excess DMBD, which masks many of the signals. Here we report the observable characteristic peaks for complex **12**. ¹H NMR (400 MHz, CD₂Cl₂, 10 °C): δ 6.42 (s, 3H, mesAr_H), 5.66 (br. t, 1H, H_{olefin}), 5.43 (t, 1H, ³J_{H-H} = 8.5 Hz, H_{olefin}), 3.38 (s, 1H, H_{syn}), 2.65 (s, 1H, H_{anti}), 2.31 (s, 9H, mesCH₃), 0.89 (s, 3H, CH₃). The resonances for the methyl and methylene groups are masked by excess DMBD and oligomers in solution.



Observation of [(cyclopentadienyl)Ni(η^4 -cyclopentadiene)][B(Ar_F)₄] (10). Complex **10** can be generated in situ starting from ligand-free species **3** and cyclopentadiene.

Complex **2** (0.010 g, 0.009 mmol) was added to a screw cap NMR tube and cooled to -80 °C in a cold bath. The complex was dissolved in 600 μ L CD₂Cl₂ and mixed. Cyclopentadiene (2.17 μ L, 0.027 mmol) was added and the reaction was quickly mixed again. The solution remained red until the temperature rose to 0 °C. At temperatures above 0 °C, the solution turned yellow-green. ¹H NMR (300 MHz, CD₂Cl₂, 25 °C): δ 7.09 (br. s, 2H, H₂), 6.79 (s, free mesitylene), 5.78 (s, 5H, Cp_H), 5.66 (s, free cyclohexene), 5.41 (t, 2H, ³J_{H-H} = 2.4 Hz, H₁), 3.30 (roofed dt, 1H, ²J_{H-H} = 22.0 Hz, ³J_{H-H} = 2.4 Hz, H_{endo}), 3.03 (roofed d, 1H, ²J_{H-H} = 22.0 Hz, H_{exo}), 1.61 (bs, free cyclohexene), 1.26 (bs, free cyclohexene).

In situ generation of [(cyclopentadienyl)Ni(η^4 -cyclopentadiene)][B(Ar_F)₄] (10**).** A screw cap NMR tube was charged with nickolecene (0.015 g, 0.075 mmol) and [H(OEt)₂][B(Ar_F)₄] (0.097 g, 0.095 mmol) and immediately cooled to -80 °C. The solids were dissolved in 600 μ L CD₂Cl₂ and mixed by inversion. The solution turned green-yellow. Quantitative conversion to complex **10** is observed in the ¹H NMR spectrum. ¹H NMR (300 MHz, CD₂Cl₂, 25 °C): δ 7.05 (br. s, 2H, H₂), 5.73 (s, 5H, Cp_H), 5.37 (br. s, 2H, H₁, under CD₂Cl₂), 3.25 (roofed d, 1H, ²J_{H-H} = 21.9 Hz, H_{endo}), 2.97 (roofed d, 1H, ²J_{H-H} = 21.6 Hz, H_{exo}).

General Procedure for Polymerization of 1,3-Dienes.

A flame-dried Schlenk tube was charged with complex **2** and dissolved in 1.0 mL of CH₂Cl₂. Monomer was added via syringe and the reaction was stirred at room temperature. It is very important that the monomers are freshly dried and distilled prior to polymerization to ensure reproducible reactions. For the addition of DMBD and 1,3-CHD the solutions turn color from red to yellow upon monomer addition. Each trial was run in triplicate. The polymerizations were quenched by the addition of cold MeOH. The polymers were collected and dried in vacuum oven at 120 °C. The polymerization of 1,3-CHD was exothermic and

within 2 minutes the solution temperature had risen substantially. PolyCHD is insoluble in CH_2Cl_2 and precipitates out as a white powder during the course of the reaction. For DMBD polymerizations, the reactions turn colorless after time, which indicates catalyst decomposition. PolyDMBD is insoluble in CH_2Cl_2 and also precipitates out of solution. Results for the polymerizations are found in Table III.2 of the Appendix.

Crystallographic Information.

The molecular structure for complex **2** was determined using a Bruker APEX II diffractometer at $-173\text{ }^\circ\text{C}$ using Mo radiation. All necessary information regarding the crystal structure data can be found in Appendix Tables III.1, III.3, and III.4, and Figure 5.1.

References

1. Stevens, M. P., In *Polymer chemistry, an introduction*. Oxford University Press, Inc.: **1999**.
2. Kaminsky, W. Polyolefins. In *Handbook of polymer synthesis*, Kricheldorf, H. R., Nuyken, O., Swift, G. Eds.; Marcel Dekker: New York, **2005**; 1-72.
3. Kaita, S.; Yamanaka, M.; Horiuchi, A. C.; Wakatsuki, Y. *Macromolecules* **2006**, *39*, 1359-1363.
4. Szwarc, M. *Nature* **1956**, *178*, 1168-1169.
5. Coates, G. W.; Hustad, P. D.; Reinhartz, S. *Angew. Chem. Int. Ed.* **2002**, *41*, 2236-2257.
6. Gottfried, A. C.; Brookhart, M. *Macromolecules* **2001**, *34*, 1140-1142.
7. Killian, C. M.; Tempel, D. J.; Johnson, L. K.; Brookhart, M. *J. Am. Chem. Soc.* **1996**, *118*, 11664-11665.
8. Grubbs, R. H.; Tumas, W. *Science* **1989**, *243*, 907-915.
9. Maughon, B. R.; Grubbs, R. H. *Macromolecules* **1997**, *30*, 3459-3469.
10. Shrock, R. R. *Acc. Chem. Res.* **1990**, *23*, 158-165.
11. Osakada, K.; Takeuchi, D. Coordination polymerization of dienes, allenes, and methylenecycloalkanes. In *Advances in Polymer Science*, Eds.; Springer-Verlag: Berlin, **2004**; Vol. 171, 137-194.
12. Ricci, G.; Italia, S.; Porri, L. *Polym. Commun.* **1988**, *29*, 305-307.
13. Wilke, G.; Bogdanovic, B.; Heimbach, P.; Keim, W.; Kröner, M.; Oberkirch, W.; Tanaka, K.; Steinrücke, E.; Walter, D.; Zimmerman, H. *Angew. Chem. Int. Ed.* **1966**, *5*, 151-164.
14. Babitskii, B. D.; Dolgoplosk, B. A.; Kormer, V. A.; Lobach, M. I.; Yakovlev, V. A. *Dokl. Akad. Nauk SSSR* **1965**, *166*, 583-585.
15. Porri, L.; Natta, G.; Gallazzi, M. C. *J. Polym. Sci., Part C* **1967**, 2525-2537.
16. Taube, R.; Schmidt, U.; Gehrke, J. P.; Anacker, U. *J. Prakt. Chem.* **1984**, *326*, 1-11.
17. Taube, R.; Windisch, H.; Weissenborn J. *Organomet. Chem.* **1997**, *548*, 229-236.

18. Quirk, R. P.; Kells, A. M.; Yunlu, K.; Cuif, J.-P. *Polymer* **2000**, *41*, 5903-5908.
19. Nickaf, J. B.; Burford, R. P.; Chaplin, R. P. *J. Polym. Sci. Part A* **1995**, *33*, 1125-1132.
20. Kobayashi, E.; Hayashi, N.; Aoshima, S.; Furukawa, J. *J. Polym. Sci. Part A* **1998**, *36*, 1707-1716.
21. Porri, L.; Giarrusso, A.; Ricci, G. *Prog. Polym. Sci.* **1991**, *16*, 405-441.
22. Taube, R.; Sylvester, G. Stereospecific Polymerization of Butadiene or Isoprene. In *Applied Homogeneous Catalysis with Organometallic Complexes*, Cornils, B., Herrmann, W. A. Eds.; VCH: Weinheim, Germany, **1996**; 280-318.
23. O'Connor, A. R.; White, P. S.; Brookhart, M. *J. Am. Chem. Soc.* **2007**, *129*, 4142-4143.
24. Hadjiandreou, P.; Julémont, M.; Teyssié, P. H. *Macromolecules* **1984**, *17*, 2455-2456.
25. Deming, T. J.; Novak, B. M.; Ziller, J. W. *J. Am. Chem. Soc.* **1994**, *116*, 2366-2374.
26. Winter, H.; Aagaard, O. *Macromol. Rapid Commun.* **1998**, *19*, 345-348.
27. Taube, R.; Wache, S.; Kehlen, H. *J. Mol. Cat. A* **1995**, *97*, 21-27.
28. Taube, R.; Wache, S.; Langlotz, J. Mol mass regulation in the allyl nickel complex catalyzed 1,4-cis polymerization of butadiene. In *Catalyst design for tailor-made polyolefins. Studies in surface science and catalysis.*, Soga, K., Terano, M. Eds.; Elsevier: Toyko, **1994**; 315-325.
29. Tobisch, S. *Macromolecules* **2003**, *36*, 6235-6244.
30. O'Connor, A. R.; Moorhouse, R. M.; Urbin, S. A.; White, P. S.; Brookhart, M. *Manuscript in Preparation* **2008**.
31. See Appendix for X-Ray structure data.
32. Tobisch, S.; Bögel, H.; Taube, R. *Organometallics* **1996**, *15*, 3563-3571.
33. Porri, L.; Gallazzi, M. C.; Destri, S.; Bolognesi, A. *Macromol. Chem., Rapid Commun.* **1983**, *4*, 485-489.
34. Tolman, C. A. *J. Am. Chem. Soc.* **1970**, *92*, 6785-6790.
35. Kuhn, N.; Winter, M. *Chemiker-Zeitung* **1983**, *107*, 14.

36. Turner, G. K.; Klæui, W.; Scotti, M.; Werner, H. J. *Organomet. Chem.* **1975**, *102*, C9-C11.
37. Pangborn, A. B.; Giardello, M. A.; Grubbs, R. H.; Rosen, R. K.; Timmers, F. J. *Organometallics* **1996**, *15*, 1518-1520.
38. Yakelis, N. A.; Bergman, R. G. *Organometallics* **2005**, *24*, 3579-3581.
39. Wilkinson, G.; Pauson, P. L.; Cotton, F. A. *J. Am. Chem. Soc.* **1956**, *76*, 1970-1974.
40. Brookhart, M.; Grant, B.; Volpe, A. F. *Organometallics* **1992**, *11*, 3290-3922.

Appendix I

Table I.1. X-ray crystal data and structure refinement.

	6	10
Formula	C ₅₃ H ₂₃ BF ₃₆ N ₂ Ni	C ₄₇ H ₃₅ BF ₂₄ Ni
Formula Weight	1441.25	1125.27
Crystal System	Triclinic	Orthorhombic
Space Group	P-1	Pbca
Unit Cell Dimensions	a = 13.0417(17)Å α = 94.317(2)° b = 14.5598(19)Å β = 108.821(2)° c = 16.336(2)Å γ = 104.061(2)°	a = 17.6927(6)Å α = 90° b = 19.4801(6)Å β = 90° c = 26.9426(9)Å γ = 90°
Volume	2808.0(6)Å ³	9285.9(5)Å ³
Z	2	8
Absorption Coefficient	0.505 mm ⁻¹	1.809 mm ⁻¹
Data/restraints/parameters	9805/0/838	8031/71/735
Final R indices [I>2σ(I)]	R1 = 0.0766, wR2 = 0.1294	R1 = 0.0972, wR2 = 0.2564

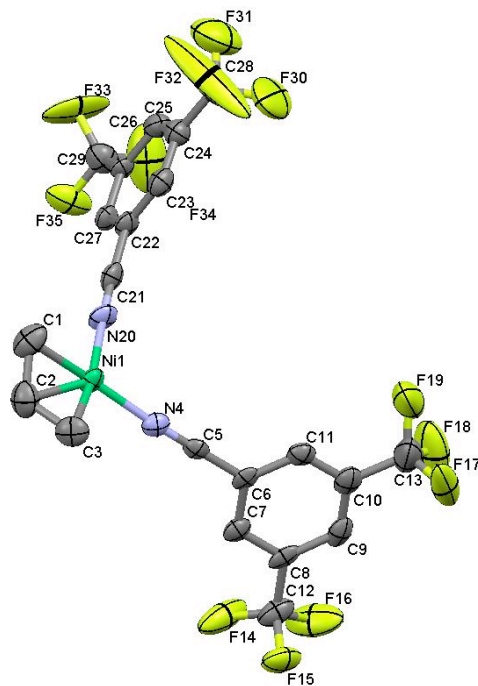


Figure I.1. ORTEP diagram showing the molecular structure for complex **6**. Thermal ellipsoids are drawn at 50 % probability. Selected bond lengths are (Å): Ni(1)-N(4) 1.874(5), Ni(1)-N(20) 1.886(5), Ni(1)-C(2) 1.960(6), Ni(1)-C(1) 1.983(6), Ni(1)-C(3) 2.013(5), C(1)-C(2) 1.354(8), C(2)-C(3) 1.356(7). The hydrogen atoms and [B(ArF)₄]⁻ counteranion have been omitted for clarity.

Table I.2. Selected bond lengths (Å) for complex **6**.

Ni(1)-N(4)	1.874(5)	C(22)-C(27)	1.393(7)
Ni(1)-N(20)	1.886(5)	C(23)-C(24)	1.393(8)
Ni(1)-C(2)	1.960(6)	C(23)-H(23)	0.9300
Ni(1)-C(1)	1.983(6)	C(24)-C(25)	1.388(7)
Ni(1)-C(3)	2.013(5)	C(24)-C(28)	1.482(9)
C(1)-C(2)	1.354(8)	C(25)-C(26)	1.385(7)
C(1)-H(1A)	0.9700	C(25)-H(25)	0.9300
C(1)-H(1B)	0.9700	C(28)-F(32)	1.168(9)
C(2)-C(3)	1.365(7)	C(28)-F(30)	1.317(10)
C(2)-H(2)	0.9800	C(28)-F(31)	1.345(8)
C(3)-H(3A)	0.9700	C(26)-C(27)	1.383(7)
C(3)-H(3B)	0.9700	C(26)-C(29)	1.503(8)
N(4)-C(5)	1.156(6)	C(27)-H(27)	0.9300
C(5)-C(6)	1.437(7)	C(29)-F(33)	1.276(7)
C(6)-C(7)	1.382(7)	C(29)-F(35)	1.299(7)
C(6)-C(11)	1.387(7)	C(29)-F(34)	1.323(7)
C(7)-C(8)	1.385(7)	B(40)-C(41)	1.645(7)
C(7)-H(7)	0.9300	B(40)-C(51)	1.652(7)
C(8)-C(9)	1.391(8)	B(40)-C(71)	1.659(7)
C(8)-C(12)	1.482(8)	B(40)-C(61)	1.662(7)
C(9)-C(10)	1.385(8)	C(41)-C(42)	1.389(6)
C(9)-H(9)	0.9300	C(41)-C(46)	1.419(6)
C(10)-C(11)	1.361(7)	C(42)-C(43)	1.391(6)
C(10)-C(13)	1.482(9)	C(42)-H(42)	0.9300
C(11)-H(11)	0.9300	C(43)-C(44)	1.388(7)
C(12)-F(16)	1.330(7)	C(43)-C(47)	1.489(7)
C(12)-F(14)	1.340(7)	C(44)-C(45)	1.387(7)
C(12)-F(15)	1.341(6)	C(44)-H(44)	0.9300
C(13)-F(17)	1.281(7)	C(45)-C(46)	1.383(6)
C(13)-F(19)	1.322(9)	C(45)-C(48)	1.480(7)
C(13)-F(18)	1.365(9)	C(46)-H(46)	0.9300
N(20)-C(21)	1.130(6)	C(47)-F(43)	1.340(6)
C(21)-C(22)	1.467(8)	C(47)-F(41)	1.345(6)
C(22)-C(23)	1.376(7)	C(47)-F(42)	1.361(5)

C(48)-F(46)	1.343(6)	C(64)-H(64)	0.9300
C(48)-F(44)	1.346(6)	C(65)-C(66)	1.376(6)
C(48)-F(45)	1.352(6)	C(65)-C(68)	1.506(7)
C(51)-C(56)	1.387(6)	C(66)-H(66)	0.9300
C(51)-C(52)	1.416(6)	C(67)-F(58)	1.316(6)
C(52)-C(53)	1.382(6)	C(67)-F(59)	1.318(5)
C(52)-H(52)	0.9300	C(67)-F(57)	1.333(6)
C(53)-C(54)	1.374(7)	C(68)-F(62)	1.284(6)
C(53)-C(57)	1.504(7)	C(68)-F(60)	1.302(6)
C(54)-C(55)	1.391(7)	C(68)-F(61)	1.335(6)
C(54)-H(54)	0.9300	C(71)-C(76)	1.387(6)
C(55)-C(56)	1.406(6)	C(71)-C(72)	1.396(6)
C(55)-C(58)	1.488(8)	C(72)-C(73)	1.386(6)
C(56)-H(56)	0.9300	C(72)-H(72)	0.9300
C(57)-F(52)	1.312(7)	C(73)-C(74)	1.386(7)
C(57)-F(53)	1.323(7)	C(73)-C(77)	1.465(7)
C(57)-F(51)	1.332(7)	C(74)-C(75)	1.378(7)
C(58)-F(54)	1.326(7)	C(74)-H(74)	0.9300
C(58)-F(56)	1.335(7)	C(75)-C(76)	1.408(6)
C(58)-F(55)	1.347(6)	C(75)-C(78)	1.498(7)
C(61)-C(62)	1.404(6)	C(76)-H(76)	0.9300
C(61)-C(66)	1.407(6)	C(77)-F(71)	1.297(7)
C(62)-C(63)	1.381(6)	C(77)-F(73)	1.301(7)
C(62)-H(62)	0.9300	C(77)-F(72)	1.308(6)
C(63)-C(64)	1.386(6)	C(78)-F(76)	1.313(6)
C(63)-C(67)	1.529(7)	C(78)-F(74)	1.322(6)
C(64)-C(65)	1.389(6)	C(78)-F(75)	1.329(6)

Table I.3. Selected bond angles (°) for complex **6**.

N(4)-Ni(1)-N(20)	96.11(18)	C(8)-C(7)-H(7)	120.4
N(4)-Ni(1)-C(2)	132.4(2)	C(7)-C(8)-C(9)	119.4(5)
N(20)-Ni(1)-C(2)	130.4(3)	C(7)-C(8)-C(12)	119.9(6)
N(4)-Ni(1)-C(1)	166.0(2)	C(9)-C(8)-C(12)	120.7(6)
N(20)-Ni(1)-C(1)	94.6(2)	C(10)-C(9)-C(8)	120.8(6)
C(2)-Ni(1)-C(1)	40.1(2)	C(10)-C(9)-H(9)	119.6
N(4)-Ni(1)-C(3)	96.2(2)	C(8)-C(9)-H(9)	119.6
N(20)-Ni(1)-C(3)	165.2(2)	C(11)-C(10)-C(9)	119.6(6)
C(2)-Ni(1)-C(3)	40.2(2)	C(11)-C(10)-C(13)	121.5(7)
C(1)-Ni(1)-C(3)	72.0(2)	C(9)-C(10)-C(13)	118.9(6)
C(2)-C(1)-Ni(1)	69.0(4)	C(10)-C(11)-C(6)	120.2(6)
C(2)-C(1)-H(1A)	116.8	C(10)-C(11)-H(11)	119.9
Ni(1)-C(1)-H(1A)	116.8	C(6)-C(11)-H(11)	119.9
C(2)-C(1)-H(1B)	116.8	F(16)-C(12)-F(14)	107.6(5)
Ni(1)-C(1)-H(1B)	116.8	F(16)-C(12)-F(15)	104.6(5)
H(1A)-C(1)-H(1B)	113.8	F(14)-C(12)-F(15)	104.4(6)
C(1)-C(2)-C(3)	119.5(6)	F(16)-C(12)-C(8)	113.7(6)
C(1)-C(2)-Ni(1)	70.8(4)	F(14)-C(12)-C(8)	112.9(5)
C(3)-C(2)-Ni(1)	72.0(3)	F(15)-C(12)-C(8)	112.9(5)
C(1)-C(2)-H(2)	119.8	F(17)-C(13)-F(19)	109.7(8)
C(3)-C(2)-H(2)	119.8	F(17)-C(13)-F(18)	105.8(6)
Ni(1)-C(2)-H(2)	119.8	F(19)-C(13)-F(18)	100.3(7)
C(2)-C(3)-Ni(1)	67.8(3)	F(17)-C(13)-C(10)	115.6(7)
C(2)-C(3)-H(3A)	116.9	F(19)-C(13)-C(10)	113.8(6)
Ni(1)-C(3)-H(3A)	116.9	F(18)-C(13)-C(10)	110.3(7)
C(2)-C(3)-H(3B)	116.9	C(21)-N(20)-Ni(1)	174.3(5)
Ni(1)-C(3)-H(3B)	116.9	N(20)-C(21)-C(22)	176.4(6)
H(3A)-C(3)-H(3B)	113.9	C(23)-C(22)-C(27)	122.1(5)
C(5)-N(4)-Ni(1)	175.7(4)	C(23)-C(22)-C(21)	118.5(5)
N(4)-C(5)-C(6)	177.9(5)	C(27)-C(22)-C(21)	119.4(5)
C(7)-C(6)-C(11)	120.8(5)	C(22)-C(23)-C(24)	119.3(5)
C(7)-C(6)-C(5)	119.2(5)	C(22)-C(23)-H(23)	120.3
C(11)-C(6)-C(5)	119.9(5)	C(24)-C(23)-H(23)	120.3
C(6)-C(7)-C(8)	119.2(5)	C(25)-C(24)-C(23)	119.4(6)
C(6)-C(7)-H(7)	120.4	C(25)-C(24)-C(28)	120.6(6)

C(23)-C(24)-C(28)	120.0(6)	C(42)-C(43)-C(47)	119.2(5)
C(26)-C(25)-C(24)	120.1(6)	C(45)-C(44)-C(43)	119.0(5)
C(26)-C(25)-H(25)	120.0	C(45)-C(44)-H(44)	120.5
C(24)-C(25)-H(25)	120.0	C(43)-C(44)-H(44)	120.5
F(32)-C(28)-F(30)	110.3(8)	C(46)-C(45)-C(44)	120.3(5)
F(32)-C(28)-F(31)	106.8(10)	C(46)-C(45)-C(48)	120.9(5)
F(30)-C(28)-F(31)	93.2(7)	C(44)-C(45)-C(48)	118.8(5)
F(32)-C(28)-C(24)	118.3(8)	C(45)-C(46)-C(41)	122.6(5)
F(30)-C(28)-C(24)	111.7(8)	C(45)-C(46)-H(46)	118.7
F(31)-C(28)-C(24)	113.6(6)	C(41)-C(46)-H(46)	118.7
C(27)-C(26)-C(25)	121.4(5)	F(43)-C(47)-F(41)	106.7(4)
C(27)-C(26)-C(29)	120.4(6)	F(43)-C(47)-F(42)	105.7(4)
C(25)-C(26)-C(29)	118.3(5)	F(41)-C(47)-F(42)	104.8(4)
C(26)-C(27)-C(22)	117.6(5)	F(43)-C(47)-C(43)	113.7(4)
C(26)-C(27)-H(27)	121.2	F(41)-C(47)-C(43)	112.5(4)
C(22)-C(27)-H(27)	121.2	F(42)-C(47)-C(43)	112.8(4)
F(33)-C(29)-F(35)	108.3(6)	F(46)-C(48)-F(44)	105.4(4)
F(33)-C(29)-F(34)	105.7(6)	F(46)-C(48)-F(45)	106.2(4)
F(35)-C(29)-F(34)	103.1(6)	F(44)-C(48)-F(45)	104.2(5)
F(33)-C(29)-C(26)	113.9(6)	F(46)-C(48)-C(45)	114.2(5)
F(35)-C(29)-C(26)	114.1(6)	F(44)-C(48)-C(45)	112.9(4)
F(34)-C(29)-C(26)	110.9(5)	F(45)-C(48)-C(45)	113.0(4)
C(41)-B(40)-C(51)	109.6(4)	C(56)-C(51)-C(52)	115.1(4)
C(41)-B(40)-C(71)	109.6(4)	C(56)-C(51)-B(40)	124.7(4)
C(51)-B(40)-C(71)	109.8(4)	C(52)-C(51)-B(40)	120.2(4)
C(41)-B(40)-C(61)	109.2(4)	C(53)-C(52)-C(51)	122.0(5)
C(51)-B(40)-C(61)	109.5(4)	C(53)-C(52)-H(52)	119.0
C(71)-B(40)-C(61)	109.2(4)	C(51)-C(52)-H(52)	119.0
C(42)-C(41)-C(46)	115.0(5)	C(54)-C(53)-C(52)	121.4(5)
C(42)-C(41)-B(40)	125.2(4)	C(54)-C(53)-C(57)	119.4(5)
C(46)-C(41)-B(40)	119.7(4)	C(52)-C(53)-C(57)	119.3(5)
C(41)-C(42)-C(43)	123.4(5)	C(53)-C(54)-C(55)	118.9(5)
C(41)-C(42)-H(42)	118.3	C(53)-C(54)-H(54)	120.5
C(43)-C(42)-H(42)	118.3	C(55)-C(54)-H(54)	120.5
C(44)-C(43)-C(42)	119.8(5)	C(54)-C(55)-C(56)	119.0(5)
C(44)-C(43)-C(47)	121.0(5)	C(54)-C(55)-C(58)	119.6(5)

C(56)-C(55)-C(58)	121.3(5)	F(59)-C(67)-F(57)	106.6(4)
C(51)-C(56)-C(55)	123.5(4)	F(58)-C(67)-C(63)	111.7(4)
C(51)-C(56)-H(56)	118.3	F(59)-C(67)-C(63)	112.4(4)
C(55)-C(56)-H(56)	118.3	F(57)-C(67)-C(63)	110.9(5)
F(52)-C(57)-F(53)	106.2(5)	F(62)-C(68)-F(60)	107.9(5)
F(52)-C(57)-F(51)	106.6(5)	F(62)-C(68)-F(61)	104.5(5)
F(53)-C(57)-F(51)	102.7(6)	F(60)-C(68)-F(61)	104.1(5)
F(52)-C(57)-C(53)	114.2(6)	F(62)-C(68)-C(65)	112.8(5)
F(53)-C(57)-C(53)	112.9(5)	F(60)-C(68)-C(65)	114.3(5)
F(51)-C(57)-C(53)	113.2(5)	F(61)-C(68)-C(65)	112.4(5)
F(54)-C(58)-F(56)	107.3(5)	C(76)-C(71)-C(72)	116.0(4)
F(54)-C(58)-F(55)	105.6(5)	C(76)-C(71)-B(40)	123.5(4)
F(56)-C(58)-F(55)	105.5(6)	C(72)-C(71)-B(40)	120.3(4)
F(54)-C(58)-C(55)	112.4(6)	C(73)-C(72)-C(71)	123.0(5)
F(56)-C(58)-C(55)	112.8(5)	C(73)-C(72)-H(72)	118.5
F(55)-C(58)-C(55)	112.6(5)	C(71)-C(72)-H(72)	118.5
C(62)-C(61)-C(66)	114.5(4)	C(72)-C(73)-C(74)	119.6(5)
C(62)-C(61)-B(40)	124.0(4)	C(72)-C(73)-C(77)	120.2(5)
C(66)-C(61)-B(40)	121.4(4)	C(74)-C(73)-C(77)	120.1(5)
C(63)-C(62)-C(61)	122.9(4)	C(75)-C(74)-C(73)	119.2(5)
C(63)-C(62)-H(62)	118.5	C(75)-C(74)-H(74)	120.4
C(61)-C(62)-H(62)	118.5	C(73)-C(74)-H(74)	120.4
C(62)-C(63)-C(64)	120.9(4)	C(74)-C(75)-C(76)	120.2(5)
C(62)-C(63)-C(67)	119.6(4)	C(74)-C(75)-C(78)	120.5(5)
C(64)-C(63)-C(67)	119.4(5)	C(76)-C(75)-C(78)	119.4(5)
C(63)-C(64)-C(65)	117.9(5)	C(71)-C(76)-C(75)	121.8(5)
C(63)-C(64)-H(64)	121.1	C(71)-C(76)-H(76)	119.1
C(65)-C(64)-H(64)	121.1	C(75)-C(76)-H(76)	119.1
C(66)-C(65)-C(64)	120.7(4)	F(71)-C(77)-F(73)	105.0(6)
C(66)-C(65)-C(68)	120.4(5)	F(71)-C(77)-F(72)	104.1(5)
C(64)-C(65)-C(68)	118.8(5)	F(73)-C(77)-F(72)	102.9(6)
C(65)-C(66)-C(61)	123.1(4)	F(71)-C(77)-C(73)	114.4(5)
C(65)-C(66)-H(66)	118.4	F(73)-C(77)-C(73)	113.7(5)
C(61)-C(66)-H(66)	118.4	F(72)-C(77)-C(73)	115.6(5)
F(58)-C(67)-F(59)	107.1(5)	F(76)-C(78)-F(74)	105.8(5)
F(58)-C(67)-F(57)	107.8(5)	F(76)-C(78)-F(75)	105.1(5)

F(74)-C(78)-F(75)	107.4(5)	F(74)-C(78)-C(75)	113.2(5)
F(76)-C(78)-C(75)	113.6(5)	F(75)-C(78)-C(75)	111.2(5)

Table I.4. Selected bond lengths (Å) for complex **10**.

Ni(1)-C(14)	2.051(8)	C(11)-H(11A)	0.9900
Ni(1)-C(13)	2.087(8)	C(11)-H(11B)	0.9900
Ni(1)-C(15)	2.116(9)	C(12)-C(13)	1.501(9)
Ni(1)-C(1)	2.189(8)	C(12)-H(12A)	0.9900
Ni(1)-C(2)	2.218(8)	C(12)-H(12B)	0.9900
Ni(1)-C(5)	2.248(7)	C(13)-C(14)	1.480(9)
Ni(1)-C(6)	2.285(7)	C(13)-H(13)	1.0000
Ni(1)-C(10)	2.465(10)	C(14)-C(15)	1.493(9)
C(1)-C(2)	1.467(8)	C(14)-H(14)	1.0000
C(1)-H(1A)	0.9900	C(15)-H(15A)	0.9900
C(1)-H(1B)	0.9900	C(15)-H(15B)	0.9900
C(2)-C(3)	1.484(8)	B(40)-C(41)	1.637(6)
C(2)-H(2)	1.0000	B(40)-C(51)	1.642(7)
C(3)-C(4)	1.489(8)	B(40)-C(71)	1.648(7)
C(3)-H(3A)	0.9900	B(40)-C(61)	1.662(6)
C(3)-H(3B)	0.9900	C(41)-C(42)	1.399(7)
C(4)-C(5)	1.465(8)	C(41)-C(46)	1.399(6)
C(4)-H(4A)	0.9900	C(42)-C(43)	1.391(7)
C(4)-H(4B)	0.9900	C(42)-H(42)	0.9500
C(5)-C(6)	1.447(8)	C(43)-C(44)	1.383(7)
C(5)-H(5)	1.0000	C(43)-C(47)	1.508(7)
C(6)-C(7)	1.488(8)	C(44)-C(45)	1.392(7)
C(6)-H(6)	1.0000	C(44)-H(44)	0.9500
C(7)-C(8)	1.492(8)	C(45)-C(46)	1.396(6)
C(7)-H(7A)	0.9900	C(45)-C(48)	1.502(7)
C(7)-H(7B)	0.9900	C(46)-H(46)	0.9500
C(8)-C(9)	1.492(8)	C(47)-F(43)	1.29(3)
C(8)-H(8A)	0.9900	C(47)-F(41)	1.29(2)
C(8)-H(8B)	0.9900	C(47)-F(431)	1.29(3)
C(9)-C(10)	1.473(9)	C(47)-F(421)	1.300(16)
C(9)-H(9)	0.9500	C(47)-F(42)	1.30(2)
C(10)-C(11)	1.501(8)	C(47)-F(411)	1.35(2)
C(10)-H(10)	1.0000	C(48)-F(44)	1.341(6)
C(11)-C(12)	1.496(9)	C(48)-F(46)	1.345(6)

C(48)-F(45)	1.346(6)	C(63)-C(67)	1.495(7)
F(41)-F(411)	0.57(4)	C(64)-C(65)	1.398(7)
F(41)-F(421)	1.69(4)	C(64)-H(64)	0.9500
F(42)-F(421)	0.69(4)	C(65)-C(66)	1.392(7)
F(42)-F(431)	1.71(4)	C(65)-C(68)	1.502(7)
F(43)-F(431)	0.57(6)	C(66)-H(66)	0.9500
F(43)-F(411)	1.74(4)	C(67)-F(62)	1.320(7)
C(51)-C(52)	1.400(7)	C(67)-F(63)	1.323(7)
C(51)-C(56)	1.402(7)	C(67)-F(61)	1.352(8)
C(52)-C(53)	1.401(7)	C(68)-F(66)	1.329(6)
C(52)-H(52)	0.9500	C(68)-F(65)	1.343(6)
C(53)-C(54)	1.385(8)	C(68)-F(64)	1.358(7)
C(53)-C(57)	1.502(7)	C(71)-C(76)	1.404(6)
C(54)-C(55)	1.381(7)	C(71)-C(72)	1.413(6)
C(54)-H(54)	0.9500	C(72)-C(73)	1.381(7)
C(55)-C(56)	1.400(7)	C(72)-H(72)	0.9500
C(55)-C(58)	1.498(7)	C(73)-C(74)	1.398(7)
C(56)-H(56)	0.9500	C(73)-C(77)	1.496(7)
C(57)-F(53)	1.307(8)	C(74)-C(75)	1.381(7)
C(57)-F(52)	1.316(7)	C(74)-H(74)	0.9500
C(57)-F(51)	1.325(8)	C(75)-C(76)	1.394(7)
C(58)-F(54)	1.321(7)	C(75)-C(78)	1.498(7)
C(58)-F(56)	1.327(6)	C(76)-H(76)	0.9500
C(58)-F(55)	1.328(6)	C(77)-F(71)	1.336(7)
C(61)-C(62)	1.396(6)	C(77)-F(73)	1.346(6)
C(61)-C(66)	1.414(6)	C(77)-F(72)	1.348(8)
C(62)-C(63)	1.407(7)	C(78)-F(74)	1.332(6)
C(62)-H(62)	0.9500	C(78)-F(75)	1.339(6)
C(63)-C(64)	1.372(7)	C(78)-F(76)	1.348(7)

Table I.5. Selected bond angles (°) for complex **10**.

C(14)-Ni(1)-C(13)	41.9(3)	H(1A)-C(1)-H(1B)	113.4
C(14)-Ni(1)-C(15)	41.9(3)	C(1)-C(2)-C(3)	122.0(8)
C(13)-Ni(1)-C(15)	70.2(4)	C(1)-C(2)-Ni(1)	69.5(4)
C(14)-Ni(1)-C(1)	131.5(4)	C(3)-C(2)-Ni(1)	106.3(6)
C(13)-Ni(1)-C(1)	169.6(3)	C(1)-C(2)-H(2)	116.3
C(15)-Ni(1)-C(1)	99.8(4)	C(3)-C(2)-H(2)	116.3
C(14)-Ni(1)-C(2)	98.4(4)	Ni(1)-C(2)-H(2)	116.3
C(13)-Ni(1)-C(2)	139.1(4)	C(2)-C(3)-C(4)	113.7(7)
C(15)-Ni(1)-C(2)	85.1(4)	C(2)-C(3)-H(3A)	108.8
C(1)-Ni(1)-C(2)	38.9(2)	C(4)-C(3)-H(3A)	108.8
C(14)-Ni(1)-C(5)	100.5(4)	C(2)-C(3)-H(3B)	108.8
C(13)-Ni(1)-C(5)	95.7(3)	C(4)-C(3)-H(3B)	108.8
C(15)-Ni(1)-C(5)	136.7(4)	H(3A)-C(3)-H(3B)	107.7
C(1)-Ni(1)-C(5)	93.7(3)	C(5)-C(4)-C(3)	108.8(7)
C(2)-Ni(1)-C(5)	80.1(3)	C(5)-C(4)-H(4A)	109.9
C(14)-Ni(1)-C(6)	119.5(3)	C(3)-C(4)-H(4A)	109.9
C(13)-Ni(1)-C(6)	90.7(3)	C(5)-C(4)-H(4B)	109.9
C(15)-Ni(1)-C(6)	160.2(3)	C(3)-C(4)-H(4B)	109.9
C(1)-Ni(1)-C(6)	99.5(3)	H(4A)-C(4)-H(4B)	108.3
C(2)-Ni(1)-C(6)	107.5(3)	C(6)-C(5)-C(4)	122.4(8)
C(5)-Ni(1)-C(6)	37.2(2)	C(6)-C(5)-Ni(1)	72.8(4)
C(14)-Ni(1)-C(10)	108.4(4)	C(4)-C(5)-Ni(1)	107.2(5)
C(13)-Ni(1)-C(10)	79.3(3)	C(6)-C(5)-H(5)	115.4
C(15)-Ni(1)-C(10)	91.3(4)	C(4)-C(5)-H(5)	115.4
C(1)-Ni(1)-C(10)	98.5(3)	Ni(1)-C(5)-H(5)	115.4
C(2)-Ni(1)-C(10)	135.0(3)	C(5)-C(6)-C(7)	130.3(7)
C(5)-Ni(1)-C(10)	127.2(3)	C(5)-C(6)-Ni(1)	70.0(4)
C(6)-Ni(1)-C(10)	90.0(3)	C(7)-C(6)-Ni(1)	113.1(5)
C(2)-C(1)-Ni(1)	71.6(4)	C(5)-C(6)-H(6)	111.8
C(2)-C(1)-H(1A)	116.4	C(7)-C(6)-H(6)	111.8
Ni(1)-C(1)-H(1A)	116.4	Ni(1)-C(6)-H(6)	111.8
C(2)-C(1)-H(1B)	116.4	C(6)-C(7)-C(8)	110.3(7)
Ni(1)-C(1)-H(1B)	116.4	C(6)-C(7)-H(7A)	109.6
		C(8)-C(7)-H(7A)	109.6

C(6)-C(7)-H(7B)	109.6	C(13)-C(14)-C(15)	108.8(9)
C(8)-C(7)-H(7B)	109.6	C(13)-C(14)-Ni(1)	70.4(4)
H(7A)-C(7)-H(7B)	108.1	C(15)-C(14)-Ni(1)	71.4(5)
C(9)-C(8)-C(7)	112.3(7)	C(13)-C(14)-H(14)	125.6
C(9)-C(8)-H(8A)	109.1	C(15)-C(14)-H(14)	125.6
C(7)-C(8)-H(8A)	109.1	Ni(1)-C(14)-H(14)	125.6
C(9)-C(8)-H(8B)	109.1	C(14)-C(15)-Ni(1)	66.7(4)
C(7)-C(8)-H(8B)	109.1	C(14)-C(15)-H(15A)	117.0
H(8A)-C(8)-H(8B)	107.9	Ni(1)-C(15)-H(15A)	117.0
C(10)-C(9)-C(8)	125.7(10)	C(14)-C(15)-H(15B)	117.0
C(10)-C(9)-H(9)	117.1	Ni(1)-C(15)-H(15B)	117.0
C(8)-C(9)-H(9)	117.1	H(15A)-C(15)-H(15B)	114.1
C(9)-C(10)-C(11)	124.3(9)	C(41)-B(40)-C(51)	107.4(4)
C(9)-C(10)-Ni(1)	81.5(5)	C(41)-B(40)-C(71)	112.0(4)
C(11)-C(10)-Ni(1)	100.7(7)	C(51)-B(40)-C(71)	112.3(4)
C(9)-C(10)-H(10)	114.5	C(41)-B(40)-C(61)	108.9(4)
C(11)-C(10)-H(10)	114.5	C(51)-B(40)-C(61)	113.0(4)
Ni(1)-C(10)-H(10)	114.5	C(71)-B(40)-C(61)	103.4(3)
C(12)-C(11)-C(10)	104.7(9)	C(42)-C(41)-C(46)	115.3(4)
C(12)-C(11)-H(11A)	110.8	C(42)-C(41)-B(40)	119.1(4)
C(10)-C(11)-H(11A)	110.8	C(46)-C(41)-B(40)	125.6(4)
C(12)-C(11)-H(11B)	110.8	C(43)-C(42)-C(41)	122.7(5)
C(10)-C(11)-H(11B)	110.8	C(43)-C(42)-H(42)	118.6
H(11A)-C(11)-H(11B)	108.9	C(41)-C(42)-H(42)	118.6
C(11)-C(12)-C(13)	113.0(8)	C(44)-C(43)-C(42)	121.2(5)
C(11)-C(12)-H(12A)	109.0	C(44)-C(43)-C(47)	120.0(5)
C(13)-C(12)-H(12A)	109.0	C(42)-C(43)-C(47)	118.8(5)
C(11)-C(12)-H(12B)	109.0	C(43)-C(44)-C(45)	117.3(4)
C(13)-C(12)-H(12B)	109.0	C(43)-C(44)-H(44)	121.4
H(12A)-C(12)-H(12B)	107.8	C(45)-C(44)-H(44)	121.4
C(14)-C(13)-C(12)	125.4(9)	C(44)-C(45)-C(46)	121.3(4)
C(14)-C(13)-Ni(1)	67.7(4)	C(44)-C(45)-C(48)	119.1(4)
C(12)-C(13)-Ni(1)	108.8(6)	C(46)-C(45)-C(48)	119.4(4)
C(14)-C(13)-H(13)	114.9	C(45)-C(46)-C(41)	122.1(4)
C(12)-C(13)-H(13)	114.9	C(45)-C(46)-H(46)	118.9
Ni(1)-C(13)-H(13)	114.9	C(41)-C(46)-H(46)	118.9

F(43)-C(47)-F(41)	105.2(18)	F(41)-F(411)-C(47)	72(4)
F(43)-C(47)-F(431)	25(2)	F(41)-F(411)-F(43)	116(5)
F(41)-C(47)-F(431)	121.7(16)	C(47)-F(411)-F(43)	47.5(12)
F(43)-C(47)-F(421)	124.8(15)	F(42)-F(421)-C(47)	75(3)
F(41)-C(47)-F(421)	81.6(16)	F(42)-F(421)-F(41)	122(3)
F(431)-C(47)-F(421)	105.2(16)	C(47)-F(421)-F(41)	49.0(10)
F(43)-C(47)-F(42)	106.8(19)	F(43)-F(431)-C(47)	77(5)
F(41)-C(47)-F(42)	111.2(19)	F(43)-F(431)-F(42)	124(6)
F(431)-C(47)-F(42)	82(2)	C(47)-F(431)-F(42)	49.0(14)
F(421)-C(47)-F(42)	30.8(19)	C(52)-C(51)-C(56)	115.8(4)
F(43)-C(47)-F(411)	82.2(18)	C(52)-C(51)-B(40)	124.8(4)
F(41)-C(47)-F(411)	25.0(18)	C(56)-C(51)-B(40)	119.4(4)
F(431)-C(47)-F(411)	102.9(18)	C(51)-C(52)-C(53)	121.7(5)
F(421)-C(47)-F(411)	102.9(15)	C(51)-C(52)-H(52)	119.1
F(42)-C(47)-F(411)	128.9(17)	C(53)-C(52)-H(52)	119.1
F(43)-C(47)-C(43)	112.0(13)	C(54)-C(53)-C(52)	121.2(5)
F(41)-C(47)-C(43)	112.0(11)	C(54)-C(53)-C(57)	120.0(5)
F(431)-C(47)-C(43)	115.6(13)	C(52)-C(53)-C(57)	118.8(5)
F(421)-C(47)-C(43)	115.6(8)	C(55)-C(54)-C(53)	118.2(4)
F(42)-C(47)-C(43)	109.5(11)	C(55)-C(54)-H(54)	120.9
F(411)-C(47)-C(43)	113.0(11)	C(53)-C(54)-H(54)	120.9
F(44)-C(48)-F(46)	106.7(4)	C(54)-C(55)-C(56)	120.6(5)
F(44)-C(48)-F(45)	106.2(4)	C(54)-C(55)-C(58)	120.2(5)
F(46)-C(48)-F(45)	105.2(4)	C(56)-C(55)-C(58)	119.1(5)
F(44)-C(48)-C(45)	113.3(4)	C(55)-C(56)-C(51)	122.4(4)
F(46)-C(48)-C(45)	112.9(4)	C(55)-C(56)-H(56)	118.8
F(45)-C(48)-C(45)	111.9(4)	C(51)-C(56)-H(56)	118.8
F(411)-F(41)-C(47)	83(3)	F(53)-C(57)-F(52)	107.2(6)
F(411)-F(41)-F(421)	124(5)	F(53)-C(57)-F(51)	104.8(6)
C(47)-F(41)-F(421)	49.4(11)	F(52)-C(57)-F(51)	104.4(6)
F(421)-F(42)-C(47)	74(3)	F(53)-C(57)-C(53)	112.4(5)
F(421)-F(42)-F(431)	111(4)	F(52)-C(57)-C(53)	113.7(5)
C(47)-F(42)-F(431)	48.6(13)	F(51)-C(57)-C(53)	113.7(5)
F(431)-F(43)-C(47)	77(5)	F(54)-C(58)-F(56)	105.2(5)
F(431)-F(43)-F(411)	118(7)	F(54)-C(58)-F(55)	107.2(5)
C(47)-F(43)-F(411)	50.2(14)	F(56)-C(58)-F(55)	105.1(5)

F(54)-C(58)-C(55)	112.1(4)	C(73)-C(72)-C(71)	122.4(4)
F(56)-C(58)-C(55)	113.6(4)	C(73)-C(72)-H(72)	118.8
F(55)-C(58)-C(55)	113.0(5)	C(71)-C(72)-H(72)	118.8
C(62)-C(61)-C(66)	115.9(4)	C(72)-C(73)-C(74)	121.0(5)
C(62)-C(61)-B(40)	123.9(4)	C(72)-C(73)-C(77)	120.8(5)
C(66)-C(61)-B(40)	119.8(4)	C(74)-C(73)-C(77)	118.2(5)
C(61)-C(62)-C(63)	122.0(4)	C(75)-C(74)-C(73)	117.8(4)
C(61)-C(62)-H(62)	119.0	C(75)-C(74)-H(74)	121.1
C(63)-C(62)-H(62)	119.0	C(73)-C(74)-H(74)	121.1
C(64)-C(63)-C(62)	121.2(4)	C(74)-C(75)-C(76)	121.3(4)
C(64)-C(63)-C(67)	120.7(5)	C(74)-C(75)-C(78)	119.4(4)
C(62)-C(63)-C(67)	118.0(5)	C(76)-C(75)-C(78)	119.3(4)
C(63)-C(64)-C(65)	118.0(4)	C(75)-C(76)-C(71)	122.0(4)
C(63)-C(64)-H(64)	121.0	C(75)-C(76)-H(76)	119.0
C(65)-C(64)-H(64)	121.0	C(71)-C(76)-H(76)	119.0
C(66)-C(65)-C(64)	121.1(5)	F(71)-C(77)-F(73)	106.3(5)
C(66)-C(65)-C(68)	121.0(4)	F(71)-C(77)-F(72)	106.0(5)
C(64)-C(65)-C(68)	117.8(4)	F(73)-C(77)-F(72)	106.6(4)
C(65)-C(66)-C(61)	121.7(4)	F(71)-C(77)-C(73)	113.2(5)
C(65)-C(66)-H(66)	119.1	F(73)-C(77)-C(73)	111.7(4)
C(61)-C(66)-H(66)	119.1	F(72)-C(77)-C(73)	112.6(5)
F(62)-C(67)-F(63)	107.2(5)	F(74)-C(78)-F(75)	105.4(4)
F(62)-C(67)-F(61)	102.9(5)	F(74)-C(78)-F(76)	106.1(4)
F(63)-C(67)-F(61)	106.5(5)	F(75)-C(78)-F(76)	105.6(4)
F(62)-C(67)-C(63)	114.1(5)	F(74)-C(78)-C(75)	114.1(4)
F(63)-C(67)-C(63)	113.9(5)	F(75)-C(78)-C(75)	113.1(4)
F(61)-C(67)-C(63)	111.5(5)	F(76)-C(78)-C(75)	111.9(4)
F(66)-C(68)-F(65)	107.3(4)		
F(66)-C(68)-F(64)	105.7(4)		
F(65)-C(68)-F(64)	104.9(4)		
F(66)-C(68)-C(65)	114.0(4)		
F(65)-C(68)-C(65)	112.2(4)		
F(64)-C(68)-C(65)	112.1(4)		
C(76)-C(71)-C(72)	115.5(4)		
C(76)-C(71)-B(40)	126.1(4)		
C(72)-C(71)-B(40)	118.4(4)		

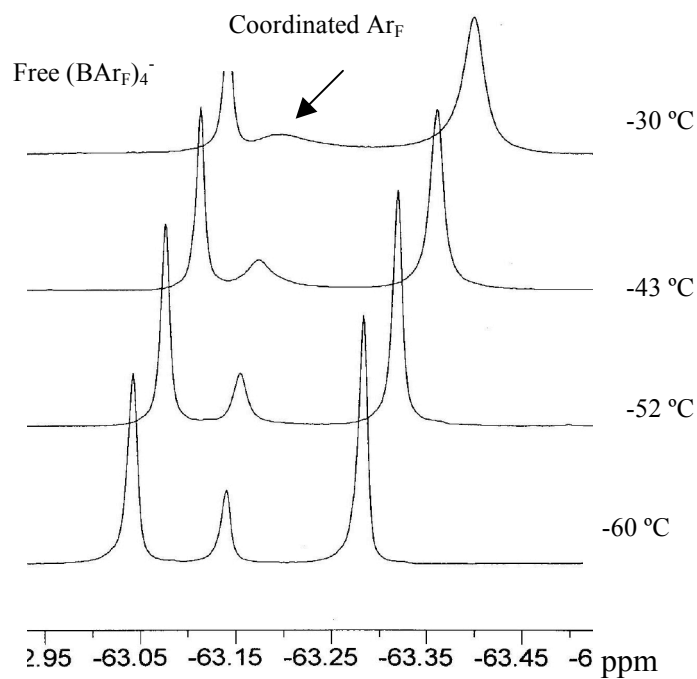


Figure I.2. ^{19}F NMR overlay showing intramolecular Ar_F exchange for species **2**.

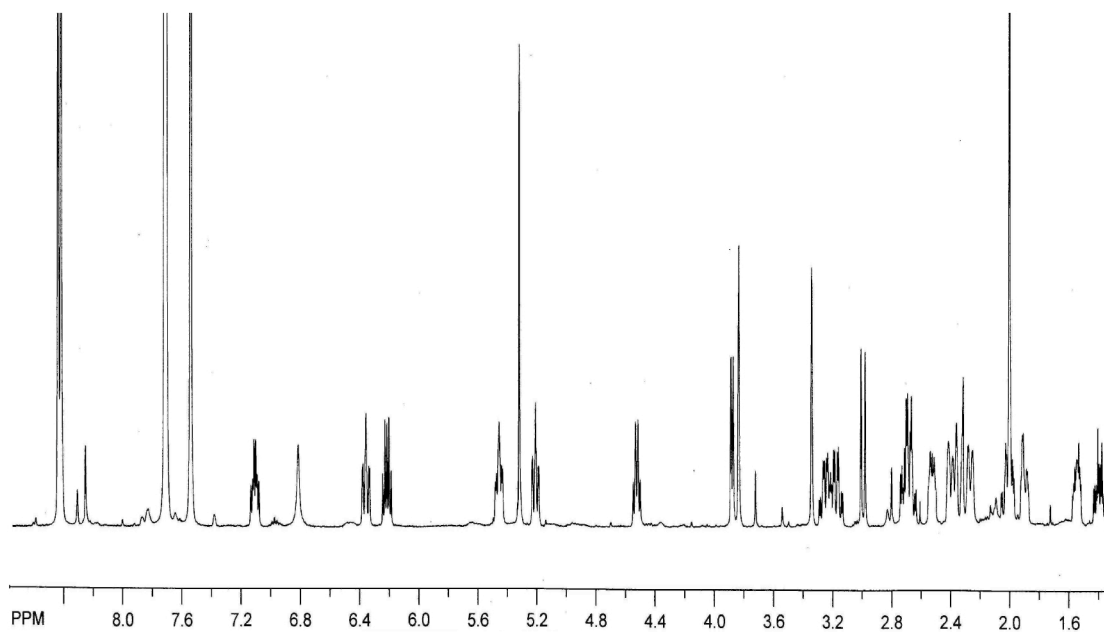


Figure I.3. ^1H NMR spectrum of complex **11** (500 MHz) in CD_2Cl_2 at -40°C .

Appendix II

Table II.1. X-ray crystallographic data for complexes **5** and **7**.

	5	7
Formula	C ₄₄ H ₂₉ BF ₂₄ Ni	C ₄₈ H ₃₇ BF ₂₄ Ni
Formula Weight	1083.19	1139.30
Temperature (°C)	-173	-173
Wavelength (Å)	0.71073	1.54178
Crystal System	Orthorhombic	Monoclinic
Space Group	P2 ₁ 2 ₁ 2 ₁	P2(1)/c
Unit Cell Dimensions	a = 13.3171(3)Å α = 90° b = 14.5598(19)Å β = 90° c = 16.336(2)Å γ = 90°	a = 12.4231(10)Å α = 90° b = 19.4054(16)Å β = 104.801(4)° c = 20.6838(17)Å γ = 90°
Volume	4544.34(17)Å ³	4820.9(7)Å ³
Z	4	4
D _{calcd} , mg/m ⁻³	1.583	1.570
Abs coeff, mm ⁻¹	0.558	1.750
F(000)	2168	2296
Crystal size (mm ³)	0.25 x 0.20 x 0.10	0.30 x 0.30 x 0.05
Theta range (°)	1.62-27.00	3.17-69.60
Index range	-17<=h<=17, -19<=k<=19, -28<=l<=28	-14<=h<=, -22<=k<=23, -24<=l<=24
Reflections collected	78781	34611
Independent Reflections	9927[(R(int) 0.0314]	8776[R(int) 0.0239]
Absorption Correction	SADABS	Numerical
Refinement Method	Full-matrix least squared on F ²	Full-matrix least squared on F ²
Data/restraints/parameters	9927/0/742	8776/33/834
Goodness-of-fit on F ²	1.044	1.046
Final R indices [I>2σ(I)]	R1 = 0.0555, wR2 = 0.1176	R1 = 0.0377, wR2 = 0.0923
Largest diff peak and hole	1.983; -1.740e/Å ⁻³	0.548; -0.428e/Å ⁻³

Table II.2. Selected bond lengths (Å) for complex **5**.

Ni(1)-C(2)	1.962(4)	C(27)-F(21)	1.297(18)
Ni(1)-C(1)	1.994(4)	C(27)-F(123)	1.319(13)
Ni(1)-C(3)	2.061(6)	C(27)-F(121)	1.32(2)
Ni(1)-C(6)	2.121(4)	C(27)-F(22)	1.355(18)
Ni(1)-C(8)	2.130(4)	C(28)-F(26)	1.317(5)
Ni(1)-C(5)	2.142(4)	C(28)-F(25)	1.329(5)
Ni(1)-C(9)	2.157(3)	C(28)-F(24)	1.334(4)
Ni(1)-C(4)	2.176(4)	C(31)-C(32)	1.395(5)
Ni(1)-C(7)	2.192(4)	C(31)-C(36)	1.401(5)
C(1)-C(2)	1.414(8)	C(32)-C(33)	1.395(5)
C(2)-C(3)	1.401(10)	C(33)-C(34)	1.378(5)
C(4)-C(9)	1.383(5)	C(33)-C(37)	1.493(5)
C(4)-C(5)	1.402(5)	C(34)-C(35)	1.379(5)
C(5)-C(6)	1.432(6)	C(35)-C(36)	1.387(5)
C(5)-C(10)	1.528(6)	C(35)-C(38)	1.497(6)
C(6)-C(7)	1.392(5)	C(37)-F(32)	1.335(5)
C(7)-C(8)	1.402(5)	C(37)-F(31)	1.340(5)
C(7)-C(11)	1.504(5)	C(37)-F(33)	1.351(4)
C(8)-C(9)	1.419(5)	C(38)-F(35)	1.314(6)
C(9)-C(12)	1.512(5)	C(38)-F(36)	1.326(5)
B(20)-C(41)	1.641(5)	C(38)-F(34)	1.326(5)
B(20)-C(51)	1.642(4)	C(41)-C(42)	1.400(4)
B(20)-C(31)	1.646(5)	C(41)-C(46)	1.403(4)
B(20)-C(21)	1.653(5)	C(42)-C(43)	1.401(5)
C(21)-C(26)	1.394(4)	C(43)-C(44)	1.392(5)
C(21)-C(22)	1.399(5)	C(43)-C(47)	1.501(5)
C(22)-C(23)	1.402(5)	C(44)-C(45)	1.384(5)
C(23)-C(24)	1.379(5)	C(45)-C(46)	1.384(5)
C(23)-C(27)	1.504(6)	C(45)-C(48)	1.505(5)
C(24)-C(25)	1.393(5)	C(47)-F(41)	1.334(4)
C(25)-C(26)	1.390(5)	C(47)-F(43)	1.338(4)
C(25)-C(28)	1.501(5)	C(47)-F(42)	1.341(4)
C(27)-F(23)	1.274(12)	C(48)-F(45)	1.251(9)
C(27)-F(122)	1.28(2)	C(48)-F(146)	1.256(10)

C(48)-F(145)	1.259(11)	C(58)-F(155)	1.246(14)
C(48)-F(44)	1.316(9)	C(58)-F(54)	1.284(8)
C(48)-F(46)	1.388(10)	C(58)-F(56)	1.316(10)
C(48)-F(144)	1.399(10)	C(58)-F(55)	1.326(11)
C(51)-C(52)	1.397(5)	C(58)-F(154)	1.331(15)
C(51)-C(56)	1.403(5)	F(21)-F(121)	0.54(4)
C(52)-C(53)	1.393(5)	F(22)-F(122)	0.75(3)
C(53)-C(54)	1.389(6)	F(22)-F(121)	1.76(3)
C(53)-C(57)	1.498(5)	F(23)-F(122)	1.67(3)
C(54)-C(55)	1.377(5)	F(45)-F(144)	0.825(13)
C(55)-C(56)	1.402(4)	F(45)-F(146)	1.367(15)
C(55)-C(58)	1.504(6)	F(46)-F(146)	0.914(15)
C(57)-F(151)	1.27(3)	F(46)-F(145)	1.754(18)
C(57)-F(52)	1.309(14)	F(54)-F(154)	0.61(3)
C(57)-F(152)	1.309(16)	F(54)-F(156)	1.57(3)
C(57)-F(53)	1.342(13)	F(55)-F(155)	0.62(3)
C(57)-F(153)	1.374(15)	F(56)-F(156)	0.63(3)
C(57)-F(51)	1.38(3)	F(56)-F(155)	1.67(2)
C(58)-F(156)	1.224(15)		

Table II.3. Selected bond angles (°) for complex **5**.

C(2)-Ni(1)-C(1)	41.9(2)	C(5)-Ni(1)-C(7)	69.28(15)
C(2)-Ni(1)-C(3)	40.7(3)	C(9)-Ni(1)-C(7)	69.37(14)
C(1)-Ni(1)-C(3)	70.7(3)	C(4)-Ni(1)-C(7)	80.99(14)
C(2)-Ni(1)-C(6)	123.3(2)	C(2)-C(1)-Ni(1)	67.8(3)
C(1)-Ni(1)-C(6)	160.72(19)	C(3)-C(2)-C(1)	113.0(6)
C(3)-Ni(1)-C(6)	105.3(2)	C(3)-C(2)-Ni(1)	73.5(3)
C(2)-Ni(1)-C(8)	134.5(3)	C(1)-C(2)-Ni(1)	70.3(3)
C(1)-Ni(1)-C(8)	112.1(3)	C(2)-C(3)-Ni(1)	65.9(3)
C(3)-Ni(1)-C(8)	168.8(2)	C(9)-C(4)-C(5)	120.9(3)
C(6)-Ni(1)-C(8)	68.26(15)	C(9)-C(4)-Ni(1)	70.7(2)
C(2)-Ni(1)-C(5)	137.9(2)	C(5)-C(4)-Ni(1)	69.7(2)
C(1)-Ni(1)-C(5)	158.3(2)	C(4)-C(5)-C(6)	118.9(4)
C(3)-Ni(1)-C(5)	99.5(3)	C(4)-C(5)-C(10)	121.7(4)
C(6)-Ni(1)-C(5)	39.24(16)	C(6)-C(5)-C(10)	119.4(4)
C(8)-Ni(1)-C(5)	81.34(15)	C(4)-C(5)-Ni(1)	72.4(2)
C(2)-Ni(1)-C(9)	152.2(2)	C(6)-C(5)-Ni(1)	69.6(2)
C(1)-Ni(1)-C(9)	110.7(2)	C(10)-C(5)-Ni(1)	131.8(4)
C(3)-Ni(1)-C(9)	151.8(3)	C(7)-C(6)-C(5)	121.5(4)
C(6)-Ni(1)-C(9)	81.96(15)	C(7)-C(6)-Ni(1)	73.9(2)
C(8)-Ni(1)-C(9)	38.66(15)	C(5)-C(6)-Ni(1)	71.2(2)
C(5)-Ni(1)-C(9)	68.62(14)	C(6)-C(7)-C(8)	117.2(3)
C(2)-Ni(1)-C(4)	155.6(2)	C(6)-C(7)-C(11)	120.9(4)
C(1)-Ni(1)-C(4)	129.65(18)	C(8)-C(7)-C(11)	121.9(4)
C(3)-Ni(1)-C(4)	119.2(3)	C(6)-C(7)-Ni(1)	68.5(2)
C(6)-Ni(1)-C(4)	69.19(15)	C(8)-C(7)-Ni(1)	68.7(2)
C(8)-Ni(1)-C(4)	68.03(15)	C(11)-C(7)-Ni(1)	132.7(3)
C(5)-Ni(1)-C(4)	37.89(15)	C(7)-C(8)-C(9)	122.6(4)
C(9)-Ni(1)-C(4)	37.21(14)	C(7)-C(8)-Ni(1)	73.5(2)
C(2)-Ni(1)-C(7)	122.1(2)	C(9)-C(8)-Ni(1)	71.7(2)
C(1)-Ni(1)-C(7)	131.8(2)	C(4)-C(9)-C(8)	118.6(3)
C(3)-Ni(1)-C(7)	132.0(2)	C(4)-C(9)-C(12)	121.4(3)
C(6)-Ni(1)-C(7)	37.60(14)	C(8)-C(9)-C(12)	120.0(3)
C(8)-Ni(1)-C(7)	37.83(15)	C(4)-C(9)-Ni(1)	72.1(2)
		C(8)-C(9)-Ni(1)	69.6(2)

C(12)-C(9)-Ni(1)	131.5(2)	F(21)-C(27)-C(23)	110.5(11)
C(41)-B(20)-C(51)	109.6(3)	F(123)-C(27)-C(23)	114.4(8)
C(41)-B(20)-C(31)	109.4(3)	F(121)-C(27)-C(23)	114.9(11)
C(51)-B(20)-C(31)	107.7(2)	F(22)-C(27)-C(23)	110.8(7)
C(41)-B(20)-C(21)	111.7(2)	F(26)-C(28)-F(25)	106.9(4)
C(51)-B(20)-C(21)	107.5(3)	F(26)-C(28)-F(24)	106.8(3)
C(31)-B(20)-C(21)	110.8(3)	F(25)-C(28)-F(24)	104.8(3)
C(26)-C(21)-C(22)	115.4(3)	F(26)-C(28)-C(25)	113.1(3)
C(26)-C(21)-B(20)	123.2(3)	F(25)-C(28)-C(25)	112.4(3)
C(22)-C(21)-B(20)	121.1(3)	F(24)-C(28)-C(25)	112.2(3)
C(21)-C(22)-C(23)	122.1(3)	C(32)-C(31)-C(36)	115.7(3)
C(24)-C(23)-C(22)	121.0(3)	C(32)-C(31)-B(20)	122.3(3)
C(24)-C(23)-C(27)	120.6(3)	C(36)-C(31)-B(20)	121.9(3)
C(22)-C(23)-C(27)	118.4(4)	C(31)-C(32)-C(33)	122.0(3)
C(23)-C(24)-C(25)	117.9(3)	C(34)-C(33)-C(32)	121.1(3)
C(26)-C(25)-C(24)	120.5(3)	C(34)-C(33)-C(37)	118.5(3)
C(26)-C(25)-C(28)	121.3(3)	C(32)-C(33)-C(37)	120.5(3)
C(24)-C(25)-C(28)	118.2(3)	C(33)-C(34)-C(35)	118.0(3)
C(25)-C(26)-C(21)	123.0(3)	C(34)-C(35)-C(36)	121.1(3)
F(23)-C(27)-F(122)	81.4(13)	C(34)-C(35)-C(38)	120.0(3)
F(23)-C(27)-F(21)	106.7(14)	C(36)-C(35)-C(38)	118.9(3)
F(122)-C(27)-F(21)	129.0(13)	C(35)-C(36)-C(31)	122.2(3)
F(23)-C(27)-F(123)	19.7(15)	F(32)-C(37)-F(31)	106.5(3)
F(122)-C(27)-F(123)	98.1(12)	F(32)-C(37)-F(33)	105.0(3)
F(21)-C(27)-F(123)	88.1(12)	F(31)-C(37)-F(33)	105.8(3)
F(23)-C(27)-F(121)	121.6(12)	F(32)-C(37)-C(33)	113.3(4)
F(122)-C(27)-F(121)	109.8(15)	F(31)-C(37)-C(33)	114.0(3)
F(21)-C(27)-F(121)	23.6(16)	F(33)-C(37)-C(33)	111.5(3)
F(123)-C(27)-F(121)	105.8(12)	F(35)-C(38)-F(36)	105.4(5)
F(23)-C(27)-F(22)	111.3(13)	F(35)-C(38)-F(34)	107.6(4)
F(122)-C(27)-F(22)	32.9(12)	F(36)-C(38)-F(34)	104.9(4)
F(21)-C(27)-F(22)	105.3(12)	F(35)-C(38)-C(35)	112.7(4)
F(123)-C(27)-F(22)	124.1(10)	F(36)-C(38)-C(35)	112.1(4)
F(121)-C(27)-F(22)	82.4(13)	F(34)-C(38)-C(35)	113.4(4)
F(23)-C(27)-C(23)	111.9(8)	C(42)-C(41)-C(46)	115.7(3)
F(122)-C(27)-C(23)	112.4(9)	C(42)-C(41)-B(20)	123.0(3)

C(46)-C(41)-B(20)	121.3(3)	F(144)-C(48)-C(45)	109.3(6)
C(41)-C(42)-C(43)	122.1(3)	C(52)-C(51)-C(56)	115.7(3)
C(44)-C(43)-C(42)	120.7(3)	C(52)-C(51)-B(20)	122.6(3)
C(44)-C(43)-C(47)	120.7(3)	C(56)-C(51)-B(20)	121.5(3)
C(42)-C(43)-C(47)	118.6(3)	C(53)-C(52)-C(51)	122.3(3)
C(45)-C(44)-C(43)	117.6(3)	C(54)-C(53)-C(52)	120.8(3)
C(46)-C(45)-C(44)	121.5(3)	C(54)-C(53)-C(57)	120.4(3)
C(46)-C(45)-C(48)	119.2(3)	C(52)-C(53)-C(57)	118.8(4)
C(44)-C(45)-C(48)	119.3(3)	C(55)-C(54)-C(53)	118.4(3)
C(45)-C(46)-C(41)	122.2(3)	C(54)-C(55)-C(56)	120.6(3)
F(41)-C(47)-F(43)	106.7(3)	C(54)-C(55)-C(58)	120.6(3)
F(41)-C(47)-F(42)	106.0(3)	C(56)-C(55)-C(58)	118.8(3)
F(43)-C(47)-F(42)	106.1(3)	C(55)-C(56)-C(51)	122.2(3)
F(41)-C(47)-C(43)	112.4(3)	F(151)-C(57)-F(52)	112.5(13)
F(43)-C(47)-C(43)	112.9(3)	F(151)-C(57)-F(152)	110.9(17)
F(42)-C(47)-C(43)	112.3(3)	F(52)-C(57)-F(152)	89.7(11)
F(45)-C(48)-F(146)	66.1(8)	F(151)-C(57)-F(53)	101.5(17)
F(45)-C(48)-F(145)	123.6(8)	F(52)-C(57)-F(53)	105.7(11)
F(146)-C(48)-F(145)	108.9(10)	F(152)-C(57)-F(53)	16.2(16)
F(45)-C(48)-F(44)	113.8(8)	F(151)-C(57)-F(153)	106.6(13)
F(146)-C(48)-F(44)	123.5(7)	F(52)-C(57)-F(153)	13.2(13)
F(145)-C(48)-F(44)	20.1(10)	F(152)-C(57)-F(153)	103.0(12)
F(45)-C(48)-F(46)	105.8(8)	F(53)-C(57)-F(153)	118.9(12)
F(146)-C(48)-F(46)	40.1(7)	F(151)-C(57)-F(51)	8(2)
F(145)-C(48)-F(46)	82.8(9)	F(52)-C(57)-F(51)	104.8(11)
F(44)-C(48)-F(46)	102.6(6)	F(152)-C(57)-F(51)	110.6(14)
F(45)-C(48)-F(144)	35.7(6)	F(53)-C(57)-F(51)	103.3(14)
F(146)-C(48)-F(144)	99.2(8)	F(153)-C(57)-F(51)	99.3(11)
F(145)-C(48)-F(144)	101.3(9)	F(151)-C(57)-C(53)	110.6(15)
F(44)-C(48)-F(144)	84.9(7)	F(52)-C(57)-C(53)	115.6(7)
F(46)-C(48)-F(144)	135.2(6)	F(152)-C(57)-C(53)	116.0(7)
F(45)-C(48)-C(45)	112.7(5)	F(53)-C(57)-C(53)	109.7(8)
F(146)-C(48)-C(45)	118.2(5)	F(153)-C(57)-C(53)	109.1(8)
F(145)-C(48)-C(45)	117.0(6)	F(51)-C(57)-C(53)	116.6(13)
F(44)-C(48)-C(45)	112.9(5)	F(156)-C(58)-F(155)	103.5(14)
F(46)-C(48)-C(45)	108.0(5)	F(156)-C(58)-F(54)	77.6(14)

F(155)-C(58)-F(54)	120.1(9)	F(22)-F(122)-F(23)	123(4)
F(156)-C(58)-F(56)	28.5(15)	C(27)-F(122)-F(23)	49.0(9)
F(155)-C(58)-F(56)	81.3(11)	F(144)-F(45)-C(48)	82.0(12)
F(54)-C(58)-F(56)	104.0(7)	F(144)-F(45)-F(146)	133.3(16)
F(156)-C(58)-F(55)	127.1(12)	C(48)-F(45)-F(146)	57.1(6)
F(155)-C(58)-F(55)	27.7(14)	F(146)-F(46)-C(48)	62.2(9)
F(54)-C(58)-F(55)	107.1(8)	F(146)-F(46)-F(145)	95.0(12)
F(56)-C(58)-F(55)	108.4(9)	C(48)-F(46)-F(145)	45.4(5)
F(156)-C(58)-F(154)	103.4(14)	F(45)-F(144)-C(48)	62.3(10)
F(155)-C(58)-F(154)	106.3(12)	C(48)-F(145)-F(46)	51.8(6)
F(54)-C(58)-F(154)	26.9(11)	F(46)-F(146)-C(48)	77.8(13)
F(56)-C(58)-F(154)	127.3(9)	F(46)-F(146)-F(45)	133.8(16)
F(55)-C(58)-F(154)	85.5(12)	C(48)-F(146)-F(45)	56.8(6)
F(156)-C(58)-C(55)	115.1(8)	F(154)-F(54)-C(58)	80.9(18)
F(155)-C(58)-C(55)	117.5(7)	F(154)-F(54)-F(156)	128(2)
F(54)-C(58)-C(55)	114.9(6)	C(58)-F(54)-F(156)	49.5(7)
F(56)-C(58)-C(55)	112.0(5)	F(155)-F(55)-C(58)	69.0(18)
F(55)-C(58)-C(55)	110.0(7)	F(156)-F(56)-C(58)	67.7(19)
F(154)-C(58)-C(55)	109.7(8)	F(156)-F(56)-F(155)	106(2)
F(121)-F(21)-C(27)	81(4)	C(58)-F(56)-F(155)	47.6(7)
F(122)-F(22)-C(27)	68(2)	F(54)-F(154)-C(58)	72.2(18)
F(122)-F(22)-F(121)	109(3)	F(55)-F(155)-C(58)	83(3)
C(27)-F(22)-F(121)	48.0(10)	F(55)-F(155)-F(56)	133(3)
C(27)-F(23)-F(122)	49.6(9)	C(58)-F(155)-F(56)	51.2(7)
F(21)-F(121)-C(27)	76(4)	F(56)-F(156)-C(58)	84(2)
F(21)-F(121)-F(22)	124(5)	F(56)-F(156)-F(54)	132(3)
C(27)-F(121)-F(22)	49.6(9)	C(58)-F(156)-F(54)	52.9(10)
F(22)-F(122)-C(27)	79(3)		

Table II.4. Selected bond lengths (Å) for complex **7**.

Ni(1)-C(2)	1.978(2)	C(25)-C(26)	1.404(3)
Ni(1)-C(1)	2.001(2)	C(25)-C(28)	1.503(3)
Ni(1)-C(3)	2.007(2)	C(27)-F(21)	1.343(3)
Ni(1)-C(8)	2.1205(19)	C(27)-F(22)	1.347(2)
Ni(1)-C(5)	2.1392(18)	C(27)-F(23)	1.351(2)
Ni(1)-C(10)	2.1426(18)	C(28)-F(26)	1.327(3)
Ni(1)-C(7)	2.1857(19)	C(28)-F(24)	1.339(3)
Ni(1)-C(9)	2.1901(19)	C(28)-F(25)	1.343(2)
Ni(1)-C(6)	2.2563(18)	C(31)-C(32)	1.400(2)
C(1)-C(2)	1.405(3)	C(31)-C(36)	1.412(2)
C(2)-C(3)	1.402(4)	C(32)-C(33)	1.406(2)
C(2)-C(4)	1.498(3)	C(33)-C(34)	1.386(3)
C(5)-C(6)	1.427(3)	C(33)-C(37)	1.502(2)
C(5)-C(10)	1.433(3)	C(34)-C(35)	1.397(3)
C(5)-C(11)	1.514(3)	C(35)-C(36)	1.392(2)
C(6)-C(7)	1.414(3)	C(35)-C(38)	1.501(2)
C(6)-C(12)	1.516(3)	C(37)-F(31)	1.333(2)
C(7)-C(8)	1.435(3)	C(37)-F(32)	1.337(2)
C(7)-C(13)	1.514(3)	C(37)-F(33)	1.341(2)
C(8)-C(9)	1.418(3)	C(38)-F(36)	1.335(2)
C(8)-C(14)	1.520(3)	C(38)-F(34)	1.346(2)
C(9)-C(10)	1.417(3)	C(38)-F(35)	1.351(2)
C(9)-C(15)	1.513(3)	C(41)-C(42)	1.402(2)
C(10)-C(16)	1.512(3)	C(41)-C(46)	1.408(3)
B(20)-C(51)	1.644(3)	C(42)-C(43)	1.401(3)
B(20)-C(41)	1.646(3)	C(43)-C(44)	1.390(3)
B(20)-C(21)	1.648(3)	C(43)-C(47)	1.507(3)
B(20)-C(31)	1.656(2)	C(44)-C(45)	1.394(3)
C(21)-C(26)	1.400(3)	C(45)-C(46)	1.394(3)
C(21)-C(22)	1.408(3)	C(45)-C(48)	1.505(3)
C(22)-C(23)	1.394(3)	C(47)-F(41)	1.341(2)
C(23)-C(24)	1.396(3)	C(47)-F(43)	1.342(2)
C(23)-C(27)	1.500(3)	C(47)-F(42)	1.349(2)
C(24)-C(25)	1.382(3)	C(48)-F(44)	1.321(2)

C(48)-F(46)	1.342(2)	C(57)-F(53)	1.339(2)
C(48)-F(45)	1.349(3)	C(57)-F(52)	1.346(2)
C(51)-C(52)	1.399(2)	C(57)-F(51)	1.350(2)
C(51)-C(56)	1.412(2)	C(58)-F(57)	1.255(10)
C(52)-C(53)	1.403(3)	C(58)-F(54)	1.293(3)
C(53)-C(54)	1.386(3)	C(58)-F(59)	1.300(8)
C(53)-C(57)	1.504(2)	C(58)-F(55)	1.336(3)
C(54)-C(55)	1.396(3)	C(58)-F(56)	1.351(3)
C(55)-C(56)	1.392(3)	C(58)-F(58)	1.420(10)
C(55)-C(58)	1.505(3)		

Table II.5. Selected bond angles (°) for complex 7.

C(2)-Ni(1)-C(1)	41.33(10)	C(10)-Ni(1)-C(6)	68.59(7)
C(2)-Ni(1)-C(3)	41.19(10)	C(7)-Ni(1)-C(6)	37.08(7)
C(1)-Ni(1)-C(3)	71.62(11)	C(9)-Ni(1)-C(6)	80.06(7)
C(2)-Ni(1)-C(8)	142.10(9)	C(2)-C(1)-Ni(1)	68.46(13)
C(1)-Ni(1)-C(8)	161.76(12)	C(3)-C(2)-C(1)	113.3(2)
C(3)-Ni(1)-C(8)	103.43(9)	C(3)-C(2)-C(4)	122.2(3)
C(2)-Ni(1)-C(5)	129.31(8)	C(1)-C(2)-C(4)	123.5(3)
C(1)-Ni(1)-C(5)	105.04(10)	C(3)-C(2)-Ni(1)	70.50(13)
C(3)-Ni(1)-C(5)	168.11(11)	C(1)-C(2)-Ni(1)	70.20(13)
C(8)-Ni(1)-C(5)	83.18(7)	C(4)-C(2)-Ni(1)	118.71(16)
C(2)-Ni(1)-C(10)	146.91(8)	C(2)-C(3)-Ni(1)	68.31(12)
C(1)-Ni(1)-C(10)	105.93(9)	C(6)-C(5)-C(10)	120.27(17)
C(3)-Ni(1)-C(10)	152.47(11)	C(6)-C(5)-C(11)	119.55(18)
C(8)-Ni(1)-C(10)	70.01(7)	C(10)-C(5)-C(11)	120.12(18)
C(5)-Ni(1)-C(10)	39.12(7)	C(6)-C(5)-Ni(1)	75.57(10)
C(2)-Ni(1)-C(7)	126.74(8)	C(10)-C(5)-Ni(1)	70.57(10)
C(1)-Ni(1)-C(7)	159.30(12)	C(11)-C(5)-Ni(1)	128.09(14)
C(3)-Ni(1)-C(7)	110.02(10)	C(7)-C(6)-C(5)	118.97(17)
C(8)-Ni(1)-C(7)	38.90(8)	C(7)-C(6)-C(12)	120.41(19)
C(5)-Ni(1)-C(7)	68.92(7)	C(5)-C(6)-C(12)	120.53(19)
C(10)-Ni(1)-C(7)	82.12(7)	C(7)-C(6)-Ni(1)	68.74(10)
C(2)-Ni(1)-C(9)	157.07(8)	C(5)-C(6)-Ni(1)	66.66(10)
C(1)-Ni(1)-C(9)	128.87(10)	C(12)-C(6)-Ni(1)	135.41(15)
C(3)-Ni(1)-C(9)	121.75(10)	C(6)-C(7)-C(8)	120.04(17)
C(8)-Ni(1)-C(9)	38.36(8)	C(6)-C(7)-C(13)	120.9(2)
C(5)-Ni(1)-C(9)	69.47(7)	C(8)-C(7)-C(13)	119.08(19)
C(10)-Ni(1)-C(9)	38.15(7)	C(6)-C(7)-Ni(1)	74.17(11)
C(7)-Ni(1)-C(9)	68.89(7)	C(8)-C(7)-Ni(1)	68.10(10)
C(2)-Ni(1)-C(6)	122.73(8)	C(13)-C(7)-Ni(1)	131.20(15)
C(1)-Ni(1)-C(6)	127.55(12)	C(9)-C(8)-C(7)	120.34(17)
C(3)-Ni(1)-C(6)	135.44(11)	C(9)-C(8)-C(14)	119.77(19)
C(8)-Ni(1)-C(6)	68.57(7)	C(7)-C(8)-C(14)	119.86(19)
C(5)-Ni(1)-C(6)	37.77(7)	C(9)-C(8)-Ni(1)	73.48(11)
		C(7)-C(8)-Ni(1)	73.01(11)

C(14)-C(8)-Ni(1)	126.94(15)	F(23)-C(27)-C(23)	111.84(17)
C(10)-C(9)-C(8)	119.26(17)	F(26)-C(28)-F(24)	106.0(2)
C(10)-C(9)-C(15)	120.04(19)	F(26)-C(28)-F(25)	107.01(19)
C(8)-C(9)-C(15)	120.62(19)	F(24)-C(28)-F(25)	105.27(17)
C(10)-C(9)-Ni(1)	69.11(10)	F(26)-C(28)-C(25)	112.64(17)
C(8)-C(9)-Ni(1)	68.16(11)	F(24)-C(28)-C(25)	112.61(18)
C(15)-C(9)-Ni(1)	133.49(16)	F(25)-C(28)-C(25)	112.77(17)
C(9)-C(10)-C(5)	119.90(17)	C(32)-C(31)-C(36)	115.93(15)
C(9)-C(10)-C(16)	118.83(18)	C(32)-C(31)-B(20)	125.60(15)
C(5)-C(10)-C(16)	121.27(17)	C(36)-C(31)-B(20)	118.39(15)
C(9)-C(10)-Ni(1)	72.74(11)	C(31)-C(32)-C(33)	121.85(16)
C(5)-C(10)-Ni(1)	70.31(10)	C(34)-C(33)-C(32)	121.17(16)
C(16)-C(10)-Ni(1)	129.65(14)	C(34)-C(33)-C(37)	119.46(16)
C(51)-B(20)-C(41)	106.44(14)	C(32)-C(33)-C(37)	119.31(16)
C(51)-B(20)-C(21)	110.63(14)	C(33)-C(34)-C(35)	117.90(16)
C(41)-B(20)-C(21)	113.17(14)	C(36)-C(35)-C(34)	120.94(16)
C(51)-B(20)-C(31)	111.59(14)	C(36)-C(35)-C(38)	121.49(16)
C(41)-B(20)-C(31)	111.39(14)	C(34)-C(35)-C(38)	117.57(16)
C(21)-B(20)-C(31)	103.74(13)	C(35)-C(36)-C(31)	122.19(16)
C(26)-C(21)-C(22)	116.00(16)	F(31)-C(37)-F(32)	106.19(16)
C(26)-C(21)-B(20)	124.22(16)	F(31)-C(37)-F(33)	106.19(17)
C(22)-C(21)-B(20)	119.30(15)	F(32)-C(37)-F(33)	106.08(17)
C(23)-C(22)-C(21)	121.94(17)	F(31)-C(37)-C(33)	112.78(15)
C(22)-C(23)-C(24)	120.91(17)	F(32)-C(37)-C(33)	112.01(16)
C(22)-C(23)-C(27)	121.12(18)	F(33)-C(37)-C(33)	113.04(16)
C(24)-C(23)-C(27)	117.97(17)	F(36)-C(38)-F(34)	106.85(16)
C(25)-C(24)-C(23)	118.23(17)	F(36)-C(38)-F(35)	106.34(15)
C(24)-C(25)-C(26)	120.76(17)	F(34)-C(38)-F(35)	105.90(15)
C(24)-C(25)-C(28)	119.61(17)	F(36)-C(38)-C(35)	113.81(15)
C(26)-C(25)-C(28)	119.58(17)	F(34)-C(38)-C(35)	111.54(15)
C(21)-C(26)-C(25)	122.15(17)	F(35)-C(38)-C(35)	111.90(15)
F(21)-C(27)-F(22)	106.51(17)	C(42)-C(41)-C(46)	115.57(16)
F(21)-C(27)-F(23)	106.87(17)	C(42)-C(41)-B(20)	125.32(16)
F(22)-C(27)-F(23)	106.24(16)	C(46)-C(41)-B(20)	119.06(15)
F(21)-C(27)-C(23)	113.37(16)	C(43)-C(42)-C(41)	121.92(17)
F(22)-C(27)-C(23)	111.57(16)	C(44)-C(43)-C(42)	121.32(17)

C(44)-C(43)-C(47)	119.96(17)	F(51)-C(57)-C(53)	112.86(15)
C(42)-C(43)-C(47)	118.69(16)	F(57)-C(58)-F(54)	125.1(6)
C(43)-C(44)-C(45)	117.86(17)	F(57)-C(58)-F(59)	110.7(6)
C(46)-C(45)-C(44)	120.50(17)	F(54)-C(58)-F(59)	64.0(6)
C(46)-C(45)-C(48)	118.92(17)	F(57)-C(58)-F(55)	32.0(7)
C(44)-C(45)-C(48)	120.56(17)	F(54)-C(58)-F(55)	108.1(3)
C(45)-C(46)-C(41)	122.78(17)	F(59)-C(58)-F(55)	131.9(5)
F(41)-C(47)-F(43)	106.94(17)	F(57)-C(58)-F(56)	73.2(7)
F(41)-C(47)-F(42)	105.40(16)	F(54)-C(58)-F(56)	105.4(3)
F(43)-C(47)-F(42)	106.12(16)	F(59)-C(58)-F(56)	44.9(7)
F(41)-C(47)-C(43)	112.82(16)	F(55)-C(58)-F(56)	103.8(2)
F(43)-C(47)-C(43)	112.89(16)	F(57)-C(58)-F(58)	105.2(7)
F(42)-C(47)-C(43)	112.11(16)	F(54)-C(58)-F(58)	38.8(6)
F(44)-C(48)-F(46)	106.92(17)	F(59)-C(58)-F(58)	101.9(5)
F(44)-C(48)-F(45)	107.67(18)	F(55)-C(58)-F(58)	76.9(7)
F(46)-C(48)-F(45)	104.14(16)	F(56)-C(58)-F(58)	136.3(5)
F(44)-C(48)-C(45)	113.65(16)	F(57)-C(58)-C(55)	116.2(6)
F(46)-C(48)-C(45)	112.56(17)	F(54)-C(58)-C(55)	114.8(2)
F(45)-C(48)-C(45)	111.31(17)	F(59)-C(58)-C(55)	113.5(4)
C(52)-C(51)-C(56)	115.94(16)	F(55)-C(58)-C(55)	112.3(2)
C(52)-C(51)-B(20)	125.42(15)	F(56)-C(58)-C(55)	111.65(19)
C(56)-C(51)-B(20)	118.65(15)	F(58)-C(58)-C(55)	107.9(5)
C(51)-C(52)-C(53)	121.86(16)		
C(54)-C(53)-C(52)	121.32(16)		
C(54)-C(53)-C(57)	119.76(16)		
C(52)-C(53)-C(57)	118.83(16)		
C(53)-C(54)-C(55)	117.70(17)		
C(56)-C(55)-C(54)	121.02(17)		
C(56)-C(55)-C(58)	118.95(17)		
C(54)-C(55)-C(58)	120.03(17)		
C(55)-C(56)-C(51)	122.12(17)		
F(53)-C(57)-F(52)	106.78(15)		
F(53)-C(57)-F(51)	106.56(15)		
F(52)-C(57)-F(51)	105.19(15)		
F(53)-C(57)-C(53)	112.85(15)		
F(52)-C(57)-C(53)	112.06(15)		

Appendix III

Table III.1. Crystal data and structure for complex **2**.

Empirical formula	C ₄₇ H ₃₃ B F ₂₄ Ni	
Formula weight	1123.25	
Temperature	100(2) K	
Wavelength	0.71073 Å	
Crystal system	Monoclinic	
Space group	P2 ₁ /c	
Unit cell dimensions	a = 12.4433(13) Å	a = 90°.
	b = 18.9381(19) Å	b = 106.340(5)°.
	c = 20.323(2) Å	g = 90°.
Volume	4595.7(8) Å ³	
Z	4	
Density (calculated)	1.623 Mg/m ³	
Absorption coefficient	0.555 mm ⁻¹	
F(000)	2256	
Crystal size	0.25 x 0.15 x 0.15 mm ³	
Theta range for data collection	1.50 to 25.00°.	
Index ranges	-14 ≤ h ≤ 9, -22 ≤ k ≤ 22, -23 ≤ l ≤ 24	
Reflections collected	37841	
Independent reflections	8089 [R(int) = 0.0681]	
Completeness to theta = 25.00°	100.0 %	
Absorption correction	Numerical	
Max. and min. transmission	0.920 and 0.868	
Refinement method	Full-matrix least-squares on F ²	
Data / restraints / parameters	8089 / 0 / 662	
Goodness-of-fit on F ²	1.037	
Final R indices [I > 2σ(I)]	R1 = 0.0604, wR2 = 0.1423	
R indices (all data)	R1 = 0.0904, wR2 = 0.1591	
Largest diff. peak and hole	0.932 and -0.717 e.Å ⁻³	

Table III.2. Polymerization of 1,3-CHD and DMBD using catalyst **2**.^a

Monomer	Ratio	Time	Conversion % (Isolated)
DMBD	1000:1	6 h	32
1,3-CHD	850:1	5 min	85

^aConditions: 23 °C, 2.0 mL total volume, solvent CH₂Cl₂. All polymerizations were run in triplicate.

Table III.3. Selected bond lengths (Å) for complex **2**.

Ni(1)-C(2)	1.934(5)	B(20)-C(51)	1.641(6)
Ni(1)-C(3)	2.015(5)	C(21)-C(26)	1.396(6)
Ni(1)-C(1)	2.063(6)	C(21)-C(22)	1.399(6)
Ni(1)-C(8)	2.149(5)	C(22)-C(23)	1.392(6)
Ni(1)-C(12)	2.154(4)	C(23)-C(24)	1.382(6)
Ni(1)-C(11)	2.157(5)	C(23)-C(27)	1.491(6)
Ni(1)-C(7)	2.159(4)	C(24)-C(25)	1.377(6)
Ni(1)-C(10)	2.193(5)	C(25)-C(26)	1.396(6)
Ni(1)-C(9)	2.224(5)	C(25)-C(28)	1.487(6)
C(1)-C(2)	1.408(8)	C(27)-F(23)	1.328(5)
C(1)-C(6)	1.494(8)	C(27)-F(22)	1.336(5)
C(2)-C(3)	1.399(9)	C(27)-F(21)	1.340(5)
C(3)-C(4)	1.474(8)	C(28)-F(24)	1.321(6)
C(4)-C(5)	1.463(9)	C(28)-F(25)	1.330(5)
C(5)-C(6)	1.447(9)	C(28)-F(26)	1.340(6)
C(7)-C(12)	1.398(7)	C(31)-C(32)	1.396(6)
C(7)-C(8)	1.418(7)	C(31)-C(36)	1.397(6)
C(7)-C(13)	1.500(7)	C(32)-C(33)	1.389(6)
C(8)-C(9)	1.410(7)	C(33)-C(34)	1.392(6)
C(9)-C(10)	1.392(7)	C(33)-C(37)	1.490(6)
C(9)-C(14)	1.504(7)	C(34)-C(35)	1.384(6)
C(10)-C(11)	1.406(7)	C(35)-C(36)	1.395(6)
C(11)-C(12)	1.404(7)	C(35)-C(38)	1.492(6)
C(11)-C(15)	1.505(7)	C(37)-F(32)	1.326(5)
B(20)-C(41)	1.636(6)	C(37)-F(33)	1.331(5)
B(20)-C(31)	1.638(6)	C(37)-F(31)	1.332(6)
B(20)-C(21)	1.639(6)	C(38)-F(35)	1.334(5)

C(38)-F(36)	1.338(5)	C(48)-F(45)	1.334(5)
C(38)-F(34)	1.346(5)	C(51)-C(52)	1.390(6)
C(41)-C(42)	1.386(6)	C(51)-C(56)	1.403(6)
C(41)-C(46)	1.411(6)	C(52)-C(53)	1.396(6)
C(42)-C(43)	1.402(6)	C(53)-C(54)	1.379(6)
C(43)-C(44)	1.372(6)	C(53)-C(57)	1.483(6)
C(43)-C(47)	1.495(6)	C(54)-C(55)	1.388(6)
C(44)-C(45)	1.398(6)	C(55)-C(56)	1.382(6)
C(45)-C(46)	1.383(6)	C(55)-C(58)	1.501(6)
C(45)-C(48)	1.495(6)	C(57)-F(53)	1.290(6)
C(47)-F(41)	1.322(5)	C(57)-F(52)	1.323(5)
C(47)-F(43)	1.324(5)	C(57)-F(51)	1.325(6)
C(47)-F(42)	1.336(6)	C(58)-F(54)	1.339(5)
C(48)-F(44)	1.315(5)	C(58)-F(55)	1.341(5)
C(48)-F(46)	1.327(5)	C(58)-F(56)	1.342(5)

Table III.4. Selected bond angles (°) for complex **2**.

C(2)-Ni(1)-C(3)	41.4(3)		
C(2)-Ni(1)-C(1)	41.1(2)	C(7)-Ni(1)-C(9)	68.68(17)
C(3)-Ni(1)-C(1)	71.1(3)	C(10)-Ni(1)-C(9)	36.73(18)
C(2)-Ni(1)-C(8)	131.5(2)	C(2)-C(1)-C(6)	120.3(6)
C(3)-Ni(1)-C(8)	171.9(2)	C(2)-C(1)-Ni(1)	64.5(3)
C(1)-Ni(1)-C(8)	105.7(2)	C(6)-C(1)-Ni(1)	107.4(4)
C(2)-Ni(1)-C(12)	157.3(2)	C(3)-C(2)-C(1)	115.3(5)
C(3)-Ni(1)-C(12)	119.5(2)	C(3)-C(2)-Ni(1)	72.4(3)
C(1)-Ni(1)-C(12)	132.3(2)	C(1)-C(2)-Ni(1)	74.4(3)
C(8)-Ni(1)-C(12)	68.34(17)	C(2)-C(3)-C(4)	120.6(5)
C(2)-Ni(1)-C(11)	141.2(2)	C(2)-C(3)-Ni(1)	66.2(3)
C(3)-Ni(1)-C(11)	104.2(2)	C(4)-C(3)-Ni(1)	106.3(4)
C(1)-Ni(1)-C(11)	166.1(2)	C(5)-C(4)-C(3)	113.9(6)
C(8)-Ni(1)-C(11)	80.69(18)	C(6)-C(5)-C(4)	118.7(5)
C(12)-Ni(1)-C(11)	38.01(18)	C(5)-C(6)-C(1)	113.5(5)
C(2)-Ni(1)-C(7)	149.4(2)	C(12)-C(7)-C(8)	118.3(4)
C(3)-Ni(1)-C(7)	149.3(2)	C(12)-C(7)-C(13)	121.1(4)
C(1)-Ni(1)-C(7)	108.4(2)	C(8)-C(7)-C(13)	120.6(4)
C(8)-Ni(1)-C(7)	38.42(17)	C(12)-C(7)-Ni(1)	70.9(3)
C(12)-Ni(1)-C(7)	37.82(17)	C(8)-C(7)-Ni(1)	70.4(3)
C(11)-Ni(1)-C(7)	68.70(18)	C(13)-C(7)-Ni(1)	130.2(3)
C(2)-Ni(1)-C(10)	126.2(2)	C(9)-C(8)-C(7)	122.0(4)
C(3)-Ni(1)-C(10)	112.8(2)	C(9)-C(8)-Ni(1)	74.1(3)
C(1)-Ni(1)-C(10)	156.2(2)	C(7)-C(8)-Ni(1)	71.2(3)
C(8)-Ni(1)-C(10)	67.07(18)	C(10)-C(9)-C(8)	117.7(4)
C(12)-Ni(1)-C(10)	67.85(18)	C(10)-C(9)-C(14)	121.4(5)
C(11)-Ni(1)-C(10)	37.69(18)	C(8)-C(9)-C(14)	120.8(5)
C(7)-Ni(1)-C(10)	80.43(18)	C(10)-C(9)-Ni(1)	70.4(3)
C(2)-Ni(1)-C(9)	121.8(2)	C(8)-C(9)-Ni(1)	68.3(3)
C(3)-Ni(1)-C(9)	138.1(2)	C(14)-C(9)-Ni(1)	131.7(3)
C(1)-Ni(1)-C(9)	124.7(2)	C(9)-C(10)-C(11)	121.7(4)
C(8)-Ni(1)-C(9)	37.58(18)	C(9)-C(10)-Ni(1)	72.8(3)
C(12)-Ni(1)-C(9)	80.44(17)	C(11)-C(10)-Ni(1)	69.7(3)
C(11)-Ni(1)-C(9)	67.77(18)	C(12)-C(11)-C(10)	119.5(4)

C(12)-C(11)-C(15)	120.4(5)	F(25)-C(28)-C(25)	113.4(4)
C(10)-C(11)-C(15)	120.2(5)	F(26)-C(28)-C(25)	112.7(4)
C(12)-C(11)-Ni(1)	70.9(3)	C(32)-C(31)-C(36)	115.6(4)
C(10)-C(11)-Ni(1)	72.6(3)	C(32)-C(31)-B(20)	120.8(4)
C(15)-C(11)-Ni(1)	128.1(4)	C(36)-C(31)-B(20)	123.6(4)
C(7)-C(12)-C(11)	120.7(4)	C(33)-C(32)-C(31)	123.1(4)
C(7)-C(12)-Ni(1)	71.3(2)	C(32)-C(33)-C(34)	120.0(4)
C(11)-C(12)-Ni(1)	71.1(3)	C(32)-C(33)-C(37)	119.9(4)
C(41)-B(20)-C(31)	111.6(3)	C(34)-C(33)-C(37)	120.1(4)
C(41)-B(20)-C(21)	110.8(3)	C(35)-C(34)-C(33)	118.1(4)
C(31)-B(20)-C(21)	107.2(3)	C(34)-C(35)-C(36)	121.1(4)
C(41)-B(20)-C(51)	105.6(3)	C(34)-C(35)-C(38)	119.6(4)
C(31)-B(20)-C(51)	110.5(3)	C(36)-C(35)-C(38)	119.3(4)
C(21)-B(20)-C(51)	111.2(3)	C(35)-C(36)-C(31)	122.0(4)
C(26)-C(21)-C(22)	115.2(4)	F(32)-C(37)-F(33)	106.4(4)
C(26)-C(21)-B(20)	119.0(4)	F(32)-C(37)-F(31)	106.4(4)
C(22)-C(21)-B(20)	125.8(4)	F(33)-C(37)-F(31)	105.9(4)
C(23)-C(22)-C(21)	122.6(4)	F(32)-C(37)-C(33)	113.3(4)
C(24)-C(23)-C(22)	120.6(4)	F(33)-C(37)-C(33)	112.8(4)
C(24)-C(23)-C(27)	119.6(4)	F(31)-C(37)-C(33)	111.4(4)
C(22)-C(23)-C(27)	119.7(4)	F(35)-C(38)-F(36)	106.6(4)
C(25)-C(24)-C(23)	118.3(4)	F(35)-C(38)-F(34)	105.5(3)
C(24)-C(25)-C(26)	120.6(4)	F(36)-C(38)-F(34)	105.5(4)
C(24)-C(25)-C(28)	120.9(4)	F(35)-C(38)-C(35)	113.5(4)
C(26)-C(25)-C(28)	118.5(4)	F(36)-C(38)-C(35)	113.5(4)
C(25)-C(26)-C(21)	122.6(4)	F(34)-C(38)-C(35)	111.7(4)
F(23)-C(27)-F(22)	106.3(3)	C(42)-C(41)-C(46)	115.9(4)
F(23)-C(27)-F(21)	106.2(4)	C(42)-C(41)-B(20)	126.0(4)
F(22)-C(27)-F(21)	106.1(4)	C(46)-C(41)-B(20)	118.0(4)
F(23)-C(27)-C(23)	113.1(4)	C(41)-C(42)-C(43)	122.0(4)
F(22)-C(27)-C(23)	112.8(4)	C(44)-C(43)-C(42)	121.1(4)
F(21)-C(27)-C(23)	111.8(3)	C(44)-C(43)-C(47)	119.5(4)
F(24)-C(28)-F(25)	107.4(4)	C(42)-C(43)-C(47)	119.4(4)
F(24)-C(28)-F(26)	104.6(4)	C(43)-C(44)-C(45)	118.3(4)
F(25)-C(28)-F(26)	105.0(4)	C(46)-C(45)-C(44)	120.4(4)
F(24)-C(28)-C(25)	113.0(4)	C(46)-C(45)-C(48)	120.2(4)

C(44)-C(45)-C(48)	119.3(4)	C(54)-C(53)-C(57)	118.3(4)
C(45)-C(46)-C(41)	122.3(4)	C(52)-C(53)-C(57)	121.4(4)
F(41)-C(47)-F(43)	106.6(4)	C(53)-C(54)-C(55)	118.4(4)
F(41)-C(47)-F(42)	105.6(4)	C(56)-C(55)-C(54)	121.1(4)
F(43)-C(47)-F(42)	104.7(4)	C(56)-C(55)-C(58)	120.8(4)
F(41)-C(47)-C(43)	113.2(4)	C(54)-C(55)-C(58)	118.1(4)
F(43)-C(47)-C(43)	113.6(4)	C(55)-C(56)-C(51)	121.8(4)
F(42)-C(47)-C(43)	112.5(4)	F(53)-C(57)-F(52)	106.4(4)
F(44)-C(48)-F(46)	107.8(4)	F(53)-C(57)-F(51)	105.2(5)
F(44)-C(48)-F(45)	104.3(4)	F(52)-C(57)-F(51)	103.8(4)
F(46)-C(48)-F(45)	103.7(4)	F(53)-C(57)-C(53)	114.0(4)
F(44)-C(48)-C(45)	113.3(4)	F(52)-C(57)-C(53)	113.0(4)
F(46)-C(48)-C(45)	113.9(4)	F(51)-C(57)-C(53)	113.5(4)
F(45)-C(48)-C(45)	112.9(4)	F(54)-C(58)-F(55)	106.5(3)
C(52)-C(51)-C(56)	116.1(4)	F(54)-C(58)-F(56)	106.8(4)
C(52)-C(51)-B(20)	126.0(4)	F(55)-C(58)-F(56)	106.3(4)
C(56)-C(51)-B(20)	117.9(3)	F(54)-C(58)-C(55)	111.7(4)
C(51)-C(52)-C(53)	122.4(4)	F(55)-C(58)-C(55)	112.2(4)
C(54)-C(53)-C(52)	120.3(4)	F(56)-C(58)-C(55)	112.8(3)